

**MOLECULAR ANALYSIS OF *CINNAMATE CoA-LIGASE*
FROM PHYTOALEXIN PRODUCING APPLE CELL
CULTURES**

Ph.D. THESIS

by

DEEPA TEOTIA



**DEPARTMENT OF BIOTECHNOLOGY
INDIAN INSTITUTE OF TECHNOLOGY ROORKEE
ROORKEE-247667, INDIA
FEBRUARY, 2018**

**MOLECULAR ANALYSIS OF *CINNAMATE CoA-LIGASE*
FROM PHYTOALEXIN PRODUCING APPLE CELL
CULTURES**

A THESIS

*Submitted in partial fulfilment of the
requirements for the award of the degree*

of

DOCTOR OF PHILOSOPHY

in

BIOTECHNOLOGY

by

DEEPA TEOTIA



**DEPARTMENT OF BIOTECHNOLOGY
INDIAN INSTITUTE OF TECHNOLOGY ROORKEE
ROORKEE-247667, INDIA
FEBRUARY, 2018**



**©INDIAN INSTITUTE OF TECHNOLOGY ROORKEE, ROORKEE- 2018
ALL RIGHTS RESERVED**



INDIAN INSTITUTE OF TECHNOLOGY ROORKEE ROORKEE

CANDIDATE'S DECLARATION

I hereby certify that the work which is being presented in the thesis entitled “**MOLECULAR ANALYSIS OF CINNAMATE CoA-LIGASE FROM PHYTOALEXIN PRODUCING APPLE CELL CULTURES**”, in partial fulfilment of the requirements for the award of the degree of Doctor of Philosophy and submitted in the Department of Biotechnology of the Indian Institute of Technology Roorkee, Roorkee is an authentic record of my own work carried out during a period from August, 2013 to February 2018, under the supervision of Dr. Debabrata Sircar, Assistant Professor, Department of Biotechnology, Indian Institute of Technology Roorkee, Roorkee.

The matter presented in the thesis has not been submitted by me for the award of any other degree of this or any other institution.

(DEEPA TEOTIA)

This is to certify that the above statement made by the candidate is correct to the best of my knowledge.

(Debabrata Sircar)
Supervisor

The Ph. D. Viva-Voce Examination of **Ms. Deepa Teotia**, Research Scholar has been held on **03/07/18**.

Chairman, SRC

Signature of External Examiner

This is to certify that the student has made all the corrections in the thesis.

Signature of Supervisor

Head of the Department

Dated:

ABSTRACT

Apple is an important fruit crop, grown mainly in the temperate region of the world. Apple fruits have high nutritional value and tremendous health protective properties. Routine consumption of apples is linked with low risk of life-threatening diseases. Despite huge economic importance, apple production is badly affected by scab disease. Except for few wild apple cultivars, most of the commercial apple cultivars are susceptible to the apple scab-disease, caused by the fungus *Venturia inaequalis*. To date, the scab-resistance mechanisms in apples are not well understood. The present study investigates the biochemical and molecular basis of scab-resistance mechanisms in apple. First, cell cultures of moderately scab-susceptible apple cultivar cv. Golden Delicious were developed as a model system to understand apple -*Venturia* (scab) interactions, both at metabolite and molecular levels. A validated HPLC-mass spectrometry based analytical method was developed to rapidly separate and quantify biphenyl and dibenzofurans, the scab-induced phytoalexins of apple. Further this thesis investigates the comparative metabolomics profile of elicitor-treated cell culture of apple cv. Golden Delicious to identify defense responsive metabolites. Gas chromatography–mass spectrometry (GC-MS) coupled with multivariate analysis were applied to analyze the metabolite profiles of elicited cell cultures. Using non-targeted comparative metabolomics a total of 43 differentially accumulating metabolites were identified in Golden Delicious cell culture treated with *Venturia*-elicitor, out of which phenolics and biphenyl accumulation was significantly enhanced upon elicitor-treatment. Furthermore, using a genome database of Rosaceae and sequence information from plant secondary metabolism- specific CoA ligase, a cDNA encoding *cinnamate:CoA ligase (CNL)* was cloned and functionally characterized from the VIE-treated cell cultures of cv. Golden Delicious. This enzyme channels carbon flux from the phenylpropanoid pathway towards benzenoid-metabolism and finally towards biphenyl phytoalexin biosynthesis. *MdCNL* preferred cinnamic acid as a substrate but failed to accept benzoic acid. *MdCNL* activity was found to be strictly dependent on the presence of K^+ and Mg^{2+} ions in the assay buffer at optimum concentrations of 100 and 2.5 mM, respectively. Coordinated increase in the *phenylalanine ammonia-lyase (PAL)* and *MdCNL* transcript levels preceded accumulation of biphenyl phytoalexin noraucuparin and aucuparin in VIE-treated cell cultures of apple cv. Golden Delicious. When greenhouse-grown apple plants of cv. Shireen (scab-resistant cultivar) and cv. Golden Delicious (moderately scab-susceptible cultivar) were infected with the scab fungus *V. inaequalis*, up-regulation of *MdCNL* transcript levels was observed in the

internodal region with accumulation of aucuparin and noraucuparin phytoalexins. Both phytoalexin levels and *MdCNL* transcript levels were significantly higher in the cultivar Shireen than that of Golden Delicious. No phytoalexins were detected in the leaves. *MdCNL* contained a C-terminal type 1 peroxisomal targeting signal consisting of SRL tri-peptide, which directed an N-terminal reporter fusion (YFP-CNL) to the peroxisomes. Together, the data suggest that *MdCNL* catalyzed cinnamoyl-CoA formation is required for biphenyl phytoalexin biosynthesis in apple.

Key words: Apple, Golden Delicious, Shireen, Cinnamate-CoA-ligase, metabolomics, biphenyl, cell culture.



Acknowledgements

Thanks to Braham Swarup Almighty, the creator of universe and source of all knowledge for his divine sanction on me and allowing me to see immensity in his creatures.

I take immense pleasure in expressing my deep sense of gratitude to my supervisor and mentor **Dr. Debabrata Sircar** for giving me the opportunity to join his research laboratory. We Shashank, Amol and me were the first three students of Dr. Sircar. PhD students use to get help and guidance from their seniors, but we had the opportunity to learn directly from our guide. We had the opportunity to learn how to establish the lab and to understand how much effort it takes to completely build it. I am very thankful to him for always giving his precious time for healthy discussions, be at tea or at office. He had also worked extremely hard to bring projects in lab, for providing us with all the facilities required for the experiments, including the expensive chemicals and instruments. Whenever my experiments had failed, he had always encouraged me to be optimistic. His trust in me and constant supervision has been a constant source of positive energy for me. He has supervised and supported me throughout my Ph.D. His enthusiasm and profound concern for my success has made this journey a joyous one. It has been a great privilege and honour to work and study with his precious guidance. His sincerity, dynamism, vision and motivation deeply inspired me to learn new things. Along with academic support his affectionate behaviour and moral support also helped me through the rough road to finish my thesis. I express my wholehearted indebtedness to him.

I would also like to express my profound gratitude to **Dr. A.K. Sharma** (current) and **Prof. Partha Roy** (previous) Head of Department of Biotechnology for providing the basic infrastructural facilities in the department that allowed me to successfully complete my Ph.D. During my PhD work I am thankful to Prof. Partha Roy for giving me access to his laboratory instrumentation. His punctuality and sense of duty have been a source of motivation.

Besides, I would like to thank the Department of Biotechnology and Institute Instrumentation Centre (IIC), IIT Roorkee for instrument facilities to carry out the research work. I am also grateful to my SRC committee members: **Dr. Pravindra Kumar, Dr. R. Prasad and Dr. R.K. Peddinti**, for their continuous advice and kind support.

I also express my sincere gratitude towards **Dr. Harsh Chauhan** and **Dr. Sri Ram Yadav** for their kind and valuable suggestions and other faculty members of Department of Biotechnology

during my PhD. I am also thankful to **Dr. M. Sankar** from chemistry department for giving access to his lab instruments.

I am very thankful to Shashank for never saying no to any help. He had always helped in those lengthy experiments, which takes more than 12 hours continuous work, where you cannot leave the instrument. Also helping in experiments where I had to leave because of hostel deadlines. I also want to thank my emergency friend Meenu for always helping me in need. I remember two times, once when I had to leave home and had to do experiment which I could not delay, she and Shashank did it for me. Another once in the night at 12, I needed laptop and I was locked in the hostel, she as always helped me again.

I am also thankful to Mr. Amol Sarkate, Ms. Kriti Juneja, Mr. Ashwani Kumar, Mr. Mukund Kumar, Ms. Varsha Tomar, Mr. Bhairavnath Waghmode, Ms. Komal Kushwaha and Mr. Prabhu for the pleasant working environment and companionship during laboratory works.

I am also thankful to the office staff, Department of Biotechnology, for their kind help and support, campus administration their hard work made my stay comfortable in campus.

I also want to appreciate great campus environment with all the greenery, safety inside the campus and also very good sports facility at the campus. I am going to miss this environment in outside world.

A special note of thanks to my colleagues in IIT Roorkee namely Malik, Benzo, Nishu and Poonam for their encouragement, support and giving unforgettable moments during my stay in IIT.

I would also like to express my deep gratitude to Mrs. Rakhi Sircar and two little angels Ishika and Annie for their moral support, kind blessings and for letting me feel like home during my stay in IIT Roorkee.

Finally, my sincere thanks to my family for standing with me in every situation of my life.

Deepa Teotia

CONTENTS

	Page No	
Title page		
Candidate's declaration		
Abstract	(i-ii)	
Acknowledgement	(iii-iv)	
Contents	(v-xii)	
List of Abbreviations	(xiii-xv)	
List of Figures	(xvi-xviii)	
List of Tables	(xix-xxi)	
Chapter 1	Introduction and Literature Review	1 - 35
	1.1: The Rosaceae family	1-3
	1.2: The origin, distribution and taxonomy of apple	3-6
	1.3: Apple production	6 - 9
	1.4: Apple scab disease	9-11
	1.4.1: <i>Venturia inaequalis</i>	10
	1.4.2 Life cycle of <i>Venturia inaequalis</i>	10-11
	1.5: Metabolomics of apple: A new tool to understand plant's disease resistance mechanism	11-14
	1.5.1: Apple phytochemicals	13-14
	1.6: Defense mechanisms to the apple scab	15-24
	1.6.1: Structural defense mechanisms	15
	1.6.2: Biochemical defense mechanisms	16-18

1.6.2.1:	Phytoanticipins	16
1.6.2.2:	Pathogenesis-related (PR) proteins	16-17
1.6.2.3:	Phytoalexins	17- 18
1.6.3:	Venturia inaequalis- Malus gene- for-gene (GfG) relationships	18-21
1.6.3.1	Hypervariability of <i>Venturia</i> <i>inaequalis</i>	20-21
1.6.4:	Breeding, cisgenesis and transgenesis	22-24
1.7:	Inducible defense metabolites of Maliane: the Biphenyls and the dibenzofurans	25-27
1.8:	Biosynthesis of the biphenyl and the dibenzofuran	27-28
1.9:	Benzoic acid biosynthesis in plants	28-32
1.9.1:	CoA-dependent and β -oxidative route of benzoic acid biosynthesis	30-31
1.9.2:	CoA-dependent and non β -oxidative route of benzoic acid biosynthesis	31
1.9.3:	CoA-independent and non β -oxidative route of benzoic acid biosynthesis	32
1.10:	Benzoate-CoA ligase (BZL) activity	32-33
1.11:	Cinnamate-CoA ligase in plants	33-34
1.12:	Aim of the work	34
1.13:	Plant material used	35
1.14:	Objectives	35

Chapter 2

Materials and Methods **36-78**

2.1:	Chemicals and reagents	36-38
2.2:	Equipments	39
2.3:	Nutrient media	40-42
2.3.1:	Nutrient media for plant tissue culture	40
2.3.2:	Nutrient media for fungal culture (scab- fungus)	41

2.3.3:	Nutrient media for <i>E.coli</i> culture	41
2.3.4:	Nutrient media for <i>A. tumefaciens</i> growth	42
2.3.5:	Activation medium for <i>A. tumefaciens</i> transformation	42
2.4:	Buffer and solutions	43-46
2.5:	Materials for molecular biology	46-49
2.5.1:	mRNA extraction, cDNA synthesis and real time PCR reagents	46-47
2.5.2:	Host cells (Competent <i>E. coli</i>)	47
2.5.3:	Vectors	48
2.5.4:	Primers	48-49
2.6:	<i>Venturia inaequalis</i> elicitor and spores used	49-50
2.7:	Plant material	51
2.8:	Development and validation HPLC method for the determination of biphenyl and dibenzofuran phytoalexins in Rosaceae	52-55
2.8.1:	Plant material	52
2.8.2:	HPLC condition	52
2.8.3:	ESI-MS-conditions	53
2.8.4:	Chemical synthesis of aucuparin, noraucuparin	53-54
2.8.5:	Preparation of standards and plant sample	54
2.8.6:	Calibration procedure	54
2.8.7:	Recovery, precision, accuracy and specificity	55
2.8.8:	Analytical Sensitivity (AS), Limit of detection (LOD) and quantification (LOQ)	55
2.9:	Induction of callus and establishment of suspension cultures of apple	55-56
2.10:	GC-MS based metabolomics of apple cell cultures treated with <i>Venturia inaequalis</i> elicitor (VIE)	56- 60

2.10.1:	Cell culture and elicitor-treatment	56
2.10.2:	Extraction of polar metabolites	56
2.10.3:	GC-MS analysis	56-57
2.10.4:	Metabolite identification	57
2.10.5:	Pre-processing and statistical analysis of metabolite data	57-58
2.10.6:	Quantitative Real-Time PCR	58-60
2.11:	Molecular cloning and functional analyses of a cinnamate-CoA ligase (CNL) from cell suspension culture of apple cv. Golden Delicious	60- 77
2.11.1:	Cell cultures and plant treatment	60-61
2.11.2:	Extraction and HPLC analysis of biphenyl phytoalexins	61
2.11.3:	Isolation and cloning of apple cDNA encoding <i>MdCNL</i>	62-68
2.11.3.1:	Reverse transcription	63
2.11.3.2:	PCR amplification and gel electrophoresis	63-64
2.11.3.3:	Agarose gel electrophoresis	65
2.11.3.4:	DNA purification from agarose gel or after digestion reactions	65
2.11.3.5:	Restriction digestion	65-65
2.11.3.6:	Ligation of DNA fragments	66-67
2.11.3.7:	Transformation of DNA products into <i>E.coli</i>	67
2.11.3.8:	Isolation of plasmid DNA by alkaline hydrolysis	67-68
2.11.4:	Heterologous expression of <i>MdCNL</i> in <i>E. coli</i>	68
2.11.5:	SDS-PAGE gel electrophoresis	68-69
2.11.6:	<i>MdCNL</i> activity assay	69
2.11.7:	Analyses of enzymatic product by ESI-	69

	MS	
	2.11.8: Substrate specificity test	70
	2.11.9: Analyses of Kinetic parameters of <i>MdCNL</i>	70
	2.11.10 : Phylogeny analyses	71-73
	2.11.11: Quantitative Real-Time PCR of <i>MdCNL</i> , <i>MdPAL</i> and <i>MdBIS</i> expression	73-75
	2.11.12: Identification of molecular weight of <i>MdCNL</i> by Matrix-Assisted Laser Desorption/Ionisation Mass Spectrometry (MALDI-MS)	75-76
	2.11.13: Agrobacterium-mediated transient expression and sub-cellular localization	76-77
	2.11.14: Homology modeling and substrate docking with <i>MdCNL</i>	77-78
	2.12: Databases and software	78
Chapter 3	Results	79-116
	3.1: To develop cell suspension culture of apple cv. <i>Golden Delicious</i>	79-81
	3.1.1: Callus induction from apple leaves	79-80
	3.1.2: Establishment of cell suspension culture	80-81
	3.2: Development and validation of a new HPLC method for the determination of biphenyl and dibenzofuran phytoalexins in Rosaceae	81-86
	3.2.1: Chemical synthesis of aucuparin, noraucuparin	81-82
	3.2.2: Optimization of chromatographic condition	82-83
	3.2.3: HPLC Method Validation	83-85

3.2.3.1:	Linearity	83-84
3.2.3.2:	AS, LOD and LOQ	84
3.2.3.3:	Precision and Accuracy	85
3.2.4:	Analysis of the plant extract with RP-HPLC method	85-86
3.3:	GC-MS based metabolomics analyses of <i>Venturia inaequalis</i> elicitor-treated cell culture of apple cv. <i>Golden Delicious</i>	87-100
3.3.1:	Comparative metabolomics of VIE-treated apple culture	87-94
3.3.1.1:	Organic acids	90
3.3.1.2:	Amino acids	90
3.3.1.3:	Sugars	90
3.3.1.4:	Sugar alcohols	91
3.3.1.5:	Vitamin	91
3.3.1.6:	Phenolics and biphenyl-dibenzofuran phytoalexins	93-94
3.3.2:	Principal component analysis (PCA) reveals significant alteration in metabolite pattern after VIE-treatment	95-96
3.3.3:	Hierarchical clustering analysis of the metabolite profiles	96-97
3.3.4:	Changes in metabolic pathways and metabolic pathway network	98-99
3.3.5:	Expression analysis of phenylpropanoid biosynthetic genes in the VIE-treated apple cell cultures	100
3.4:	Molecular cloning and functional analyses of a cinnamate-CoA ligase (CNL) from cell suspension	101-116

	culture of apple cv. <i>Golden Delicious</i>	
	3.4.1: Accumulation of biphenyl phytoalexin	101-103
	3.4.2: cDNA Cloning of a cinnamate CoA-ligase from cell culture of <i>Malus domestica</i> cv. <i>Golden Delicious</i>	103-106
	3.4.3: Functional characterization of <i>MdCNL</i>	107-110
	3.4.4: Expression of <i>MdPAL</i> , <i>MdCNL</i> and <i>MdBIS3</i>	111-113
	3.4.5: Phylogenetic reconstruction of CNL and related amino acid sequences	113-115
	3.4.6: Subcellular localization of <i>MdCNL</i>	115-116
	3.4.7: Molecular modeling and molecular docking	116-123
Chapter 4	Discussion	124-136
	4.1 General Discussion	124
	4.1.1: Development of cell suspension culture of apple cv. <i>Golden Delicious</i>	125
	4.1.2: Development of a validated HPLC method for the simultaneous detection of biphenyl and dibenzofuran phytoalexins.	126-127
	4.1.3: GC-MS based metabolomics analyses of <i>Venturia inaequalis</i> elicitor (VIE)-treated cell culture of apple cv. <i>Golden Delicious</i> .	127-131
	4.1.4: Molecular cloning and functional analyses of cinnamate-CoA-ligase (<i>MdCNL</i>) from VIE-treated cell culture of cv. Golden Delicious.	131-136
Chapter 5	Summary, Conclusion and Future scopes	137-141
	5.1: Summary	137-139
	5.1.1: Development of cell suspension culture of	137

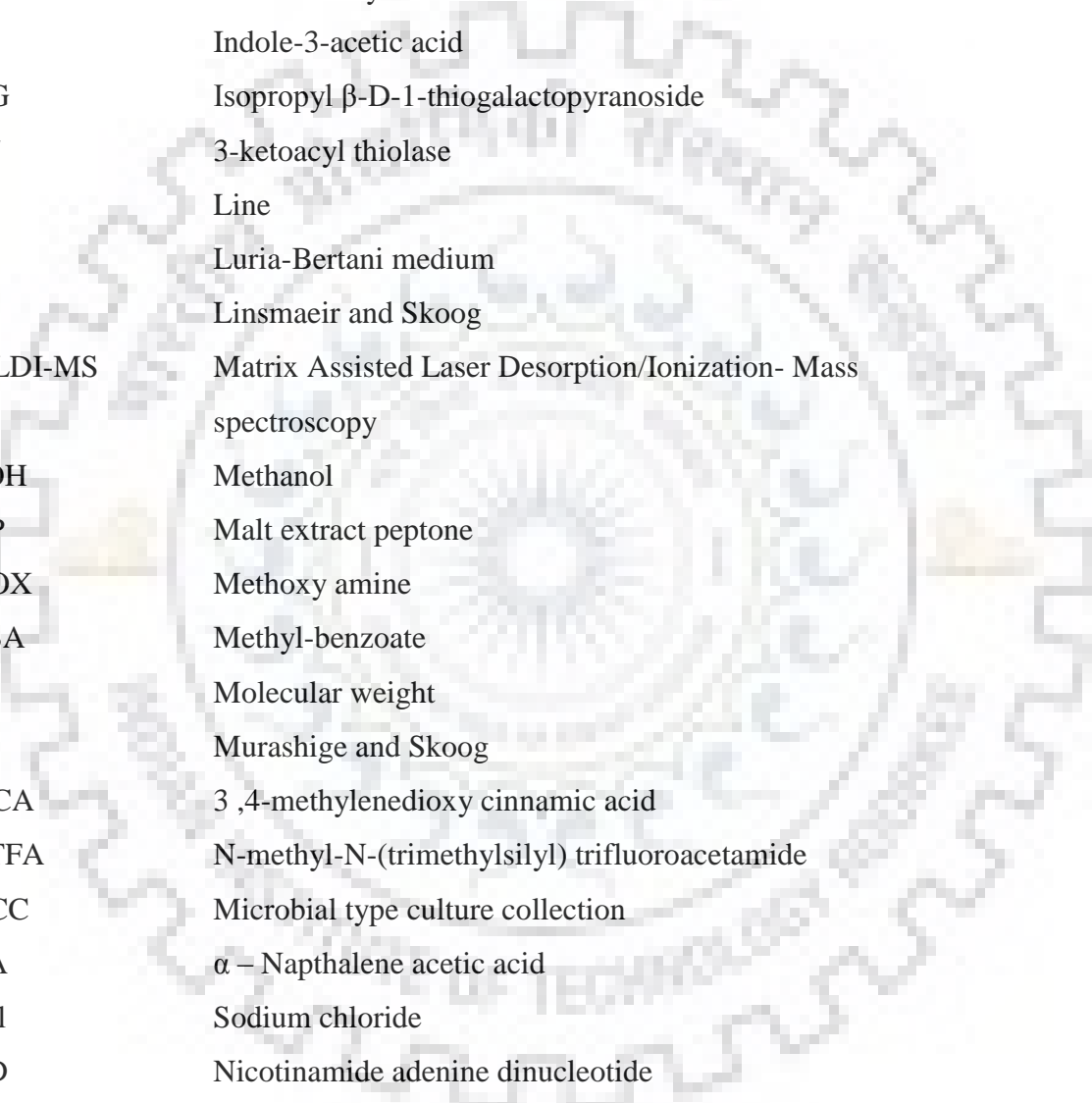
	apple cv. Golden Delicious	
	5.1.2: Development of a validated HPLC method for the simultaneous detection of biphenyl and dibenzofuran phytoalexins	137-138
	5.1.3: GC-MS based metabolomics analyses of <i>Venturia inaequalis</i> elicitor (VIE)-treated cell culture of apple cv. Golden Delicious	138
	5.1.4: Molecular cloning and functional analyses of cinnamate-CoA-ligase (<i>MdCNL</i>) from VIE-treated cell culture of cv. Golden Delicious	139
	5.2: Conclusion	140
	5.3: Future scopes	141
Chapter 6	References	142-163
Chapter 7	Publications	164

LIST OF ABBREVIATIONS



ATP	Adenosine triphosphate
AOX	Alternate oxidase
BA	Benzoate or benzoic acid
BD	Benzaldehyde dehydrogenase
BS	Benzaldehyde synthase
BIS	Biphenyl synthase
BZL	Benzoate-CoA-ligase
cDNA	Complimentary deoxy ribose nucleic acid
CoA	Coenzyme A
C4H	Cinnamate -4-hydroxylase
4CL	4-Coumarate CoA-ligase
CNL	Cinnamate CoA-ligase
CHD	Cinnamic acid CoA- hydratase / dehydrogenase
CHY	3-hydroxyisobutyryl CoA- hydrolase
DEPC	Diethyl pyrocarbonate
DMSO	Dimethyl sulfoxide
2,4-D	2,4-Dichlorophenoxyacetic acid
DTT	Dithiothreitol
dNTPs	Deoxyribose nucleotide tri phosphates
ESI-MS	Electro-spray-ionization mass spectrometry
E	Elicited
EDTA	Ethylene di amine tetra acetic acid
FAD	Flavin adenine dinucleotide
FMN	Flavin mononucleotide
F3H	Flavanone-3-hydroxylase
GC-MS	Gas chromatography- mass spectrometry
GD	Golden Delicious
HBD	4-Hydroxybenzaldehyde dehydrogenase
HBS	4-Hydroxybenzaldehyde synthase

LIST OF ABBREVIATIONS



HPLC	High-performance liquid chromatography
HBA	Hydroxybenzoate or hydroxybenzoic acid
HCHL	Hydroxycinnamoyl-CoA hydratase/lyase
4-HBA	4-Hydroxybenzoic acid
IFS	Isoflavone synthase
IAA	Indole-3-acetic acid
IPTG	Isopropyl β -D-1-thiogalactopyranoside
<i>KAT</i>	3-ketoacyl thiolase
L	Line
LB	Luria-Bertani medium
LS	Linsmaeir and Skoog
MALDI-MS	Matrix Assisted Laser Desorption/Ionization- Mass spectroscopy
MeOH	Methanol
MEP	Malt extract peptone
MEOX	Methoxy amine
MeBA	Methyl-benzoate
MW	Molecular weight
MS	Murashige and Skoog
MDCA	3,4-methylenedioxy cinnamic acid
MSTFA	N-methyl-N-(trimethylsilyl) trifluoroacetamide
MTCC	Microbial type culture collection
NAA	α – Naphthalene acetic acid
NaCl	Sodium chloride
NAD	Nicotinamide adenine dinucleotide
NADP	Nicotinamide adenine dinucleotide phosphate
NE	Non-elicited
NaOH	Sodium hydroxide
ORF	Open reading frame
PAL	Phenylalanine ammonia-lyase
PCR	Polymerase chain reaction
RT	Retention time

SAS	Salicylic aldehyde synthase
SDS	Sodium dodecyl sulfate
TEMED	Tetra methyl ethylene diamine
TIC	Total ion current
TMS	Tri-methyl-silylation
VIE	<i>Venturia inaequalis</i>
YE	Yeast-extract
YMB	Yeast manitol broth
YMA	Yeast manitol agar



LIST OF FIGURES

Figure No.		Page No.
1.1:	Origin and evolutionary history of the cultivated apple	4
1.2:	Average geographical distribution of apple production (from 2015-2016)	7
1.3:	Top ten apple producing countries of the world (from year 2015-2016)	8
1.4:	World production of apple and area harvested (from year 1997-2016)	8
1.5:	Apple scab symptoms	9
1.6:	<i>Venturia inaequalis</i> spores	10
1.7:	Life cycle of <i>Venturia inaequalis</i> causing scab disease in apples.	11
1.8:	Methodologies to prevent apple disease	15
1.9:	Major preformed defense metabolites detected from apples and other members of Malinae	17
1.10:	Comparison between transgenesis and cisgenesis	22
1.11:	Possible routes of benzoic acid biosynthesis in plants	30
1.12:	CNL catalyzed formation of Cinnamoyl CoA and subsequent benzoyl CoA	34
2.1:	<i>V. inaequalis</i> mycelium growing on agar plate	50
2.2:	Apple plants growing in green house	51
2.3:	Chemical synthesis of aucuparin and noraucuparin	54
2.4:	Growth curve of <i>M. domestica</i> cv. Golden Delicious cell suspension culture based on fresh weight	61
3.1:	Friable callus induced from the leaves of apple	80
3.2:	Cell suspension culture of apple cv. Golden Delicious	81
3.3:	TIC and mass-spectrum (GC-MS) of chemically synthesized (A) aucuparin and (B) nor-aucuparin	82
3.4:	HPLC chromatogram showing separation of standard noraucuparin, aucuparin and eriobofuran. Detection wavelength 254 nm	83
3.5:	HPLC chromatogram of the elicited cell culture of <i>S. aucuparia</i>	86
3.6:	ESI-MS/MS spectrum of HPLC eluted noraucuparin	86

3.7:	A representative GC-MS chromatograms (TIC) of detected metabolites from the VIE-treated (24h post elicitation) cell cultures of apple	88
3.8:	Metabolites grouped under specific class	88
3.9:	Differentially accumulating metabolites in the VIE-treated cell culture of apple cv. Golden Delicious	92-93
3.10:	Differential accumulation of phenolics and biphenyl phytoalexins in the VIE-treated cell cultures of apple cv. Golden Delicious	94
3.11:	PCA analyses of detected metabolites from VIE-treated cell cultures of apple	95-96
3.12:	Hierarchical clustering analyses of 43 detected metabolites from VIE-treated cell culture of apple cv. Golden Delicious	97
3.13:	The metabolic pathways network analyses of VIE-treated apple cell culture.	99
3.14:	Changes in the <i>MDPAL</i> , <i>MdF3H</i> <i>MdAOX</i> , <i>MdBIS3</i> expression levels in <i>V. inaequalis</i> elicitor-treated cell cultures of apple cv. Golden Delicious	100
3.15:	HPLC analysis showing accumulation of biphenyl	102
3.16:	Time course accumulation of biphenyl phytoalexins	102
3.17:	Time course accumulation of noraucuparin and aucuparin in the <i>Venturia inaequalis</i> infected greenhouse-grown shoots	103
3.18:	Construction of the expression vector for MdCNL cDNA	104
3.19:	Molecular weight determination of <i>MdCNL</i> by using MALDI-TOF	105
3.20:	Amino acid sequence alignment of <i>M. domestica</i> CNL (<i>MdCNL</i>)	106
3.21:	Temperature (A) and pH (B) optimum of <i>MdCNL</i> .	108
3.22:	Effect of selected monovalent and divalent cation supplementation on CNL activity	108
3.23:	Substrate specificity of recombinant <i>MdCNL</i>	109
3.24:	LC-ESI-MS/MS analysis of CNL-catalyzed cinnamoyl-CoA formation, represented in the mass spectrum by the molecular ion [M-H] ⁻ at m/z 896.2	110
3.25:	Changes in the gene expression levels.	112
3.26:	Progression of scab symptoms in <i>V. inaequalis</i> -infected leaves of apple	113
3.27:	Phylogenetic tree demonstrating the evolutionary relationships between <i>Malus domestica</i> cv.	114-115
3.28:	Localization studies of Golden Delicious CNL in leaf epidermis cells of <i>N. benthamiana</i> .	116
3.29:	Ramachandran plot of MdCNL generated by PROCHECK.	117

3.30:	Cartoon representation of modeled structure of <i>MdCNL</i> protein with α helices (cyan color) and β sheets (red color).	118
3.31:	Cartoon representation of superposition of cinnamate CoA ligase from <i>M. domestica</i> model (green color) and crystal structure of tt0168 from <i>Thermus thermophiles</i> HK8 (PDB ID: 1ULT) (cyan color).	118
3.32:	Topology diagram of secondary structures of cinnamate-CoA ligase from <i>MdCNL</i> model represented in figure 3.31.	119
3.33:	The cartoon representation of <i>MdCNL</i> from showing binding with: (A) cinnamic acid (cyan color); (B) 4-coumaric acid (magenta color); (C) caffeic acid (pink color); (D) ferulic acid (yellow color) and E) sinapic acid (violet color). Interacting residues of <i>MdCNL</i> are shown in stick format while red dotted lines show the intermolecular hydrogen bond interactions.	120
3.34:	Pictographic representation of hydrophobic interaction involved in <i>MdCNL</i> with: (A) cinnamic acid, (B) 4-coumaric acid, (C) caffeic acid, (D) ferulic acid and (E) sinapic acid.	121
3.35:	Electrostatic potential surface view of <i>MdCNL</i> . Zoom window shows the binding pocket with cinnamic acid (cyan color), 4-coumaric acid (magenta color), caffeic acid (pink color), ferulic acid (yellow color) and sinapic acid (violet color).	123
4.1:	Proposed role of cinnamate-CoA ligase (CNL) in benzoyl-CoA biosynthesis.	135
4.2:	Figure showing incorporation of benzoyl-CoA into biphenyl phytoalexin backbone.	136

LIST OF TABLES

Table No.		Page No.
1.1:	Taxonomic classification of Rosaceae family based on tribes and fruit, flower and morphologies	1-2
1.2:	Taxonomy and classification of apple	5
1.3:	List of scab-resistant and susceptible apple cultivars	6
1.4:	Indian apple production and percentage share among six apple producing states	9
1.5:	Major bioactive metabolites detected from apple.	14
1.6:	Gene-for-gene (GfG) relationships nomenclature for <i>Venturia inaequalis</i> and <i>Malus</i> pathosystem. The races are defined by the avirulence (avr) genes that are absent, thus the complementary host is susceptible	18-19
1.7:	Physiological races of <i>V. inaequalis</i> .	20
1.8:	Pathogenicity and virulence governing factors of <i>V. inaequalis</i>	21
1.9:	Genes shown to impact scab resistance in apple	23
1.10:	Genetic transformation of apple for scab resistance	24
1.11a:	Structures of biphenyl-derivatives (1-10) recorded from Malinae.	26
1.11b:	Structures of dibenzofuran-derivatives (1-17) recorded from Malinae	26-27
2.1:	Chemicals used for various experimental purposes	36-38
2.2:	Equipment used	39
2.3:	Media composition for callus and suspension culture	40
2.4:	Culture medium for <i>Venturia inaequalis</i> growth	41
2.5:	Culture medium and reagents for <i>E.coli</i> growth	41

2.6:	Culture medium and reagents for <i>A. tumefaciens</i> growth	42
2.7:	Activation medium for <i>A. tumefaciens</i> growth for transient expression in <i>Nicotiana benthamiana</i> leaves	42
2.8:	Buffers for affinity purification of His ₆ -tag fusion protein	43
2.9:	Buffers for plasmid isolation (miniprep)	43
2.10:	Buffer for DNA gel electrophoresis	44
2.11:	Buffers and reagents for SDS-PAGE electrophoresis	45
2.12:	Washing solution for regeneration of PD ₁₀ column and Ni-NTA agarose regeneration	46
2.13:	Composition of Bradford reagent used for protein estimations	46
2.14:	Enzymes and kits used in molecular biology	47
2.15:	Host cells	47
2.16:	Cloning and expression vectors used	48
2.17:	Primers used	48-49
2.18:	Elicitors used	49-50
2.19a:	Composition of qPCR reaction	59
2.19b:	qPCR reaction program	60
2.20:	Homology of apple unigenes present in GDR with other plant secondary metabolite specific <i>cinnamate-CoA-ligase</i> (CNL) sequences	62
2.21:	Reverse transcription (RT) reaction mixture for cDNA synthesis	63
2.22:	PCR reaction program	64
2.23:	Components for restriction digestion reaction	66
2.24:	Components for de-phosphorylation reaction	66
2.25:	Components for ligation reaction	67
2.26:	Accession numbers of amino acid sequences used for phylogenetic	71-73

	reconstruction	
2.27:	qPCR reaction program	75
3.1:	The effect of various growth regulator supplementations on callus induction in apple cultivar "Golden Delicious" after 25 days of culture. Values are mean \pm standard deviation (n = 3)	79
3.2:	Regression parameters of calibration curve (n = 3)	84
3.3:	Performance characteristics	84
3.4:	Recovery, precision (intra- and inter-day) and accuracy (%) data for the simultaneous determination of noraucuparin, aucuparin and eriobofuran	85
3.5:	List of 43 identified metabolites from VIE-treated cell cultures of apple cv. Golden Delicious	89-90
3.6:	Kinetic properties of <i>MdCNL</i>	110
3.7:	Docking results of <i>MdCNL</i> with cinnamic acid (CID444539), 4-coumaric (CID637542), caffeic (CID689043), ferulic (CID445858) and sinapic acids (CID637775) along with their binding energy and interacting residues.	122


Chapter 1


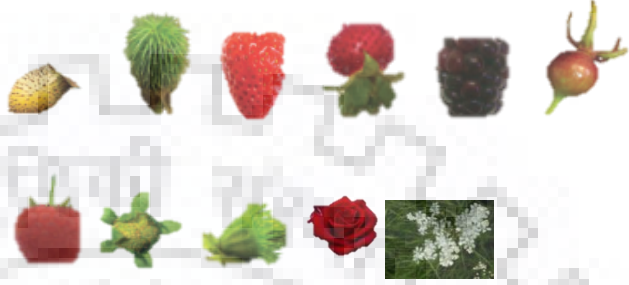

Introduction and Literature Review

1.1. The Rosaceae Family:

The flowering plants (Angiosperms) have 416 families, out of which 25 families constitute the most economically important plant families (Bennett, 2010). The Rosaceae is economically one of the most important plant families within the order Rosales, which is well known for producing pome bearing fruits. This family comprise of approximately 100 genera and 3000 species (Phipps, 2014), distributed worldwide. Rosaceae have important commercial fruit species including apple, pear, peach, strawberry, etc (Xiang et al., 2017). Apart from fruit species, Rosaceae also includes many ornamental flowers including roses, meadowsweets, hawthorns, crabapples and rowans. Previously Rosaceae was divided into four sub-families, Rosoideae, Maloideae, Amygdaloideae and Spiraeoideae, according to fruit and morphological characteristics. But as per recent molecular taxonomy (based on chloroplast gene sequence), Rosoideae sub-family is separted into Rosoideae (approx. 2000 species) and Dryadoideae (approx.30 species). Previouslyproposed Maloideae, Amygdaloideae and Spiraeoideae are now combined together into a single sub-family Amygdaloideae (approx. 1000 species) (Xiang et al., 2017). Taxonomy of Rosaceae family is given in Table 1.1.

Table 1.1: Taxonomic classification of Rosaceae family based ontribes and fruit, flower and morphologies (Xiang et al., 2017).

Rosaceae		
Subfamilies	Tribe	Fruit / flower morphologies
Amygdaloideae	Maleae	
	Kerrieae	
	Gillenieae	
	Exochordeae	
	Amygdaleae	
	Sorbarieae	

	Lyonothamneae Maleae Neillieae Spiraeaceae	
Rosoideae	Agrimoniaeae Roseae Potentilleae Colurieae Ulmarieae Rubeae	
Dryadoideae	Dryadeae	

The genome sequence of a number of Rosaceae members have been published, such as woodland strawberry (*Fragaria vesca*), domesticated apple (*Malus domestica* Brokh), pear (*Pyrus bretschneideri*), peach (*Prunus persica*), and Mei (*Prunus mume*, related to apricot) (Shulaev et al., 2011; Velasco et al., 2010; Wu et al., 2013; Verde et al., 2013; Zhang et al., 2012b). These genome sequences provide important resources for molecular analyses. The genome sequence of apple (*Malus × domestica* Borkh cv. Golden Delicious) is made publically available [Genome Data base of Rosaceae (GDR) www.rosaceae.org]. The complete genome sequence of Golden Delicious (Velasco et al., 2010) showed 603.9 Mb total contig size with reconstruction of total 17 chromosome / linkage groups. There are 57,386 putative genes out of which, 42.4% were transposable genetic element, 4021 are transcription factors, 178 miRNA, 992 resistant genes and 1246 biosynthetic genes. Availability of apple genome sequence will be beneficial for studying fruit and plant characteristics and developing new disease resistant cultivars. Furthermore, apple genome sequence provides the opportunity to perform functional genomics and marker / genome assisted breeding.

Rosaceae exhibited polyploidization and species radiation events in the family, which is the reason for it's high species diversity (Xiang, Y. et al., 2017). It is proposed that ancestor of Maleae (e.g. apples, pears) is hybrid of the ancestors of the Spiraeoideae and the Amygdaleae. Because of this,

all members of Maleae have basic chromosome number of 17, with an exception of early branching genus *Vauquelinia* which have chromosome number 15, whereas Spiraeoideae and Amygdaleae have chromosome number of 9 and 8 respectively. Recently a hypothesis was proposed that Maleae originated from a whole-genome duplication event in a relative of the ancestor of *Gillenia* ($x=9$) (Evans et al., 2000; Evans and Campbell, 2002; Velasco et al., 2010; Verde et al., 2013).

1.2. The origin, distribution and taxonomy of apple:

The domestication of apples were due to initial introduction of apple in Europe and thereafter hybridization occurred between cultivars and wild species (Harris et al., 2002; Pereira-Lorenzo et al., 2007). The nuclear DNA and chloroplast DNA analysis of apples indicate that domesticated apples are most closely related to wild *Malus* species. The presence of 18-bp duplication in the chloroplast DNA sequence supports the close relationship between wild and cultivated *Malus* species (Harris et al., 2002).

The wild apples in Almaty (Kazakhstan) were the major progenitors of the domesticated apples. The forest of Tian Shan was identified as the area where the apple was domesticated for the first time (Dzhangaliev, 2003; Cornille et al., 2012). Apples are self-incompatible and progeny obtained from their seeds show high degree of variability with mother plant. Asian wild apple species have wide range of colors, sizes, flowers and forms, while its allozyme diversity is significantly higher than North American wild apples (Janick, 2005). In Late Neolithic or early Bronze age period, farmers frequently collected the fruits of wild relatives of domesticated apple in the middle-east and Europe, seeds carried in saddle bags or horse dropping along the trade routes by caravans or carried by birds through which apples reach the Western Europe from Central Asia (Figure 1.1). Microsatellite markers study of five *Malus* species from Europe indicates that multiple wild species have contributed in domestication of apples. *M. sylvestris*, the wild European crabapple was the major secondary contributor (Cornille et al., 2012).

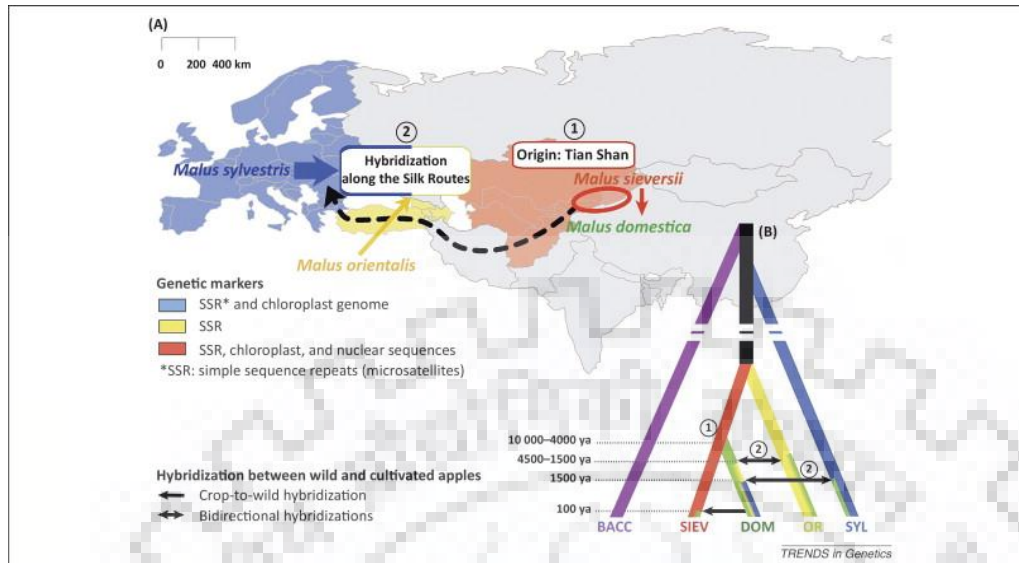


Figure 1.1: Origin and evolutionary history of the cultivated apple (A) Based on molecular markers studies. 1: Origin of domesticated apple from the *Malus sieversii* in the mountains of Tian Shan; 2: migration of domesticated apple to Europe from Asia; (B) Genealogical relationships between the domesticated and the wild apples. Abbreviations: SIEV, *M. sieversii*; BACC, *Malus baccata*; DOM, *M. domestica*; SYL, *Malus sylvestris*; OR, *Malus orientalis*; (Source: Cornille et al., 2014).

The main problem with *Malus* taxonomy is the similarity between cultivated and wild species and hence identification of different categories becomes difficult. Furthermore the scientific names used for domesticated apple are legion, such as *Malus pumila* Miller and *Malus domestica* Borkh. Recent study indicates that *M. pumila* (*M. sieversii*) is the correct name, and represents major progenitor of domesticated apple (Cornille et al., 2012). Taxonomy of domesticated apple is given in Table 1.2

Table 1.2: Taxonomy and classification of apple.

Kingdom	Plantae
Phylum	Magnoliophyta
Class	Magnoliopsida
Order	Rosales
Family	Rosaceae
Subfamily	Amygdaloideae
Tribe	Maleae
Subtribe	Malinae
Genus	<i>Malus</i>
Species	<i>Domestica</i>

There are more than 7500 known cultivars of apple that are grown worldwide with range of desired characteristics (Matsumoto, 2014). Different cultivars are bred to obtain better taste and quality of apple. Wild apples grow directly from seeds while domestic apple are generally propagated by clonal propagation. The most common varieties of apple grown worldwide are Red Delicious, Liberty, Empire, Golden Delicious, Gala, Fuji, McIntosh and Granny smith. In India, based on ripening season, apple cultivars are divided into three categories, in early season (from early march to June) Michal, Shlomit, Vista Bella, Anna, Mayan; in mid season (from mid July to mid September) Royal Delicious, Red Delicious, Gala, Red Chief, Starkrimson and Granny Smith, while in case of late season (from early September to late December) Firdaus, Lal Ambary, Sunahari, Shireen, Golden Delicious, Red Gold Ambri and Fuji cultivars are cultivated. Many of these late-ripening apples tend to have prolonged storage life. Till date more than 100 apple cultivars are released which have different resistance towards scab disease (Belete et al., 2017) (Table: 1.3).

Table 1.3: List of scab-resistant and susceptible apple cultivars.

Scab-resistant cultivars	Scab-susceptible cultivars
Pristine	Jonathan
William's Pride	Red Delicious
Redfree	Jonamac
Prima	Imperial Gala
Goldrush	McIntosh
Priscilla	Honeycrisp
Crimson Crisp	Cortland
Jonafree	Campbell Redchief
Florina	Golden Delicious
Scarlet	Empire
Prima	Fuji
Liberty	Northern Spy
Freedom	Granny Smith
Firdaus	Crispin
Enterprise	Braeburn

1.3. Apple production:

Apples are deciduous fruits which grow mostly in temperate regions around the world and constitutes one of the most consumed fruits in Europe. The main apple producing regions are Europe, South America, North America, South Africa, Oceania (Australia and nearby islands) and Asia. Asia is the largest producer of apple among different continents (Figure 1.2).

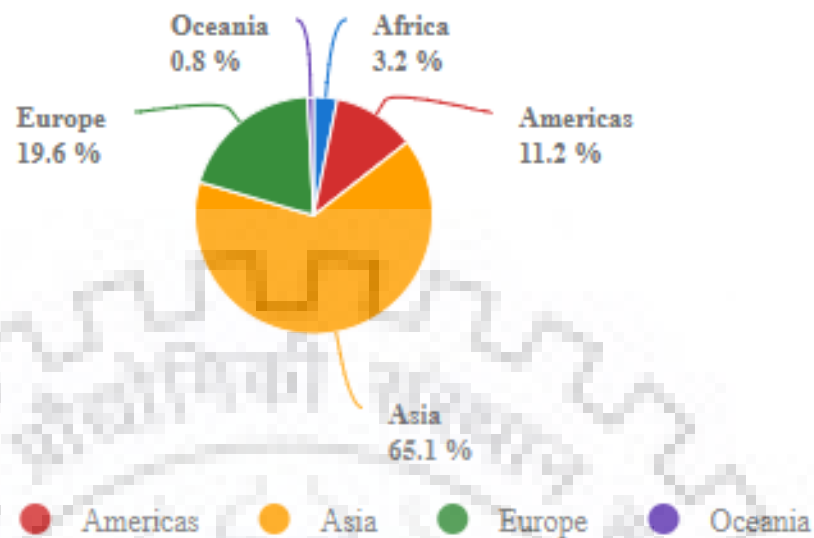


Figure 1.2: Average geographical distribution of apple production in the world (from the year 2015-2016) (source: FAOSTAT 2016).

Total worldwide production of apple is 8.93 million tons (FAOSTAT 2016) out of which approximately 65.1 % of total world productions are obtained from Asia (Figure 1.2), China being the highest producer of apple (Figure 1.3). China and India are the largest producers of apple in Asia, India being 6th in rank in terms of global apple production (Figure 1.3). From 1997 to 2016 production of apple increased continuously, whereas area harvested decreased then increased, making increase in overall yield from 1997 to 2016 (Figure 1.4)

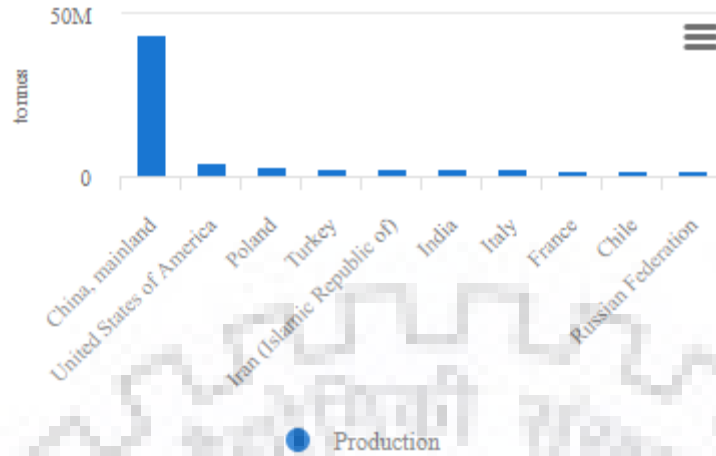


Figure 1.3: Top ten apple producing countries of the world (from the year 2015-16) (source: FAOSTAT 2016).

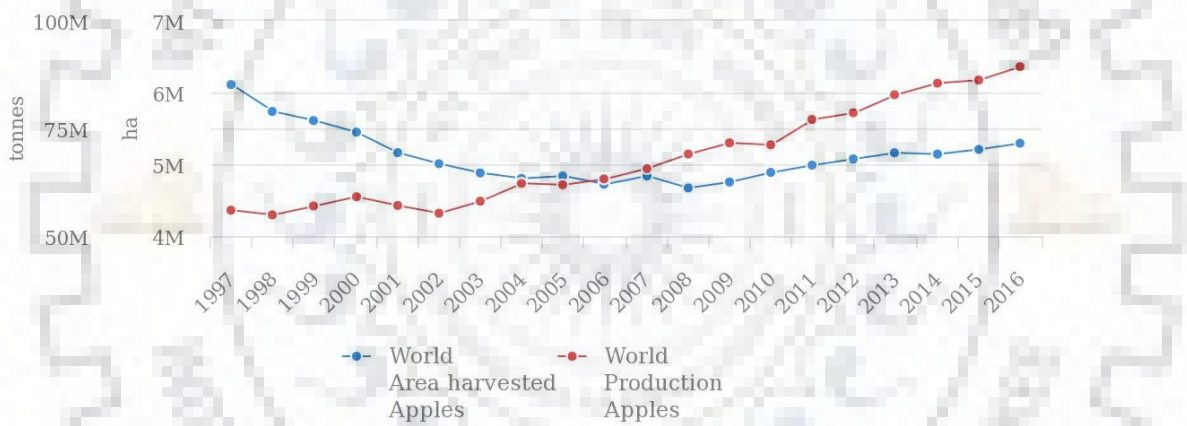


Figure 1.4: World production of apple and area harvested (from the year 1997-2016) (source: FAOSTAT 2016).

The total annual apple production in India is approximately 0.21 million tones with a total land area under cultivation of 313040 ha. According to National Horticulture Board data (2014-15), among Indian states, Jammu and Kashmir is the largest producer of apples sharing 64.14% of total Indian production followed by Himachal Pradesh and Uttrakhand (Table 1.4)

Table 1.4: Indian apple production and percentage share among six apple producing states
(source: APEDA Agri Exchange data 2014).

Position	State	Production in kilo tones	Percentage Share
1	Jammu & Kashmir	1,368.63	64.14
2	Himachal Pradesh	625.20	29.30
3	Uttarakhand	106.10	4.97
4	Arunachal Pradesh	32.00	1.50
5	Nagaland	1.89	0.09
6	Tamil Nadu	0.02	<0.09

1.4. Apple scab disease:

Scab disease is caused by *Venturia inaequalis* fungus, which belongs to the Ascomycota. Apple scab is one of the most damaging diseases in economic terms, as the climate is in favour of scab where apples are grown (MacHardy, 1996). An array of fungicide applications are required to control this disease (Bus et al., 2011). Symptoms of scab include circular velvety olive green, chlorotic or necrotic lesions; spots on pedicels and sepals; and dark colored brown corky lesions or small black spots on fruits (Figure 1.5). Scab leads to distortion in fruits, and premature fruit and leaf fall (Jha et al., 2009).

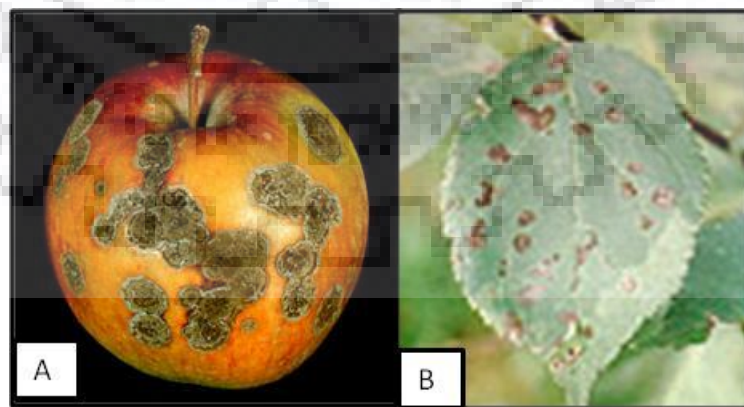


Figure 1.5: Apple scab symptoms. A. fruit; B. leaf (Source: Vaillancourt and Hartman, 2000).

1.4.1. *Venturia inaequalis*:

Venturia inaequalis is a heterothallic fungus including seven chromosomes. Fungal species of *Venturia* infects their particular fruit hosts, e.g. *Venturia carpophila* (peach), *Venturia pirina* (pear) and *Venturia cerasi* (cherry). The host range of *V. inaequalis* includes a number of genera such as, *Malus*, *Pyrus*, *Sorbus*, *Crataegus* etc (Bus et al., 2011). *V. inaequalis* produces two types of spores, the sexual (ascospore) and the asexual (conidia) spores, both capable of infecting apples (Figure 1.6). Recently, transcriptome data of *V. inaequalis* was published to understand *Venturia*-apple interaction (Thakur et al., 2013).

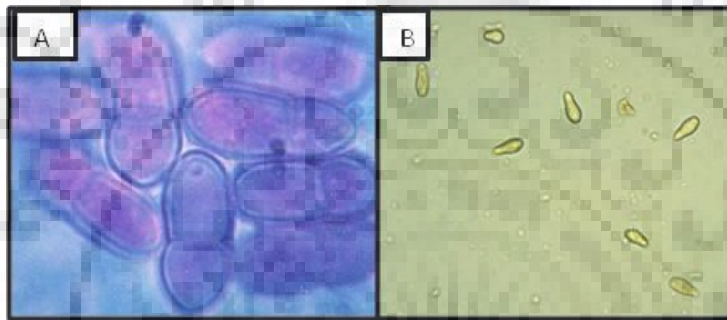


Figure 1.6: *Venturia inaequalis* spores. A. Ascospore (two unequal sized cells with characteristic "footprint" shape (Source: MacHardy, 1996); B. Conidia (0-1 septate, pale brown in color having obpyriform to obclavate shape (Source: Vaillancourt and Hartman, 2000).

1.4.2. Life cycle of *Venturia inaequalis*: Primary source of inoculum is the germination of sexual (ascospore) spores, which causes the initiation of the disease, whereas conidia serve as the secondary source of infections. Development of fungus begins within the pre-infected leaves fallen on earth during the winter season, sexual fruiting bodies are formed in stroma of leaves called as pseudothecium which contains asci. Ascospores are present in tetrad (four pairs) in each ascus which results into meiotic division followed by mitotic division. These microscopic spores are released in the following spring season. The number of ascospore released is maximum in the flowering season because of wet environment. These ascospores formed are carried to young susceptible leaves and fruits by wind currents. Infection occurs after 10 to 25 hours of wet period on leaf and viable symptoms occur approximately 14 to 21 days after infection (Figure 1.7). The secondary infection starts on newly infected young leaves and fruits by second type of spores

called conidiospores (asexual spores). During spring, several secondary cycles of infection occurs resulting into a wide spreading of infection.

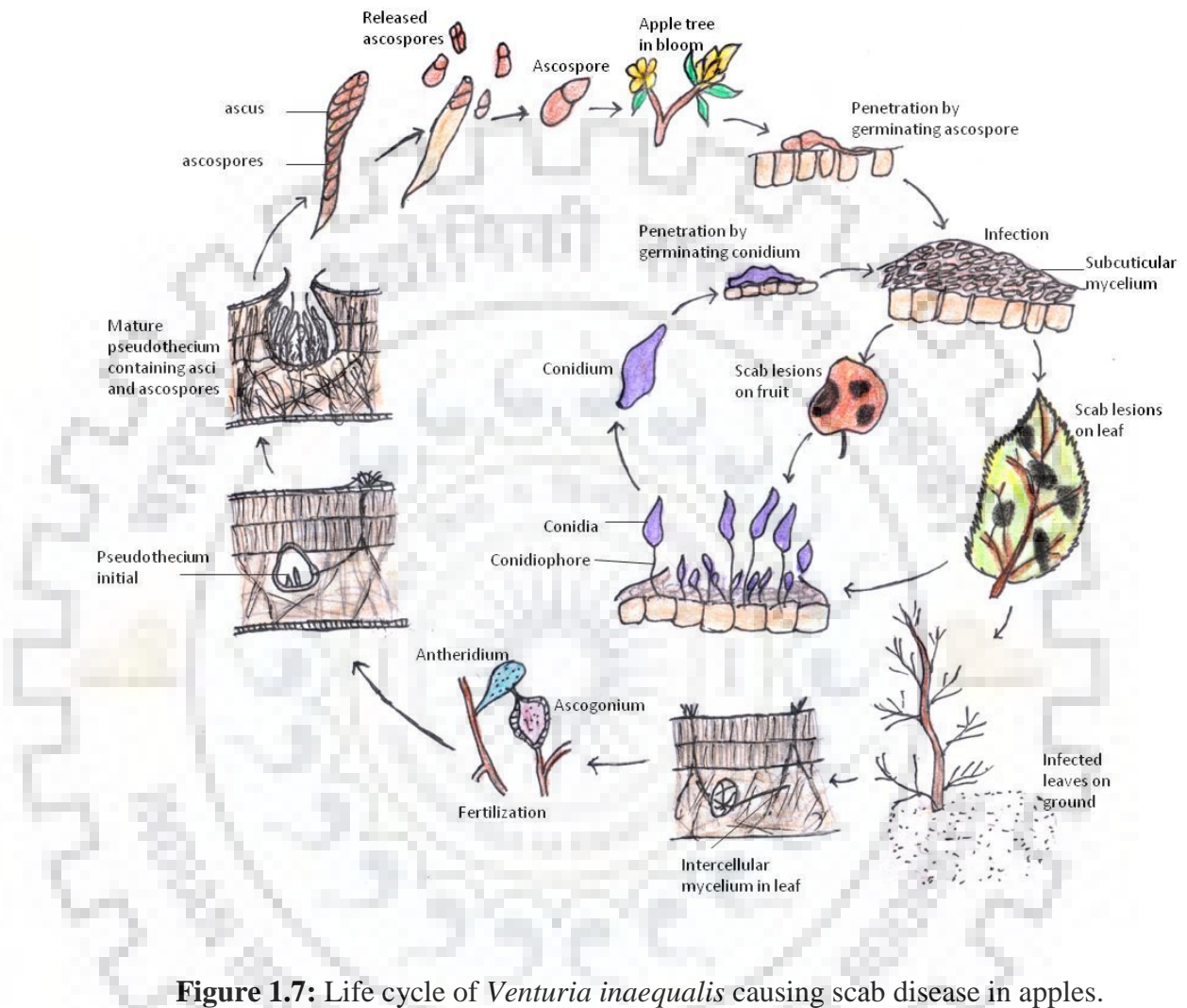


Figure 1.7: Life cycle of *Venturia inaequalis* causing scab disease in apples.

1.5. Metabolomics of apple: A new tool to understand plant's disease resistance mechanism:

The accomplishment of plant metabolomics predominantly depends on methodologies and instrumentations to comprehensively recognize measure and localize each and every metabolite, which helps in analysis and monitoring of plant metabolome. Nowa day's number of integrated techniques and methodologies are accessible for analyses of highly complex samples and broad range of biological targets with the integration of metabolomics with functional genomics and other omics technologies to analyze biochemical and genetic mechanism of cellular function and metabolic regulation. The plant metabolome consists of the entire set of metabolites synthesized

by the primary and secondary metabolic pathways which give rise to the biochemical phenotype to that particular plant tissue.

Gas chromatography-mass spectrometry (GC-MS) is an emerging technology, routinely used in plant metabolomics (Shuman et al., 2011), especially for facilitating the identification and quantification of the primary metabolites such as amino acids, sugars, organic acids (Schauer and Fernie, 2006) and an wide array of secondary metabolites such as phenolics, flavonoids and biphenyls (Chizzali et al., 2012). GC-MS has been used to identify and measure metabolites in many plant samples (Bisht et al., 2013; Kumar and Nagar, 2014). Most metabolomics studies on apples published so far were targeted analyses focusing on specific metabolites and limited to only fruit quality analyses (Aprea et al., 2011; Vanzo et al., 2013). Recently, (Sciubba et al., 2015) identified new scab-preventive metabolites from resistant apple cultivar by NMR-based metabolomics. However, untargeted metabolomics analysis provides a more comprehensive view on the differential accumulation of metabolites upon pathogen infection (Eisenmann et al., 2016). Till date, there is no report available on metabolic re-programming of apple plants upon scab-infection. Very recently, targeted HPLC-based metabolite profiling of the cell suspension cultures of *M. domestica* cv. Florina showed massive metabolic reprogramming in response to yeast-extract (YE) elicitor-treatment (Sarkate et al., 2017). The authenticity and purity of apple juices has been accessed currently using LC-MS based metabolomics platform (Vaclavic et al., 2012). Attempts have been made to differentiate and correlate the volatiles released after fungal infection from apple fruits (Rowan et al., 2009; Schmarr et al., 2010). The spatial gradients of metabolites accumulated in apple have also been analyzed using metabolomic imaging technique (Zhang et al., 2007). Metabolic flux map study can be used for studying different metabolism reactions (Masakapalli et al., 2013, 2014). So far, any single metabolome analytical technique (GC-MS, LC-MS, NMR) alone cannot detect complete metabolomics profile, due to their intrinsic limitations in either detection or quantification (Lakhera et al., 2017).

The prime approach in the study of plant metabolomics is to construct the metabolite library which promotes metabolite identification and biological elucidation of results and bioinformatics tools for visualization and analysis of its metabolome. In general, upon pathogen infection, the plant starts synthesizing an array of defense-responsive metabolites, both primary and secondary. Alteration in the metabolic profiles of a plant in response to pathogen infection can be studied with metabolomics approach. This technology provides the opportunity to evaluate pathogen-induced local and systemic alterations in plant metabolite patterns without any prior assumptions.

Measuring the level of metabolites prior and after pathogen infection may give an exact picture of the physiological status of the plant tissue. This approach helps to decipher the plant metabolic regulation under biotic stress (Kumar et al., 2014) and also provides identification of potential metabolite biomarker for applications in crop breeding and crop protection. Metabolomics also provide clues to clone target genes for developing transgenic plants with higher resistance (Harish et al., 2013). Mostly, phenylpropanoid biosynthetic genes such as *phenylalanine ammonia-lyase* (PAL), *cinnamate-4-hydroxylase* (C4H), *4-coumarate-CoA-ligase* (4CL) are up-regulated upon pathogen infection (Mandal, 2010; Mandal et al., 2011; Mukherjee et al., 2016). Till date, there is no report available on comprehensive metabolic re-programming of apple plants upon scab-infection, which opens an area of considerable research interest.

1.5.1. Apple phytochemicals: Apple fruits have high nutritional values and enormous health promoting properties (Sarkate et al., 2017). Apples are rich source of soluble as well as insoluble fibers, minerals and vitamins (Gerhauser, 2008). Apple has free radical scavenging activity due to the phytochemical content rather than that of vitamin C (Eberhardt et al., 2000). The antiradical activity is analogous with the presence of major amount of polyphenols, phenolic acids and flavonoids in apple peel as compared to its flesh (Leontowicz et al., 2002). Consumption of apples are related with lower mortality rate due to the presence of dietary flavonoids and phenolics (Vinson et al. 2001; Boyer and Liu, 2004). Apple fruits have good anti-proliferative, antioxidant, gastrointestinal protection from drug injury and cholesterol lowering properties (Eberhardt et al., 2000; Leontowicz et al., 2002; Wolfe et al., 2003; Dianne, 2011). Quercetin-derivatives, catechin, epicatechin, procyanidin, cyanidin-3-galactoside, chlorogenic acid, gallic acid and p-coumaric acid are the major health-protective antioxidant metabolites present in apples, with minor amount of phloridzin (Lee et al., 2003). The major categories of polyphenols detected in apples are proanthocyanidins, catechins, epicatechin, flavonols, hydroxycinnamates, dihydrochalcones and anthocyanins (Lee et al., 2003; Tsao et al., 2003; Wolfe et al., 2003; Chizzali et al., 2012). In addition to phenolics, apples are also rich source of many bioactive triterpenes (He and Liu, 2007). Daily consumption of apple can help in reducing risk of heart disease and cancer (Gerhauser, 2008). Many biological activities are exhibited by apples and apple-derived products such as anticancer potential, anti-diabetic properties and cholesterol-lowering properties (Dianne, 2011; Sarkate et al., 2017). Major bioactive metabolites detected from apples are listed in Table 1.5.

Table 1.5: Major bioactive metabolites detected from apple.

Metabolite class	Types of metabolite	Reference
Terpenes	Mono-terpenes [(ϵ)- β -Ocimene, Linalool] Sesquiterpenes α -Farnesene, (ϵ , ϵ)- α -Farnesene, β -Caryophyllene, Germacrene δ , α -Curcumene].	(Rupasinghe et al., 1998; Nieuwenhuizen et al., 2013).
Phenolics: free form	Caffeic acid, gallic acid, chlorogenic acid, benzoic acid and syringic acid.	(Francini and Sebastiani, 2013; Boyer and Liu, 2004).
Phenolics: ester-linked	Hydroxybenzoic acid, 4-p-coumaroylquinic acid, 4-caffeoylquinic acid, p-coumaric acid, vanillic acid, vanillin, <i>cis</i> -ferulic acid, <i>trans</i> -ferulic acid.	(Rana and Bhushan, 2016; Francini and Sebastiani, 2013)
Flavanoids	Flavan-3-ols [(catechin, epicatechin,) and procyanidins (procyanidins B1, B2 and C1)].	(Rana and Bhushan, 2016; Tsao et al., 2003).
	Quercetin and its glycosides [quercetin 3-galactoside, quercetin 3-rutinoside (Rutin), quercetin 3-glucoside, quercetin 3-arabinoside, quercetin 3-xyloside and quercetin 3-rhamnoside].	(Tsao et al., 2003; Lee et al., 2003)
	Dihydrochalcones and their glycosides (phloretin, Phloridzin and hydroxyphloretin, phloretin- <i>O</i> -glycosides, phloretin-2'- <i>O</i> -glucoside and phloretin-2'- <i>O</i> -(2''- <i>O</i> -xylosyl) glucoside).	(Francini and Sebastiani, 2013; Lee et al., 2003).
Carotenoids	Carotenes (α -, β -, γ -, ζ - carotenes and β -zeacarotene), Xanthophylls (neoxanthin, violaxanthin, Lutein, antheraxanthin, Chrysanthemaxanthin, Flavaxanthin)	(Delgado-Pelayo et al., 2014; Valadon and Rosemary, 1967)
Vitamins	Vitamin A, Vitamin B1 (thiamine), Vitamin B2 (riboflavin), Niacin, Folic acid, Vitamin B6, Pantothenic acid, Vitamin C (Ascorbic acid), Vitamin E and Vitamin K.	(Lee and Mattick, 1989).

1.6. Defense mechanisms of apple:

In orchards, apple trees are generally multiplied by clonal propagation of single elite cultivar, which brings genetic uniformity within the population, thereby adversely affect plant's disease resistance potential (Gessler and Patocchi, 2007). Interestingly, most of the top selling commercial apple cultivars are highly susceptible to apple scab disease, however, few wild apple cultivars are resistant towards scab-infection. There are many defence mechanisms against apple scab, with either one having their advantages and disadvantages (Figure 1.8). Some of these methods includes external application like chemical control, cultural control and biological control, whereas in other methods plant have defence mechanisms internally such as scab resistance genes in scab resistant varieties, structural defence and biochemical defence mechanisms.

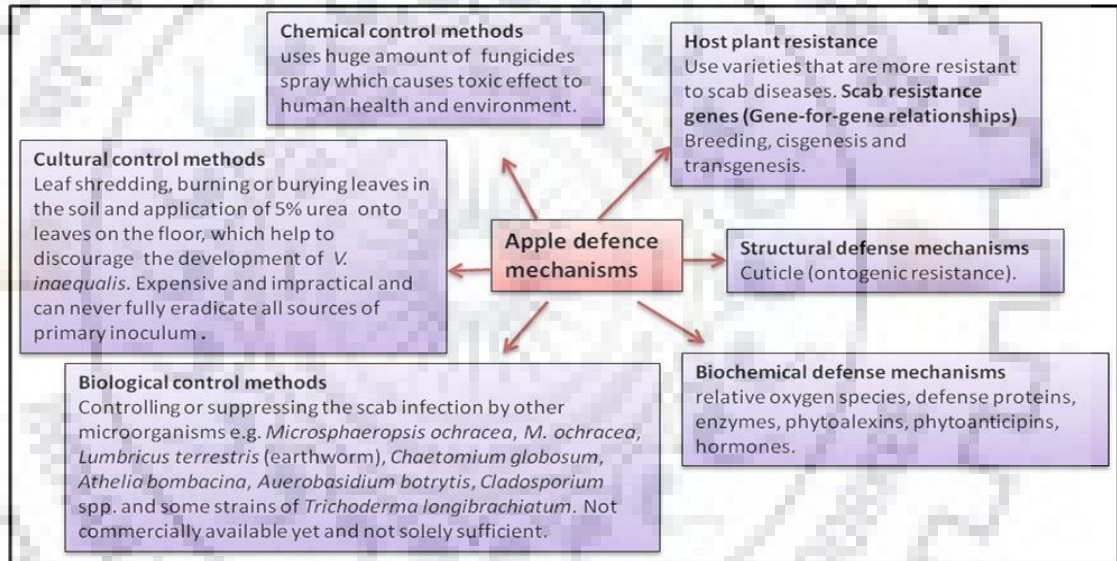


Figure 1.8: Methodologies to prevent apple disease (Source: Belete and Boyraz, 2017; Bus et al., 2011).

1.6.1. Structural defense mechanisms:

The amount of free water on the leaf surface and the composition and the thickness of the cuticle determines the infection and penetration capacity of *Venturia inaequalis* (ontogenic resistance) (Belete and Boyraz, 2017).

1.6.2. Biochemical defense mechanisms:

1.6.2.1. Phytoanticipins: Ontogenic resistance is exhibited by preformed antimicrobial compounds known as phytoanticipins. Phenolic acids and flavon-3-ols, such as quinic acid and its derivatives, epicatechin and catechin play major role as preformed defense metabolites in apple (Mikulic Petkovsek et al., 2008; Schwalb and Feucht, 1999). Phenolic acids like caffeic-, chlorogenic-, benzoic- and salicylic acids were found to help plant under variable stress condition including pathogen attack (Vasco et al., 2009). It has been found that quercetin-3-O-galactoside, chlorogenic acid present in *Malus* play a crucial role against fungal pathogen, moreover quinic acid also serves as an intermediate of phenylpropanoid pathway (Kanwal et al., 2010). Quercetin-3-O-galactoside found in leaves and fruits show nonspecific and very potent anti-fungal activity (Kanwal et al., 2010) and was shown to reduce the growth of several fungus up to 99 percent. Chlorogenic acid which is found in high concentration in fruits of Malinae reported to help plants in repelling brown rot infection (Villarino et al., 2011). Earlier it has been shown that differential accumulation of flavonols (catechins and proanthocyanidins) was key factors in providing scab resistance in apple cultivars (Treutter and Feucht, 1990). (Picinelli et al., 1995; Mayr et al., 1997) have shown a positive association between procyanidins content and scab resistance in apple. In contrary, (Sierotzki and Gessler, 1993) have shown that there was no positive correlation between scab-resistance and basal level of flavonols in terms of scab susceptibility of apples. In our study, high basal level of catechin (flavonol) content was also observed in the Florina cell culture. It was also reported that scab-resistant apple cultivars are particularly rich in the content of caffeic, chlorogenic and ferulic acids and their concentration rapidly increases after scab-infection as compared to susceptible cultivars (Mikulic Petkovšek et al., 2003). Furthermore, Liaudanskas et al. (2014) had shown that high phenolic content of scab-resistant apple is associated with higher nutritional quality and antioxidant properties. Scab resistant apple cultivars bears high amount of phloridzin, which is broken down into phloretin after pathogen infection (Lattanzio et al., 2001). A list of major pre-formed defense metabolites in Malinae is listed in Figure 1.9.

1.6.2.2. Pathogenesis-related (PR) proteins: PR-2 (β -1,3-glucanase), PR-3 (chitinase) and PR-8 (endochitinase type III) proteins are higher in resistant cultivar 'Remo' than in the susceptible cultivar 'Elstar' prior to infection by *Venturia inaequalis*. After infection concentration of these proteins in susceptible cultivar becomes similar to resistant. Therefore, suggesting constitutive accumulation of PR proteins only in the resistant cultivar. Other PR proteins are also

present which are functioning in plant scab defence, PR-1, PR-5, PR-10, PR-12 and PR-14 (Belete and Boyraz, 2017).

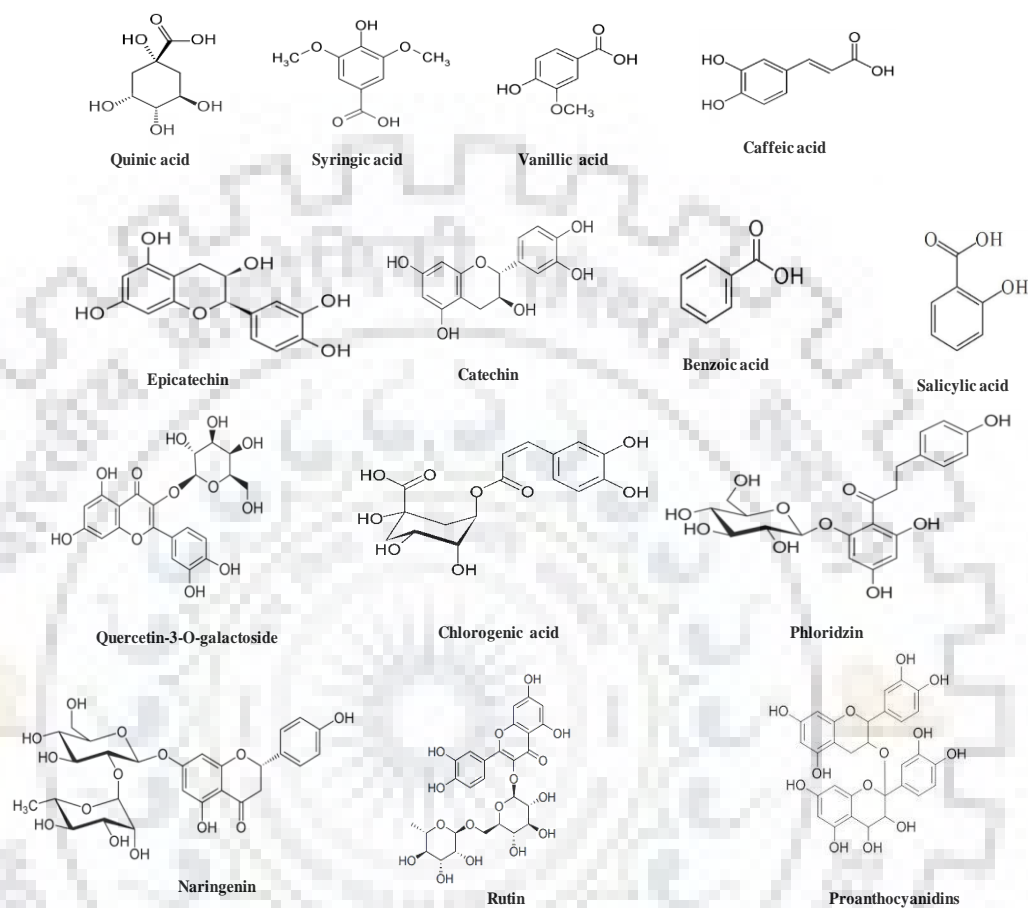


Figure 1.9: Major preformed defense metabolites detected from apples and other members of Malinae.

1.6.2.3. Phytoalexins: Phytoalexins are low molecular weight toxic substances produced and accumulated in plants with response to pathogen infection, physiochemical stresses and confer protection against infecting parasite. These are non-specific toxic chemicals formed only post infectionally, that inhibits growth and development of microbial inducers on hypersensitive tissues formed when host plant cells comes in contact with these parasites. Phytoalexins tend to fall into several classes including terpenoids, alkaloids and glycoesteroid derived mostly from simple phenylpropanoid pathway, shikimate pathway and mevalonate pathway (Hammerschmidt et

al., 1999). These compounds are much diverse in chemical structure and produced by any plant families fall into the same class.

1.6.3. *Venturia inaequalis*- *Malus* gene-for-gene (GfG) relationships:

The apple scab disease makes one of the first (*Venturia inaequalis*-*Malus*) pathosystem for GfG relationships given by Flor, 1971. Flor postulated ‘for each gene that gives resistance in the host, there is respective gene that gives pathogenicity in the parasite’ (Flor, 1971).

Ascospores give rise to haploid mycelium producing either virulence (avr) or avirulence (Avr) locus. It is commonly hypothesized that there is a specific recognition event between a product from host *R* gene and a product from respective pathogen *Avr* gene (Jones & Dangl, 2006). 17 GfG relationships are being defined till date. Relationship (0) to (17) having host (0) to (17) respectively. Host (0) is defined for host which does not contain any resistance gene, therefore these are susceptible to all the isolates of *Venturia inaequalis*. Distinct phenotypic reactions are shown by numerous major *R* gene loci in apple: Class 1: hypersensitive response (HR); Class 2: stellate necrosis (SN); and Class 3: chlorosis (Chl) with limited sporulation (Bowen et al., 2011; Shay & Hough, 1952) (Table 1.6).

Table 1.6: Gene-for-gene (GfG) relationships nomenclature for *Venturia inaequalis* and *Malus* pathosystem. The races are defined by the avirulence (*avr*) genes that are absent, thus the complementary host is susceptible (Source: Bus et al., 2011).

<i>Malus</i>					<i>Venturia inaequalis</i>			
Differential host		Phenotype	Resistance locus			Avirulence locus		Race
Number	Accession		Historical	LG ^a	New	New	Old	
h(0)	Royal Gala	Susceptibility			-	-		(0)
h(1)	Golden Delicious	Necrosis	<i>Vg</i>	12	<i>Rvi1</i>	<i>AvrRvi1</i>		(1)
h(2)	TSR34T15	Stellate necrosis	<i>Vb2</i>	02	<i>Rvi2</i>	<i>AvrRvi2</i>	<i>p-9</i>	(2)
h(3)	Geneva ^b	Stellate necrosis	<i>Vb3</i>	04	<i>Rvi3</i>	<i>AvrRvi3^d</i>	<i>p-10</i>	(3)
h(4)	TSR33T239	Hypersensitive response	<i>Vb4 = Vx = Vr1</i>	02	<i>Rvi4</i>	<i>AvrRvi4^d</i>		(4)

h(5)	9-AR2T196	Hypersensitive response	<i>Vm</i>	17	<i>Rvi5</i>	<i>AvrRvi⁵</i>		(5)
h(6)	Priscilla	Chlorosis	<i>Vf</i>	01	<i>Rvi6</i>	<i>AvrRvi⁶</i>		(6)
h(7)	Malus x floribunda 821 ^b	Hypersensitive response	<i>Vfb</i>	08	<i>Rvi7</i>	<i>AvrRvi⁷</i>		(7)
h(8)	B45	Stellate necrosis	<i>Vb8</i>	02	<i>Rvi8</i>	<i>AvrRvi⁸</i>		(8)
h(9)	K2	Stellate necrosis	<i>Vdg</i>	02	<i>Rvi9</i>	<i>AvrRvi⁹</i>	<i>p-8</i>	(9)
h(10)	A723-6 ^b	Hypersensitive response	<i>Va</i>	01 ^c	<i>Rvi10</i>	<i>AvrRvi10^d</i>		(10)
h(11)	A722-7	Stellate necrosis/chlorosis	<i>Vbj</i>	02	<i>Rvi11</i>	<i>AvrRvi11^d</i>		(11)
h(12)	Hansen's baccata #2 ^b	Chlorosis	<i>Vb</i>	12	<i>Rvi12</i>	<i>AvrRvi12^d</i>		(12)
h(13)	Durello di Forli	Stellate necrosis	<i>Vd</i>	10	<i>Rvi13</i>	<i>AvrRvi13^d</i>		(13)
h(14)	Dülmener Rosenapfel ^b	Chlorosis	<i>VdrI</i>	06	<i>Rvi14</i>	<i>AvrRvi14^d</i>		(14)
h(15)	GMAL2473	Hypersensitive response	<i>Vr2</i>	02	<i>Rvi15</i>	<i>AvrRvi15^d</i>		(15)
h(16)	MIS op 93.052 G07-098 ^b	Hypersensitive response	<i>Vmis</i>	03	<i>Rvi16</i>	<i>AvrRvi16^d</i>		(16)
h(17)	Antonovka APF22 ^b	Chlorosis	<i>Val</i>	01	<i>Rvi17</i>	<i>AvrRvi17^d</i>		(17)

^aLG = apple linkage group

^bTemporary differential host until the host has been confirmed as being monogenic, or a monogenic progeny from this polygenic host has been selected.

^cProvisional placement is based on the assumption that the resistance in source PI 172623 are identical.

^aTo date GfG relationship not confirmed

1.6.3.1. Hypervariability of *Venturia inaequalis*: Generally different populations of *Venturia inaequalis* are present in both within and different areas (Bus et al., 2011). Also their virulence differs in different regions (Luby et al., 2001). In the nomenclature only those isolates of *Venturia inaequalis* are taken which shows resistance against broad spectrum resistance genes (MacHardy, 1996), making a total of eight races to date (Table 1.7). *Venturia inaequalis* isolates are hypervariable exhibiting differential pathogenicity on apple cultivars thus giving the name differential hosts. However as some of the isolates can grow on two differential hosts, categorizing them into particular race is difficult.

Table 1.7: Physiological races of *V. inaequalis*.

Races	apple cultivars Pathological characteristics on	Reference
Race1	Dolgo, Geneva and R 12740-7A(a Russian cultivar) have non sporulating lesion	MacHardy 1996
Race2	Geneva, Dolgo and some progenies of R 12740-7A have sporulating lesion.	
Race3	Geneva have sporulating lesion whereas, Dolgo, and R 12740-7A have non sporulating lesion.	
Race4	Dolgo and Geneva have non sporulating lesion whereas, those progenies of R 12740-7A on which race 2 isolates cannot sporulate have sporulating lesion.	
Race5	<i>Vm</i> R gene containing cultivars have sporulating lesions.	
Race6	<i>Vf</i> hybrids have sporulating lesion but cannot infect <i>Malus floribunda</i> 821 containing <i>Vfh</i> R gene.	Benaouf and Parisi, 2000
Race7	<i>Vf</i> and <i>Vfh</i> R gene containing cultivars can be infected but Golden delicious which contains <i>Vg</i> gene cannot be infected.	
Race8	Can infect Royal gala, Golden delicious and <i>Vh8R</i> gene containing cultivars.	Bus et al., 2005

It is predicted that certain factors like avirulence factor, pectinolytic, cutinolytic, cellulolytic and β -D-glucosidase activities are responsible for pathogenicity and virulence of the scab fungus *Venturia inaequalis* (Table 1.8).

Table 1.8: Pathogenicity and virulence governing factors of *V. inaequalis* (Source: Jha, 2009).

Locus/Gene	Function associated with it
Avirulence Factor	
<i>avrVg(avrRvi1)</i>	Apple cultivars containing <i>Vg(avrRvi1)</i> are avirulent.
<i>avrVf(avrRvi6)</i>	Apple cultivars containing <i>Vf(avrRvi6)</i> are avirulent.
<i>avrVh2(avrRvi2)</i>	Apple cultivars containing <i>Vh2(avrRvi2)</i> are avirulent.
<i>avrVm(avrRvi5)</i>	Apple cultivars containing <i>Vm(avrRvi5)</i> are avirulent.
<i>avrVfh(avrRvi7)</i>	Apple cultivars containing <i>Vfh(avrRvi7)</i> are avirulent.
<i>avrVd(avrRvi13)</i>	Apple cultivars containing <i>Vd(avrRvi13)</i> are avirulent.
<i>avrVh8(avrRvi8)</i>	Apple cultivars containing <i>Vh8(avrRvi8)</i> are avirulent.
Cell Wall Degrading Enzymes (CWDEs)	Promote pathogen entry into the host and facilitates nutrients uptake
Cellulase	
β -D-glucosidase	
Polygalacturonase (endo- and exo-PG)	
Cutinase	Assists pathogen in cuticle penetration and sub-cuticular growth
Esterase	Assists pathogen in cuticle penetration by softening cutin
Melanoprotein	Assists in slow release of CWDEs and diverting the solute/nutrient flow towards the site of infection
Cellophane induced	
<i>Cin1</i>	Induced during apple infections
<i>Cin3</i>	Induced during apple infection

1.6.4. Breeding, cisgenesis and transgenesis:

In order to control scab disease, several apple breeding programs have been conducted for the introgression of scab-resistance gene from resistant cultivars to scab-susceptible cultivars (Gessler and Pertot, 2011). Classical breeding method is very slow and also many unwanted genes are inherited along with the gene of interest e.g. it took approximately 50 years to introduce *Vf* (*Rvi6/HcrVf2*) scab resistance gene from *Malus floribunda* 821 to scab susceptible cultivars in making a high quality marketable apple cultivars (Schouten et al., 2009). Thus classical breeding methods are not very promising way of producing scab resistant varieties. New approach have been developed to genetically modify the plant from one or more genes either inserted from crossable donor plant known as cisgenesis or foreign genes from outside the gene pool of the conventional breeder known as transgenic. The benefit of cisgenic plants are absence of any foreign genes and preserving the fruit quality and other desired traits of the cultivars (Schouten et al., 2014). Cisgenic plants are exempted from the GMO regulation. Therefore cisgenesis is a fast, safe and acceptable way than transgenesis. A comparison between cisgenesis and transgenesis is given in Figure 1.10.

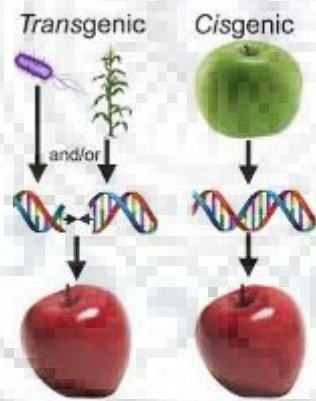


Figure 1.10: Comparison between transgenesis and cisgenesis

A list of genes from apple and other sources are present that have shown resistance against apple scab (Table 1.9). Several scab-resistance genes (*Rvi1* - *Rvi17*) have been isolated and mapped from various apple cultivars across the globe (Bus et al., 2011). Two genes, *Rvi6* (formerly *HcrVf2*) and *Rvi15* (formerly *Vr2*) are currently the only two monogenic scab resistance genes that are publically available (Wurdig et al., 2015). In the meanwhile new *V.inaequalis* (race 6 and 7) were detected which overcome *Rvi6* resistance (Parisi et al., 1993; Trapman, 2006). However, full resistance against apple scab is provided by *Rvi15* gene, which is originated from the accession

GMAL 2473. The virulence of *Venturia inaequalis* against this accession is being monitored in 16 countries since 2009 and till date there are no reports of any scab, proving it to be a good candidate (Schouten et al., 2014). However, there is an urgent need for searching new scab-resistance gene in apple to provide durable resistance.

Table 1.9: Genes shown to impact scab resistance in apple (Source: Jha et al., 2009).

Gene	Gene sequence	Apple cultivar (s) used in study	Inference
Chitinase			
<i>ech42</i> (Endo)	<i>Trichoderma atroviride</i>	McIntosh	Transgenic plants are resistant to mix of Races 1-5
<i>nag70</i> (Exo)	<i>Trichoderma atroviride</i>	McIntosh	Transgenic plants are resistant to mix of Races 1-5
<i>ech42</i> (Endo) and <i>nag70</i> (Exo)	<i>Trichoderma atroviride</i>	McIntosh	Exhibit synergism in imparting scab resistance against mix of Races 1-5
		Galaxy, Araine	Transgenic plants are resistant to Race 1 and 6
Puriondoline B (<i>PinB</i>)	Wheat	Galaxy, Araine	Transgenic plants are resistant to race 6
<i>MpNPR1-1</i>	Apple	Galaxy	Transgenic plants are resistant to mix of Race 1 and 5
<i>LRPKm1</i>	Apple	Florina, Golden Delicious	Upregulated by SA treatment and during <i>Venturia</i> infections

The scab-resistance in apple is controlled by several quantitative trait loci (QTL). Polygenic resistance against scab can be created with broad range of *R* genes and QRLs (Quantitative resistance loci). Durability of all *R* genes is not equal. To create durable scab resistance apple plants, pyramiding of both *R* genes and available quantitative resistance genes are required (Bus et al., 2011). It can be achieved through cisgenic technology which seems to be a promising approach to impart more effective and durable resistance in commercial apple cultivars. Cisgenic

apple plants have already being in development in the recent past (Vanblaere et al., 2011; Würdig et al., 2015) (Table 1.10).

Table 1.10: Genetic transformation of apple for scab resistance.

Gene	Donator	Reference	Plant
<i>Rvi6</i> (formerly <i>HcrVf2</i>)	<i>Malus floribunda</i> 821	Belfanti et al., 2004	Gala
<i>HcrVf1</i> (R-genes)	<i>M. floribunda</i> 821	Malnoy et al., 2008	Gala
<i>Rvi6</i> (formerly <i>HcrVf2</i>)promoter	<i>M. floribunda</i> 821	Szankowski et al., 2008	Gala
<i>Rvi6</i> (formerly <i>HcrVf2</i>)	<i>M. floribunda</i> 821	Vanblaere et al., 2011	Gala; the first true cisgenic plant.
<i>Rvi6</i> (formerly <i>HcrVf2</i>)	Florina	Vanblaere et al., 2014	Gala
<i>Rvi15</i> (previously <i>Vr2</i>)	GMAL 2473	Schouten et al., 2014	Gala
<i>ech42</i> (Endochitinase)	<i>Trichoderma atroviride</i> (previously <i>T. harzianum</i>)	Wong et al., 1999	Royal Gala
<i>ech42</i> (Endochitinase)		Bolar et al., 2000	Marshall McIntosh
<i>ech42</i> and <i>nag 70</i> (exo chitinase) cotransformed		Bolar et al., 2001	Galaxy and Ariane apple
<i>pinB</i> (puroinduline B antifungal protein)	Wheat	Faize et al., 2004	Ariane and Galaxy

1.7. Inducible defense metabolites of Malinae: the Biphenyls and the dibenzofurans:

Resistant apple cultivars combat scab or fire-blight infection by producing chemically specialized defense metabolites, the biphenyls and the dibenzofurans (Chizzali and Beerhues, 2012). The ability to produce these phytoalexins is only confined to this sub-tribe Malinae (Saini et al., 2017). The most common biphenyls are aucuparin and noraucuparin, and most common dibenzofurans is eriobofuran. These biphenyls and dibenzofurans exhibited significant antifungal and anti-bacterial properties, however, their mode-of-actions remain largely elusive (Chizzali et al., 2012). Both biphenyls and dibenzofurans inhibited the fungal spore germination and fungal mycelial growth. Later, thirteen biphenyls and four dibenzofurans phytoalexins specific to Malinae were also tested for in vitro antibacterial activity against fire blight infection (Chizzali et al., 2012). Interestingly, all scab-susceptible apple cultivars either completely failed to produce these two classes of phytoalexins upon pathogen infection or produce these phytoalexins in small quantities. Earlier, it has been shown that biphenyls and dibenzofurans mainly localized in the sapwood of the plants (Kokubun and Harborne, 1995). These phytoalexins were not found in the leaves (Hrazdina, 2003), with only exception of *Sorbus aucuparia*, which accumulates aucuparin, a biphenyl-derivative, in the leaves in response to biotic and abiotic elicitor-treatment (Kokubun and Harborne, 1994). Until now, any biphenyl- or dibenzofuran- glycosides have not been identified from any intact plants for Malinae. However, scab-resistant apple cell cultures produced these 2'-glucosyloxyaucuparin (biphenyl-glycoside) and dibenzofuran-glycoside, malusfuran in response to elicitor-treatment (Borejsza-Wysocki et al., 1999). It has been reported that biphenyls and dibenzofurans do not occur simultaneously (Kokubun and Harborne, 1995b), however, yeast extract-treated cell cultures of the scab-resistant apple cultivar Liberty accumulated both biphenyls and dibenzofurans simultaneously, which suggested a biogenic relationship between the two classes of compounds. Recently, elicitor-treated cell cultures of *S. aucuparia* or *Pyrus pyrifolia* also showed simultaneous accumulation of both the biphenyls and dibenzofuran (Hüttner et al., 2010; Saini et al., 2017). Till date, ten (10) biphenyls (Table 1.11a) and seventeen (17) dibenzofurans (Table 1.11b) have been detected so far in Malinae (out of 30 genera) (Chizzali and Beerhues, 2012). Out of total 10 biphenyls, aucuparin is the most widely distributed biphenyl whereas γ -cotonefuran is the most abundant dibenzofuran. Among all detected biphenyls, 2'-glucosyloxyaucuparin is unique to *Malus* species, similarly among dibenzofurans, malusfuran is unique to the genus *Malus* (Chizzali and Beerhues, 2012).

Table 1.11a: Structures of biphenyl-derivatives (1-10) recorded from Malinae.

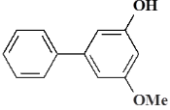
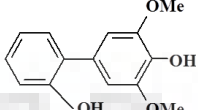
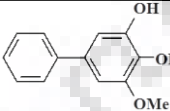
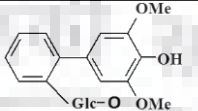
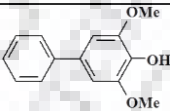
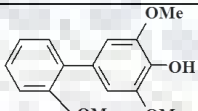
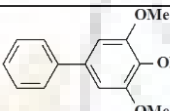
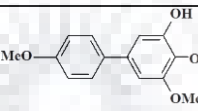
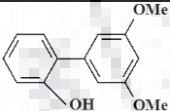
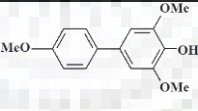
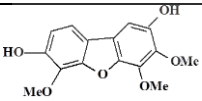
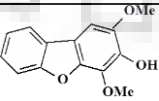
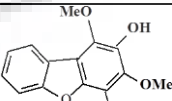
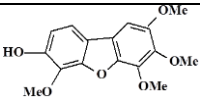
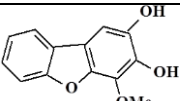
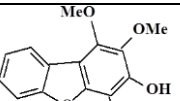
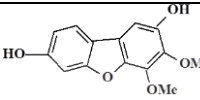
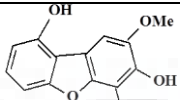
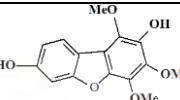
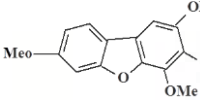
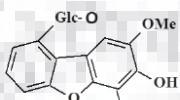
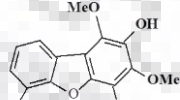
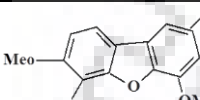
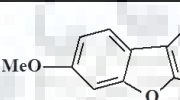
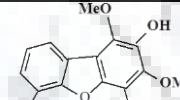
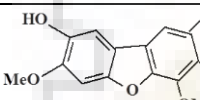
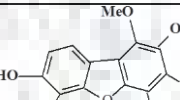
Biphenyls	
 3-hydroxy-5-methoxybiphenyl	 2'-hydroxy-aucuparin
 Noraucuparin	 2'-glucosyloxy-aucuparin
 Aucuparin	 2'-methoxy-aucuparin
 3,4,5-trimethoxy-biphenyl	 Rhaphiolepsin
 Isoaucuparin	 4'-methoxyaucuparin

Table 1.11b: Structures of dibenzofuran-derivatives (1-17) recorded from Malinae.

Dibenzofurans		
Cotonefurans	Eriobofurans	Pyrufurans
 α -cotonefuran	 Eriobofuran	 α -pyrufuran

 <p>β-cotonefuran</p>	 <p>Noreriobofuran</p>	 <p>β-pyrufuran</p>
 <p>γ-cotonefuran</p>	 <p>9-hydroxy-eriobofuran</p>	 <p>γ-pyrufuran</p>
 <p>δ-cotonefuran</p>	 <p>Malusfuran</p>	 <p>6-hydroxy-α-pyrufuran</p>
 <p>ϵ-cotonefuran</p>	 <p>7-methoxyeriobofuran</p>	 <p>6-methoxy-α-pyrufuran</p>
 <p>2,8-dihydroxy-3,4,7-trimethoxydibenzofuran</p>		 <p>7-hydroxy-6-methoxy-α-pyrufuran</p>

1.8. Biosynthesis of the biphenyl and the dibenzofuran:

The formation biphenyl scaffold is well studied both at biochemical and molecular level (Liu et al., 2004; 2007). Biphenyl scaffold is known to be catalyzed by a type III polyketide synthase, biphenyl synthase (BIS) (Liu et al., 2007). Very recently crystal structure of BIS has been elucidated (Stewart et al., 2017). The BIS enzyme catalyzes the condensation of one molecule of benzoyl-CoA with three molecules of malonyl-CoA to produce one molecule of 3,5-dihydroxybiphenyl, the precursor for other substituted biphenyl phytoalexins (Saini et al., 2017). Biphenyls are known to be converted into dibenzofurans, however biochemical and molecular details of such conversion remains still elusive (Khalil et al., 2015). These biphenyls and dibenzofurans are benzoate-derived metabolites. The starter substrate benzoyl-CoA for biphenyl biosynthesis, is either derived from cinnamoyl-CoA (in β -oxidative pathway) or from free benzoic acid (non- β -oxidative pathway) in a reaction catalyzed by benzoate:CoA ligase (BZL), which

promotes thio-esterification of benzoic acid by coenzyme A. BZL activity has been detected in *Clarkia breweri* and *Hypericum androsaemum* (Abd El-Mawla and Beerhues, 2002; Beuerle and Pichersky, 2002b). Although biosynthesis of core biphenyl pathway is well studied (Liu et al., 2007; Sircar et al., 2015; Khalil et al., 2015) but how the precursor benzoyl-CoA is formed, is not well understood in apples.

1.9. Benzoic acid biosynthesis in plants:

Benzoic acid and its coenzyme A (CoA) derivative in plants act as a central molecule for biosynthesis of several plant natural products which play crucial role as plant hormones, defense metabolites, co-factors, attractant for pollinators and seed dispersers (Abd El-Mawla and Beerhues, 2002). Benzoate-derived metabolites have high nutraceutical values for humans. Benzoate-derived C₆-C₁ building block is found in a number of plant natural product constituents, such as the antihypertension drug reserpine, the anticancer drug paclitaxel, and the red naphthoquinone dye shikonin (Dewick, 2009). Salicylic acid (2-hydroxybenzoic acid) and methyl-salicylate are known to be the defense signaling molecules in many plants, playing key role in regulating plant defense responses upon pathogen attack (Baldwin et al., 2006; Vlot et al., 2009). Derivatives playing roles in primary metabolism are respiratory co-factor ubiquinones, aromatic-cytokinin such as meta-topolin and vitamin B9 (Block et al., 2014; Werbrouck et al., 1996; Mutui et al., 2012; Hanson and Gregory, 2011). Benzoate-derived volatile derivatives, such as methyl benzoate, methyl salicylate, benzyl-benzoate and anthraniloyl are involved in plant-insect and plant-plant interactions. They serve as aroma and flavor compounds in floral and fruit scent, attractants for pollinators and seed dispersers, respectively (Dudareva and Pichersky, 2008; Gaid et al., 2012; Dudareva et al., 2013). Benzoic acid-derived volatile compound also serve as antimicrobial compounds involved in plant protection (Köllner et al., 2010; Widhalm and Dudareva, 2015). A number of non-volatile benzoyl (benzoic acid-derived) and benzyl (benzyl alcohol-derived) compounds such as benzoylglucosinolates and salicortin can also acts as plant defense molecule (Lee et al., 2012; Babst et al., 2010; Widhalm and Dudareva, 2015). Simple phenols, for example hydroquinone, are likely to arise from benzoic acid by oxidative decarboxylation (Dewick, 2009), whereas conjugated phenols such as ellagitannins, are derived from gallic acid (3,4,5-trihydroxybenzoic acid; Dewick, 2009). Benzoyl-CoA serves as a precursor molecule for the biosynthesis of biphenyl and dibenzofuran class of phytoalexins in the Rosaceous sub-tribe Malinae (Saini et al., 2017).

Despite simple structure and widespread distribution in plant kingdom, biosynthesis of benzoic acid and its derivatives are not completely understood. This complexity is mainly due to the existence of multiple benzoic acid biosynthetic pathways between different species and even within different compartments of same species (Wildermuth, 2006). Plant benzoic acids arise either from shikimate or chorismate pathway intermediates or from the phenylpropanoid pathway. The examples of benzoic acid biosynthesis from the intermediates of shikimate pathway are 3-hydroxybenzoic acid biosynthesis in *Centaureum erythraea* and *Swertia chirata*, salicylic acid biosynthesis in *Arabidopsis thaliana* and *Nicotiana benthamiana*, 2,3-dihydroxybenzoic acid biosynthesis in *Catharanthus roseus*, and gallic acid biosynthesis in *Rhus typhina* (Abd El-Mawla et al., 2001; Wang et al., 2001; Catinot et al., 2008; Moreno et al., 1994; Ishikura et al., 1984; Werner et al., 1997; Gaid et al., 2012). It has also been reported that many plants synthesize isochorismate which serves as the intermediate for the biosynthesis of *o*-succinylbenzoic acid, salicylic acid, and 2,3-dihydroxybenzoic acid (Gross et al., 2006; Mustafa et al., 2009; Bartsch et al., 2010).

In phenylpropanoid pathway, formation of benzoic acids and its derivatives starts from *trans*-cinnamic acid (CA) or its derivatives (hydroxyl- and methoxy-derivatives). *Trans*-cinnamic acid or its derivatives originate from L-phenylalanine by a deamination reaction catalyzed by phenylalanine ammonia-lyase (PAL; Gaid et al., 2012, Mir et al., 2013). PAL catalyzed formation of cinnamic acid is well established in plants (Mir et al., 2010). Benzoic acid is derived from cinnamic acid by C₂ shortening of the propyl side chain. This shortening of C₂ unit of the propyl side chain of cinnamic acid proceeds by three major pathways.

However, multiple biosynthetic pathways have been reported for C₂ chain shortening of cinnamic acid, proceeding either *via* a (1) **CoA-dependent and β -oxidative mechanism**; (2) **CoA-dependent and non- β -oxidative** and (3) **CoA-independent and non- β -oxidative** mechanism (Figure 1.11).

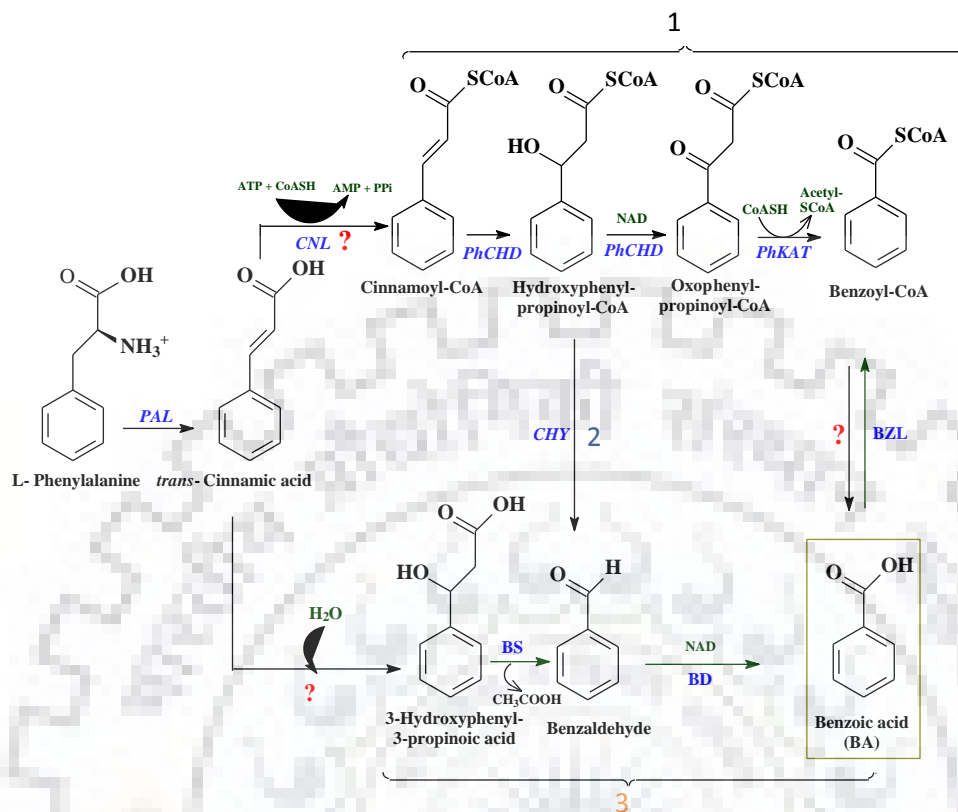


Figure 1.11: Possible routes of benzoic acid biosynthesis in plants. **1:** CoA-dependent and β -oxidative route; **2:** CoA-dependent and non β -oxidative route; **3:** CoA-independent and non β -oxidative route. Question marked reaction steps has not been yet identified for benzoic acid biosynthesis in Malinae. [PAL = Phenylalanine ammonia-lyase; CNL = Cinnamate-CoA-ligase; PhCHD = cinnamic acid-CoA hydratase / dehydrogenase; PhKAT = 3-ketoacyl thiolase; CHY = 3-hydroxyisobutyryl-CoA hydrolase; BD = benzaldehyde dehydrogenase; BS = benzaldehyde synthase].

1.9.1. CoA-dependent and β -oxidative route of benzoic acid biosynthesis:

The CoA-dependent and β -oxidative route mirrors fatty acid β -oxidation, the intermediates being maintained as CoA thioesters. The CoA-dependent and β -oxidative pathway of benzoic acid biosynthesis has been detected in *Cucumis sativus*, *Nicotiana attenuata*, *Arabidopsis thaliana*, and *Petunia hybrida* (Ribnický et al., 1998; Jarvis et al., 2000; Bussell et al., 2014; Klempien et al., 2012; Gaid et al., 2012; Lee et al., 2012; Widhalm and Dudareva, 2015). Recently, all of the genes

and enzymes involved in the core β -oxidative pathway of benzoic acid biosynthesis were identified and functionally characterized (Figure 1.12). In this route, cinnamic acid is first activated into cinnamoyl-CoA in a reaction catalyzed by cinnamate-CoA-ligase (CNL; Colquhoun et al., 2012; Gaid et al., 2012; Klempien et al., 2012). A cDNA encoding *CNL* has been cloned and functionally characterized from *Petunia hybrida* (Colquhoun et al., 2012; Klempien et al., 2012) and from cell cultures of *Hypericum calycinum* (Gaid et al., 2012). The function of *BZO1* gene identified from *Arabidopsis thaliana*, has now re-established as *CNL* (Kliebenstein et al., 2007; Lee et al., 2012). Cinnamoyl-CoA is later converted into 3-oxo-3-phenylpropanoyl-CoA through intermediate formation of 3-hydroxy-3-phenylpropanoyl-CoA in a reaction catalyzed by a bi-functional enzyme, cinnamic acid-CoA hydratase / dehydrogenase (*PhCHD*) (Bussell et al., 2014; Qualley et al., 2012). Finally, 3-oxo-3-phenylpropanoyl-CoA is converted to benzoyl-CoA by 3-ketoacyl thiolase (*PhKAT*) (Van Moerkercke et al., 2009). In this route, formation of free benzoic acid has not been detected yet, thereby raising question on conversion of benzoyl-CoA to benzoic acid. Till date *CNL*, *CHD*, and *KAT* gene function has not been detected from apple or any other member of Malinae.

1.9.2. CoA-dependent and non β -oxidative route of benzoic acid biosynthesis:

Another route of C₂ side chain shortening involving CoA-dependent and non- β -oxidative C₂ cleavage was reported in few plant species via direct conversion of cinnamoyl-CoA into benzaldehyde (Figure 1.12). A *CHY* gene encoding 3-hydroxyisobutyryl-CoA hydrolase, which converts cinnamoyl-CoA into benzaldehyde, was reported in *A. thaliana* (Ibdah and Pichersky, 2009). Similar C₂ side chain shortening was observed in the hairy root cultures of *Datura stramonium*, which express a bacterial gene encoding hydroxycinnamoyl-CoA hydratase/lyase (HCHL) (Mitra et al., 2002), the cell cultures of *H. androsaemum* (Abd El-Mawla and Beerhues, 2002), and *Vanilla planifolia* pods (Gallage et al., 2014). Benzaldehyde was then converted into benzoic acid by dehydrogenase activity, yet not cloned from Malinae.

1.9.3. CoA-independent and non β -oxidative route of benzoic acid biosynthesis:

Furthermore, the CoA-independent and non- β -oxidative route of C₂ side chain shortening was detected for benzoic acid formation in cell cultures of *Sorbus aucuparia* (Gaid et al., 2009), *Pyrus pyrifolia* (Saini et al., 2017) as well as 4-hydroxybenzoic acid formation in *Solanum tuberosum* (French et al., 1976) and *Daucus carota* (Schnitzler et al., 1992; Sircar and Mitra, 2008). In this route, cinnamic acid is supposed to undergo C₂-side chain cleavage to yield benzaldehyde, which subsequently converted into benzoic acid by benzaldehyde dehydrogenase activity. Previously, analogous C₂-side chain shortening enzyme activity was shown by the 4-hydroxybenzaldehyde synthase (HBS), detected from few plant species. HBS-catalyzed conversion of 4-coumaric acid to 4-hydroxybenzaldehyde was detected in the tubers of *Solanum tuberosum* (French et al., 1976), in the cell cultures of *Lithospermum erythrorhizon* (Yazaki et al., 1991), in *Daucus carota* (Schnitzler et al., 1992; Sircar and Mitra, 2008) and in the *Vanilla planifolia* cell culture (Podstolski et al., 2002). A similar salicylaldehyde synthase (SAS) activity catalyzing conversion of *o*-coumaric acid to salicylaldehyde has also been observed in the *Nicotiana tabacum* (Malinowski et al., 2007; Sarkate et al., 2018). Oxidation of the intermediate benzaldehyde or 4-hydroxybenzaldehyde by a NAD⁺ dependent dehydrogenase is a key feature of this route. Subsequently, a benzaldehyde dehydrogenase activity converts benzaldehyde into benzoic acid. A benzaldehyde dehydrogenase-encoding cDNA was cloned from *Antirrhinum majus* (Long et al., 2009) and shown to contribute to methyl benzoate biosynthesis. Benzaldehyde dehydrogenase activity has also been detected in cell cultures of *Sorbus aucuparia* and *Pyrus pyrifolia* (Gaid et al., 2009; Saini et al., 2017). Moreover, a gene encoding aldehyde oxidase, which exhibits high affinity for benzaldehyde, was identified in developing *A. thaliana* seeds (Ibdah et al., 2009). Interestingly, in the flowers of *P. hybrida*, both the β -oxidative and the non- β -oxidative pathway contribute towards benzenoid production (Boatright et al., 2004; Van Moerkercke et al., 2009). Though benzaldehyde dehydrogenase activity has been well characterized in plants, the upstream chain shortening enzyme catalyzing the conversion of *trans*-cinnamic acid into benzaldehyde has not been identified in Malinae so far.

1.10. Benzoate-CoA ligase (BZL) activity:

In order to participate into biphenyl phytoalexin biosynthesis, benzoic acid needs to be converted onto benzoyl-CoA. In CoA-dependent and β -oxidative route, no free benzoic acid is formed, rather,

cinnamoyl-CoA is directly converting into benzoyl-CoA with the help of two successive enzymes, cinnamic acid-CoA hydratase/ dehydrogenase (CHD) and 3-ketoacyl thiolase (KAT). Recently, cDNA encoding *CHD* (Bussell et al., 2014; Qualley et al., 2012) and *KAT* (Van Moerkercke et al., 2009) has been cloned and functionally characterized from *Petunia hybrida*. In CoA-dependent and non β -oxidative and in CoA-independent and non β -oxidative route free benzoic acid is formed. Benzoic acid is further converted into benzoyl-CoA in a reaction catalyzed by the benzoate-CoA ligase (BZL) (Fig 1.11). BZL activity has been detected from *Clarkia breweri* (Beuerle and Pichersky, 2002a). A similar enzyme catalyzing conversion of 3-hydroxybenzoic acid into 3-hydroxybenzoate-CoA has also been detected from cell cultures of *Centaurium erythraea* (Barillas and Beerhues, 1997, 2000). *BZO1* from Arabidopsis was initially proposed as a putative benzoate:CoA ligase (BZL) (Kliebenstein et al., 2007), however it has recently been identified as cinnamate-CoA ligase (Lee et al., 2012).

1.11. Cinnamate-CoA ligase in plants:

Cinnamic acid is the first branch point of phenylpropanoid pathway which diverts carbon flux in various sub-pathways. In most of the plant species, cinnamic acid is first converted into 4-coumaric acid, in a reaction catalyzed by *cinnamate-4-hydroxylase* (Yang et al., 2005). 4-Coumaric acid is then thioesterified by *4-coumaroyl-CoA ligase (4CL)* to form 4-coumaroyl-CoA, which serve as precursors for an array of plant natural products, such as lignin, flavonoids, anthocyanins, and cell wall-bound phenolics (Li et al., 2015). In many plants, in addition to *4CL* route, cinnamic acid is thioesterified with CoA by *Cinnamate-CoA ligase (CNL)* to form cinnamoyl-CoA, which then directs carbon flow from the general phenylpropanoid pathway into benzenoid metabolism (Figure 1.12). *Cinnamate-CoA ligase* from four plants have been cloned so far, *CNL (BZO1)* from *Arabidopsis thaliana* (Kliebenstein et al., 2007), *CNL* from *Petunia hybrid* (Klempien et al., 2012), *CNL* from *Hypericum calycinum* (Gaid et al., 2012), *CNL / BZL* from *Clarkia breweri* (Unpublished).

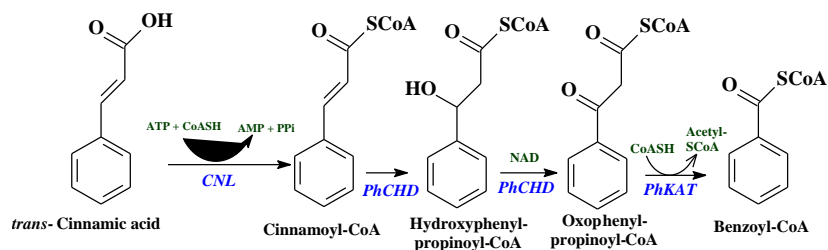


Figure 1.12: CNL-catalyzed formation of cinnamoyl-CoA and subsequent benzoyl-CoA. [CNL = Cinnamate-CoA-ligase; PhCHD = cinnamic acid-CoA hydratase / dehydrogenase; PhKAT = 3-ketoacyl thiolase; CHY = 3-hydroxyisobutyryl-CoA hydrolase].

1.12. Aim of the work:

Upon pathogen infection, resistant apple cultivars are known to produce specialized biphenyl and dibenzofuran class of phytoalexins. These biphenyls and dibenzofurans are originated from benzoic acid. Though biphenyl biosynthesis is well understood in apple and other members of Malinae, but early steps of benzoic acid biosynthesis are not well elucidated. Further, after pathogen attack, how metabolic re-programming takes place in apple to synthesize an array of defense metabolites is not known. The first aim of my doctoral thesis work is to develop a cell suspension culture of scab-resistant apple cultivar “Shireen” as a model system to understand apple *Venturia* (scab) interactions, both at metabolite and molecular levels. The second aim of my thesis work is to perform a comparative metabolomics of *Venturia inaequalis* elicitor (VIE)-treated cell cultures of apple (*Malus domestica* cv. Shireen) to identify differential accumulation of scab-induced metabolites in cell culture. The third aim of my research is to develop a validated HPLC method for the rapid and precise detection of biphenyl-dibenzofuran phytoalexins. The fourth aim of my research is to clone and functionally characterize *cinnamate-CoA-ligase* (CNL), the early gene involved in the benzoic acid / benzoyl-CoA biosynthesis gene from elicitor-treated cell cultures of apple cv. Golden Delicious. The overall goal of this doctoral research work is to improve our understanding of the defense metabolites biosynthesis in apples and their regulation after scab-infection, so that successful metabolic engineering strategies can be framed in future to fortify defense potentials of apple plants against scab disease.

1.13. Plant material used:

Cell suspension culture of apple cultivar Golden Delicious; green house grown plants of scab-resistant apple cultivar Shireen and moderately scab-susceptible apple cultivar Golden Delicious.

1.14. Objectives:

To fulfill described aim of my research, following objectives were set:

1. To develop cell suspension culture of apple (*Malus domestica*) cultivar Golden Delicious.
2. To develop a validated HPLC-mass spectrometry based analytical method for the rapid separation and precise detection of biphenyl phytoalexins.
3. To study the comparative metabolomics of scab-resistant (cv. Shireen) and scab-susceptible (cv. Golden Delicious) apple cultivar upon scab-infection.
4. To clone and functionally characterize *cinnamate CoA-ligase (CNL)* gene involved in the early steps of phytoalexin biosynthesis from apple cell cultures.

Chapter 2

Materials and Methods

2.1. Chemicals and reagents:

The deionized water used for media preparation, buffers, HPLC solvents and aqueous solutions was obtained from Milli-Q water purification system (Millipore). All solutions were sterilized by autoclaving for 20 minutes at 121°C and a pressure of 15 psi. All antibiotics and other thermolabile substances were sterile-filtered with 0.22 µ filter (Sartorius, India) before use. Chemicals used for different experiments are listed in [Table 2.1](#).

Table 2.1: Chemicals used for various experimental purposes.

Chemicals	Brand / supplier
Phytohormones for callus induction and maintenance	
2,4- Dichlorophenoxy acetic acid (2,4 D)	Duchefa Biochemie
Kinetin	Himedia
α-Naphthalene acetic acid (NAA)	Himedia
Reagents for GC-MS derivatization	
N-Methyl-N-(trimethylsilyl)-trifluoroacetamide(MSTFA)	Sigma
Methoxy amine hydrochloride (MeOX)	Sigma
Pyridine	SRL
Reagents for biochemistry and molecular biology	
IPTG	Sigma
dNTPs	NEB
DEPC treated water	SRL
ATP	Himedia

CoA (Coenzyme A)	Sigma
NaH ₂ PO ₄	Himedia
NaCl	Himedia
Imidazole	Himedia
Luciferase	Sigma
Luciferin	Sigma
Antibiotics	
Ampicillin	Himedia
Chloramphenicol	Himedia
Rifampicin	Himedia
Kanamycin	Himedia
Stationary phases used in protein desalting and affinity purification	
PD ₁₀ -cartidge Sepharose G-25 columns	GE Healthcare
Ni-NTA agarose	Qiagen
Various metabolite standards used in HPLC / GC-MS	
3,5-Dihydroxybiphenyl	Synthesized in our research group
Aucuparin	Synthesized in our research group
Benzoic acid	Sigma
Caffeic acid	Sigma
Catechin	Sigma
Chlorogenic acid	Sigma
Ferulic acid	Sigma
L-Phenylalanine	Himedia
Noraucuparin	Synthesized in our research group
<i>p</i> -Coumaric acid	Sigma
Protocatechuic acid	Sigma

Rutin	Sigma
Sinapic acid	Sigma
<i>trans</i> -Cinnamic acid	Sigma
Vanillic acid	Sigma
Vanillin	SRL
Reagents for gel electrophoresis	
Ultrapure Agarose	Thermofisher Scientific
Ethidium bromide (EtBr)	Hi media
TEMED	SRL
Acrylamide and Bisacrylamide	Merck
SDS	Hi media
EDTA	Hi media
β -Mercaptoethanol	Merck
Aluminium persulphate	Hi media
Bromophenol blue	SRL
Coomassie blue R-250 and G-250	Merck
Ladder	
1 kb / 100 bp DNA ladder	NEB
Gene ruler DNA ladder Mix	Fermantas
Long range SDS PAGE Standard	Bio-Rad

2.2. Equipments:

The major equipments used for various analyses are listed in [Table 2.2](#).

Table 2.2: Equipments used.

Equipment	Model	Brand
Balance	ME 204 (mg range)	MettlerToledo
Centrifuge 1	1-14 K (cooling)	Sigma
Centrifuge 2	5810-R	Eppendorf
Clean bench	Horizontal laminar flow	Clean air
Digital pH meter	CL54	Toschon
Dry bath	MK-20 (pelltier controlled)	BiochemLifescience
GC-MS	Agilent 6890 gas chromatograph	Agilent
Gel doc	Gel Doc™ XR+ System	Bio-Rad
Hot plate	2MLH	Remi
HPLC	LC- 20 AP	Shimadzu
Incubator shaker	LSI 4018 R	Labtech
Magnetic stirrer	MS 500	Remi
Real time PCR system	Quant studio 3	Applied Biosystem
Rotary vacuum	Centrivap	Labconco
Sonicator	Q 700	Q SONICA
Spectrophotometer	Carry 400	Agilent
Thermocycler	Veriti	Applied Biosystem
Vacuum pump	Millipore	Millipore
Vortex	3003-100	Rivotek
Water bath	Rivotek	Polular Ltd

2.3. Nutrient media:

2.3.1. Nutrient media for plant tissue culture:

Readymade plant growth LS medium (Linsmaier and Skoog 1965) was used for tissue culture (Table 2.3). 50 mL of media were poured into Erlenmeyer flask (250 mL capacity), then sealed with aluminum foil followed by autoclaving at 121°C for 20 min.

Table 2.3: Media composition for callus and suspension culture.

Medium	Brand name	Preparation and storage
A. For callus Linsmaier and Skoog (LS) medium (without sugar and hormone)	Himedia, India	4.2 g media powder was dissolved in deionized water along with 30 g sucrose (3%), 2 µM 2,4-dichlorophenoxyacetic acid (2,4-D), 1 µM kinetin and 1 µM naphthaleneacetic acid (NAA). pH 5.8-6 was adjusted with NaOH, then final volume was adjusted to 1 L. For sterilization autoclave was done at 121°C for 20 min. For solid media, 0.7-0.8% agar was added prior to autoclaving.
B. For cell suspension culture Linsmaier and Skoog (LS) medium (without sugar and hormone)	Himedia, India	4.2 g media powder was dissolved in deionized water along with 30 g sucrose (3%), 2 µM 2,4-D and 1 µM NAA. pH 5.8-6 was adjusted with NaOH (1N), , then final volume was adjusted to 1 L. For sterilization autoclave was done at 121°C for 20 min. Stored at room temperature.

2.3.2. Nutrient media for fungal culture (scab-fungus):

Table 2.4: Culture medium for *Venturia inaequalis* growth.

Medium	Composition	Preparation & Storage
Malt extract peptone (MEP) medium	Malt Extract 30 g/L Peptone 3 g/L Agar (Solid media) 1.5 %	Mix deionized water; pH7.0 is adjusted with HCl (1N), then final volume was adjusted to 1 L. For sterilization autoclave was done at 121°C for 20 min.

2.3.3. Nutrient media for *E. coli* culture:

Table 2.5: Culture medium and reagents for *E. coli* growth.

Medium	Components
Luria-Bertani (LB) medium	Bacteriological peptone 10g Yeast extract 5g NaCl 10g For solid media, 1.2 % agar was added prior to autoclaving.
Antibiotics	Ampicillin 100 mg/ml Prepared in autoclaved water and then filter sterilized. Chloramphenicol 30 mg/ml Prepared in pure ethanol and then filter sterilized.
For induction of protein expression	IPTG (Stock 0.5 M) Final concentration in bacterial culture 0.5 mM
For preservation at -80°C	Glycerol 400 µl Bacterial culture 600 µl

2.3.4. Nutrient media for *Agrobacterium tumefaciens* culture:

Table 2.6: Culture medium and reagents for *A. tumefaciens* growth.

Medium	Composition	Preparation and Storage												
Yeast mannitol Broth (YMB) / Yeast manitol Agar (YMA)	<table border="0"> <tr> <td>K₂HPO₄</td> <td>0.05 g/L</td> </tr> <tr> <td>MgSO₄.7H₂O</td> <td>0.02 g/L</td> </tr> <tr> <td>NaCl</td> <td>0.01 g/L</td> </tr> <tr> <td>Yeast Extract</td> <td>0.04 g/L</td> </tr> <tr> <td>Manitol</td> <td>1.0 g/L</td> </tr> <tr> <td>Agar (for YMA)</td> <td>15.0 g/L</td> </tr> </table>	K ₂ HPO ₄	0.05 g/L	MgSO ₄ .7H ₂ O	0.02 g/L	NaCl	0.01 g/L	Yeast Extract	0.04 g/L	Manitol	1.0 g/L	Agar (for YMA)	15.0 g/L	Mix deionized water; pH 7.0 adjusted with HCl (1N), then final volume was adjusted to 1 L. For sterilization autoclave was done at 121 ⁰ C for 20 min.
K ₂ HPO ₄	0.05 g/L													
MgSO ₄ .7H ₂ O	0.02 g/L													
NaCl	0.01 g/L													
Yeast Extract	0.04 g/L													
Manitol	1.0 g/L													
Agar (for YMA)	15.0 g/L													
Antibiotics	<table border="0"> <tr> <td>Kanamycin</td> <td></td> </tr> <tr> <td>Rifampicin</td> <td></td> </tr> </table>	Kanamycin		Rifampicin		<p>30 mg/10 ml final stock solution was prepared in water and filter sterilized. Final concentration used 250 mg/L. Used freshly or before one week.</p> <p>10 mg/ml stock solution prepared in methanol and filter sterilized. Final concentration used 50µg/ml.</p>								
Kanamycin														
Rifampicin														

2.3.5. Activation medium for *A. tumefaciens* transformation:

Table 2.7: Activation medium for *A. tumefaciens* growth for transient expression in *Nicotiana benthamiana* leaves.

Medium	Composition	Preparation & Storage						
Activation medium	<table border="0"> <tr> <td>MES/KOH (pH 5.6)</td> <td>10 mM</td> </tr> <tr> <td>MgCl₂</td> <td>10 mM</td> </tr> <tr> <td>Acetosyringone</td> <td>150 mM</td> </tr> </table>	MES/KOH (pH 5.6)	10 mM	MgCl ₂	10 mM	Acetosyringone	150 mM	Prepared freshly. MES and MgCl ₂ dissolved in deionized water while acetosyringone mixed in ethanol.
MES/KOH (pH 5.6)	10 mM							
MgCl ₂	10 mM							
Acetosyringone	150 mM							

2.4. Buffers and solutions:

Table 2.8: Buffers for affinity purification of His₆-tag fusion protein.

Name of buffer	Ingredient	
Lysis buffer pH 8	NaH ₂ PO ₄	3.4 g
	NaCl	0.9 g
	20 mM imidazole	0.7 g
	dH ₂ O	500 ml
Washing buffer pH 8	NaH ₂ PO ₄	3.4 g
	NaCl	0.04 g
	50 mM imidazole	1.7 g
	dH ₂ O	500 ml
Elution buffer pH 8	NaH ₂ PO ₄	3.4 g
	NaCl	8.8 g
	250 mM imidazole	8.5 g
	dH ₂ O	500 ml

Table 2.9: Buffers for plasmid isolation (miniprep).

Buffer 1	Tris-HCl	50 mM
	EDTA	10 mM
	RNaseA	100 µg/ml
	Adjust to pH 8 with HCl	
	RNase A was freshly added prior to use	
Buffer 2	NaOH	0.2 M
	SDS	1% (w/v)
Buffer 3	Potassium acetate	2.55 M
	Adjust to pH 5.5 with glacial acetic acid	

Table 2.10: Buffer for DNA gel electrophoresis.

Name of Buffer	Ingredient	Preparation and storage
50 X TAE Buffer (diluted to 1 X for use).	Tris buffer 242 g EDTA 18.61 g Glacial acetic acid 57.1 ml Water 1L	pH 8.0 was adjusted by later addition of glacial acetic acid, autoclaved and stored at room temperature.



Table 2.11: Buffers and reagents for SDS-PAGE electrophoresis.

Name of Buffer	Ingredient	Preparation and storage
Stacking Gel (5 %)	Tris buffer (0.5 M) 1.25 ml (pH 6.8) Acrylamide/Bis (30 %) 2.0 ml SDS (10 % w/v) 0.05 ml APS (10 % w/v) 0.05 ml TEMED 5 μ l Water 3.0 ml	TEMED added in the last for polymerization and the mixture was poured immediately and gently to avoid bubble formation using pipette. Allowed it to solidify.
Resolving Gel (12 %)	Tris buffer (0.5 M) 1.3 ml (pH 8.8) Acrylamide/Bis (30 %) 0.6 ml SDS (10 % w/v) 0.05 ml APS (10 % w/v) 0.05 ml TEMED 5 μ l Water 1.2 ml	TEMED added in the last for polymerization and the mixture was poured immediately and gently to avoid bubble formation using pipette on solidified stacking gel.
Electrophoresis tank buffer	Tris HCl 3.0 g Glycine 14.4 g Na-SDS 1.0 g Water 1000 ml	Mixed well and check pH without adjustment should be 8.3
Staining solution	Ethanol 30 ml Coomassie brilliant blue – 250 200 mg Glacial acetic acid 7 ml Water 43 ml	Mixed well and used for staining the protein bands on gel
Destaining solution	Ethanol 30 ml Glacial acetic acid 7 ml Water 63 ml	Mixed well used for destaining the gel to get clear protein bands

Table 2.12: Washing solution for regeneration of PD₁₀ column and Ni-NTA agarose regeneration.

Name	Ingredient	Washing procedure
NaOH Cleaning solution	NaOH 0.16 M	Wash PD ₁₀ column with five column volumes of NaOH(1N) cleaning solution followed by five volume of distilled water. After washing pH was checked to confirm cleaning, which should be neutral.
Ni-NTA agarose washing and regeneration solution	Acetic acid 0.2 M Glycerol 30 % Deionized water	Wash with the following solutions in the same order.

Table 2.13: Composition of Bradford reagent used for protein estimations.

Name	Ingredient	Preparation and storage
Bradford dye solution	Coomassie Brilliant 100 mg Blue G-250 Ethanol (96%) 50 ml Orthophosphoric Acid 100 ml (85%) Water to 1000 ml	Dissolve well Coomassie Brilliant blue G-250 in ethanol, add orthophosphoric acid and adjust volume to 1 L with water. Filter the solution with filter paper (Whatman No. 1) and keep in refrigerator in dark bottle.

2.5. Materials for molecular biology:

2.5.1. mRNA extraction, cDNA synthesis and real time PCR reagents:

Various enzymes and kits used for mRNA extraction, cDNA synthesis and real time PCR analyses are listed in [Table 2.14](#).

Table 2.14: Enzymes and kits used in molecular biology.

Enzyme	Brand
M-MuLV reverse transcriptase	NEB
Taq DNA polymerase	NEB
Phusion HF DNA polymerase	NEB
Fast Alkaline phosphatase (FastAP)	Thermofisher Scientific
Restriction endonuclease	NEB
RiboLock RNase inhibitor	Thermofisher Scientific
T4 DNA ligase	NEB
RNase A	Thermofisher Scientific
RNase-free DNase I	Qiagen
Kits	
DNeasy Plant Mini kit	Qiagen
RNeasy Plant Mini kit	Qiagen
Minelute Gel extraction kit	Qiagen
Genelute PCR Clean-up kit	Sigma
Power Up™ SYBR™ Green Master Mix	Applied Biosystems
SMART RACE cDNA Amplification Kit	Clontech

2.5.2. Host cells (Competent *E. coli*):**Table 2.15:** Host cells.

<i>E. coli</i>	Purpose	Genotype
DH5α	This strain was used for the initial cloning and plasmid amplification into various vectors	F' φ80δlacZ9M15 end A1 hsdR17(rk-mk+)supE44thi- 1 λ-gyrA96 relA1 9(lacZYA-argFV169) deoR
BL21(DE3)pLysS – For overexpression of protein	Used for protein expression of target gene cloned in pRSET B vector	F- <i>ompT hsdSB</i> (rB-mB-) <i>gal dcm</i> (DE3) pLysS (CamR)

2.5.3. Vectors:

Table 2.16: Cloning and expression vectors used.

Vectors	Characters/purpose	Supplier
Cloning vector		
pGEM-T easy	3 Kb T-overhanged vector with <i>lacZ</i> and ampicillin resistance genes for subcloning of Taq DNA polymerase-amplified PCR products.	Invitrogen
Expression vector		
pRSET B	2.9 Kb expression vector with N-terminal His ₆ -tag and ampicillin resistance gene	Invitrogen

2.5.4. Primers:

All primers used in various PCR amplifications were obtained from Eurofin genomics (Bangalore, India) as mentioned in [Table 2.17](#).

Table 2.17: Primers used.

SN	Label	Sequence (5' - 3')*	GDR Acc. No
1	<i>MdCNL</i> FP	GATGCTAGC ATGGCCTTTGAATCAATGAATACG ^a	MDP0000576682
2	<i>MdCNL</i> RP	GATGGTACCTCAAAGACGAGACAAAGCAAG ^b	
3	3' <i>MdCNL</i> UTR	GGCAAAGACATTCGTCTTATC	
4	5' <i>MdCNL</i> UTR FP	CTTGGTAATTTCCACACAAG	
5	5' <i>MdCNL</i> UTR RP	GAAGCGAGTGCATTCATAG	
6	<i>MdCNL</i> FPq	ACACGGGCACCCAAAGG	
7	<i>MdCNL</i> RPq	CGAGGGTGTGGCATTGC	
8	<i>MdPAL</i> FPq	CACCACCCTGGACAGATTGAG	MDP0000261492
9	<i>MdPAL</i> RPq	ATAAGAGCTGCCATCCAAAATATG	
10	<i>MdBIS3</i> FPq	CGCCTTTGGTTAAGAATGAGCCTC	MDP0000287919
11	<i>MdBIS3</i> RPq	CCTCAATGTTACAAATGTCTTGGCGC	
12	<i>MdProfilin</i> FPq	GGCAGCGTTTGGTCTCAG	MDP0000264119
13	<i>MdProfilin</i> RPq	GCAGCAATCTCCTCAGGC	
14	<i>attB1</i> FP	GGGACAAGTTTGTACAAAAAAGCAGGCTTAACCAT GGCCTTTGAATCAATGAATACG	

15	<i>attB2a</i> RP	GGGGACCACTTTGTACAAGAAAGCTGGGTC TCA AAG ACG AGA CAA AGC AAG AAT CTG	
16	<i>attB2b</i> RP	GGGGACCACTTTGTACAAGAAAGCTGGGTC AAG ACG AGA CAA AGC AAG AAT CTG	
17	<i>F3HFP</i>	GCTCTCCCTGCCTCGAATG	MDP0000190489
18	<i>F3HRP</i>	GGATGTGGAACCGTTGATT	
19	<i>AOX</i> FP	GGAGCGGCGACGGTTT	MDP0000643331
20	<i>AOX</i> RP	GCGCGCTGCTCATCATC	
21	<i>Actin</i> FP	GTGAGGCTCTATTCCAACCATC	MDP0000921834
22	<i>Actin</i> RP	GGAACACAAATTGGGCAAGTAT	

*Restriction sites underlined; a, *Nhe*I; b, *Kpn*I; q, quantitative RT-PCR; FP, forward primer; RP, reverse primer.

2.6. *Venturia inaequalis* elicitor and spores used:

Yeast-extract (YE) and elicitor prepared from *Venturia inaequalis* (VIE) was used to up-regulate metabolite / biphenyl-dibenzofuran biosynthesis in cell suspension culture of apple. Moreover, *Venturia inaequalis* conidio-spores were used to infect apple plants (Table 2.18).

Table 2.18: Elicitors used.

Elicitor	Company	Preparation method
Yeast extract (YE)	Himedia, India	1.5 g of yeast extract is dissolved in 10 ml of distilled water and then filter sterilized. Seventh day is taken from the linear growth phase for the elicitation of cell suspension culture of apple cv. Golden Delicious. The final concentration used for yeast-extract solution is 3g/L.
<i>Venturia inaequalis</i> elicitor(VIE)	Prepared in laboratory	The strain of <i>V. inaequalis</i> (MTCC No.: 1109) was purchased from the MicrobialType Culture Collection and Gene Bank (MTCC), Chandigarh, India. It is grown on MEP medium plate. VIE was prepared from fungal cell extracts as described by (Sarkate et al., 2018). Briefly, 10 g ground fungal mycelium (Figure 2.1) was added to 1 L acidified water with a final pH of 2. The water extract was then boiled for 1 h, cooled to room temperature and filter

		sterilized. After filtration, the pH of the fungal extract solution was adjusted to 5.0 and the final volume adjusted to 1 L by adding distilled water. This solution was used as the VIE. For elicitation, 2.5 ml VIE (equivalent to 70 mg fungal polysaccharide) was added to the seven-day-old cell suspension culture (50 mL).
<i>Venturia inaequalis</i> spores for infection in green house grown plants	Prepared in laboratory	Conidia were harvested from suspension culture of <i>Venturia inaequalis</i> growing in MEP (as given in Table 2.4) medium. Distilled water is used for washing the conidia followed by centrifugation and finally adding the distilled water. The conidial concentration was made to $\approx 5 \times 10^6$ conidia/ml. On the upper epidermis of leaves of potted plants $\approx 20 \mu\text{l}$ of the conidial suspension were placed. After air drying, the inoculated plants were placed in a moist chamber at 25°C for 48 h and maintained at 25°C. Then inoculated leaves were detached and used for experiments (Holzapfel et al., 2012 ; Ishii et al., 1992).

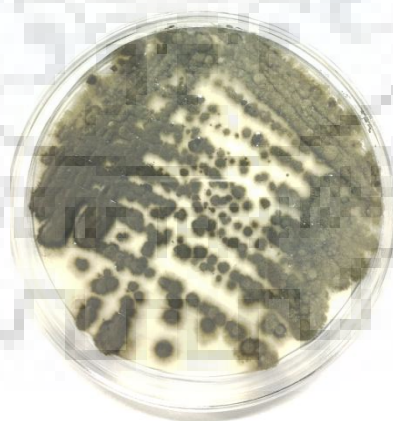


Figure 2.1: *V. inaequalis* mycelium growing on agar plate

2.7. Plant material:

Apple (*Malus domestica*) cultivar 'Shireen' and 'Golden Delicious' were brought from the **Central Institute of Temperate Horticulture** (ICAR-CITH), Srinagar, India. These plants were maintained under temperate condition in a micro-climate control green house (temperature 20 - 22°C and relative humidity of 65± 5%) in Department of Biotechnology of Indian Institute of Technology Roorkee (Roorkee, India). These plants were used for developing callus and cell suspension culture.



Figure 2.2: Apple plants growing in green house.

2.8. Development and validation HPLC method for the determination of biphenyl and dibenzofuran phytoalexins in Rosaceae:

2.8.1. Plant material:

Sorbus aucuparia (mountain ash) cell culture is known to produce biphenyl and dibenzofuran phytoalexins (Liu et al., 2004). In order to develop a rapid and validated HPLC method for simultaneous detection of biphenyl and dibenzofuran phytoalexins, *S. aucuparia* cell culture was used (as a kind gift from Prof. Ludger Beerhues of Technical University Braunschweig, Germany). *Venturia inaequalis* elicitor (VIE) (as described in table 2.19) was used to treat five days old cell cultures of *Sorbus aucuparia* for biphenyl / dibenzofuran phytoalexin induction. 2.5 mL of the VIE (~ 70 mg of fungal polysaccharide) was added to the *S. aucuparia* cell cultures (50 ml). Samples were extracted 48 h post elicitation. Cells were collected by filtration and 2g fresh cell mass was extracted in 4 ml of methanol and centrifuged at 10,000 rpm for 20 min. Supernatant was directly injected into HPLC for analyses of phytoalexins.

2.8.2. HPLC condition:

HPLC analyses were performed on a Shimadzu-HPLC system (Shimadzu Corporation, Kyoto, Japan) equipped with a CBM-20A controller, LC-20AT pump, SPD-20A PDA detector and CTO-10ASvp column oven. Sample injection was made through Rheodyne™ 7725i injection valve with a 20 µl sample loop. Chromatographic separation was achieved on Luna C₁₈ reversed-phase column 250 x 4.6 mm, 5 µm particle size (Phenomenex, Torrance, California, USA) coupled with a Phenomenex Security Guard™ C₁₈ guard column 4 x 3 mm (Torrance, California, USA). The mobile phase was degassed as well as vacuum filtered through 0.45 µm nylon membranes. The mobile phase consisted of an isocratic solvent mixture comprising 1mM TFA in water: methanol [40:60; (v/v)] with a flow rate of 0.5 ml min⁻¹. Detection wavelength was set at 254 nm. Peaks were identified by comparing their retention time and UV-spectra with those of authentic standards. Data was acquired and processed with LC-Solution software (Shimadzu Corporation, Kyoto, Japan) on Windows 7™ platform. Peaks from the plant samples corresponding to aucuparin, noraucuparin and eriobofuran were eluted and subjected to electron spray ionization mass spectrometry (ESI-MS/MS) under negative ion mode for the confirmation of their chemical identity.

2.8.3. ESI-MS-conditions:

ESI-MS analyses were carried out on a QTrap 3200 system (Applied Biosystems/MDS Sciex). HPLC elutes were directly introduced to an ESI source (Turbo V; Applied Biosystems/MDS Sciex) using a Hamilton syringe pump and a flow rate of 5 $\mu\text{l min}^{-1}$. The mass spectrometer was operated in the positive mode with a source voltage and declustering potential of 5.5 kV and 76 V, respectively. Nitrogen gas was used for nebulization, with the curtain gas, gas 1 and gas 2 settings at 10, 14 and 0 respectively. Putative product molecular ion peaks $[\text{M}+\text{H}]^+$ were further analyzed by MS/MS experiments in the enhanced product ion mode of the instrument using nitrogen gas for collision-induced dissociation at the high-level setting. The collision energy was set at 76 V. Compounds were identified by comparison with their reference standards. Data was acquired and processed with Analyst software (version 1.4.2; Applied Biosystems / MDS Sciex).

2.8.4. Chemical synthesis of aucuparin and noraucuparin:

Aucuparin and noraucuparin were synthesized from 3,4,5-trimethoxybiphenyl by following the protocols of [Hüttner et al. \(2010\)](#). Aucuparin was synthesized from 3,4,5-trimethoxybiphenyl by position selective single demethylation (removal of methoxy group at carbon number 4) using MgI_2 reagent ([Bao et al., 2009](#)). The second demethylation reaction was done by using BBr_3 to produce noraucuparin ([Figure 2.3](#)). Chemically synthesized aucuparin and noraucuparin were subjected to GC-MS analyses of their silylated-derivatives. In GC-MS, the temperature program used was: 70°C initial temperature for 3 min, then temperature increased to 300°C at the ramp rate of 10°C/min and finally a 3 min hold at 300°C. Total run time calculated was 29 min. Helium gas of ultra-high purity was used as carrier gas at a flow rate of 1ml/min. Split ratio was 1/10. The MS scan range was set at m/z 80–600 and the 1700 V voltage was set for detector. The purity and correctness of structure of noraucuparin and aucuparin, were confirmed by comparing the mass-spectrum of silylated-derivative of newly synthesized aucuparin and noraucuparin with the previously published data ([Hüttner et al., 2010](#)). Chemical synthesis of aucuparin and noraucuparin was shown below in [figure 2.3](#).

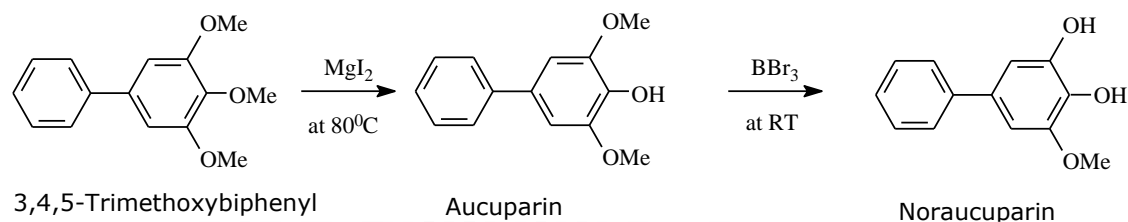


Figure 2.3: Chemical synthesis of aucuparin and noraucuparin

2.8.5. Preparation of standards and plant sample:

Standard stock solutions of 1 mg ml^{-1} of each of aucuparin, noraucuparin and eriobofuran were prepared in aqueous methanol (50:50, v/v). Working standard solutions of $1.5\text{--}400 \text{ }\mu\text{g ml}^{-1}$ range were prepared by dilution of standard stock solution with aqueous methanol (50:50, v/v). All stock solutions were stored at -20°C . For the sample preparation, 5-day old *S. aucuparia* cell culture was treated with *Venturia inaequalis* elicitor and cells were harvested after 48 hour post elicitation (hpe). Liquid nitrogen is used for crushing cell mass and then extracted in methanol at concentration of 1 g ml^{-1} of methanol. The suspension was homogenized for 5 min and then centrifuged at 10,000 rpm for 20 min. The supernatant was collected, filtered through $0.45 \text{ }\mu\text{m}$ filters (Millipore, Bangalore, India) and directly used as sample for HPLC analyses.

2.8.6. Calibration procedure:

Nine different concentration levels were used to prepare the standard calibration plot for noraucuparin, aucuparin and eriobofuran. Noraucuparin and aucuparin was used in the concentration range of $1.5\text{--}400 \text{ }\mu\text{g ml}^{-1}$ whereas eriobofuran concentration was used in the range of $3\text{--}400 \text{ }\mu\text{g ml}^{-1}$. The working calibration concentrations were prepared by diluting the stock solutions with aqueous methanol (50:50, v/v). Each calibration solution was injected into HPLC in triplicate. The calibration curve was prepared by plotting the peak area against the concentration of the compound. The calibration curves, characterized by slope, intercept and correlation coefficient were used to determine the concentration of respective analyte in the sample, limit of detection (LODs), limit of quantification (LOQs) and analytical sensitivity (AS).

2.8.7. Recovery, precision, accuracy and specificity:

The relative recoveries were determined by the method of standard addition. Homogenized elicited cell culture of *S. aucuparia* were spiked with three known concentrations of each of the three standards (50, 100, 200 µg ml⁻¹) before following the described extraction procedure. Three replicate analyses were run for all the three standards at defined concentration level and the peak area ratios of three extracted sample solution at each concentration level were compared with standard solutions to get the percent recovery. These samples were analyzed next day to obtain inter-day precision. The precision was expressed in terms of relative standard deviation (RSD %). The accuracy was expressed as the percentage of the analyte concentration measured in each sample relative to the known amount of analyte spiked to the sample.

2.8.8. Analytical Sensitivity (AS), Limit of detection (LOD) and quantification (LOQ):

Analytical sensitivity was calculated according to ALAMIN program as describe before ([Garcia et al., 1997](#)) Analytical sensitivity was expressed as the ratio of Ss/b , where Ss is the residual standard deviation and b is the slope of the calibration curve. The limit of detection (LOD_{approx}) and limit of quantification (LOQ_{approx}) were determined by the following equations:

$$\text{LOD}_{\text{approx}} = 3 (\text{AS}) \times [(n-2) / (n-1)]^{1/2}$$

$$\text{LOQ}_{\text{approx}} = 10 (\text{AS}) \times [(n-2) / (n-1)]^{1/2}$$

Where n is the number of total measurement for each calibration set and AS is the analytical sensitivity.

2.9. Induction of callus and establishment of suspension cultures of apple:

From the young leaves of apple cv. Golden Delicious primary callus culture was derived. Callus and cell cultures were developed using different combinations of 2,4-D, NAA and kinetin hormones. Immature young green leaves of green house grown apple plants were used for callus induction. Leaves were surface sterilized and then cut into small segments (approx. 10 mm). Leaf segments were put on solid basal LS medium (pH 5.8-6) ([Linsmaier and Skoog, 1965](#)) with 30 g l⁻¹ sucrose, 7 g l⁻¹ agar and growth regulators [2,4-D, NAA and kinetin]. The cultures were kept in dark at 26°C for callus induction. Regular sub-culturing of callus was done at 4-weeks interval. For initiating the cell suspension culture soft friable calli were used, which were grown in the dark in a shaker at constant agitation of 180 rpm. Same media and growth regulator composition was used to develop cell suspension culture, except for non addition of kinetin in the medium. Sub-culturing

was done after every 16 days by transferring 2.5 g of cultured cell mass into 50 ml of fresh LS medium.

2.10. GC-MS based metabolomics of apple cell cultures treated with *Venturia inaequalis* elicitor (VIE):

2.10.1. Cell culture and elicitor-treatment:

Apple (*Malus domestica* cv. Golden Delicious) cell cultures were used for metabolomics analyses. VIE was used to elicit the cell culture. Elicitor-treatment was performed by adding 2.5 ml of the VIE (~ 70 mg of fungal polysaccharide) to the seven-day-old cell apple suspension culture (50 ml). Upon elicitor-treatment, defined time points were used for harvesting cells: 0, 6, 12, 24 and 48 hpe. Instead of the VIE, sterile distilled water is used in the control experiment in similar volume. All experiments were performed with at least three biological repeats.

2.10.2. Extraction of polar metabolites:

The VIE-treated apple cell cultures were harvested by vacuum filtration at defined time points (0-48h). Dried cell mass (2g) were crushed in liquid nitrogen and fine powdered samples were used for metabolite extraction. The extraction of polar metabolites for GC-MS analyses was performed by crushing 2 gm of sample in 4 ml of methanol. In order to identify extraction efficiency, 50 µl of 2-phenylphenol (2 mg/ml methanol stock) was spiked in the extraction mixture as the internal standard (IS) and re-vortexed for 1 min. The homogenized extracts were then centrifuged at 14000 g for 5 min. The resulting supernatant was transferred into a new 1.5 ml tube and was used for metabolite measurements by GC-MS. The extract was dried out in a vacuum concentrator (Labconco, Centrivap; USA) without heating for 2 h followed by freeze drying for 12 h in a lyophilizer. Finally dried material was subjected to derivatization for GC-MS analyses as described by (Lisec et al., 2006). For GC-MS derivatization, 80 µl of N-methyl-N-(trimethylsilyl)-trifluoroacetamide (MSTFA) was added to each vial at 37°C for 30 min. One derivatization reaction was also prepared using an empty reaction tube as a control.

2.10.3. GC-MS analysis:

An Agilent GC-MS system was used for metabolomics analyses. GC-MS system comprising of Agilent 7890A gas chromatograph (Agilent technologies, CA, USA) coupled with an Agilent

5975C mass detector (Agilent technologies, CA, USA) was used. Derivatized sample (1 μ l) was injected in GC-MS by automatic sampler (7683 B series, Agilent Technologies) with a split ratio of 1:10. Samples were separated on fused silica capillary column DB-5 MS (5 % phenyl methyl polysiloxane: 30m x 0.25mm i.d. x 0.25 μ m, Agilent technologies). The temperature program used was: Initial temperature of 80°C for 1 min, then temperature is increased to 220°C at the ramp rate of 10°C/min, followed by temperature increase to 310°C at the ramp rate of 20°C/min and finally a 15 min hold at 310°C. The total time for the run is 34.5 min. Ultra-high pure helium gas was being used as carrier gas with a flow rate of 1ml/min. The inlet temperature and interface temp was set 280°C. The MS unit was tuned to its maximum sensitivity and the total ion current was recorded for mass range was m/z 80–700, and the 1700 V voltage was set for the detector. Replication of three was used for each sample. 7 min of solvent delay was given after which scan was started with scan frequency of 4 S⁻¹ (2.0 HZ). The retention index (RI) was calculated by a set of hydrocarbons (even numbered C₁₂ to C₂₈) by linear interpolation.

2.10.4. Metabolite identification:

Metabolites present in the cell cultures were identified by matching mass spectra of each compound from library (3:1 signal to noise ratio) using the NIST-11 mass spectral library (National Institute of Standards and Technology). For the mass spectra comparison the matching value of the metabolite identity taken was more than 70 percent. For further confirmation spiking of the sample is done with the corresponding pure standard. In order to check for co-elution, the mass spectra of all peaks were analyzed at three different points, beginning, middle and end of each peak width. No coelution detected in any of the identified peaks.

2.10.5. Pre-processing and statistical analysis of metabolite data:

Raw GC-MS data files obtained from Agilent ChemStation™ software were deconvoluted by Automated Mass Spectral Deconvolution and Identification System (AMDIS) using tools available with WsearchPro (www.wsearch.com.au). Metabolite data obtained were further converted into .csv (comma separated values) format before uploading. Finally the data obtained was normalized using internal standard. After that, the data were, log transformed with Pareto scaling (mean-centered and divided by the square root of standard deviation of each variable) followed by normalization before statistical analyses. Multivariate statistical analyses like ANOVA (using Fisher's LSD method; p value < 0.05), principal component analyses (PCA) were performed by

using interactive online tool Metaboanalyst3.0 (<http://www.metaboanalyst.ca>). The output for PCA data consisted of score plots and loading plots, for conceptualizing the contrast between different samples and to understand the cluster separation respectively. A heat map was created using interactive heat map tool of Metaboanalyst 3.0. A simplified metabolic pathway was manually constructed using information from the KEGG database via pathway analyses in Metaboanalyst 3.0.

2.10.6. Quantitative Real-Time PCR:

The VIE-treated apple cell cultures are used for the extraction of total RNA at specified time points (0-48 h) using RNeasy Plant Mini Kit from Qiagen (www.qiagen.com). An aliquot of total RNA (1 µg) was reverse transcribed at 42°C using Oligo (dT) primers and RevertAid H Minus reverse transcriptase (Fermentas; www.thermoscientificbio.com) to form cDNA. Quantitative RT-PCR was performed with the QuantStudio 3 Real-Time PCR System (Thermo Fisher Scientific) using Power Up™ SYBR™ Green Master Mix (Applied bio systems) following the manufacturer's instruction (Table 2.19 a). PCR program for each gene is given in Table 2.19 b. Melt-curve analyses was performed to evaluate gene-specific amplification. Six serial dilutions of cDNA are used from all the samples for checking the amplification and correlation efficiencies of each PCR. For relative quantification cycle threshold values are converted into raw data with the help of PCR efficiency. Expression of the apple genes cv. Golden Delicious viz, *phenylalanine ammonia-lyase (Md PAL)*, *flavanone 3-hydroxylase (Md F3H)*, *alternative oxidase (Md AOX)* and *biphenyl synthase isoform 3 (Md BIS3)* were assessed using the gene-specific primers given in Table 2.18 (PAL: primers 8 forward and 9 reverse; F3H: primers 17 forward and 18 reverse; AOX: primers 19 forward and 20 reverse; BIS3: primers 10 forward and 11 reverse). Primers were designed based on the sequence of corresponding apple unigene present in GDR (Genome database of Rosaceae; www.rosaceae.org). The reference gene apple *actin* used as an internal control for all the samples for normalization (primers 21 forward and 22 reverse). Scaling of expression level was performed in relation to the respective mRNA expression levels in the control (0h) cells, which was put 1. The technical repeats were done three times. The mathematical model (Pfaffl, 2001) was used for the calculations of efficiency and gene expression level. In Pfaffl method, following algorithm was used to calculate the Ct differences. The relative expressed level was calculated based on comparison with a reference gene.

$$\text{Ratio} = (E_{\text{target}})^{\Delta C_{t_{\text{target}}(\text{control} - \text{sample})}} / (E_{\text{ref}})^{\Delta C_{t_{\text{ref}}(\text{control} - \text{sample})}}$$

Table 2.19a: Composition of qPCR reaction.

Component	Volume	Remarks
Power Up™ SYBR™ Green Master Mix (2X)	5 µl	SYBRGreen I Dye, AmpliTaq Gold DNA Polymerase, dNTPs with dUTP and buffer components.
Forward primer (10 pmole)	0.5 µl	Final concentration 0.125 µM
Reverse primer (10 pmole)	0.5 µl	Final concentration 0.125 µM
Template DNA	1 µl	Final concentration 1 ng
Water nuclease free	3 µl	Final volume to 10 µl

Table 2.19b: qPCR reaction program.

Steps	Temperature °C	Time	Remarks
Initial denaturation	95	2 min	Denaturation and activation of the hot start Taq polymerase
Denaturation	95	15s	X 40 cycles
Annealing	50 (<i>PAL</i>) 52 (<i>F3H</i>) 54 (<i>AOX, Actin</i>) 55 (<i>BIS 3</i>)	1 min	
Extension	72	1 min	
Final extension	72	1 min	

2.11. Molecular cloning and functional analyses of a *cinnamate-CoA ligase (CNL)* from cell suspension culture of apple cv. Golden Delicious:

2.11.1. Cell cultures and plant treatment:

Seven-day-old cell cultures, growing in log-phase (Figure 2.4) were treated with the *Venturia inaequalis* elicitor (VIE) as describe before in table 2.18. The VIE-treated cultures were taken at post-elicitation time points [0-72 hpe] to measure the quantity of biphenyl phytoalexins and gene expression levels. Instead of the VIE, an equal amount of sterile distilled water was used in the control experiment. A minimum of three replicates were used for each treatment. In order to check scab-induced phytoalexin accumulation in intact plants, greenhouse-grown apple plants were infected with scab fungus. For scab-infection one scab-resistant (cv. Shireen) and one moderately

scab-susceptible (cv. Golden Delicious) apple cultivar was selected. Immature leaves of both the cultivars were inoculated with conidial suspension (5×10^6 conidia / mL) of *V. inaequalis*, as described previously (as given in table 2.18). Infected leaves and shoots (internode region between two successive infected leaves) at various stages were used for the RNA isolation and phytoalexin analyses [0-480 hours post infection (hpi)]. Infected plants were routinely photographed till 20 days post infection to capture disease symptoms.

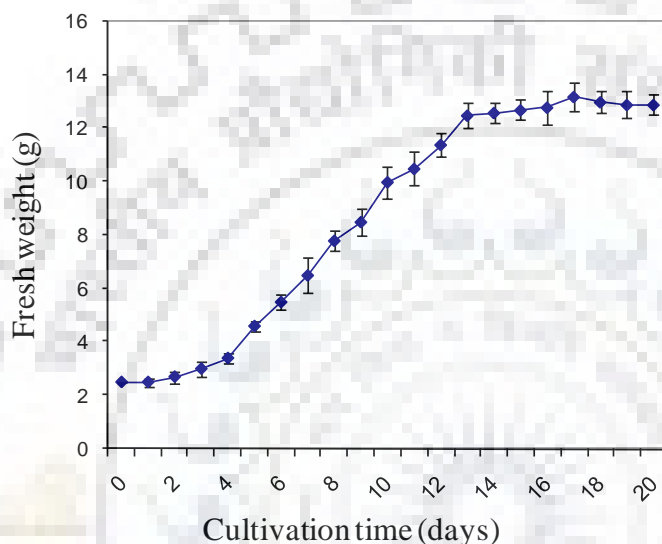


Figure 2.4: Growth curve of *M. domestica* cv. Golden Delicious cell suspension culture based on fresh weight. Culture was initiated at day zero with 2.5 g cell mass.

2.11.2. Extraction and HPLC analysis of biphenyl phytoalexins:

Elicitor-treated cell cultures were taken at defined post elicitation time points (0,3, 6, 9,12, 18, 24, 36, 48, and 72 h) and kept at -80°C till further analyses. Frozen cell culture (ca. 2g) and freeze-dried apple shoots (0-20 days) were extracted for phytoalexins isolation using 4 mL of methanol. Extract was centrifuged at 10,000 rpm for 15 min and the supernatant was used for phytoalexin analyses. Biphenyl phytoalexins were separated by using a PhenomenexTM (Torrance, USA) Luna C₁₈ column (RP-Hydro, 4 μm , 250 x 4.6 mm) coupled with a Shimadzu-HPLC system (Shimadzu Corporation, Kyoto, Japan) equipped with a CBM-20A controller, LC-20AP pump, SPD-M20A PDA detector. HPLC conditions and detection procedures were kept similar as described before (Teotia et al., 2016). Retention time and UV-spectra of the biphenyls were compared with the authentic standards.

2.11.3. Isolation and cloning of apple cDNA encoding *MdCNL*:

Apple genome sequence (version 0.1 cDNA) (Velasco et al., 2010) was searched for putative *cinnamate-CoA-ligase* (*MdCNL*) sequence involved in the conversion of cinnamic acid to cinnamoyl-CoA via the TBLASTN server of the GDR (Genome Data Base of Rosaceae: www.rosaceae.org), using available published plant benzoate metabolism specific CoA-ligase sequences as queries (Table 2.20). Based on bioinformatics processing, apple unigene MDP0000576682 served as the most promising candidate to design 5' and 3' primers for the cds amplification of the putative *MdCNL* cDNA from the elicited cell culture of apple cv. Golden Delicious.

Table 2.20: Homology of apple unigenes present in GDR with other plant secondary metabolite specific *cinnamate-CoA-ligase* (CNL) sequences.

Candidate CoA-ligase sequence	Accession No.	<i>M. domestica</i> unigenes sharing highest identity based on tblastn search
Cinnamate CoA-ligase from <i>Hypericum calycinum</i> [Gaid et al., 2012]	AFS60176	MDP0000684928, MDP0000576682 (~73%)
Cinnamate CoA-ligase from <i>Petunia hybrida</i> [Klempien et al., 2012]	AEO52693	MDP0000684928, MDP0000576682 (~67%)
Cinnamate CoA-ligase (BZO1) from <i>Arabidopsis thaliana</i> [Kliebenstein et al., 2007]	AQX17825.1	MDP0000684928, MDP0000576682 (62%)
Cinnamate CoA-ligase / benzoate-CoA-ligase from <i>Clarkia breweri</i> [Functionally un-characterized sequence]	AEO52695	MDP0000684928, MDP0000576682 (~68%)

2.11.3.1. Reverse transcription:

VIE-treated apple cell cultures were used for extraction of total RNA at different post elicitation time points (0–72 h) using the RNeasy Plant Mini Kit. Genomic DNA contamination was removed by on-column DNase I (Qiagen) treatment. Total RNA (1 µg) was reverse transcribed at 42°C with Revert Aid H Minus Moloney murine leukemia virus reverse transcriptase and an oligo (dT)

primer, as per manufacturer instruction (Table 2.21).The resulting cDNA pools were stored at -20°C till further use.

Table 2.21. Reverse transcription (RT) reaction mixture for cDNA synthesis.

Mix 1	Volume	Mix 2	Volume
RNA 1 µg	5 µl	10 X RT buffer	2 µl
Oligo dT primer (3'CDS) 10 pmol	1 µl	dNTPs (1 mM each)	2 µl
		RNase inhibitor (10 µl)	0.5 µl
Water	6.5 µl	Reverse transcriptase (200 µl)	1 µl
		Water	2 µl

Mix 1 was added in PCR tube and centrifuged briefly, incubated in PCR for 5 min at 65°C, thereafter kept on ice for 5 min. Then mix 2 was added and mixed well by providing short spin. This mixture was incubated in PCR for 90 min at 42°C and reaction terminated at 70°C for 10 min. cDNA was ready for use and divided in aliquots to avoid multiple freeze/thaw cycles and stored at -80°C

2.11.3.2. PCR amplification and gel electrophoresis:

MdCNL coding sequence was PCR amplified from the elicited (6 hpe) apple cell culture cDNA pool using Phusion High-Fidelity DNA polymerase. The forward primer 1 (with a *Nhe*1 restriction site) and reverse primer 2 (with a *Kpn*1 restriction site) (Table 2.17) was used to PCR amplify *MdCNL*. The PCR programs were set as: 98°C for 30 s, followed by 30 cycles of 98°C for 10 s, 65°C for 30 s and 72°C for 60 s, and 10 min final extension at 72°C (Table 2.22). Gel was run to check the expected size (1725 bp). The PCR product of 1725 bp was purified using GenElutePCR clean-up kit.

3' UTR was PCR amplified using gene specific forward primer 3 (Table 2.17) designed 91 bp upstream the stop codon, following 3' race protocol from SMART RACE cDNA Amplification Kit. The 5' UTR sequence was amplified using a genomic DNA fragment (genomic DNA was isolated using DNeasy Mini Kit) with gene specific forward primer 4 (derived from 200bp upstream segment of MDP0000576682) and reverse primer 5 (Table 2.17). In case of greenhouse

grown plants, *MdCNL* cds was amplified from a reverse-transcribed RNA, isolated from the shoots (internodal segment) of apple plants inoculated with conidiospores of *V. inaequalis* after 48h of infection.

Table 2.22: PCR reaction program.

Steps	Temp.°C	Time	Remarks
Initial denaturation	98	30 s	Denaturation and activation of the hot start Taq polymerase
Denaturation	98	10 s	X 30 cycles
Annealing	65	30 s	
Extension	72	1 min	
Final extension	72	10 min	

2.11.3.3. Agarose gel electrophoresis:

PCR amplified DNA was separated on agarose gel. This is based on the principle that small DNA molecules migrate faster than larger molecules through the agarose matrix under effect of electric current. In this study, 2% agarose gel was used to analyze samples shorter than 500 bp length. For larger sizes, 1% agarose gel is used. Ethidium bromide is used for visualization of bands. It intercalates in nucleic acid molecules and its fluorescence increases 20 fold after binding to nucleic acid molecules.

2.11.3.4. DNA purification from agarose gel or after digestion reactions:

DNA fragments of the right size were extracted from gel using a kit. First, the gel matrix was solubilized in a buffer at 50°C. The solution was transferred to Nucleospin column (Qiagen) where DNA binds to the silica membrane, but other components were washed away using wash buffer. Finally, DNA was eluted by water or elution buffer. In case of purification of DNA fragments after digestion reactions, the reaction product was mixed with wash buffer instead of gel solubilizer buffer. Then the process was continued as mentioned before.

2.11.3.5. Restriction digestion:

NheI (forward primer) and *KpnI* (reverse primer) restriction sites were present in the *MdCNL* and also present in MCS of pRSET B expression vector. The resulting fragment was digested with *NheI* and *KpnI* and then ligated into the *NheI* / *KpnI* linearized expression vector pRSET B. pRSET B was designed for expression of His-tag protein in *E. coli*. DNA insert was positioned in correct frame. This sequence includes an ATG translation initiation codon and permits the use of affinity chromatography for the purification of fusion protein. Digestion reaction was listed in [table 2.23](#). Reaction was incubated at 37°C for 2 h. Following digestion, the gel-purification of the digested vector was performed. Both digestion products were purified using Gene elute PCR purification kit to exclude residual protein and salts which may inhibit the ligation reaction.

Table 2.23: Components for restriction digestion reaction.

Component	Volume (Insert)	Volume (Vector)
0.2 µg purified DNA insert or vector	10 µl	5.5 µl
10 × reaction buffer Nhe1	2.0 µl	1.0 µl
Nhe1	1.0 µl	0.5 µl
Kpn1	4.0 µl	2.0 µl
Nuclease free water	3.0 µl	1.0 µl

The digested vector is subjected to dephosphorylation using shrimp alkaline phosphatase. Dephosphorylation of the 5' group of the vector ends prevent self-ligation of the vector during the ligation reaction (Table 2.24).

Table 2.24: Components for de-phosphorylation reaction.

Component	Volume (Insert)
pRSET B vector solution	3.0 µl
10 × reaction buffer	2.0 µl
Shrimp Alkaline phosphatase enzyme (1 U/1 µl)	1.0 µl
Nuclease free water	14.0 µl

The reaction was incubated in PCR at 37°C with lead temperature 60°C for 30 min. The reaction was terminated at 65°C for 5 min, which later used directly for ligation.

2.11.3.6. Ligation of DNA fragments:

To promote the ligation reaction, the insert amount should be 2-6 fold more than the vector amount. The vector and insert are mixed together in PCR tubes and kept at 55°C for 5 min, then chilled on ice. This step is done to avoid mispriming of the sticky ends. The tubes are centrifuged and then the buffer and the enzyme are added and the reaction is incubated by 4°C overnight. A negative control reaction which contains all the components except the insert is done in parallel.

Table 2.25: Components for ligation reaction.

Component	Volume
Digested vector 50 ng	1 μ l
Digested insert 50 ng	6 μ l
10x ligation buffer	1 μ l
T4-DNA-Ligase (5U/ μ l)	0.5 μ l
Nuclease free water up to	10 μ l

2.11.3.7. Transformation of DNA products into *E.coli*:

Ligation reaction (5 μ l) is used to transform 50 μ l competent cells. Transformations occurred into *E. coli* DH5 α and *BL21 (DE3)pLysS*. Chemically competent cells are prepared in the laboratory by calcium chloride method. Ligation product (5 μ l) is added to DH5 α competent cells (50 μ l) and left for 25 min on ice, then transferred to a water bath at 40°C for 45 s followed by immediate incubation on ice for 2 min. LB medium (250 μ l) and bacterial suspension is shaken by 37°C for one and a half hours. The whole bacterial suspension is plated on LB-agar plates containing ampicillin. Transformation of plasmid into BL-21(DE3) follows the same procedure except that the heat shock time is reduced to 20 s and the selection medium contains chloramphenicol, in addition to ampicillin. DH5 α produces a high yield of plasmid while the BL-21 strain is suited for expression of proteins.

2.11.3.8. Isolation of plasmid DNA by alkaline hydrolysis:

A single colony of the transformed DH5 α was inoculated into 5 ml LB medium containing 20 μ g/ml ampicillin and grown over night at 37°C. On the following day, 4 ml cultures were centrifuged. Bacterial pellets were suspended in ice-cooled buffer I (300 μ l) containing RNase A, then buffer II (300 μ l) was added and the bacterial suspension was inverted cautiously 6 times and left on ice for 5 min. Lysis of the cell wall took place in addition to denaturation of large chromosomal DNA. RNA is destroyed by RNase I. Precipitation of proteins and denaturation of large chromosomal DNA were done by adding buffer III (300 μ l), cautious inversion (6 times) and incubation on ice for 20 min. Centrifugation at 13000 rpm for 10 min was done to exclude the denatured proteins and DNA. The supernatant containing the DNA solution (800 μ l) was

transferred to a new eppendorf tube. Residual contaminants and hydrolysed protein were extracted by vortexing with 800 µl chloroform followed by centrifugation at 13000 rpm for 10 min. The aqueous layer was transferred to a new eppendorf tube. Isopropanol (0.7 volume) was added, vortexed and followed by centrifugation at 13000 rpm for 30 min to precipitate plasmid DNA. The pellets were washed with 70% ethanol (500 µl) followed by centrifugation at 13000 rpm for 10 min. The supernatant is discarded and the plasmid pellets are dried by 37°C and then dissolved in 30 µl water.

2.11.4. Heterologous expression of *MdCNL* in *E. coli*:

The PCR product for *MdCNL* coding open reading frame (ORF) sequence was double digested with *Nhe*1 and *Kpn*1 restriction enzymes and ligated into the pRSET B expression vector. After sequence verification of ORF in both the strand, *MdCNL*-pRSET B expression construct was heterologously expressed in *Escherichia coli* BL21 (DE3)-RIL cells (Stratagene) as N-terminal His₆-tagged protein. The induction of expression and affinity purification of recombinant *MdCNL* protein (64 kDa) on Ni-NTA agarose was done as described before (Liu et al., 2007). Bacterial cell wall was disrupted by sonication for 5 min at duty cycle 40% and output control of 1.5. Ni-NTA slurry (200 µl) was added to 3 ml of the cleared lysate. All procedures were carried out at 4°C. After shaking at 4°C for 1 h, put the mixture into a column. Affinity purification started with 4 ml washing buffer (four times 1 ml each). 3.5 ml elution buffer is used for eluting the His₆-tagged-fusion protein. Imidazole (used for elution) was removed from the eluate by gel filtration through a PD₁₀ column equilibrated with 0.1 M Tris-HCl pH 7.5 buffer. SDS-PAGE was routinely performed to check the efficiency of affinity purification. Protein concentrations were determined by Bradford reagent (Bradford 1976) using bovine serum albumin as a standard.

2.11.5. SDS-PAGE gel electrophoresis:

SDS-PAGE was used for confirming the expression of protein. The 12% separating gel was used for the high resolution of proteins. Protein samples to be analyzed were added with protein loading buffer in a 1:1 ratio and denatured at 95°C for 5 min. A prestained 100 bp to 10 kDa protein ladder is used to determine the molecular mass of the separated protein. The running conditions were 25 mA in the stacking gel, 35 mA in the separating gel and 200 V supplied by a Power Pack (Thermo Fisher Scientific). To check for successful protein expression, the gel was stained with coomassie

blue stain for 2-3 hrs at room temperature, followed by destaining solution until clear bands appeared.

2.11.6. *Md*CNL activity assay:

*Md*CNL activity was tested by spectrophotometric method where activity was calculated by measuring the rate of increase in the absorbance at 311 nm due to formation of the cinnamoyl-CoA. The standard assay in 100 mM potassium phosphate buffer (pH 6.5) consisted of 0.4 mM cinnamic acid, 2.5 mM ATP, 2.5 mM MgCl₂ and 10 µg affinity purified recombinant *Md*CNL protein, in final assay volume of 1 mL. The reaction was started at 25°C by addition of 0.2 mM CoA and cinnamoyl-CoA formation was observed by recording the change in absorbance at 311 nm up to 5 min. Cinnamate-CoA-ligase activity was calculated using the previously reported extinction coefficient of cinnamoyl-CoA ($\epsilon = 22 \text{ cm}^{-1} \text{ mM}^{-1}$; Gross and Zenk, 1966; Stöckigt and Zenk, 1975). In separate assays, a range of phenolic acids (4-coumaric acid, caffeic acid, ferulic acid and sinapic acid) with related structure were tested as potential substrate for *Md*CNL, keeping the other assay conditions unchanged. The activities of these assays were calculated with the help of extinction coefficient (ϵ) values of the corresponding CoA esters reported earlier (Gross and Zenk, 1966; Gaid et al., 2012). For determination of pH optima, pH values from 5.5 to 11.5 were tested. Evaluation of other incubation parameters were examined including incubation temperatures and times, and protein concentrations in the range from 20-60°C, 1-20 min and 1 - 40 µg protein, respectively. Enzyme stability was tested by keeping the protein at 4°C and -80°C for 24 h. Stability was further tested by storing recombinant protein at -80°C for six months, with or without addition of glycerol (20%, v/v).

2.11.7. Analyses of enzymatic product by ESI-MS:

The chemical identity of CNL product, cinnamoyl-CoA was further confirmed by ESI-MS analyses of the enzymatic product. For ESI-MS analyses, the assay volume used was 5 mL rather than 1 ml and incubated for 2 hrs at room temperature, the CoA ester formed was purified and analyzed following the methods previously described (Beuerle and Pichersky, 2002a). ESI-MS analysis was performed negative ion mode on a 3200 QTrap mass spectrometer (Applied Biosystem/MDS SCIEX) equipped with an electrospray ionization interface (ESI, Turbo V). For data acquisition and evaluation analyst software version 1.4.2 (Applied Biosystems/MDS SCIEX) was used.

2.11.8. Substrate specificity test:

Spectrophotometric assay is recommended to screen the substrate preference when the absorption maxima of the product is far from the CoA maxima (λ 261nm), which is not applicable for benzoate CoA esters. Due to limitation of spectrophotometric assay to test substrate specificity with a wide range of potential CNL substrate, we have carried out luciferase-based assay (Gaid et al., 2012). For luciferase assay, standard reaction volume was reduced to 200 μ l, which consisted of 200 μ M potential carboxylic acid substrate, 250 μ M MgCl₂, 50 μ M ATP, 5 μ g purified protein, 100 μ M CoA and 100 mM potassium phosphate buffer pH 6.5. This reaction mixture was incubated at room temperature for 2 h and then 2 μ l of mixture was taken out and diluted with a dilution buffer (100 mM Tris-HCL pH 7.5) to 100 μ l. Diluted mixture (100 μ l) was put into a 96-microwell plate and then a second reaction mixture (100 μ l) consisting of 1 μ g firefly luciferase, 4.6 μ g luciferin in 100 mM Tris-HCl pH 7.5, was added. After gentle shaking and 10 sec time delay, luminescence was measured by a luminometer (FLUOstar OPTIMA Labtech spectrophotometer, Germany). The data obtained was expressed as relative luciferase activity, which is inversely proportional with the remaining of ATP concentration. Normalization of ATP quantification was done by control reaction having heat denatured *MdCNL* and without any substrate. The control reaction does not use any ATP and thereby its value was given as 100%.

2.11.9. Analyses of Kinetic parameters of *MdCNL*:

For kinetic parameter determination, different concentrations of cinnamic acid and 4-coumaric acid (1 - 1000 μ M) at a fixed concentration of ATP (2.5 mM), CoA (0.2 mM), MgCl₂ (2.5 mM) were used. K_m value for ATP was measured by varying the concentration from 1 to 1000 μ M keeping a fixed concentration of cinnamic acid (0.4 mM), CoA (0.2 mM) and MgCl₂ (2.5 mM). Similarly, K_m value for CoA was calculated by varying the concentration from 1 to 1000 μ M keeping fixed concentration of cinnamic acid (0.4 mM), ATP (2.5 mM) and MgCl₂ (2.5 mM). For all the kinetic calculations experiments are done in triplicate. The K_m and V_{max} kinetic parameters were calculated by the Hanes plot using the Hyper 32 program.

(<http://homepage.ntlworld.com/john.easterby/software.html>).

2.11.10. Phylogeny analyses:

Functional plant CoA-ligase sequences, which are related to *cinnamate-CoA-ligase* reactions were used to re-construct a phylogenetic tree. The accession numbers and the sequences were given in Table 2.26. The phylogenetic tree was created following the neighbor-joining algorithm using MEGA 5.05 software (www.megasoftware.net) with 1,000 bootstrap supports (Tamura et al., 2011). The Poisson correction method was used to compute the evolutionary distances (Zuckerandl and Pauling, 1965; Sircar et al., 2015) and the units used is the number of amino acid substitutions per site. Gaps and missing data were abolished by the pair-wise deletion method.

Table 2.26: Accession numbers of amino acid sequences used for phylogenetic reconstruction. *MdCNL* sequence is represented by its nucleotide accession number.

Sequence	Accession No.
<i>Arabidopsis lyrata</i> fatty acid CL	XP_002880289
<i>Medicago truncatula</i> OSBZL8	XP_003616108
<i>Medicago truncatula</i> OSBZL7	XP_003616110
<i>Glycine max</i> OSBZL2	XP_003544347
<i>Glycine max</i> OSBZL1	XP_003518357
<i>Medicago truncatula</i> OSBZL6	XP_003616111
<i>Medicago truncatula</i> OSBZL5	XP_003609738
<i>Medicago truncatula</i> OSBZL4	XP_003629166
<i>Medicago truncatula</i> OSBZL3	XP_003610948
<i>Medicago truncatula</i> OSBZL2	XP_003610946
<i>Clarkia breweri</i> BZL/CNL	AEO52695
<i>Brassica rapa</i> subsp. <i>Pekinensis</i> BZL	ACR10278
<i>Panicum virgatum</i> 4CL1	ACD02135
<i>Arabidopsis thaliana</i> CNL	Q9SS01
<i>Petunia hybrida</i> CNL	AEO52693
<i>Hypericum calycinum</i> CNL	AFS60176
<i>Medicago truncatula</i> OSBZL1	XP_003600627
<i>Zea mays</i> 4CL	AAS67644

<i>Cenchrus purpureus</i> 4CL	AEW12812
<i>Oryza sativa</i> 4CL	CAA36850
<i>Lolium perenne</i> 4CL3	AAF37734
<i>Lolium perenne</i> 4CL2	AAF37733
<i>Neosinocalamus affinis</i> 4CL	ACA09448
<i>Camellia sinensis</i> 4CL	ABA40922
<i>Prunus avium</i> 4CL	ADZ54779
<i>Sorbus aucuparia</i> 4CL3	ADE96997
<i>Rubus idaeus</i> 4CL3	AAF91308
<i>Gossypium hirsutum</i> 4CL2	ACZ06243
<i>Populus trichocarpax deltoids</i> 4CL4	AAK58909
<i>Lolium perenne</i> 4CL1	AAF37732
<i>Glycine max</i> 4CL3	AAC97389
<i>Glycine max</i> 4CL4	CAC36095
<i>Glycine max</i> 4CL2	NP_001236236
<i>Agastache rugosa</i> 4CL	AAT02218
<i>Lithospermum erythrorhizon</i> 4CL	BAA08366
<i>Ruta graveolens</i> 4CL1	ABY60842
<i>Arabidopsis thaliana</i> 4CL3	NP_849844
<i>Scutellaria baicalensis</i> 4CL	BAD90936
<i>Petroselinum crispum</i> 4CL1	P14913
<i>Vanilla planifolia</i> 4CL	O24540
<i>Nicotiana tabacum</i> 4CL2	O24146
<i>Nicotiana tabacum</i> 4CL	AAB18638
<i>Solanum tuberosum</i> 4CL2	P31685
<i>Solanum tuberosum</i> 4CL1	P31684
<i>Nicotiana tabacum</i> 4CL1	O24145
<i>Salvia miltiorrhiza</i> 4CL2	AAP68991
<i>Sorbus aucuparia</i> 4CL1	ADF30254
<i>Populus trichocarpax deltoids</i> 4 CL3	AAK58908
<i>Ruta graveolens</i> 4CL2	ABY60843

<i>Arabidopsis thaliana</i> 4CL2	NP_188761
<i>Arabidopsis thaliana</i> 4CL1	NP_001077697
<i>Rubus idaeus</i> 4CL1	AAF91310
<i>Salvia miltiorrhiza</i> 4CL1	AAP68990
<i>Populus trichocarpaxdeltoids</i> 4CL1	AAC39366
<i>Populus trichocarpax deltoids</i> 4CL2	AAC39365
<i>Rubus idaeus</i> 4CL2	AAF91309
<i>Sorbus aucuparia</i> 4CL2	ADE96996
<i>Amorpha fruticosa</i> 4CL	AAL35216
<i>Glycine max</i> 4CL1	NP_001236418
<i>Medicago truncatula</i> 4CL	XP_003637266
<i>Malus domestica</i> CNL	MG334585
<i>Physcomitrella patens</i> 4CL1	ABY21312
<i>Selaginella moellendorffii</i> 4CL	EFJ29005
<i>Pinus taeda</i> 4CL	
<i>Pinus massoniana</i> 4CL	AAB42383
<i>Pinus radiata</i> 4CL	ACF35279
<i>Pseudotsuga menziesii</i> 4CL	AAQ05340
<i>Picea wilsonii</i> 4CL	ADC97166
<i>Nothotsuga longibracteata</i> 4CL	AAF74016
<i>Abies beshanzenensis</i> 4CL	
<i>Tsuga canadensis</i> 4CL	AAF74019
<i>Larix gmeliniivar. Olgensis</i> 4CL	AAQ05330

2.11.11. Quantitative Real-Time PCR of *MdCNL*, *MdPAL* and *MdBIS* expression:

Total RNA was isolated from 100 mg sample prepared from VIE-treated cell cultures of cv. Golden Delicious and *V. inaequalis* infected leaves and shoots of cv. Shireen and cv. Golden Delicious. Total RNA (2 µg) was reverse transcribed at 42°C to synthesize cDNA. Quantitative RT-PCR (qPCR) was done in QuantStudio 3.0 Real-Time PCR system (Thermo Fisher Scientific) using PowerUp SYBR Green Master Mix (Thermo Fisher Scientific) following the method given

in the manufacturer's instructions. Differential expression levels of *MdPAL*, *MdCNL* and *MdBIS3* genes were tested in the VIE-treated Golden Delicious cell cultures at defined post elicitation time points. Differential expression *MdCNL* gene was monitored in the scab-infected green house grown Shireen and Golden Delicious plants. Primer details for Real-Time PCR analyses were listed in Table 2.17. The $\Delta\Delta C_t$ mRNA quantification method (Pfaffl, 2001) was used to analyze the differentials expression levels of target genes. Expression of the *MdCNL* gene was calculated using the gene-specific primers 6 (forward) and 7 (reverse). Primer 8 (forward) and 9 (reverse) were used to analyze the expression of *MdPAL* gene. Forward primer 10 and reverse primer 11 were used to analyze the expression level of the phytoalexin- specific biphenyl synthase isomer 3 gene (*MdBIS3*; Hüttner et al., 2011). The mRNA of the *MdProfilin* reference gene (forward primer 12 and reverse primer 13) was used to normalize the samples, which served as an internal control sample for each line. PCR program was set as given in table 2.27. The relative change in gene expression level was calculated using the arithmetic formula $2^{-\Delta\Delta C_t}$ in combination with expression values normalized to the endogenous reference *profilin* gene. Gene-specific real-time qPCR efficiency was calculated by a standard curve using a dilution series of the cloned amplicon. In case of cell culture, scaling of target gene expressions were performed by taking VIE treated samples (0h) as a calibrator. In case of scab-infected green house grown plants, scaling was done in relation to the respective mRNA expression levels of *MdCNL* in mock inoculated stems/leaves, which were set to 1. Biological and technical experiments were done in triplicates.

$$\text{Ratio} = (E_{\text{target}})^{\Delta C_t_{\text{target}}(\text{control} - \text{sample})} / (E_{\text{ref}})^{\Delta C_t_{\text{ref}}(\text{control} - \text{sample})}$$

Table 2.27: qPCR reaction program.

Steps	Temperature°C	Time	Remarks
Initial denaturation	95	2 min	Denaturation and activation of the hot start Taq polymerase
Denaturation	95	15 s	X 40 cycles
Annealing	54 (<i>CNL, Profilin</i>) 50(<i>PAL</i>) 55 (<i>BIS 3</i>)	30 s	
Extension	72	30 s	
Final extension	72	1 min	

2.11.12. Identification of molecular weight of *MdCNL* by Matrix-Assisted Laser Desorption/Ionisation Mass Spectrometry (MALDI-MS):

The purified recombinant protein sample was eluted and deposited onto the target plate using Sinapic acid (Sigma-Aldrich) matrix prepared in 70% acetonitrile (MS grade Sigma-Aldrich) and 0.1% trifluoroacetic acid (TFA). Bruker ultrafleXtreme MALDI-TOF/TOF mass spectrometer equipped with smartbeam-II laser (Bruker Daltonics, Billerica, MA, USA) was used for analyzing the sample, which was operated in linear positive mode. FlexControl 3.4 and FlexAnalysis 3.4 software (Bruker Daltonics, Billerica, MA, USA) was used for spectral acquisition and analysis.

In addition to the protein of interest (approximately 64kDa), there was an additional peak (approximately 67kDa) was observed in the spectrum as indicated by asterix (red). To identify the protein (contaminant), eluted fraction was run on SDS-PAGE and the protein band indicated by arrow (approximately 67kDa) was excised for identification by MALDI-TOF. The gel band was excised and washed thrice in a solution of 50% v/v acetonitrile and 25 mM NH₄HCO₃, pH 7.8 at 37°C for 10 min. Subsequently, speedy-vac (Eppendorf, country) was used at room temperature to dry the gel band and finally recovered with 8 µl (15ng/µl), of sequencing grade trypsin solution (Sigma Aldrich, USA) and overnight digested at 37°C. 10 µl of 0.1% (v/v) TFA was used for

recovering the peptides from gel by sequential extractions and subsequently it is dried. Two microlitres of extract were deposited onto the MTP 384 ground steel MALDI target plate using 5 mg/ml α -cyano-4-hydroxy cinnamic acid (Bruker Daltonics, Germany) in 50% acetonitrile and 0.1% v/v TFA. Peptide mass fingerprint (PMF) and time-of-flight (TOF) -MS analyses were performed in reflectron mode. Spectral acquisition and analysis was performed using above mentioned software.

Protein identification was carried out by comparing of mass spectra to entries in the Swiss-Prot database using Mascot (2.4.1. Matrix Science, UK). Mascot MS/MS ion search criteria were as follows: taxonomy *E. coli* bacteria. Trypsin digestion allowing up to one mis-cleavage, variable modification - oxidation of methionine, cysteine as carboxyamidomethylation or propionamide, peptide tolerance of 200 ppm and MS/MS tolerance of 0.7 Da. The “ion score cutoff” was manually set to 20, thereby eliminating the lowest quality matches. A probability-based Mowse score using $-10 \log (P) > 19$ indicated identity ($p < 0.05$). To eliminate false positives, 1% FDR was applied at both protein and peptide level.

2.11.13. Agrobacterium-mediated transient expression and sub-cellular localization:

In order to check sub-cellular localization of *MdCNL*, we performed co-localization studies using transiently expressed *MdCNL* protein in *Nicotiana benthamiana* leaves. *MdCNL* transformation constructs were generated through the Gateway cloning system (Invitrogen). In order to make the CNL coding region compatible with the Gateway cloning system, PCR amplification of *MdCNL* ORF involved either a stop codon (primer 14, forward primer *attB1*; primer 15, reverse primer *attB2a*) or without stop codon (primer 14, forward primer *attB1*; primer 16, reverse primer *attB2b*) for subsequent generation of N and C terminal fusions with YFP, respectively. Primer details are given in [Table 2.17](#). The modified PCR products (CNL, with stop codon; CNL-DEL, without stop codon) were first cloned into a pDONR/Zeo donor vector by the Gateway BP reaction to create entry clones and then into the destination vectors by the Gateway LR reaction (Invitrogen). The entry clone was subsequently used to transfer the coding sequence of *MdCNL* into the pEarly-Gate 104 destination vector to generate construct with N-terminal fusion of *MdCNL* with YFP (35S::YFP-CNL). Accordingly, the coding sequence of the CNL-DEL entry clone was transferred to the pEarly-Gate 101 destination vector to generate C-terminal fusion construct of CNL (35S::CNL-DEL-YFP). The binary Gateway expression vectors bearing the YFP-CNL and CNL-

DEL-YFP were transferred to the *A. tumefaciens* strain C58C1 by electroporation as exactly described before (Gaid et al., 2012). For co-localization, *A. tumefaciens* C58C1 cultures harboring YFP-CNL, CFP-PTS1 (peroxisomal marker construct; (Nowak et al., 2004) were mixed 1:1: (v/v) prior to infiltration. 10-mL needleless syringe was used for carrying the leaf infiltration. After 36 h of infiltration, the leaves of *N. benthamiana* were looked for YFP/CFP expression by confocal laser scanning microscopy (LSM-780 AxioObserver; Carl Zeiss, Germany). The argon laser (488 nm for both YFP and autofluorescence of chlorophyll, 458 nm for CFP) and the main beam-splitter (458/514/594 nm) were used. Fluorescence was detected with filter sets on channel 1 for CFP with band pass 448 to 502 and on channel 2 for YFP with band pass 517 to 588. Thered chlorophyll autofluorescence was selected by the META channel. The spectral signature of fluorophores was observed by the λ mode. The samples were analysed using a Plan-Apochromat 40 \times 1.3 oil DIC M27 objective. The ZEN 2.3 lite software (Carl Zeiss) was used for processing of all the images.

2.11.14. Homology modeling and substrate docking with MdcNL:

BlastP of MdcNL sequence from cv. Golden Delicious shows that it has a sequence identity of 36% and query coverage of 95% with the crystal structure of tt0168 from *Therumus thermophilus* HK8 (PDB ID: 1ULT) (Hisanaga et al., 2004). 3D model of cinnamate CoA ligase was predicted by utilizing Phyre2 (Kelley et al., 2015). ModLoop and Swiss PDB viewer 4.1.0 was used for loop refinement and energy minimization of the predicted model, respectively (Fiser et al., 2003; Guex and Peitsch, 1997). PROCHECK was utilized to cross-check the stereochemical properties of the predicted model (Laskowski et al., 1996). PDBsum (<http://www.ebi.ac.uk/thornton-srv/databases/pdbsum/Generate.html>) was used to generate the topology diagram of the model (Laskowski, 2001). AutoDockVina 1.1.2 was utilized to find the interactions between protein and ligands (Trott and Olson, 2010). AutDockMGLTools version 1.5.6 was used for the addition of hydrogen atoms and Kollman charges (9.028) on protein (Morris et al., 2009). All the major tested substrate ligands, cinnamic acid (CID444539), 4-coumaric acid (CID637542), caffeic acid (CID689043), ferulic acid (CID445858) and sinapic acid (CID637775) were retrieved from PubChem compound database in the SDF format. OpenBabel 2.3.1 was utilized to convert all the SDF format of ligands into PDB format (O'Boyle et al., 2009). Gasteiger charges on cinnamic acid (-1.056), 4-coumaric acid (-2.0525), caffeic acid (-3.0527), ferulic acid (-4.0529) and sinapic acid (-5.0532) were added and all were saved in .pdbqt formats. The characteristics motif consisting of conserved Gly, His and Thr were used to create the atomic grid for docking. Atomic potential grid

map with a spacing of 0.375 Å was generated by using Autogrid4. The gridboxsize was 40 Å X 40 Å X 40 Å with dimensions of -2.861, 0.0056 and -1.722 (x,y and Z coordinates). AutoDock Vina1.1.2 was used for docking and pose with maximum binding energy was analyzed in PyMol and the hydrophobic interactions figures were made in Maestro11.2 of Schrodinger (Schrödinger Release 2017-4: Maestro, Schrödinger, LLC, New York, NY, 2017).

Sequence information for *MdCNL* could be available in the data libraries (GenBank/EMBL) with the accession number MG334585.

2.12. Databases and software:

A. MetaboAnalyst 3.0 (www.metaboanalyst.ca)

MetaboAnalyst (www.metaboanalyst.ca) is an application used for metabolomic data visualization, analysis and interpretation for the wide range of statistical metabolomics calculations.

B. The Genome Database for Rosaceae (GDR: <http://www.rosaceae.org/>)

Rosaceae genomics and transcriptomics data is available at this database for working in functional genomics. It is used to search apple genome and NCBI Malus EST for possible OMTs candidates.

C. Basic Local Alignment Search Tool (BLAST: <http://blast.ncbi.nlm.nih.gov/Blast.cgi>)

It uses nucleotide or protein query to search nucleotide and protein databases available by website or any set of sequences supplied by the user.

D. Mega 5 (Molecular Evolutionary Genetic Analysis) was used to infer the phylogenetic tree (Tamura et al., 2011).

E. Primer Express 3.0 software (ThermoFisher Scientific) was used to design primers for Quantitative Real Time expression analysis.

Chapter 3

Results

3.1. To develop cell suspension culture of apple cv. Golden Delicious:

3.1.1. Callus induction from apple leaves:

Callus induction was initiated by using various combinations of three growth regulators, 2,4-D, NAA and kinetin. Induction of friable callus was observed in response to all levels of growth regulator treatment but the combination of 2 μM 2,4-D, 1 μM NAA and 1 μM kinetin exhibited the best result for callus induction and biomass production (Table 3.1). Callus developed in this optimum combination showed friable light yellow appearance. Higher or lower concentrations of 2,4-D and NAA resulted into reduced rate of callus formation with less biomass (Figure 3.1).

Table 3.1: The effect of various growth regulator supplementations on callus induction in apple cultivar "Golden Delicious" after 25 days of culture. Values are mean \pm standard deviation (n = 3).

Growth regulator treatment			Callus Induction	
2, 4 D (μM)	NAA (μM)	Kinetin (μM)	Callus induction (%)	Callus fresh weight (g)
0	0	0	8	2.2 \pm 0.4
0.5	0	0	12	4.0 \pm 0.2
0.5	0.5	0.5	48	9.5 \pm 0.6
1.0	0.5	0.5	60	9.6 \pm 0.6
1.0	1.0	1.0	72	10.2 \pm 0.4
2.0	0.5	0	80	11.2 \pm 0.8
2.0	1.0	0.5	84	11.6 \pm 0.6
2.0	1.0	1.0	96	14.5 \pm 0.6
2.0	1.5	1.5	70	9.8 \pm 0.8
0.0	1.0	1.0	50	8.5 \pm 1.2
2.5	1.0	1.0	80	10.0 \pm 0.5
2.5	1.5	0	66	8.2 \pm 0.8

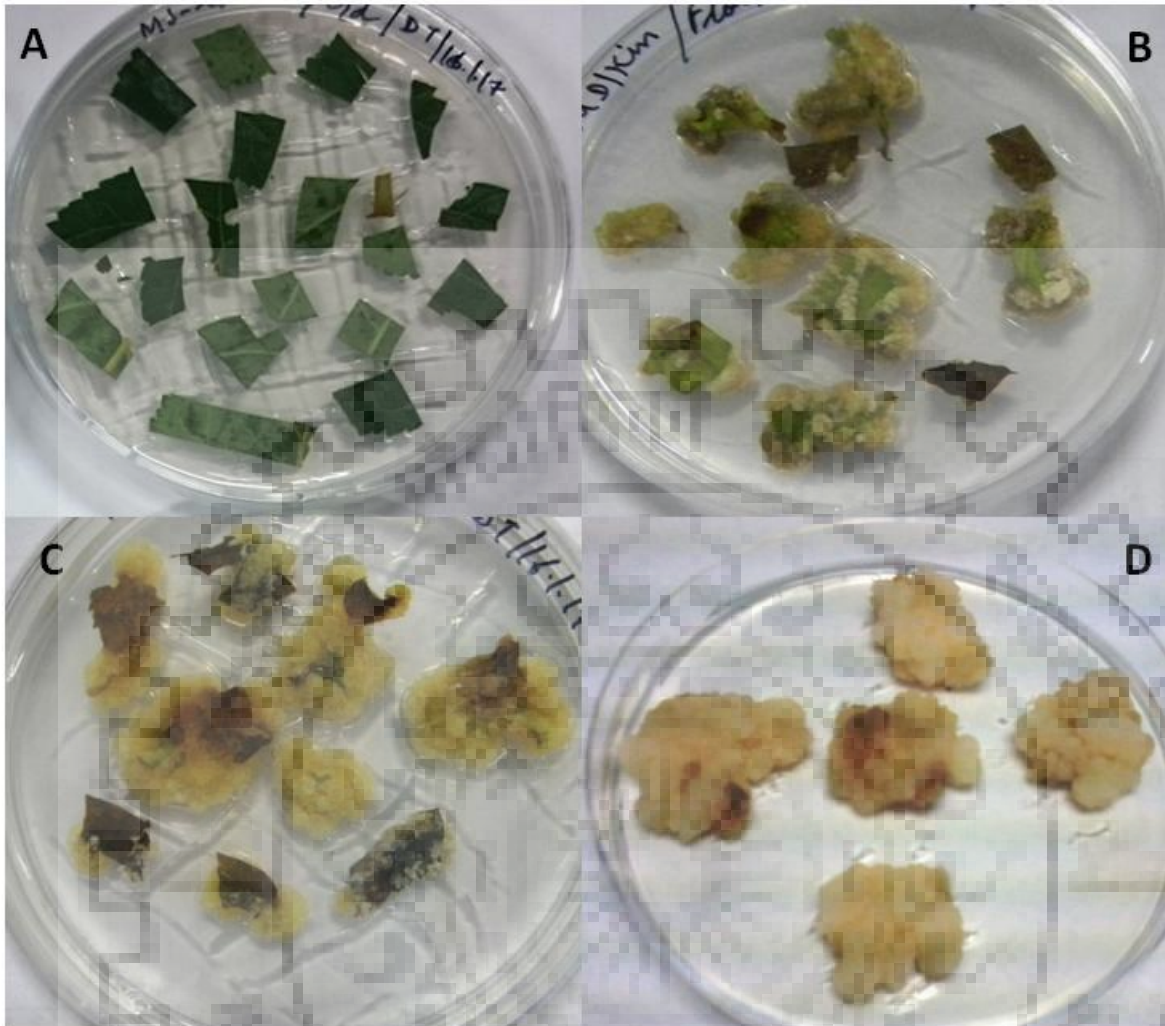


Figure 3.1: Friable callus induced from the leaves of apple (*Malus domestica* cv. Golden Delicious). Different stages for induction of callus are shown from A to D.

3.1.2. Establishment of cell suspension culture:

Friable callus was used to develop cell suspension culture. Growth of cell suspension culture in liquid LS-medium showed best result with $2\mu\text{M}$ 2,4-D and $1\mu\text{M}$ NAA as shown in [Figure 3.2](#). Kinetin addition in the medium showed cell clumping, thereby kinetin was removed.

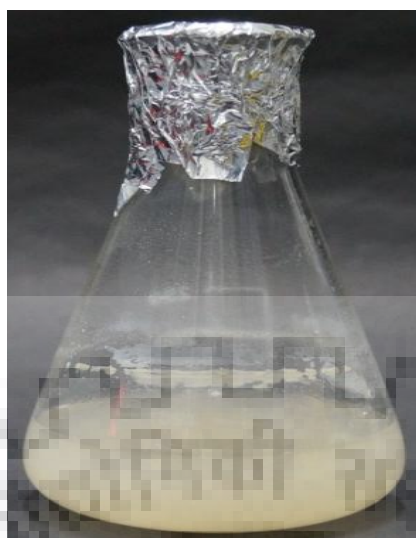


Figure 3.2: Cell suspension culture of apple cv. Golden Delicious.

3.2. Development and validation of a new HPLC method for the determination of biphenyl and dibenzofuran phytoalexins in Rosaceae:

3.2.1. Chemical synthesis of aucuparin and noraucuparin:

Since aucuparin, noraucuparin and eriobofuran are not available commercially, they were synthesized following the published protocols as described in material method section. The starter substrate for the synthesis of both aucuparin and noraucuparin were 3,4,5-trimethoxybiphenyl, which was synthesized as described by (Hüttner et al., 2010). Newly synthesized aucuparin, noraucuparin and eriobofuran were derivatize with MSTFA and subjected to GC-MS analyses. Chemical identities were confirmed by comparing the mass spectrum with standard aucuparin, noraucuparin and eriobofuran (obtained from Prof. L. Beerhues, TU-BS, Germany as gift). Silylated-derivative of aucuparin showed molecular ion peak of 302.10 (Figure 3.3 A) and noraucuparin showed molecular ion peak of 360.20 (Figure 3.3 B), which were the characteristic identity as per published record (Hüttner et al., 2010). Since mass-spectrums were in complete agreement with the standard aucuparin, noraucuparin and eriobofuran, no further structural confirmation was performed. Aucuparin, noraucuparin and eriobofuran was dissolved in methanol (100%) at 50 mM final concentration and stored at -20°C till further use.

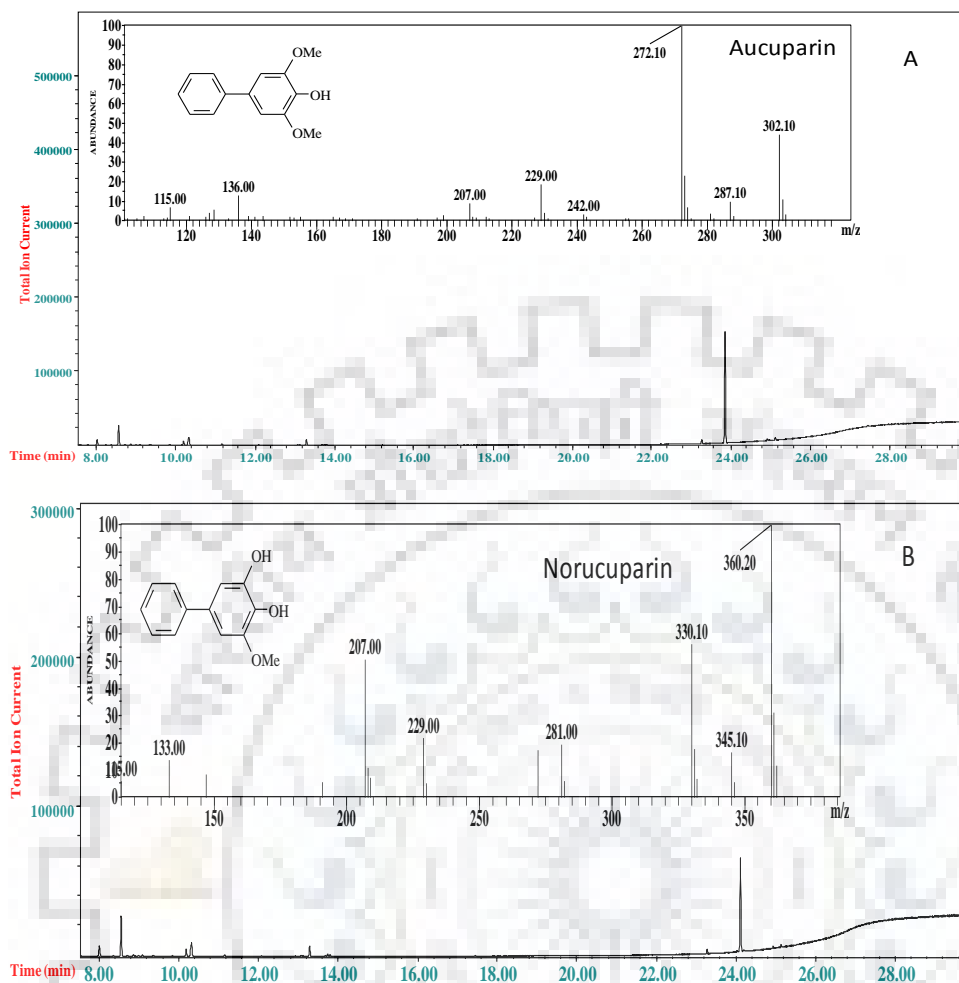


Figure 3.3: TIC and mass-spectrum (GC-MS) of chemically synthesized (A) aucuparin and (B) noraucuparin.

3.2.2. Optimization of chromatographic condition:

Various isocratic combination of acetonitrile-water or methanol-water were tried to achieve optimum chromatographic conditions for noraucuparin, aucuparin and eriobofuran. Optimum separation with good peak shapes was observed in the mobile phase comprising of 1 mM TFA in water and methanol in the ratio of 40:60 (v/v). Optimized flow rate was found to be 0.5 ml min⁻¹. Under this optimized condition the chromatograms of standard noraucuparin, aucuparin and eriobofuran was shown in [Figure 3.4](#). A good separation was achieved within 40 mins with the above described chromatographic conditions. The retention times for noraucuparin, aucuparin and eriobofuran were 20.0, 34.1 and 39.9 min, respectively.

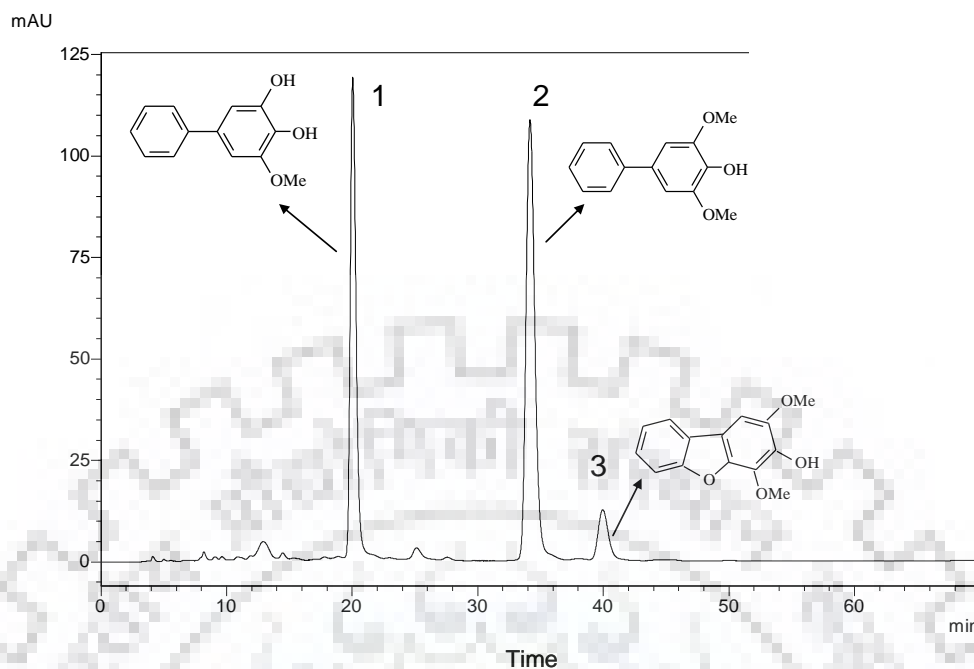


Figure 3.4: HPLC chromatogram showing separation of standard noraucuparin, aucuparin and eriobofuran. Detection wavelength 254 nm. Key to peak identity: (1) noraucuparin; (2) aucuparin; (3) eriobofuran.

3.2.3. HPLC Method Validation:

The HPLC method was validated for linearity (see calibration), limit of detection (LOD), limit of quantification (LOQ), accuracy, precision and peak purity. The method was validated according to ICH guidelines (ICH Topic Q2 B., 1996).

3.2.3.1. Linearity:

Excellent linearity was observed between peak area and concentration in the range 3–400 $\mu\text{g ml}^{-1}$ for noraucuparin and aucuparin and 6–400 $\mu\text{g ml}^{-1}$ for eriobofuran. The coefficient of regression of the calibration curve obtained for all the three analytes were more than 0.995, thereby confirming the linearity of the developed method. The parameters of the linear regression equation for each analyte was presented in (Table 3.2).

Table 3.2: Regression parameters of calibration curve (n = 3).

Analyte	Linear range ($\mu\text{g/mL}$)	$y = bx + a$ ¹	Correlation coefficient (R^2)
Noraucuparin	1.5- 400	$y = 716.8 x - 387.1$	0.999
Aucuparin	1.5- 400	$y = 620.7 x + 459.3$	0.999
Eriobofuran	6- 400	$y = 61.7 x + 187.5$	0.996

¹ y = peak area; x = concentration.

3.2.3.2. Analytical sensitivity (AS), Limit of detection (LOD) and Limit of quantification (LOQ):

The results for the AS, LOD and LOQ were listed in (Table 3.3). The limit of detection was found to be 0.76 $\mu\text{g/ml}$ for noraucuparin, 0.40 $\mu\text{g/ml}$ for aucuparin and 3.77 $\mu\text{g/ml}$ for eriobofuran. Corresponding limits of quantification were found to be 2.5, 1.3 and 12.6 $\mu\text{g ml}^{-1}$ respectively. These results clearly indicate that the analytical method has good sensitivity.

Table 3.3: Performance characteristics.

Compound	AS ($\mu\text{g/ml}$)	LOD _{approx} ($\mu\text{g/ml}$)	LOQ _{approx} ($\mu\text{g/ml}$)
Noraucuparin	0.35	0.76	2.50
Aucuparin	0.18	0.40	1.30
Eriobofuran	1.77	3.77	12.6

AS = analytical sensitivity; LOD = limit of detection; LOQ = limit of quantification

3.2.3.3. Precision and Accuracy:

The precision and accuracy data for the determination of noraucuparin, aucuparin and eriobofuran were presented in (Table 3.4). The method was found to be accurate and precise, as indicated by recovery studies close to 100 and % RSD not more than 4 (Table 3.4).

Table 3.4: Recovery, precision (intra- and inter-day) and accuracy (%) data for the simultaneous determination of noraucuparin, aucuparin and eriobofuran.

Analyte	Spiked Analyte ($\mu\text{g/ml}$)	Recovery ($\mu\text{g ml}^{-1}$)	Intra-day precision		Recovery ($\mu\text{g ml}^{-1}$)	Inter-day precision	
			(% RSD)	Accuracy (%)		(% RSD)	Accuracy (%)
Noraucuparin	50	50.50 ± 0.96	1.90	101.01	52.17 ± 0.34	0.66	104.33
	100	104.03 ± 0.13	0.12	104.03	103.16 ± 0.31	0.30	103.16
	200	203.95 ± 1.58	0.77	101.98	207.58 ± 3.51	1.70	103.79
Aucuparin	50	52.04 ± 0.42	0.81	104.08	52.33 ± 0.89	1.70	104.67
	100	102.84 ± 0.23	0.22	102.85	103.86 ± 2.63	2.53	103.86
	200	202.62 ± 0.77	0.38	101.31	204.99 ± 0.39	0.19	102.49
Eriobofuran	50	47.92 ± 0.72	1.50	95.85	48.62 ± 0.25	0.52	97.24
	100	102.33 ± 3.90	3.82	102.33	103.00 ± 3.72	3.61	103.00
	200	203.34 ± 3.65	1.79	101.67	206.03 ± 1.24	0.60	103.01

RSD = Relative standard deviation.

3.2.4. Analysis of the plant extract with RP-HPLC method:

The methanolic extract of elicited *Sorbus aucuparia* cell culture was directly injected to the HPLC system and separated under the optimum chromatographic condition as described above. The chromatogram (Figure 3.5) showed some non-identified peaks as well. However the retention time of these non-identified peaks did not overlap with the peaks of phytoalexins under study, thereby the interference of these non-identified peaks did not influence the precision and validity of this analytical method. The peak purity of the analytes was checked by the comparison of UV-spectra and mass-spectra of the HPLC eluted fraction of the corresponding peaks with those of authentic standards. Mass-spectra were recorded in negative ESI-mode, which led to unambiguous chemical

identities of peaks of interest (Figure 3.6). In the mass-spectra, molecular ion of m/z 215 represented noraucuparin, m/z 229 represented aucuparin and molecular ion of m/z 243 represented eriobofuran.

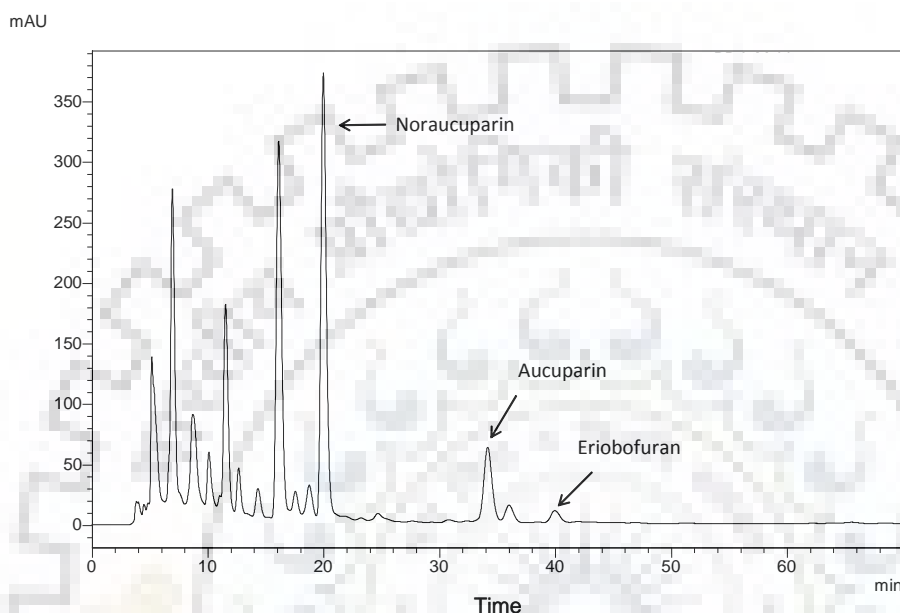


Figure 3.5: HPLC chromatogram of the elicited cell culture of *S. aucuparia*. HPLC conditions are same as used in Figure 3.4. Detection wavelength was set at 254 nm.

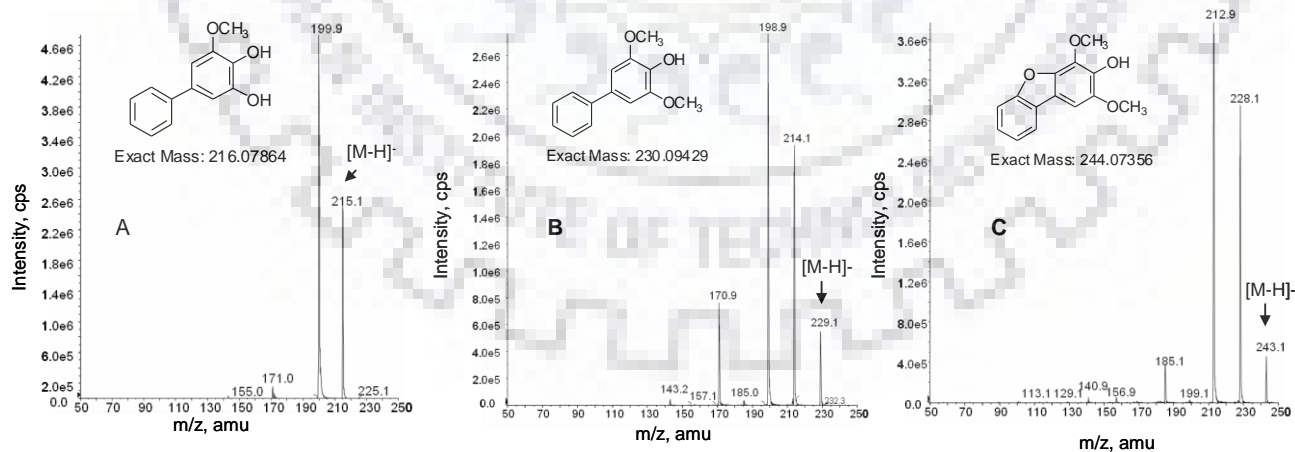


Figure 3.6: ESI-MS/MS spectrum of HPLC eluted noraucuparin (A), aucuparin (B) and eriobofuran (C) from elicited *S. aucuparia* cell cultures. ESI-MS/MS analyses was carried out in negative ion mode.

3.3. GC-MS based metabolomics analyses of *Venturia inaequalis* elicitor-treated cell culture of apple cv. Golden Delicious:

3.3.1. Comparative metabolomics of VIE-treated apple culture:

In order to understand scab-induced metabolic re-programming, Golden Delicious cell cultures were treated with elicitor prepared from *V. inaequalis* and resulting time course changes in the concentration of differentially accumulating metabolites were analyzed by GC-MS based metabolomics. VIE-treated cells were extracted for isolation of metabolites and after TMS-derivatization, submitted to GC-MS metabolomics analyses. Dynamic changes in the metabolite levels post elicitation were compared with the non-elicited control cells. One representative GC-MS chromatogram (TIC; total ion chromatogram) of apple cell culture (24 h post elicitation) was shown in [Figure 3.7](#). A total of 43 low-molecular weight metabolites were detected ([Table 3.5](#)). Metabolites were characterized based on their retention time and specific fragmentation pattern. Detected metabolites were grouped under primary metabolites comprising of amino acids (8), sugars (3), sugar alcohols (3), organic acids (12), vitamin (2) and, secondary metabolites comprising phenolics (11) and Flavonoids (4) ([Figure 3.8](#)). The dominance of organic acids and phenolics were detected in the elicited cell cultures. When compared with the untreated control cultures, two new metabolites, noraucuparin and aucuparin were detected from the elicited cell cultures. From metabolomics point of view, VIE-treatment appears to trigger a metabolic alteration, in both the primary and secondary metabolism. Metabolite concentration was represented after normalization using the area of internal standard.

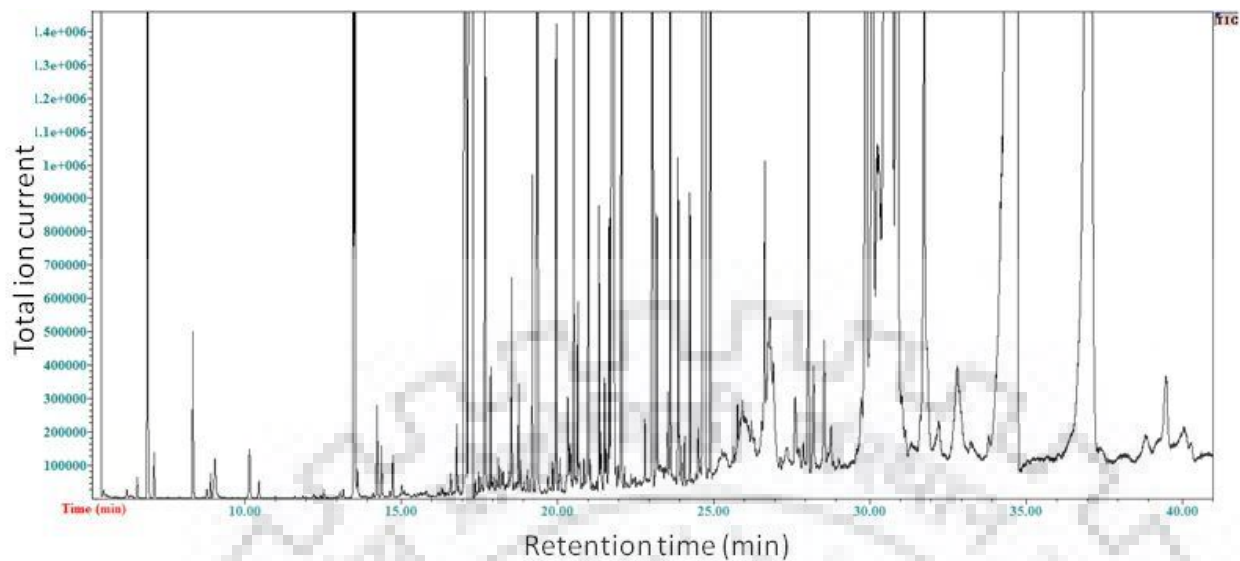


Figure 3.7: A representative GC-MS chromatograms (TIC) of detected metabolites from the VIE-treated (24h post elicitation) cell cultures of apple.

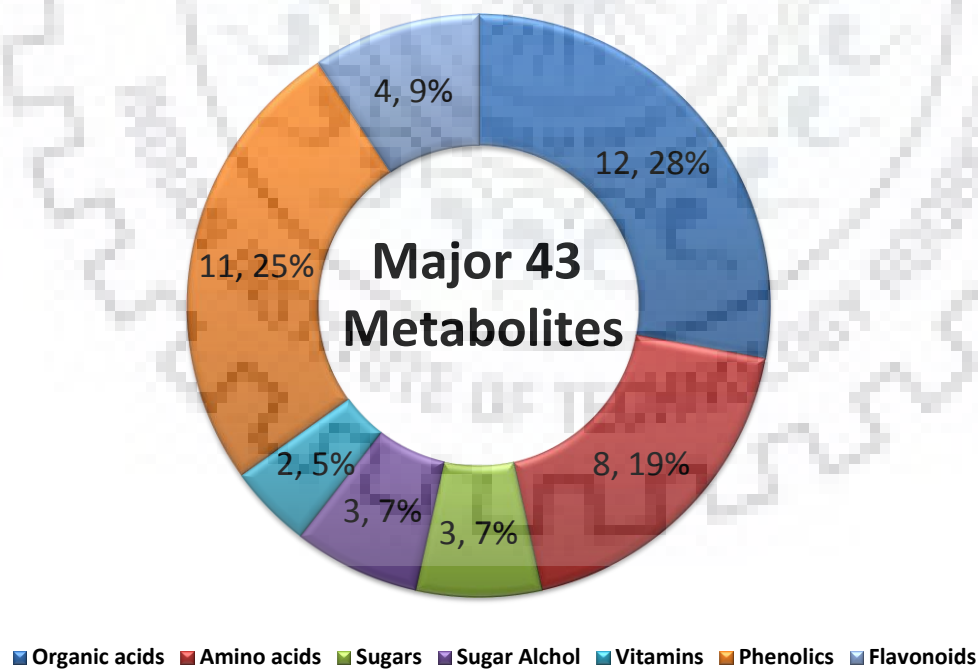


Figure 3.8: Metabolites grouped under specific class.

Table 3.5: List of 43 identified metabolites from VIE-treated cell cultures of apple cv. Golden Delicious.

S. No	Metabolite	Derivate	KEGG ID/ Pubchem ID	Retention Time	Qualification Ions [m/z]
1	L-Alanine	2 TMS	C01401	6.3	233,218
2	Aspartic acid	3 TMS	C00049	13.52	349,334
3	Ascorbic acid	4 TMS	C00072	18.26	449, 374
4	Aucuparin	1 TMS	C09918	24.08	302, 287
5	Benzoic acid	1 TMS	C00180	10.66	194, 179
6	p-OH Benzoic acid	2 TMS	C00156	15.65	282, 267
7	Caffeic acid	3TMS	C01481	19.4	396, 381
8	Catechin	5 TMS	C06562	25.27	649, 461
9	Chlorogenic acid	6TMS	C00852	29.97	419, 345
10	t-Cinnamic acid	1 TMS	C00423	14.82	220, 205
11	Citric acid	4 TMS	C00158	16.53	363, 375
12	p-Coumaric acid	2TMS	C00811	18.35	308, 293
13	Epicatechin	5 TMS	C09727	26	649,461
14	Ferulic acid	2TMS	C01494	23.6	338, 323
15	Fructose	5 TMS	C02336	17.33	437, 347
16	Fumaric acid	2 TMS	C00122	11.32	245, 230
17	D- Glucose	5 TMS	C00031	18.17	358, 319
18	Glyceric acid	3 TMS	C00258	14.35	322, 248
19	Glycine	2 TMS	C00037	9.33	204, 176
20	Glycolic acid	2 TMS	C00160	13.53	205, 177
21	L-Histidine	3 TMS	C00135	10.96	371,356
22	L-Isoleucine	2 TMS	C00407	12.07	260,232
23	2-Ketoglutaric acid	2 TMS	C00026	18.06	318,288
24	Linoleic acid	1 TMS	C01595	24.65	352,337
25	Linolenic acid	1 TMS	C06427	24.72	350,335
26	Malic acid	3 TMS	C00149	14.41	335, 319
27	Malonic acid	2 TMS	C00383	15.51	233, 148
28	Mannitol	6 TMS	C00392	24.85	421, 319
29	Myo-inositol	6 TMS	C00137	19.18	432, 318
30	Noraucuparin	2 TMS	44605718	23.8	330, 313

31	Oleic acid	1 TMS	C00712	24.7	354, 339
32	Protocatechuic acid	3TMS	C00230	17.36	370, 355
33	Pyruvic acid	2 TMS	C00022	7.58	232, 217
34	Rutin	10 TMS	C05625	28.75	354, 309
35	Salicylic acid	2 TMS	C00156	17.2	303, 233
36	Serine	3 TMS	C00065	12.75	306, 218
37	D-Sorbitol	6 TMS	C00794	24.89	497, 421
38	Succinic acid	2 TMS	C00042	12.03	247, 218
39	Sucrose	8 TMS	C00089	21.63	451, 437
40	L-Threonine	3 TMS	C00188	13.89	335,291
41	α-Tocopherol	1 TMS	C02477	30.67	502, 487
42	4,5,7-trihydroxyflavanone	3 TMS	C01477	31.82	488,416
43	Valine	1TMS	C00183	10.31	246, 218

3.3.1.1. Organic acids: Twelve organic acids were detected from the VIE-treated apple cell cultures. Except for glycolic acid and oleic acid, the levels of all identified organic acids (glyceric acid, pyruvic acid, succinic acid, fumaric acid, malic acid, malonic acid, linoleic acid, linolenic acid, citric acid and 2-ketoglutaric acid) were up-regulated upon VIE-treatment (Figure 3.9 A-L). Glycolic acid content remained more or less constant throughout the time-course studied. We hypothesized that, high organic acid accumulation after VIE-treatment was probably due to higher turnover number of glycolysis and TCA cycle which generated more abundant intermediate.

3.3.1.2. Amino acids: A total of 8 amino acids were detected from both, control and VIE-treated cells (Figure 3.9 M-T). No significant changes in the level of serine, threonine and alanine were observed in the elicited cells over the time-course studied. The content of valine, histidine, isoleucine, aspartic acid, and glycine were up-regulated after elicitor-treatment.

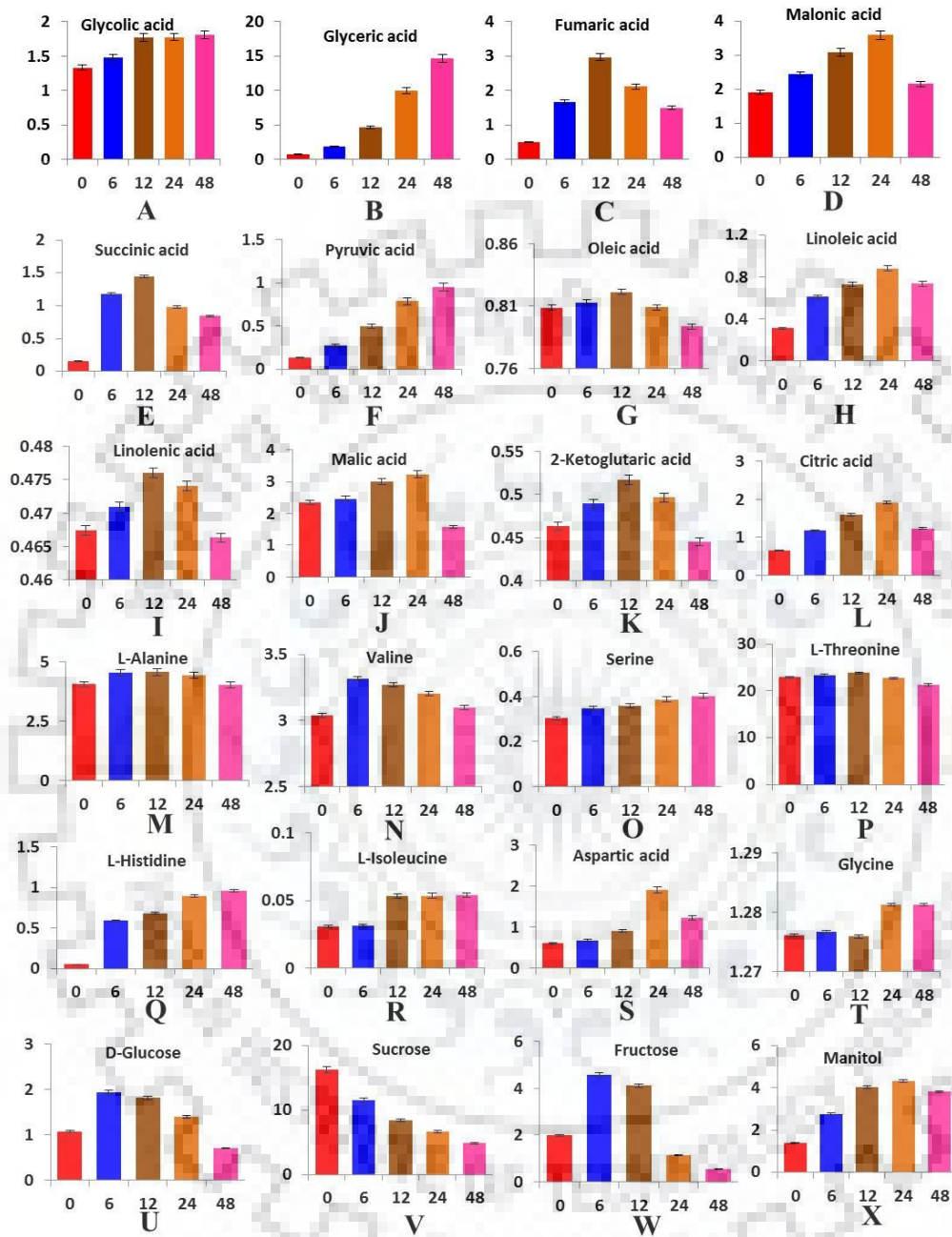
3.3.1.3. Sugars: Sucrose, fructose, and glucose sugars (Figure 3.9 U-W) were detected from both the elicited and non-elicited apple cell cultures. Glucose and fructose is derived from sucrose after hydrolyses. The sucrose content was down-regulated upon VIE-treatment, whereas glucose and fructose contents were up-regulated. Fructose and glucose showed highest accumulation at 6 h. This indicates that sucrose catabolism was higher in VIE-treated cell culture.

3.3.1.4. Sugar alcohols: Three sugar alcohols, manitol, sorbitol and myo-inositol, were identified in VIE-treated apple cell cultures (Figure 3.9 X-Z). Manitol and sorbitol content up-regulated upon VIE-treatment with highest accumulation at 24 h. No significant change in myo-inositol content was observed over the time course studied.

3.3.1.5. Vitamin: Ascorbic acid (vitamin C) and tocopherol was the two vitamins identified from both the non-elicited and elicited cell cultures (Figure 3.9 α - β). After VIE-treatment ascorbic acid level was first increased, reached peak at 12 h and decreased thereafter, whereas tocopherol almost remain same.



Primary metabolites



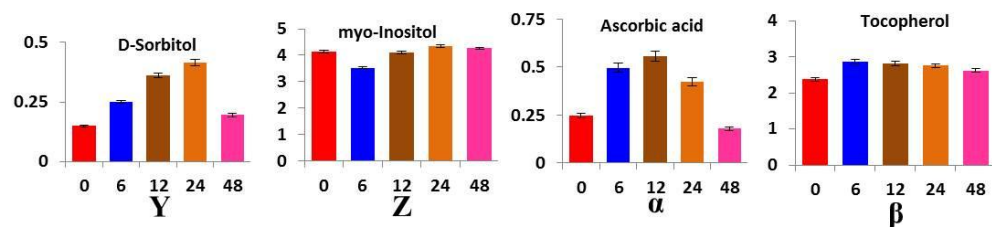


Figure 3.9: Differentially accumulating metabolites in the VIE-treated cell culture of apple cv. Golden Delicious. Organic acids (A-L); Amino acids (M-T); Sugars (U-W); Sugar alcohols (X-Z); Vitamin (α - β). Error bars represent standard deviations. The y-axis gives the normalized relative metabolite abundance in terms of the area of internal standard. The x-axis represents post-elicitation time points (h).

3.3.1.6. Phenolics and biphenyl-dibenzofuran phytoalexins:

Metabolomics analyses showed that phenolics were the most abundant metabolites in apple cell cultures. Plant phenolics play crucial role in pathogen defense (Lattanzio et al., 2006; Bera et al., 2017) as well as they constitute the major proportion of plant anti-oxidant system (Kaufholdt et al., 2015, 2016). In this study, a total of 11 phenolics were detected from the VIE-treated apple cell cultures (Figure 3.10). Phenolics detected in apple cell cultures were caffeic acid, protocatechuic acid, chlorogenic acid, benzoic acid, ferulic acid, 4-coumaric acid, *trans*-cinnamic acid, *p*-hydroxybenzoic acid and salicylic acid (Figure 3.10 A-I). The biphenyl phytoalexins detected were noraucuparin and aucuparin (Figure 3.10 J-K). Flavonoids detected were catechin, epicatechin, 4,5,7-trihydroxyflavone and rutin (Figure 3.10 L-O). All these phenolics showed differential accumulation upon VIE-treatment. The content of these phenolics were up-regulated after VIE-treatment. In this study a rapid enhancement of benzoic acid was observed after VIE-treatment. It was known that benzoic acid serves as the precursor for biphenyl and dibenzofuran class of phytoalexins of apple and other members of Malinae. Upon scab-infection, benzoic acid forms benzoyl-CoA, which combines with malonyl-CoA to produce 3,5-dihydroxybiphenyl, the precursor for all other biphenyl and dibenzofurans. Enhanced biosynthesis of benzoic acid in VIE-treated apple cells might attribute its higher resistance against scab fungus *V. inaequalis* and *E. amylovora* by facilitating rapid formation of biphenyl phytoalexins upon pathogen attack. Furthermore, a considerable up-regulation of salicylic acid (SA) biosynthesis was observed in VIE-treated apple cell (Figure 3.10 D). SA can induce local resistance in form of hypersensitive

reaction or long distance systemic acquired resistance (SAR) by triggering the production of pathogenesis-related proteins (PR proteins). VIE-treatment to apple cell culture led to production of aucuparin, and noraucuparin, the marker phytoalexins of Malinae. It has been shown that biphenyls phytoalexin can efficiently inhibit the growth of *Venturiainaequalis* and *E. amylovora* (Chizzali et al., 2012). Interestingly, in our study, biphenyl phytoalexins were absent from the control cells and only formed after VIE-treatment.

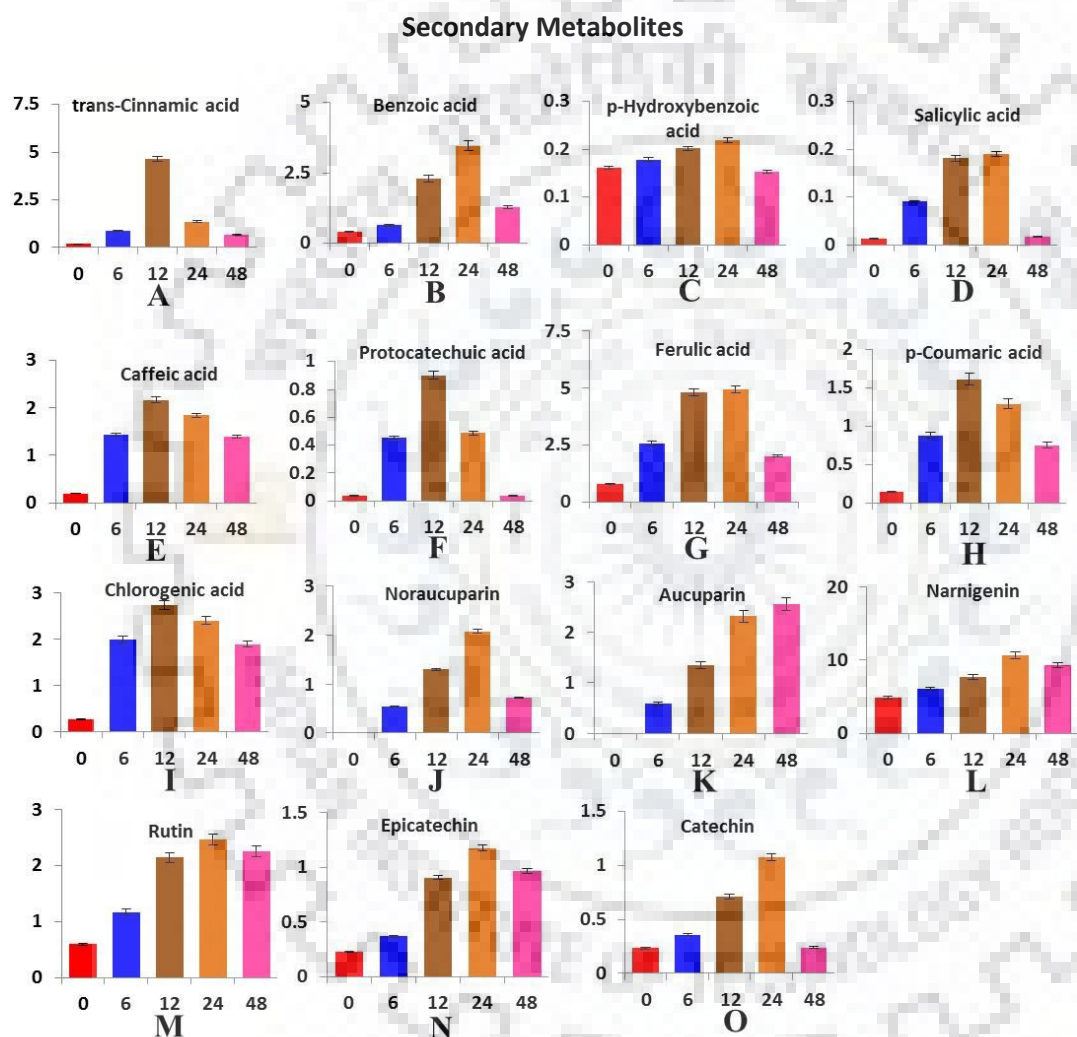
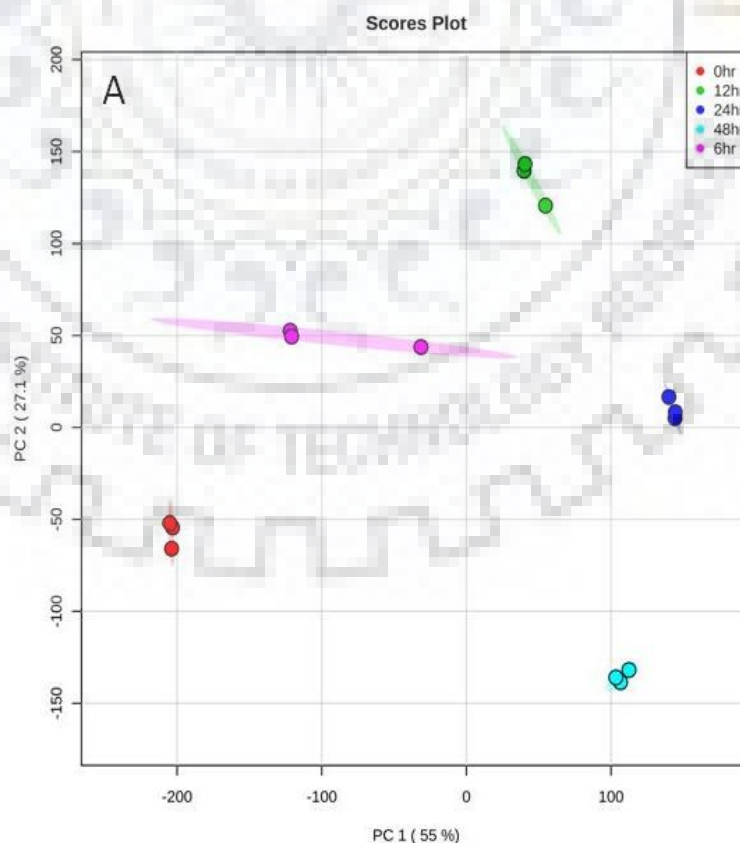


Figure 3.10: Differential accumulation of phenolics and biphenyl phytoalexins in the VIE-treated cell cultures of apple cv. Golden Delicious. Error bars represent standard deviations. The y-axis gives the normalized relative metabolite abundance in terms of the area of internal standard (area of metabolite divided by area of internal standard). The x-axis represents post-elicitation time points (h).

3.3.2. Principal component analysis (PCA) reveals significant alteration in metabolite pattern after VIE-treatment:

The differential accumulation of metabolites in VIE-treated samples at defined post-elicitation time points was analyzed by PCA. The PCA helps to reduce the dimensionality of complex data sets. PCA analyses uses, linear orthogonal transformation of the original data variables to generate a new set of uncorrelated variables known as principal components (PCs) (Park et al.,2015). As shown in Figure 3.11A, the first PC and the second PC of the analyzed PCA score plot represented 27.1 % (PC1) and 55 % (PC 2) of the total variance of the samples. The PC 1 difference between the metabolomics profiles of control and VIE-treated cells were represented by PC1. The metabolomics profile at various time points in VIE-treated cells was separated by PC 2. Furthermore, a PCA loading plot (Figure 3.11 B) was constructed to show the abundant variable (metabolites) contributing the PCA results. Metabolites included in loading plot were differentially accumulating 43 metabolites as shown in Table 3.5. These results suggest that differentially accumulating metabolites are probably contributing to the different degree of defense responses against scab-infection.



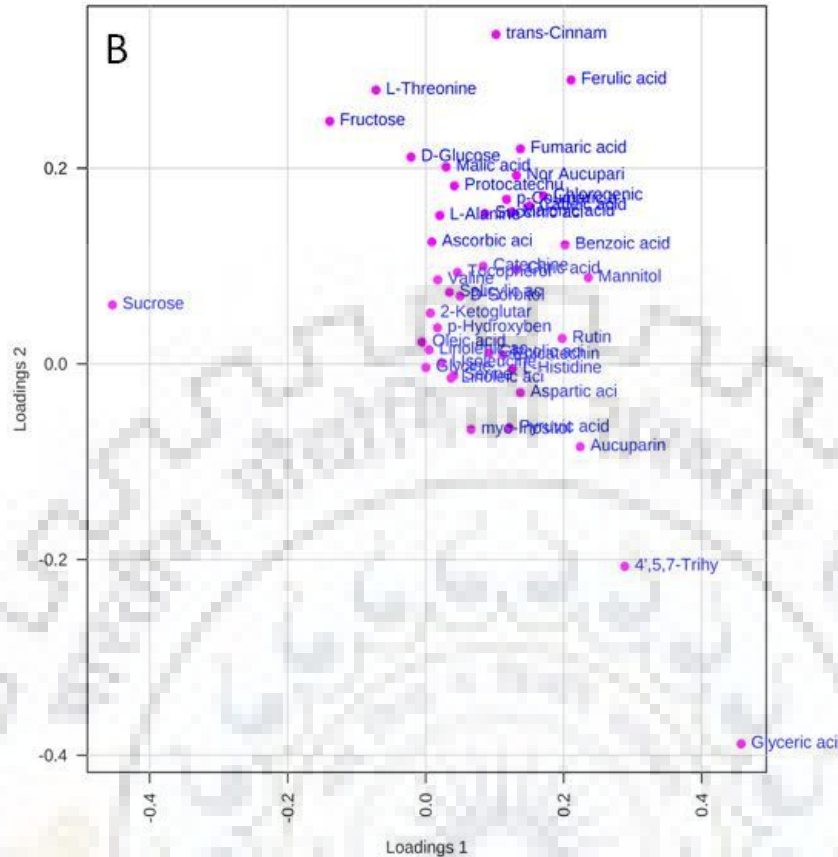


Figure 3.11: PCA analyses of detected metabolites from VIE-treated cell cultures of apple. (A) Scores plot; (B) loading plot.

3.3.3. Hierarchical clustering analysis of the metabolite profiles:

In order to search for any probable discrepancies in the metabolite profiles of all the analyzed samples from the five time points (0-48 h), the 43 detected metabolites were organized and visualized by hierarchical clustering analysis (HCA) tool of Metaboanalyst 3.0 (Figure 3.12) (Shen et al., 2015). The hierarchical clustering offered excellent separation of the metabolite trend between the non-elicited (0h) and VIE-treated (6-48h) cells. VIE-treated cells were the major source of variance in the result, which indicated that change in metabolite concentration by VIE-treatment.

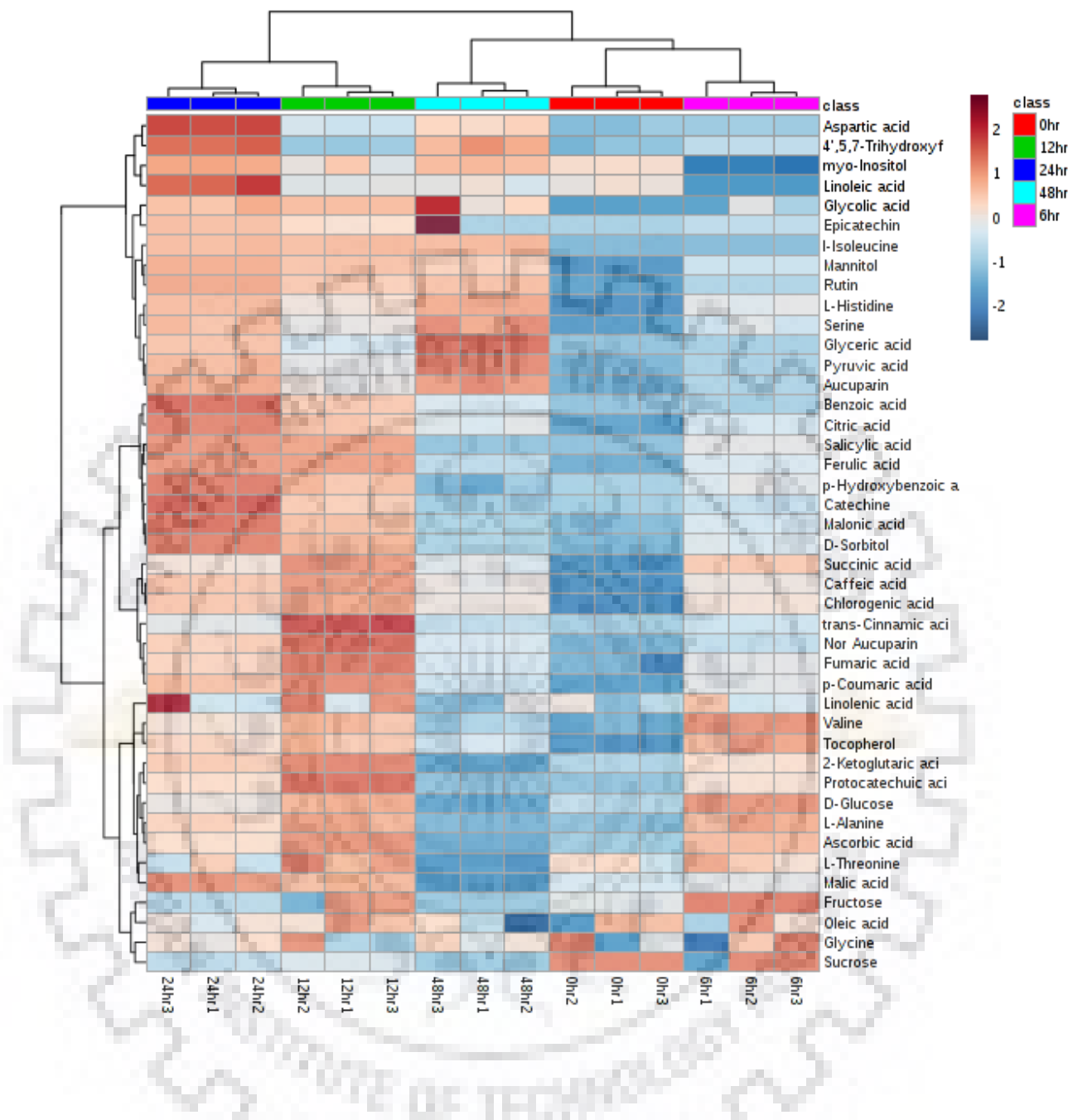


Figure 3.12: Hierarchical clustering analyses of 43 detected metabolites from VIE-treated cell culture of apple cv. Golden Delicious. Similarity assessment for clustering was done on the basis of Euclidean distance coefficient and the average linkage method of metaboanalysts 3.0 tool. Rows and columns represent individual metabolites and different samples, respectively.

3.3.4. Changes in metabolic pathways and metabolic pathway network:

A simplified metabolic pathway network was reconstructed using key metabolic pathways, such as the shikimic acid pathway, the phenylpropanoid pathway, the glycolytic pathway, the TCA cycle, the pentose phosphate pathway, the biphenyl biosynthetic pathway, the flavonoids biosynthesis pathway and the amino acid biosynthetic pathway to show the regulated pattern diversity of each detected metabolites with respect to their proportional incorporation into key metabolic pathways. As shown in [Figure 3.13](#), sucrose as the precursor for glucose and fructose was higher in non-elicited cells than that of VIE-treated cells. However, sucrose hydrolysis product, the glucose and the fructose were higher in the VIE-treated cells, suggesting that more active sucrose catabolism occurred after VIE treatment. The level of sorbitol and manitol were higher in VIE-treated cells suggesting that fructose is metabolized more towards these metabolites rather than re-entering into glycolytic pathway through fructose-6-phosphate. Metabolites of glycolysis pathway, especially pyruvic acid level were up-regulated in the VIE-treated cells, whereas glycine and serine levels remained mostly unaltered. The level of identified TCA cycle metabolites such as citric, succinic, fumaric and malic acids were up-regulated after VIE-treatment suggesting higher turn-over number of TCA cycle. The metabolites derived from shikimate pathway showed an absolutely distinct accumulation pattern. The level of all the detected shikimate-derived metabolites such as caffeic acid, protocatechuic acid, catechin, chlorogenic acid, benzoic acid, ferulic acid, 4-coumaric acid, *trans*-cinnamic acid, rutin, and salicylic acid were higher in the VIE-treated cells. Aucuparin and noraucuparin were only synthesized after VIE-treatment.

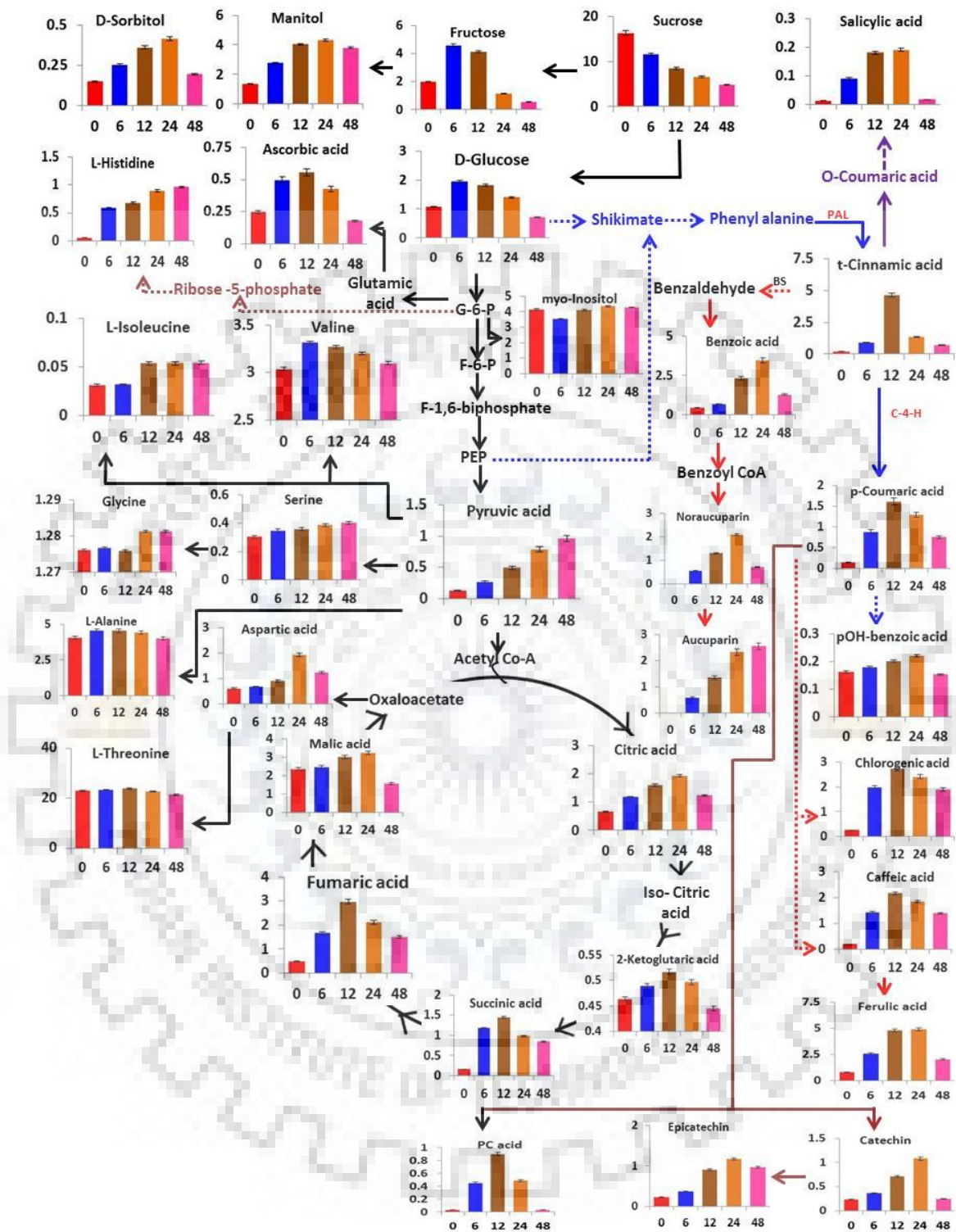


Figure 3.13: The metabolic pathways network analyses of VIE-treated apple cell culture. The bar graph represent the abundance of each metabolite in the control and VIE-treated apple cell culture.

3.3.5. Expression analysis of phenylpropanoid biosynthetic genes in the VIE-treated apple cell cultures:

Since the level of phenolics and biphenyl phytoalexins were significantly higher in the VIE-treated apple cells, the expression levels of four genes (*PAL*, *F3H*, *AOX* and *BIS3*) related to phenylpropanoid, flavonoids and biphenyl biosynthesis were examined using qRT-PCR at defined post elicitation time points (0, 1, 3, 6, 9, 12, 24, 36 and 48h). The expression levels of *PAL*, *F3H*, *AOX* and *BIS3* are shown in Figure 3.14. The expression levels of all the four genes were up-regulated upon VIE-treatment demonstrating that phenylpropanoid and biphenyl biosynthesis was triggered by the VIE-treatment. High *AOX* expression level is probably associated with the enhanced biosynthesis of phenylpropanoid (Costa et al., 2009; Costa et al., 2017). Previously, it was demonstrated that *AOX* expression is linked with high phenylpropanoid biosynthesis in many plant species (Campos et al., 2016a, 2016 b). These gene expression data were well correlated with the enhanced accumulation of phenylpropanoids such as cinnamic acid, flavonoids and biphenyls in the elicited cell cultures of apple.

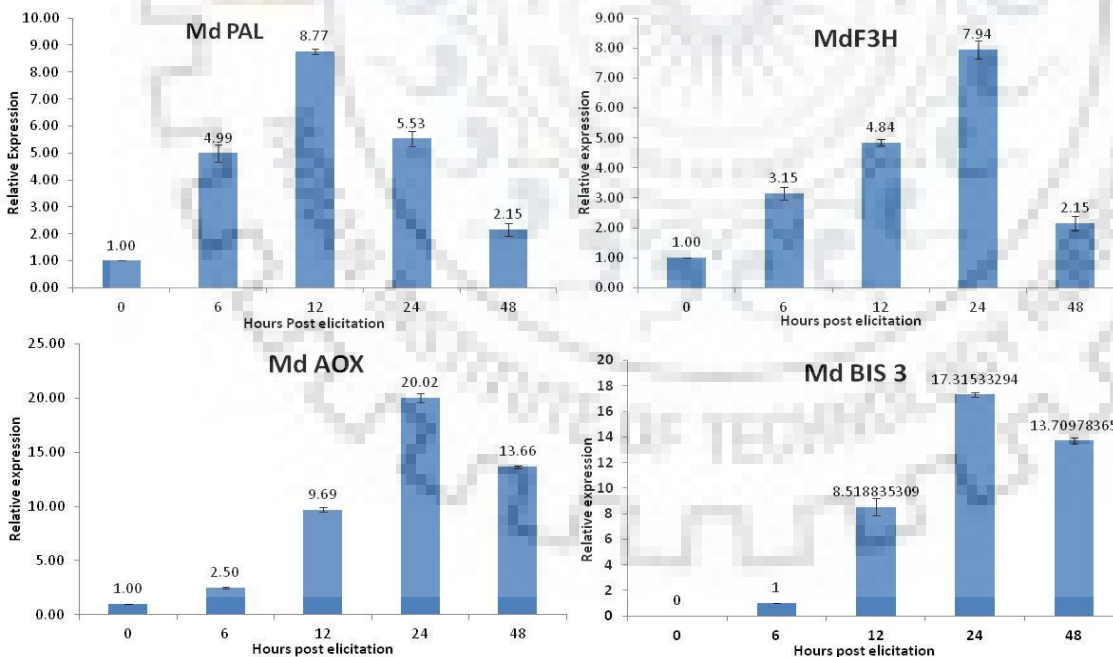


Figure 3.14: Changes in the *MDPAL*, *MdF3H*, *MdAOX*, *MdBIS3* expression levels in *V. inaequalis* elicitor-treated cell cultures of apple cv. Golden Delicious. The relative transcript levels were determined by real-time-PCR. Results are means \pm SD (n = 3).

3.4. Molecular cloning and functional analyses of a cinnamate-CoA ligase (CNL) from cell suspension culture of apple cv. Golden Delicious:

3.4.1. Accumulation of biphenyl phytoalexin:

Golden Delicious cell cultures grown in LS-medium responded to VIE-treatment by producing two biphenyl phytoalexin, as shown by HPLC-DAD analysis (Figure 3.15). Time-course analyses of phytoalexin accumulation showed induced accumulation of two biphenyl phytoalexins, the noraucuparin and the aucuparin (Figure 3.16). Noraucuparin accumulation started at 6hpe and reached peak at 24 hpe ($4.2 \pm 0.4 \mu\text{g/g DW}$). After attaining peak, noraucuparin concentrations decreased as rapidly as it was increased and reached to almost a basal level at 72 hpe ($1.1 \pm 0.1 \mu\text{g/g DW}$). In contrary, aucuparin accumulation started after 9 hpe and its level continues to increase during the studied time-course. Maximum aucuparin level was recorded at 72 hpe ($5.4 \pm 0.16 \mu\text{g/g DW}$). Control cultures treated with equal amount of water (in lieu of VIE) showed no phytoalexin accumulation over the time course studied. Phytoalexins were detected only inside the cells, a minor traces of phytoalexins were detected in the culture media, which was probably due to occasional cell death during elicitation process. Noraucuparin and aucuparin accumulation was also observed from the internode region of *V. inaequalis* infection green-house-grown plants of Shireen and Golden Delicious. However, in case of scab-resistant cultivar Shireen, accumulation of both noraucuparin and aucuparin peaked earlier than that of moderately scab-susceptible cultivar Golden Delicious (Figure 3.17). At peak, the level of noraucuparin and aucuparin were 2.0-fold and 3.2-fold respectively in Shireen as compared to Golden Delicious. Leaves failed to show any accumulation of biphenyl phytoalexins.

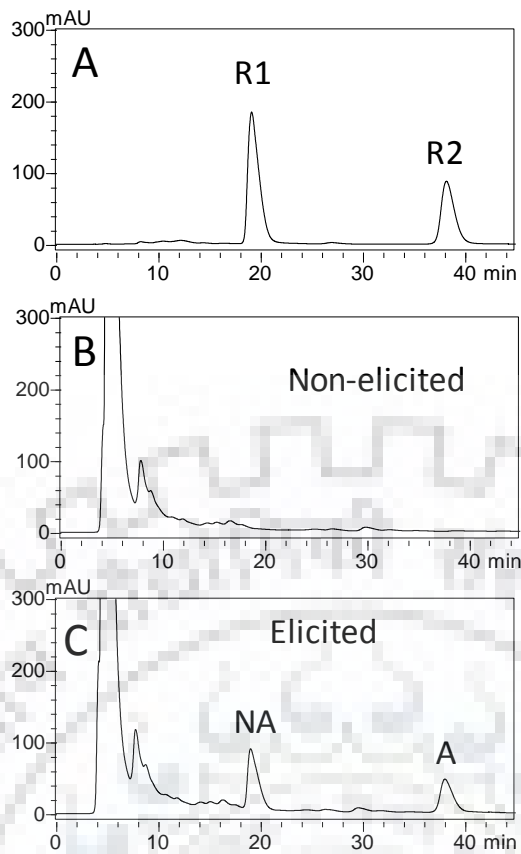


Figure 3.15: HPLC analysis showing accumulation of biphenyl [noraucuparin (NA) and aucuparin (A)] phytoalexins in the VIE-treated and untreated cell culture of apple cv Golden Delicious. (A) Reference compounds (R1: noraucuparin; R2: aucuparin); (B) phytoalexin profile of untreated control cells after 24 h; (C) phytoalexin profile of VIE-treated cells after 24 h. The chromatograms were monitored at 254 nm.

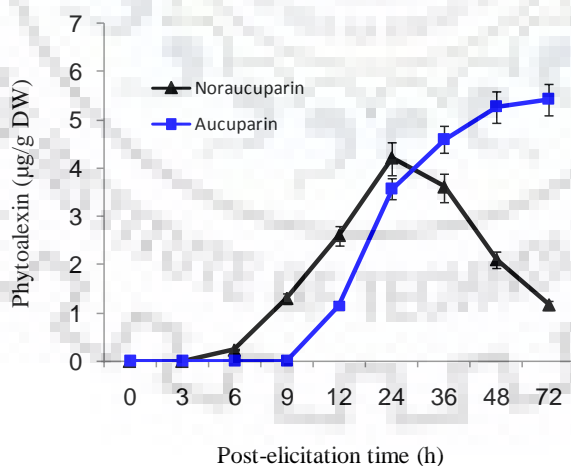


Figure 3.16: Time course accumulation of biphenyl phytoalexins (noraucuparin and aucuparin) in the *Venturia inaequalis* elicitor-treated cell cultures of *M. domestica* cv. Golden Delicious. Results are means \pm SD (n = 3).

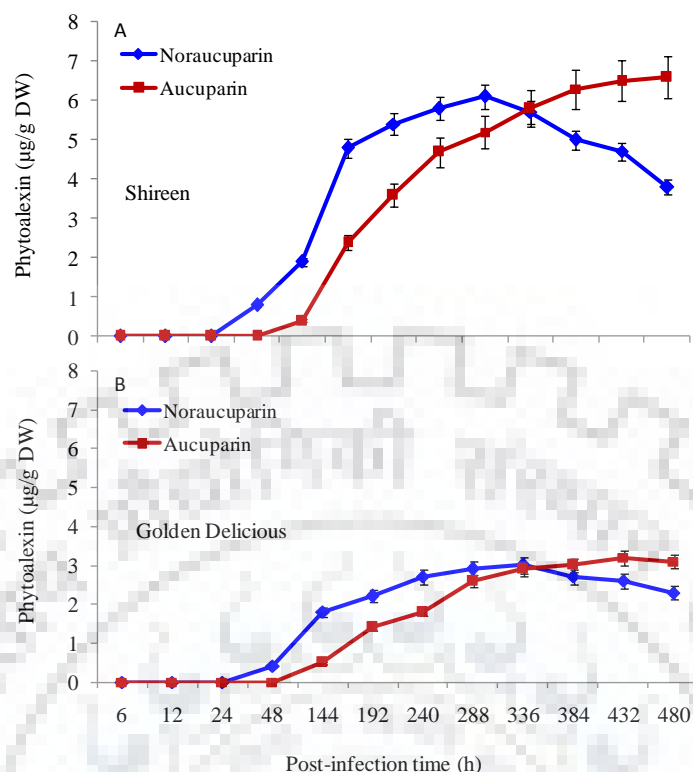


Figure 3.17: Time course accumulation of noraucuparin (blue) and aucuparin (red) in the *Venturia inaequalis* infected greenhouse-grown shoots of Shireen (A) and Golden Delicious (B). Results are means \pm SD (n = 3).

3.4.2. cDNA cloning of a cinnamate CoA-ligase from cell culture of *Malus domestica* cv. Golden Delicious:

The genome sequence of apple cv. Golden Delicious shares significant similarities with the CNL from *Hypericum calycinum* (accession no.: AFS60176) and *Petunia hybrida* (accession no.: AEO52693) (Table 2.20). *In silico* analyses of cleaned sequence from GDR database (www.rosaceae.org; Table 2.20), identified one apple unigenes [MDP0000576682] that shared considerable sequence similarity (73%) with *Hypericum calycinum* CNL. Based on sequence similarity, MDP0000576682 unigene coding sequence was used to derive gene-specific primers for the amplification of the corresponding transcript from the cDNA pool of VIE-treated (6h) cell cultures of *Malus* \times *domestica* cv. Golden Delicious. After extension of 5'- and 3'- ends, the full-length cDNA was re-amplified using Phusion High-Fidelity proof reading DNA polymerase

(Figure 3.18). The resulting full length cDNA consisted of a coding sequence (cds) of 1725 bp, a 5' untranslated region (UTR) of 240 bp, a 3' UTR of 447 bp and one 11bp long poly A tail. This coding sequence encoded a protein of 574 amino acids long with 63.67 kDa of molecular mass and an isoelectric point of 7.4. Molecular mass of recombinant was calculated by matrix-assisted laser desorption/ionisation mass spectrometry (MALDI-MS) analyses (Figure 3.19). The deduced CNL amino acid sequence contained a putative AMP-binding motif (box I) and a box II domain at a distance of 196 and 395 amino acids respectively (Figure 3.20). A glycine residue at amino acid position 254 (marked by asterisk) is supposed to provide hydrophobicity in CNL (Figure 3.20) (Schneider et al., 2003). C-terminal end of CNL peptide contained a type 1 peroxisomal targeting signal (PTS1) comprising of SRL tripeptide, as predicted by PTS predictor software (Rottensteiner et al., 2004). Sequence similarity of *MdCNL* with 4-coumarate:CoA ligases (4CLs) were low (26%-30%); however, *MdCNL* showed 62.3% homology with CNL from *Arabidopsis thaliana* (AtBZO1; Q9SS01), 66.7% homology with CNL from *Petunia hybrida* (PhCNL; AEO52693), 71.8% homology with CNL from *Hypericum calycinum* (HcCNL; AFS60176), 72.5% homology with predicted ortho-succinylbenzoate:CoA ligase1 from *Medicago truncatula* (OSBZL1; XP_003600627).

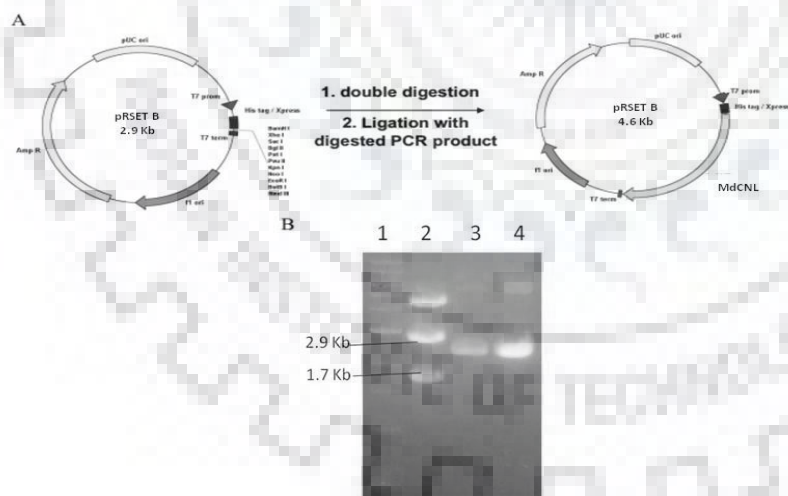


Figure 3.18: Construction of the expression vector for *MdCNL* cDNA. A. vector maps; B. confirmation of the successful ligation and presence of the insert (Lane1: 1Kb ladder; Lane 2: Double digestion of pRSETB vector (2.9Kb) containing CNL (1.7Kb) making a total of 4.6 Kb; Lane 3: complete pRSET B vector with CNL; Lane 4: same as 3).

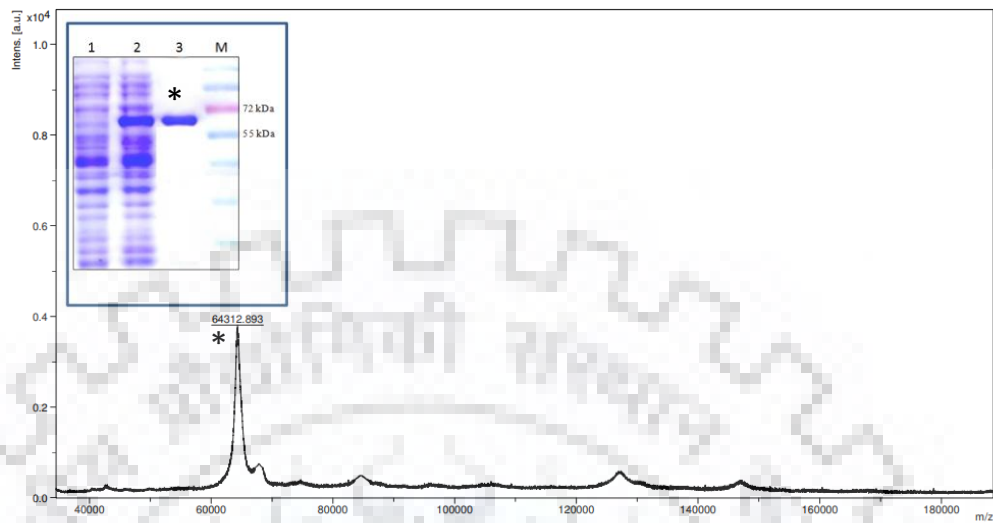


Figure 3.19: The molecular weight determination of *MdCNL* by using MALDI-TOF. The average molecular weight of the recombinant *MdCNL* was observed at 64.3 kDa. Inset showed purification of recombinant *MdCNL* (lane 1: Crude protein from un-induced bacterial cultures; lane 2: crude protein prepared from IPTG-induced cultures; lane 3: Ni-NTA affinity-purified CNL; lane 4 (M): molecular marker).

In addition, the identity of the unknown peak (approx. 67 kDa) detected in the spectrum was confirmed as Chaperone protein DnaK OS from *E. coli* with very high confidence by detecting of two unique peptides, suggesting it as a contaminant originating from host in which the protein was expressed. Inset showed purification of recombinant *MdCNL* (lane 1: uninduced crude protein; lane 2: induced crude protein; lane 3: Ni-NTA affinity purified CNL; lane 4: molecular marker).

```

1  MAFESMN-----TLPKCDA----NYTALSPT-----TFLKRAAFYAERTSVIYECTRFTWGQTYD-----RCCR MdGDCNL
1  M-----D-----KLPRKCGA----NVVPLSPI-----TFLNRAAKVYANRTSIIYENTRFTWGQTYE-----RCCR HcCNL
1  M-----D-----ELPKCGA----NVVPLTFL-----TFLTRAFKSYANRTSIIYAGARFTWEQTYK-----RCCR PhCNL
1  M-----D-----NLPKCRA----NYTILTPL-----TFLMRASASYANRTSVIHEGTRFTWSQTYD-----RCRR MtOSBZL
1  M-----D-----DLALCEA----NNVPLTPM-----TFLKRASECYPNRTSIIYGKTRFTWPQTYD-----RCCR AtCNL
1  M-----A-----IETIPNDIVYRSKLPDPIPKHLLPHSYLHNKHSKPCIIDGAT-----GDIYTFADVVELNAR--R Sa4CL1
1  M-----APQEQAQVSMVEKQSNNNNSDVI FRSKLPDIYIPNHLSLHDYIFQNISEFATKPKCLINGPT---GHVYTYSDVHVISR--Q At4CL1

57  LASSLVSLNVVVKHDVSVLAPNVPAMYEMHF-GVPMAGAVLNTINTRLNAKTIASILRHSGAKVFFVDYQVPLARDVLRILT--- MdGDCNL
52  LASYLRSINISKNDVSVLAPNVPAMLEMHF-AVPMAGAILNTINTRLDAKNIATILRHSEAKLFFVDYQLLDLAREAL----- HcCNL
52  LASSLQSLNIVKNDVSVLAPNVPATYEMHF-AVPMAGAVLNTINTRLDPMNIAIILKHSEAKLFFVDYQVLEKARKALELLMSTNFI PhCNL
52  LASSLRALNIAKNDVSVLAPNIPAMYEMHF-AVPMAGAVLNTINHRLANAANIATILQHSEAKVFFVDYEFVSKAKDALRLLME--- MtOSBZL
52  LAASLISLNIKNDVSVMAPNTPALYEMHF-AVPMAGAVLNPINTRLDATSI AAILRHAKPKILFLDRSFEALARESLLHLLSS--- AtCNL
65  VASGLNKLGIQQGDVIMLLLPNSPA-FAFAFLGASFRGAMTTAANPFFTPAEILKQAKASKAKLIITLACYDKVKD---LSS--- Sa4CL1
78  IANFHKLGVNQDVMMLLPNCP E-FVLSFLAASFRGATATAANPFFTPAEIAKQAKASNTKLIITEARYVDKIKP---LQN--- At4CL1

                                BOX I
140  ---DTAD---K---SMPLVIVIDDIDSPTGIRLGE-LEYEQLIKKGNPGEV---SVPV---DD-EWDPVVALNYTSGTTSEPKGV MdGDCNL
130  ---SGM---E---STPLVVLIDDVDKPTGIGRHG-LEYEQLIKRGRSDF A---PDEL---VD-EWDPIALNYTSGTTSAPKGV HcCNL
139  TAQNSKK---I---SMPQVILDDLYSPTRIQQQDQLEYEQLVHQGNPEYA---PENI---VDEWDPIVLNYTSGTTSAPKGV PhCNL
135  ---EKDQTEQYS---SLPLVIVIDDINNPTGIRLGE-LEYEQVMVHGGNPNYL---PEEI---QD-EWSPITLNYTSGTTSAPKGV MtOSBZL
135  ---EDSN---L---NLP-VIFIHENDFPKRASFEE-LDYECLIQRGEF---T---PSMVARMFRIQDEHDPISLNYTSGTTADPKGV AtCNL
144  ---SSD---VHDKLMC-V---DS---PPDPSC-LHFSLELLQADEN---D---MPEV---DISPDDVVALPYSSGTTGLPKGV Sa4CL1
157  ---DDGV---V---IVC-I---DDNESVPIPEGC-LRFTELTQSTTE---ASEVIDSV---EISPDDVVALPYSSGTTGLPKGV At4CL1

                                *
207  VYSHRGAYLSTMSLVLGWEMGSEP-VYLWT-----LPMFHCNGWTFWTGVAARGGTNVC-LRNTTAYDIYRNIHRHK----- MdGDCNL
196  VYSHRGAYLSTLSLILGWEMGNEP-VYLWS-----LPMFHCNGWTFWTGIAARGGTNVC-IRNTTAEADMYRNIANHG----- HcCNL
211  VYSHRGAYLSTINTIMGWEMGTEP-VYLWS-----LPMFHNGWTLTWGIAARGGTNVC-IRNTTAQEIYSNITLHK----- PhCNL
206  VYSHRGAYLSTLSLILGWEMGSEP-VYLWT-----LPMFHCNGWTFWTGVAARGGTNIC-IRNTAASDIYRAINLYN----- MtOSBZL
205  VISHRGAYLCTLSAIGWEMGTCP-VYLWT-----LPMFHCNGWTFWTGTAARGGTNSVC-MRHVTAPEIYKNIEMHN----- AtCNL
205  MLTHKGL-VTSVAQQVD---GENENLYSDDVVLVCLVPLFH-----YSLNSVLLCGLRAGAAIIMMNFIEVSLGLGIDKYK Sa4CL1
221  MLTHKGL-VTSVAQQVD---GENENLYFHSDDVILVCLVPLMFH-----LYALNSIMLCGLRVGAAILIMPKEINLLELIFQRCK At4CL1

277  --VTMCCAPIIFNFLLEAKSHERCEISTPVQILTGGAAPPAPLLKKIEPLGFKVT---HAYGLTEATGPALVCEWQAKWNMLP-GDD MdGDCNL
266  --VTMCCAPIVFNILLEAGSEARRPITRVPQVLTGGAPPESSLAKMEPLGFKIT---HAYGLTEATGPALVCEWQAKWDGLP-KGD HcCNL
281  --VTMCCAPTVFNILLEAKPHERREITTPVQVMVGGAPPPTTLIGKIEELGFHVV---HCYGLTEAGGTLVCEWQSEWNKLS-RED PhCNL
276  --VTMCCAPIIFNIIILGAKPSEKRVKSPVNILTGGAAPPASLLEKIEPLGFHVT---HAYGLTEATGPALVCEWQKKNVLP-KRE MtOSBZL
275  --VTMCCVPTVFNILLLKWSLDSLSPRGVPHVLTGGSPPPAALVKKVTLRGVQVM---HAYGQTEATGPIVCEWQDEWNRLP-ENQ AtCNL
280  VSIAP I---VPIVLAIAKFPDLDKYDLSS-IRVLKCGGAPLGELEDTVRAKFPNVTLGQGYGMTEA-GPVL T-----MSLFAFAK Sa4CL1
296  VTVA PM---VPIVLAIAKSSSETEKYDLSS-IRVVKSGAAPLGELEDVAVNAKFPNAKLGQGYGMTEA-GPVLA-----MSLGAFAK At4CL1

                                BOX II
359  QAKLKARQGISILTADVDVKNKDTMESVPHDGKTMGEIVLRGSSVMKGYFKDPKATEKAF-QNGWFWTGDVGVVHPDGYMEIKDRLK MdGDCNL
348  QAKLKARQGVSIILTADADVKNLATMESVPRDGTMGIEIVLRGSSIMMGYKDKQETTSKAF-KNGWFATGDVGVVHPDGYEIEIKDRSK HcCNL
363  QANLKARQGISVLALEDVDVKNKDTMQSPVPHNGKTMGEICLRGSSIMKGYFKNDKANSQVF-KNGWFLTGDAVVIHQDGYEIKDRCK PhCNL
358  QSMLKARQGVSVTLADVDVKNLETMESVVRDGTMGIEIMLKGSSIMMGYFKDKATEKAF-GDGWFRTGDVGVVHPDGYEIEIKDRSK MtOSBZL
357  QMELKARQGISILGLADVDVKNKDTQKSAPRDGTMGIEILKGSIMKGYLKNPKATFEAF-KHGWLNTGDVGVVHPDGHVEIKDRSK AtCNL
357  PFEVKGCGCTVVRNAELKIVDPESGASLPRNQF---GEICIRGDQIMKGYLNDPESTRITIDKEGWLHTGDIGFIDDDDELFIIVDRLK Sa4CL1
373  PFPVKSACGCTVVRNAEMKIVDPDPTGDSLNRNQF---GEICIRGHQIMKGYLNNPATAETIDKDGWLHTGDIGLIDDDDELFIIVDRLK At4CL1

446  DVIISGGENISSVEVENILHGHKPVLEAAVAVMPPHRWGESPCAFVALRSNAEG-----AA-----T---ESEIIAYCRKNLPH MdGDCNL
435  DVIISGGENISSVEVESVLYKHPRVLEAAVAVMPEKMGESPCAFVAIRKNEKG-----SR-----NDVKEVDILRFCRANMPH HcCNL
450  DVIISGGENISSIIVENAILKHPSVIEAAVAVMPPHRWGETPCAFV I---KTKNP-----EI-----K---EADIIVHCKKELPG PhCNL
445  DVIISGGENISSVEVENVLYSHKPVLEAAVAVMPPHRWGESPCAFVTLNKNKEEV-----KSDFCVVT---EDEIITYCRKNLPH MtOSBZL
444  DVIISGGENISSVEVENVLYKPKVLETAVAVMPPHTWGETPCAFVLEKSETTIKEDRVDFQT---R---ERNLIEYCRENLPH AtCNL
443  ELIKYKGFQVAPAELEALLIHPSPVDAAVVPMKDEAAGEVPAFAFVV---RSNNS-----QL---T---EDEVKQFISKQVVF Sa4CL1
459  ELIKYKGFQVAPAELEALLIGHPPDITDVAVAMKEEAAAGEVPAFAFVV---KSKDS-----EL---S---EDDVKQFVSKQV-- At4CL1

517  FMVPKKVEFLPQLPRNPMGKVLKNVLRDQA----KTFVLSESQQT---AVD-----LYRNDQQILA-----L-SRL MdGDCNL
509  FMVPKRVAFLAELPKNSFNKILKQQLRDLMA----KAFGSTIQKKK---VTGGHGGGYGDAQSPVLA-----M-SRL HcCNL
519  FMVPKHVQFLEELPKTGTGKVKKQLQREMA----KSGIFDN-----KSGIFDN-----ANQTSQILD-----L-PAFL PhCNL
521  FMVPMKVMFMDLPKTLTGKIQKFEELRAKA----KCFVNVDEKKNKPKFNQ-----VNHNDQIIMA-----L-SRL MtOSBZL
524  FMCPRKVVFELELPKNGNGKILPKPLRDLA----KGLVVEDE-----INVIKAEVKRPFVGHFI-SRL AtCNL
512  YKRINRVFFIEAIPKSPSGKILRDLRAKLAAGFPN Sa4CL1
526  -----KSCVLQENQSVL-----H At4CL1

```

Figure 3.20: Amino acid sequence alignment of *M. domestica* CNL (*MdCNL*), *H. calycinum* CNL (*HcCNL*; AFS60176), *P. hybrida* CNL (*PhCNL*; AEO52693); predicted OSBZL1 from *M. truncatula* (*MtOSBZL*; XP_003600627), *Arabidopsis thaliana* CNL (*AtCNL*, AtBZO1; Q9SS01), and 4CL1 from *A. thaliana* (*At4CL1*; NP_001077697) and *Sorbus aucuparia* (*Sa4CL1*; ADF30254). The amino acid conserved motifs (box I and box II) and 12 amino acids predicted to function as a 4CL substrate specificity code (Schneider et al., 2003) are highlighted. C-terminal (SRL / ARL) sequence represents peroxisomal targeting sequences. The asterisk marks a glycine residue whose hydrophobicity in CNLs was anticipated. Gaps introduced to maximize the alignment are indicated by dashes.

3.4.3. Functional characterization of *MdCNL*:

MdCNL cDNA was cloned and heterologously expressed in *Escherichia coli* as a His₆-tag fusion protein, which was purified by affinity chromatography using Ni-NTA agarose beads. The temperature optimum was found to be 30°C (Figure 3.21 A), whereas pH optimum was 6.5 (Figure 3.21B). The CNL activity was found to be linear up to 10 min and with the protein concentration up to 10 µg per assay. CNL activity was found to be strictly dependent on the presence of cations. Among divalent cations, Mg²⁺ gave maximum activity whereas Cu²⁺ caused enzyme inactivity. Among monovalent cations, K⁺ showed best activity whereas Na⁺ failed to give any activity. The combinations of divalent [Mg²⁺ (2.5 mM)] and monovalent [K⁺ (100 mM)] cations led to the highest CNL activity (100%) (Figure 3.22). No significant loss in CNL activity was observed upon storage at -80°C (with glycerol) for six months. At 4°C, enzyme activity decreased by 20% within 24 h. Substrate specificity of CNL was studied by using luciferase-based assay, which reflects CoA ligase activity in the assay by measuring the remaining ATP (Schneider et al., 2005). The amount of left-over ATP is inversely proportional to the CoA ligase activity. Incubation of the heat-denatured CNL without any substrate served as a negative control and the measured luciferase activity was set as 100% (Figure 3.23A). For substrate specificity test, a wide array of substrates (cinnamic acid, benzoic acid and their related acids) were tested with *MdCNL* in the presence of CoA, ATP, and 2.5 mM Mg²⁺ in potassium phosphate buffer as source for K⁺. The preferred substrate for *MdCNL* was cinnamic acid, followed by 4-coumaric and caffeic acids. Very minor activity was detected with ferulic and Sinapic acids. No enzyme activity was observed with benzoic acid, identifying the enzyme as CNL and not benzoate-CoA ligase (BZL). Further, substrate specificity was checked by spectrophotometric assay, which also confirms the preference for cinnamic acid as CNL substrate (Figure 3.23B). Caffeic, ferulic and sinapic acids were poor substrates for CNL. The product of CNL catalyzed reaction (cinnamoyl-CoA) was identified by the LC-ESI-MS in negative ion mode. The molecular ion [M-H]⁻ at m/z 896.3 was indicative peak for cinnamoyl CoA, which was further subjected to fragmentation and the resulting MS/MS spectrum signals, such as [AMP-H]⁻ at m/z 346.3, [ADP-H]⁻ at m/z 426.2, and [ADP-H₂O-H]⁻ at m/z 408.2, [M-H₂PO₃]⁻ at m/z 816.2 and [M-AMP-H]⁻ at m/z 549.2 matched with the previously reported data of cinnamoyl-CoA (Beuerle and Pichersky, 2002a; Figure 3.24). The kinetic properties of CNL were studied for cinnamic acid and 4-coumaric acid (Table 3.6). Cinnamic acid showed higher affinity and the turn over number as compared to 4-coumaric acid. Catalytic efficiency

(k_{cat}/K_m) of cinnamic acid was found to be 20-fold higher than that of 4-coumaric acid. The K_m values for co-substrate ATP and CoA were 102.4 and 108.6 μ M, respectively.

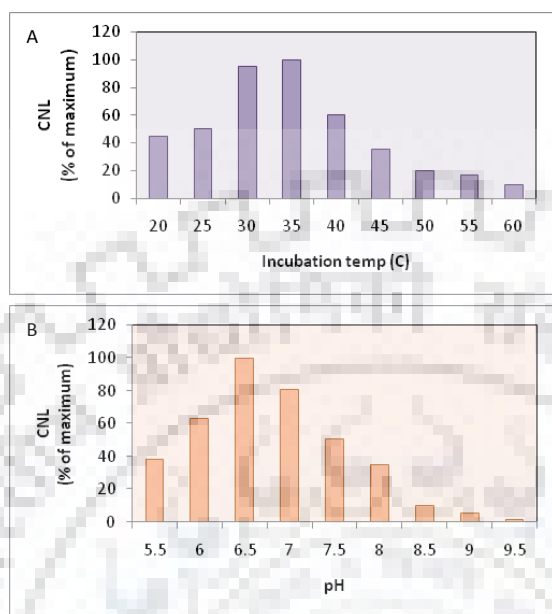


Figure 3.21: Temperature (A) and pH (B) optimum of *MdCNL*. Results are expressed as percentage of maximum.

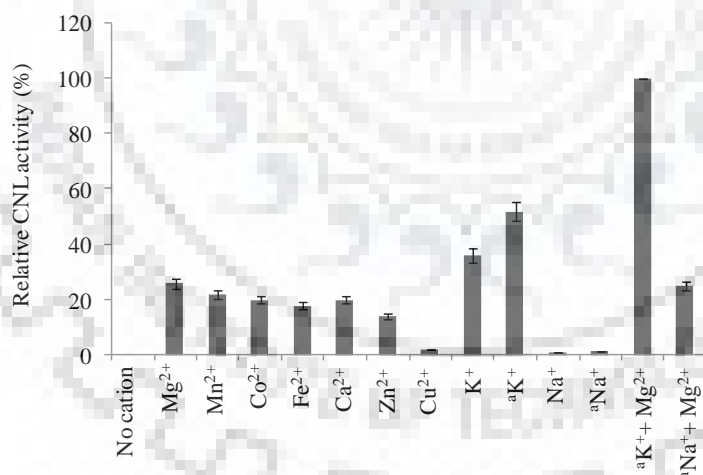


Figure 3.22: Effect of selected monovalent and divalent cation supplementation on CNL activity. Assays contained either 2.5 or 100 (100) mM concentrations of monovalent and divalent cations, respectively or a combination of both monovalent and divalent ions. Best activity was recorded for assays containing 100 K^+ and 2.5 mM Mg^{2+} and was set as 100 %. SD values are indicated (n = 3).

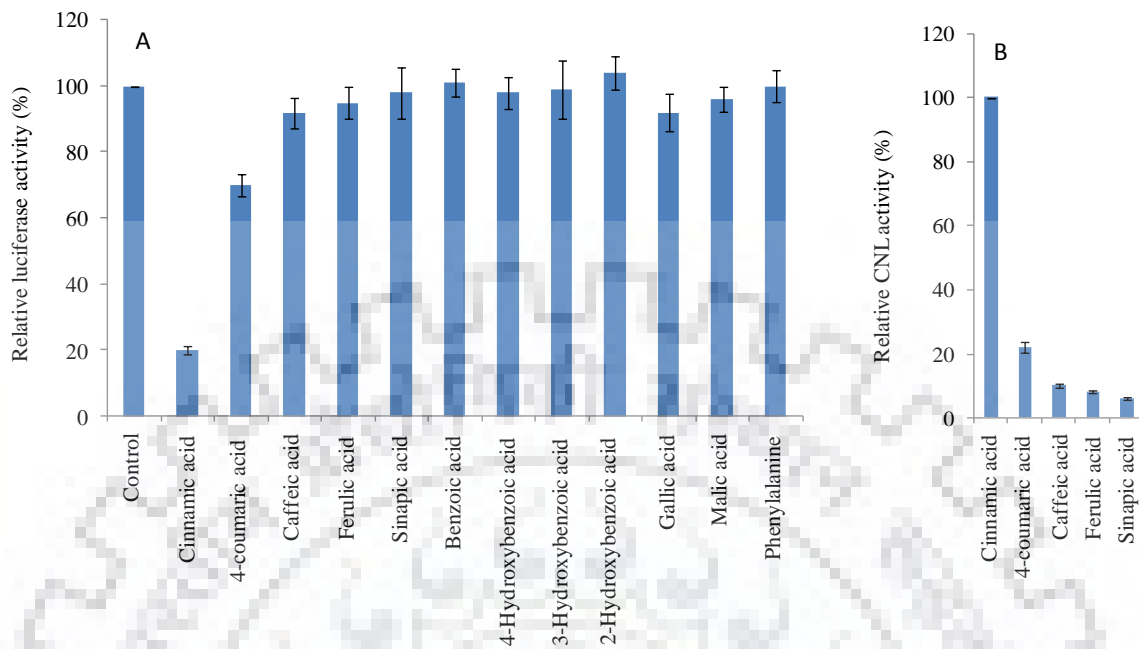


Figure 3.23: Substrate specificity of recombinant *MdCNL* (A) luciferase-based assay. The left over ATP in the CNL-assay was measured as luciferase-dependent bioluminescence, which inversely correlated with CNL activity. A control reaction with heat denatured CNL protein and without any substrate was used as negative control to normalize bioluminescence. (B) spectrophotometric-based assay in which the CNL activities were calculated using the previously reported extinction coefficients of the respective CoA esters, considering activity with cinnamic acid (cinnamoyl-CoA formation) as 100%.

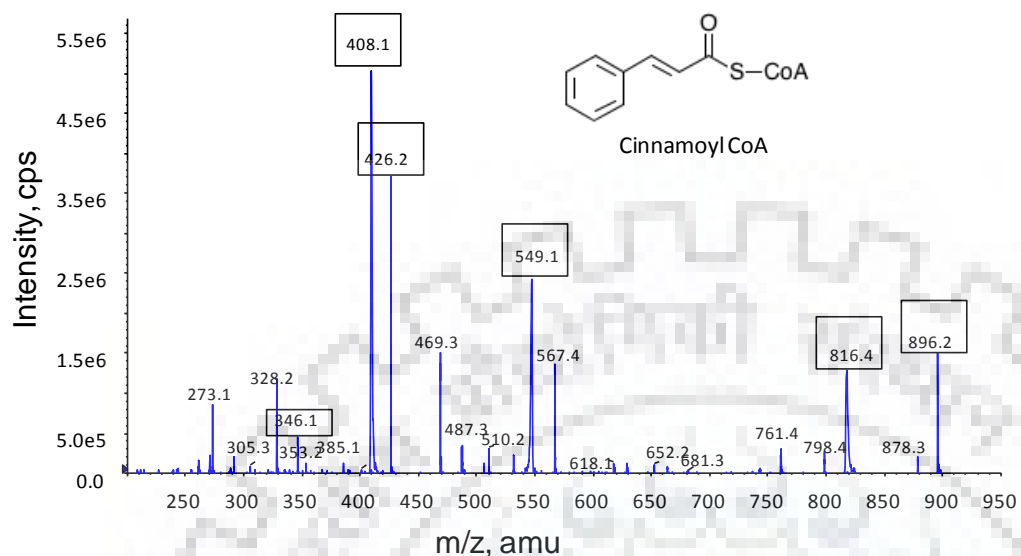


Figure 3.24: LC-ESI-MS/MS analysis of CNL-catalyzed cinnamoyl-CoA formation, represented in the mass spectrum by the molecular ion $[M-H]^-$ at m/z 896.2. MS/MS analysis showed characteristic fragments of CoA and phosphoadenosine-containing compounds as indicated by boxes (Beuerle and Pichersky, 2002a).

Table 3.6: Kinetic properties of *Md*CNL. Values are means ($n = 3$).

Substrate	K_m (μM)	V_{max} (nkat mg^{-1} protein)	K_{cat} (Sec^{-1})	K_{cat}/k_m ($\mu\text{M}^{-1} \text{Sec}^{-1}$)
Cinnamic acid	19.6	13.8	0.88	0.044
4-Coumaric acid	126.4	2.7	0.17	0.001

For ATP and CoA, K_m values were 102.4 and 108.6 μM , respectively

3.4.4. Expression of *MdPAL*, *MdCNL* and *MdBIS3*:

After VIE-treatment, transcript levels of *MdPAL*, *MdCNL* and *MdBIS3* in apple cell-cultures were analyzed by Real time-PCR over the time-course of 72h (Figure 3.25A). In order to see the involvement of general phenylpropanoid and biphenyl biosynthesis pathway in VIE-induced phytoalexin accumulation, *MdPAL* and *MdBIS3* expression levels were also monitored. Both *MdPAL* (Sircar et al., 2015; Sarkate et al., 2018) and *MdBIS3* (Chizzali et al., 2012) were known to be inducible. *Profilin* mRNA served as control for equal template amounts. *MdPAL* transcripts were detectable as early as 0.5 h after the onset of elicitation. The mRNA level peaked at 6 h and decreased thereafter slowly. Similar expression pattern were observed for the *MdCNL* transcript level which, attained peak at 6h, and rapidly decreased thereafter. *MdBIS3* showed similar induction pattern like *MdCNL*, however induction was delayed. *MdBIS3* expression attained peak at 12h and thereafter expression level rapidly decreased and reached to basal level at 72 h. mRNA followed alike the pattern of *MdBIS3*, however expression level was relatively less. The expression of *MdPAL*, *MdCNL* and *MdBIS3* preceded the accumulation of noraucuparin and aucuparin phytoalexins, suggesting involvement of these genes in biphenyl phytoalexin biosynthesis in Golden Delicious cell cultures.

V. inaequalis infected green-house grown plants of cv. Shireen did not show any visible symptoms on the leaves after 16 days of infection, however, infected Golden Delicious leaves showed minor scab symptoms after 16 days (Figure 3.26). This is possibly due to scab-resistance properties of Shireen. *MdCNL* expression in *V. inaequalis*infected stems of cv. Shireen and Golden Delicious were measured in relation to that observed in mock-inoculated control stems (internodes) over the time-course of 16 day (384 h). Compared to Golden Delicious, a rapid induction of *MdCNL* transcript level was observed in the Shireen (Figure 3.25 B). After onset of scab fungus infection, *MdCNL* expression in Shireen attained peak at day 6 whereas in Golden Delicious, a delayed induction was observed, which showed maxima at day 8. When compared with mock-inoculated control shoots, the *MdCNL* expression level was found to be 38 and 12.5 fold higher in Shireen and Golden Delicious, respectively.

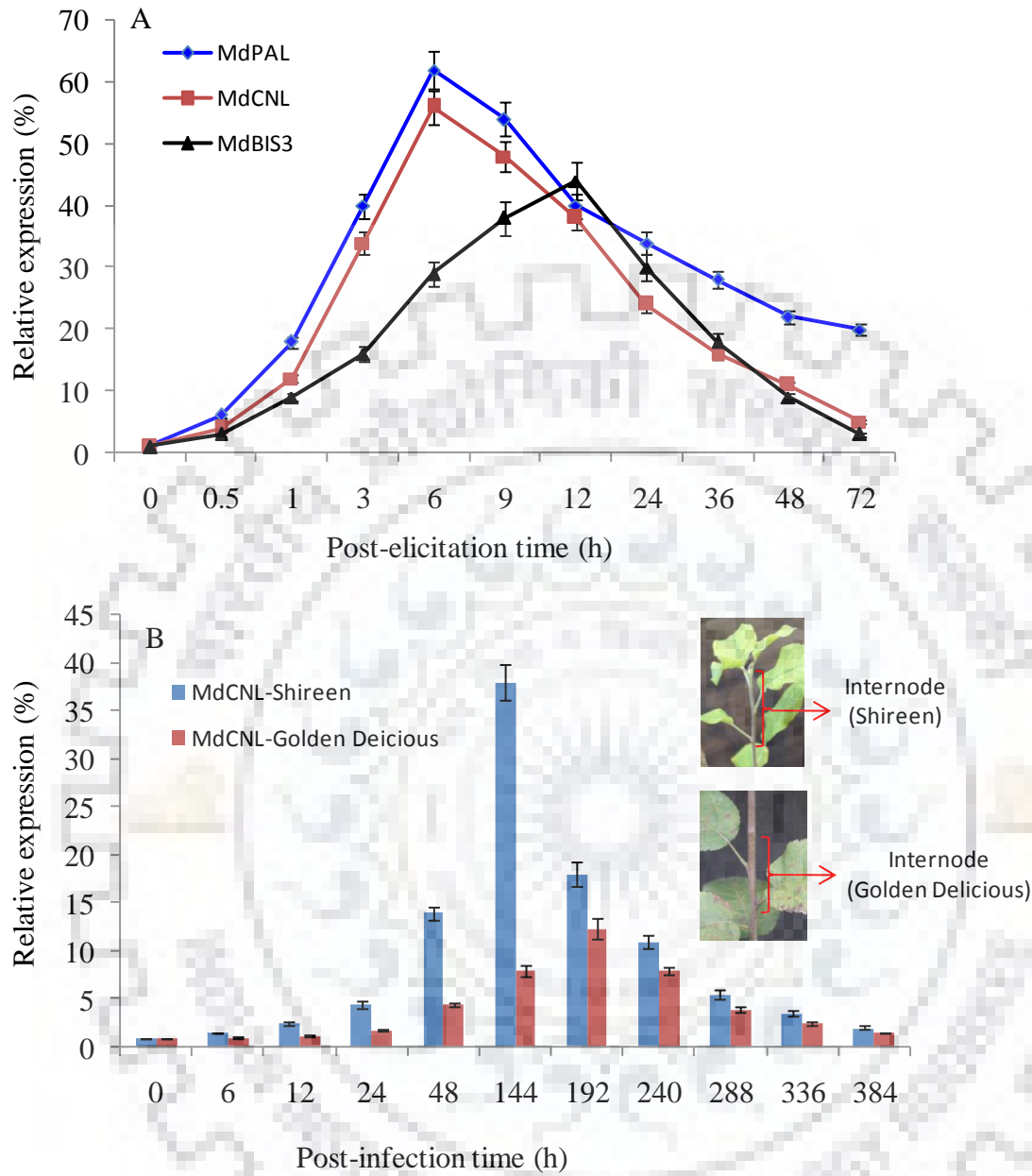


Figure 3.25: Changes in the gene expression levels. (A) Changes in the expression of *MdPAL*, *MdCNL*, and *MdBIS3* in *V. inaequalis* elicitor-treated cell cultures of cv. Golden Delicious. (B) Changes in the expression level of *MdCNL* in scab-infected shoots of apple cultivar Shireen (blue bars) and Golden Delicious (red bars). The relative transcript levels were determined by real-time-PCR. Results are means \pm SD (n = 3).

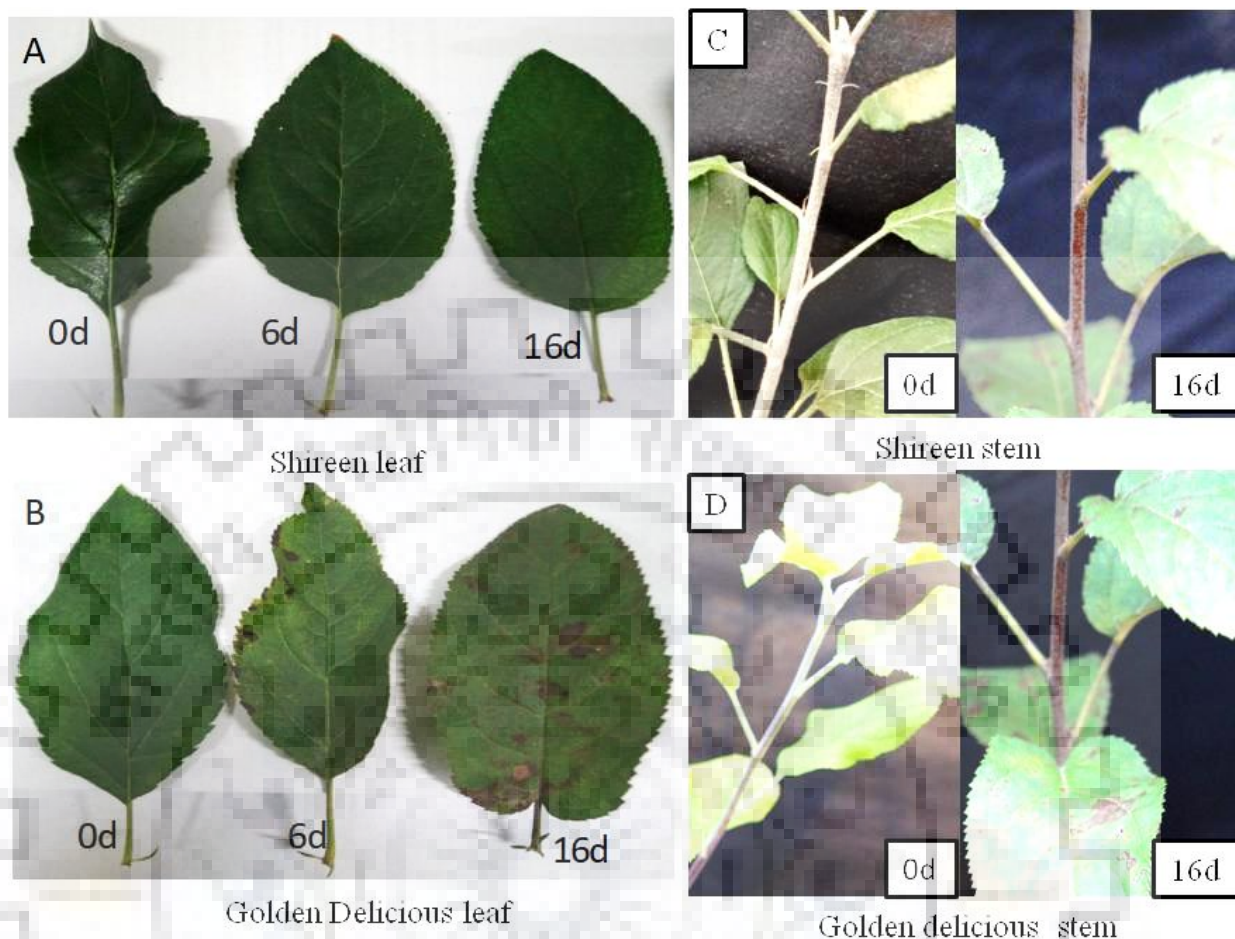


Figure 3.26: Progression of scab symptoms in *V. inaequalis*-infected leaves of apple cv. Shireen (A) and Golden Delicious (B); *V. inaequalis*-infected shoots showing transition zone of apple cv. Shireen (C) and Golden Delicious (D).

3.4.5. Phylogenetic reconstruction of CNL and related amino acid sequences:

For construction of a phylogenetic tree, benzoate- and cinnamate-specific CoA ligases were taken into consideration (Figure 3.27). The amino acid sequence accession numbers are listed in (Table 2.26). In addition to angiosperms, 4-coumarate:CoA ligase (4CL) sequences gymnosperms, pteridophytes and bryophytes were also included in the tree. Tree rooting was done using fatty acid CoA ligase sequence from *Arabidopsis lyrata*. The resulting neighbor-joining tree consisted of two major evolutionarily distinct clusters. The first cluster was constituted by benzenoid-related CoA ligases including CNL from Golden Delicious. The *H. calycinum* CNL, putative OSBZL1 from *M.*

truncatula, CNL from *Petunia hybrida*, were the closest to apple CNL. The second cluster comprised of 4CL sequences.

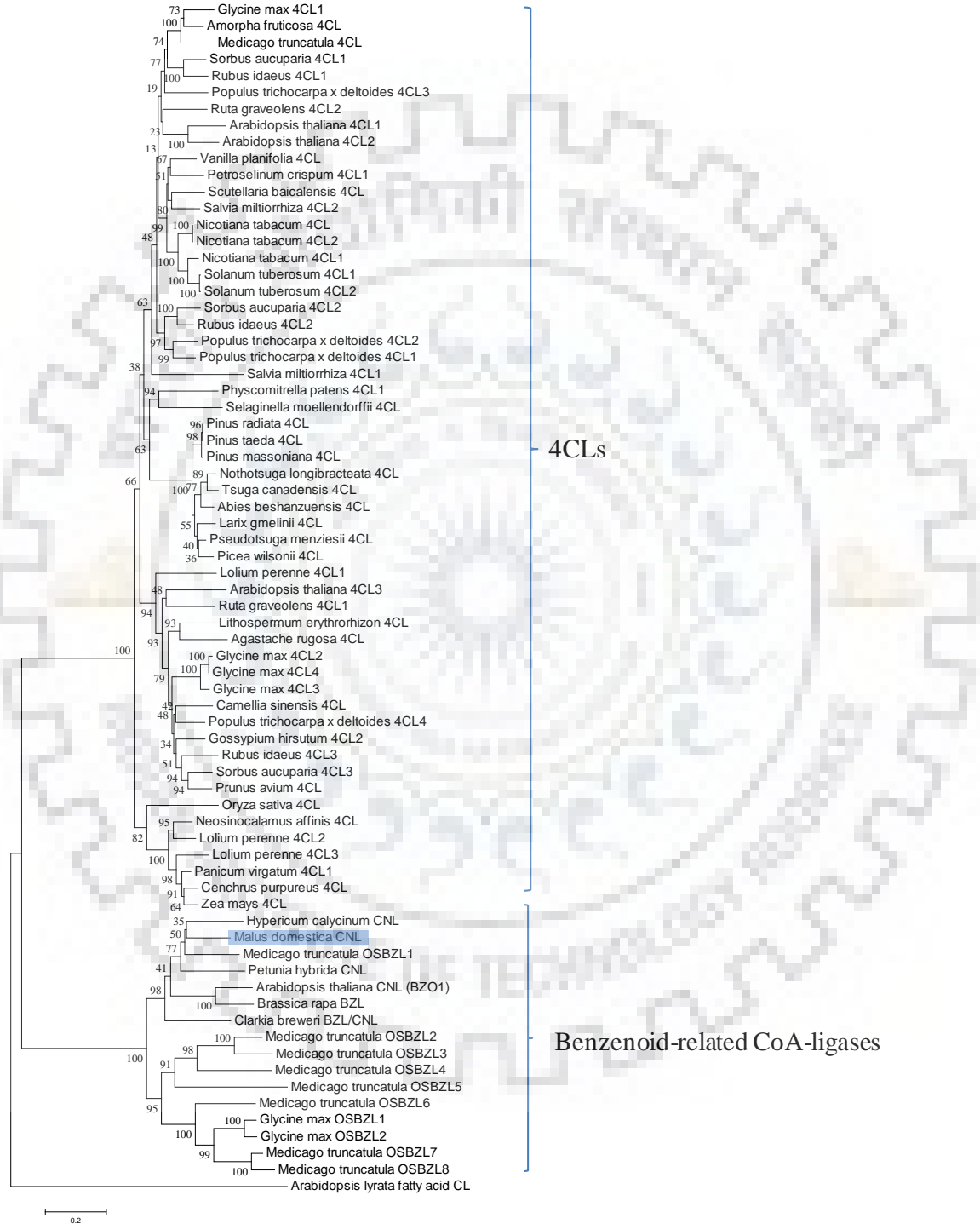


Figure 3.27: Phylogenetic tree demonstrating the evolutionary relationships between *Malus domestica* cv. Golden Delicious CNL and other benzoate- and cinnamate- related CoA-ligases. The neighbor-joining tree was constructed using amino acid sequences through MEGA 5.05 with 1,000 bootstrapped value support and a Poisson correction. The bootstrap values are indicated at the branch points. The scale bar represents 0.2 amino acid substitutions per site.

3.4.6. Subcellular localization of *MdCNL*:

Bioinformatic processing of *MdCNL* sequence showed the presence of a C-terminal PTS1 signal represented by amino acid SRL. To examine the functionality of the C-terminal PTS1 signal, gateway constructs encoding fusion proteins of CNL with yellow fluorescent protein (YFP) were generated and transiently expressed in epidermis cells of *Nicotiana benthamiana* leaves. The *MdCNL* coding sequence was fused with YFP at either the N terminus to generate YFP-CNL construct or the C terminus (without stop codon) to generate CNL-DEL-YFP construct. For co-localization, cyan fluorescent protein (CFP) as a fluorochrome was N-terminally fused with the PTS1 tripeptide and used as a peroxisomal marker protein (Nowak et al., 2004). All constructs were driven by 35S promoter from the cauliflower mosaic virus. The products of the constructs were localized by confocal laser scanning microscopy. For YFP-CNL, punctate fluorescence was observed, suggesting peroxisomal localization (Figure 3.28 A). In contrast, fluorescence was present throughout the cytoplasm when YFP was fused with the C-terminus of *MdCNL*, thereby masking PTS1 (Figure 3.28 B). In order to check peroxisomal localization of *MdCNL*, tobacco leaves were co-transformed with YFP-CNL and the marker construct CFP-PTS1. The products of both constructs were targeted to the peroxisomes (Figure 3.28 C, D). In merged condition, the most of YFP dots overlaid with CFP dots, giving pale dots (Figure 3.28 F), thereby suggesting a perfect co-localization.

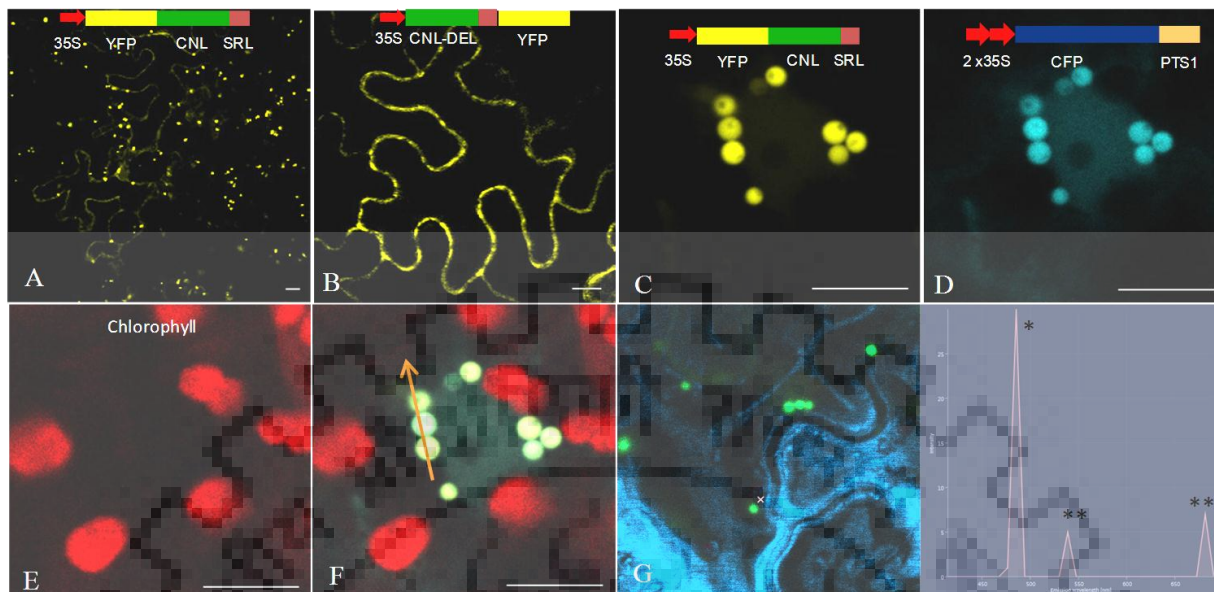


Figure 3.28: Localization studies of Golden Delicious CNL in leaf epidermis cells of *Nicotiana benthamiana*. Transient expression of YFP-CNL (A) and CNL-DEL-YFP (B) constructs resulted in the formation of peroxisomal and cytosolic localization of CNL proteins, respectively. (F) Co-transformation with YFP-CNL (C) and the marker construct CFP-PTS1 (D), where merged localization in peroxisomes indicated by arrow in F. (E) Autofluorescence of chloroplasts, (G) emission fingerprints of CFP (*), YFP (**), and chlorophyll (***) are documented. Bars = 10 μ m.

3.4.7. Molecular modeling and molecular docking:

Homology model of *MdCNL* was generated using the crystal structure of fatty acid-CoA ligase (tt0168) from *Thermus thermophilus* HB8 (Hisanaga et al., 2004) which showed highest identity (36%). *MdCNL* sequence showed 27% similarity with crystal structure of 4-coumarate:CoA ligase (5BSW) (Li and Nair, 2015). *MdCNL* homology model was generated to compare the structural and functional properties of the protein. Ramachandran plot of the model produced by PROCHECK shows that 86.0% residues are in most favored region, 13.6% are in the additional allowed region and 0.2% residues are in generously allowed and disallowed regions as shown in (Figure 3.29). The predicted model consists of 19 α helices and 24 β sheets as shown in (Figure 3.30). Superposition of validated model of *MdCNL* with the crystal structure of tt0168 from

Thermus thermophilus HK8 (PDB ID: 1ULT) shows RMSD of 0.16 Å as shown in (Figure 3.31). Topology diagram of the model generated by PDBsum is shown in Figure 3.32. Molecular docking was used to check the preference of binding of the orientation of substrates with protein. The interacting residues of *MdCNL* with cinnamic acid, 4-coumaric acid, caffeic acid, ferulic acid and sinapic acid are shown in Figure 3.33 and 3.34. Binding energy chart was shown in Table 3.7. Hydrogen bonding of all the substrates with Gly334 shows that it plays an important role in catalysis of substrates by *MdCNL*. Electrostatic potential surface view of docking results shows that all the cinnamic acid, 4-coumaric acid, caffeic acid, ferulic acid and sinapic acid bind at hydrophobic pocket of *MdCNL* as shown in Figure 3.35.

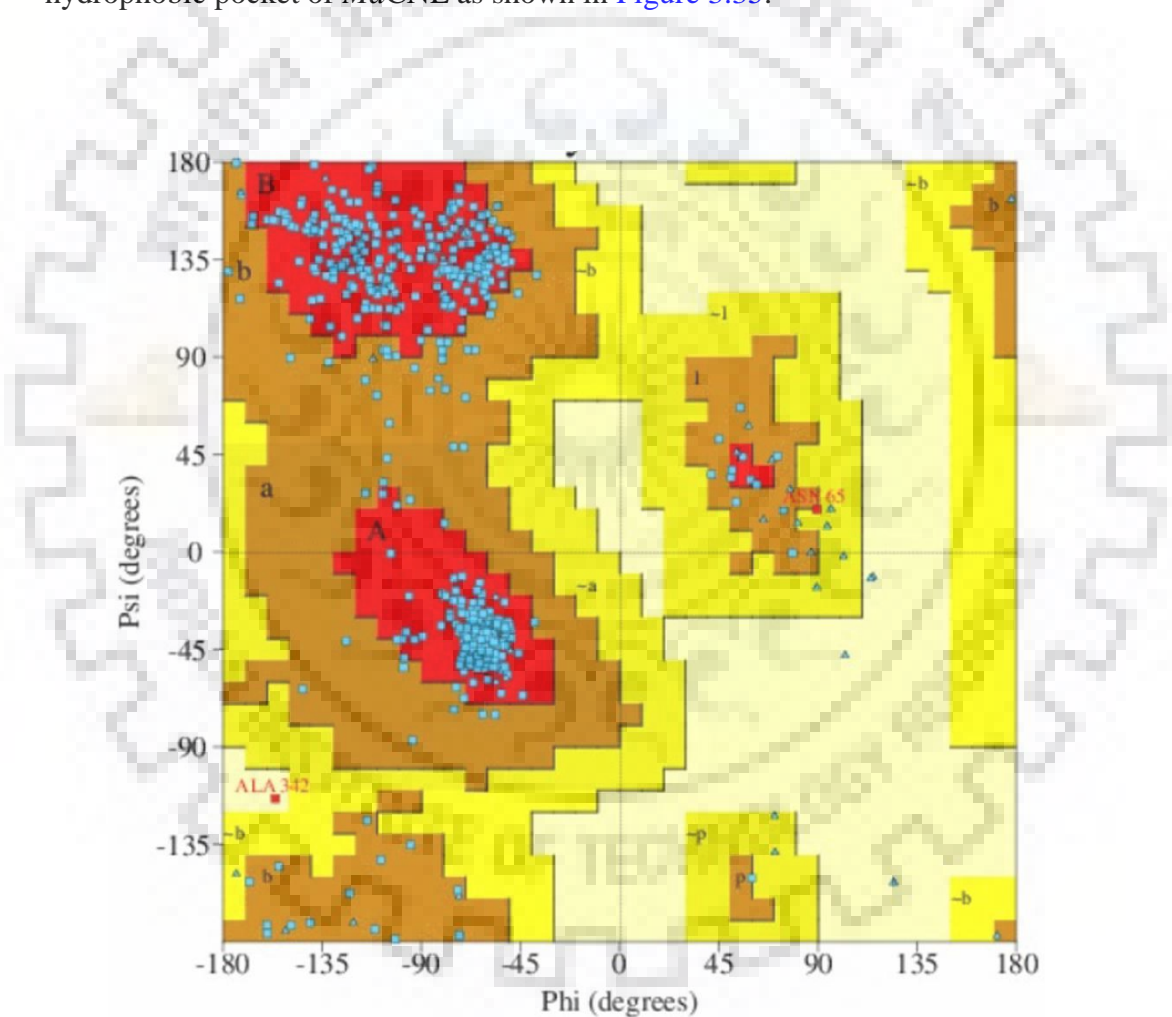


Figure 3.29: Ramachandran plot of *MdCNL* generated by PROCHECK.

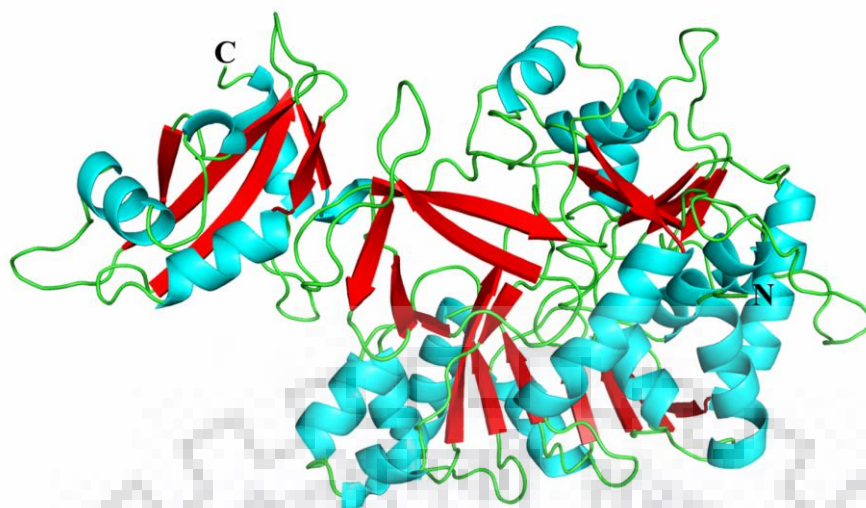


Figure 3.30: Cartoon representation of modeled structure of *MdCNL* protein with α helices (cyan color) and β sheets (red color).

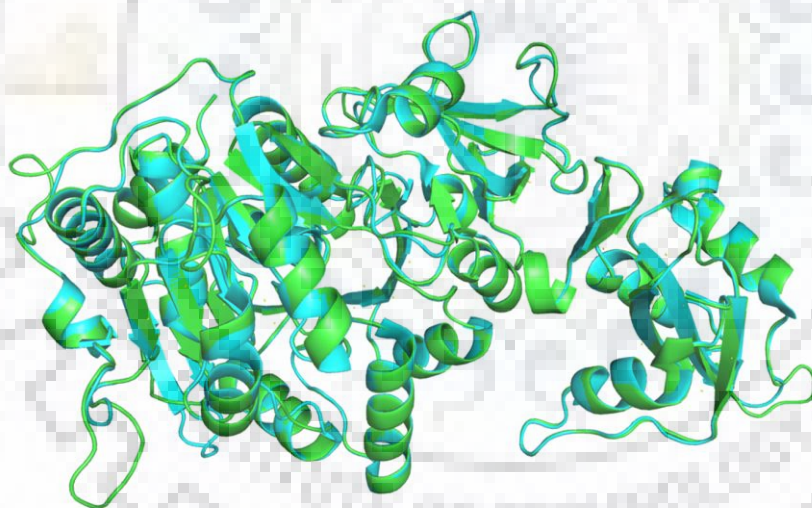


Figure 3.31: Cartoon representation of superposition of cinnamate CoA ligase from *M. domestica* model (green color) and crystal structure of tt0168 from *Thermus thermophiles* HK8 (PDB ID: 1ULT) (cyan color).

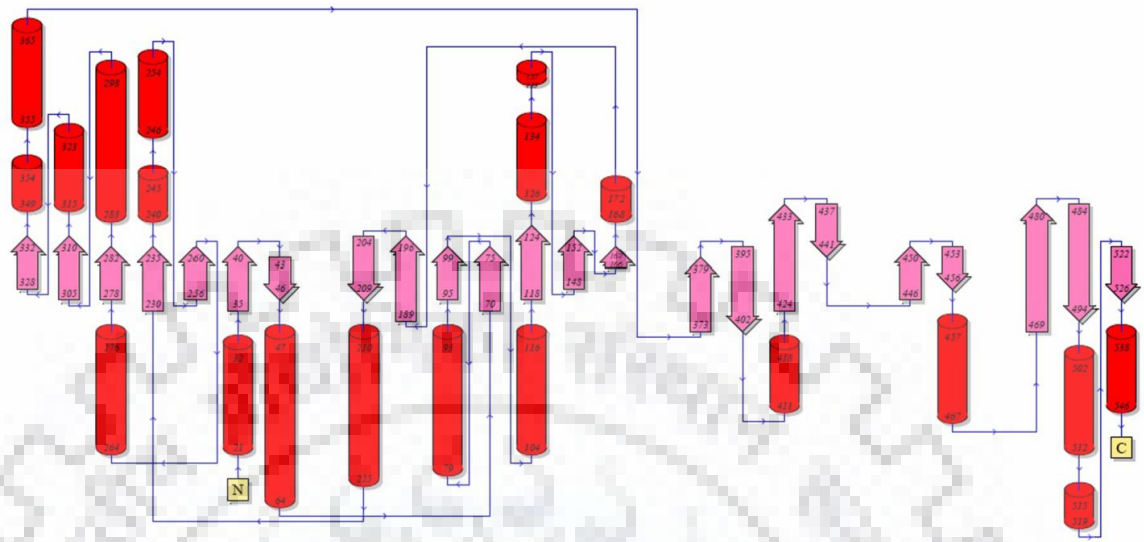


Figure 3.32: Topology diagram of secondary structures of cinnamate-CoA ligase from *MdcNL* model represented in figure 3.31.

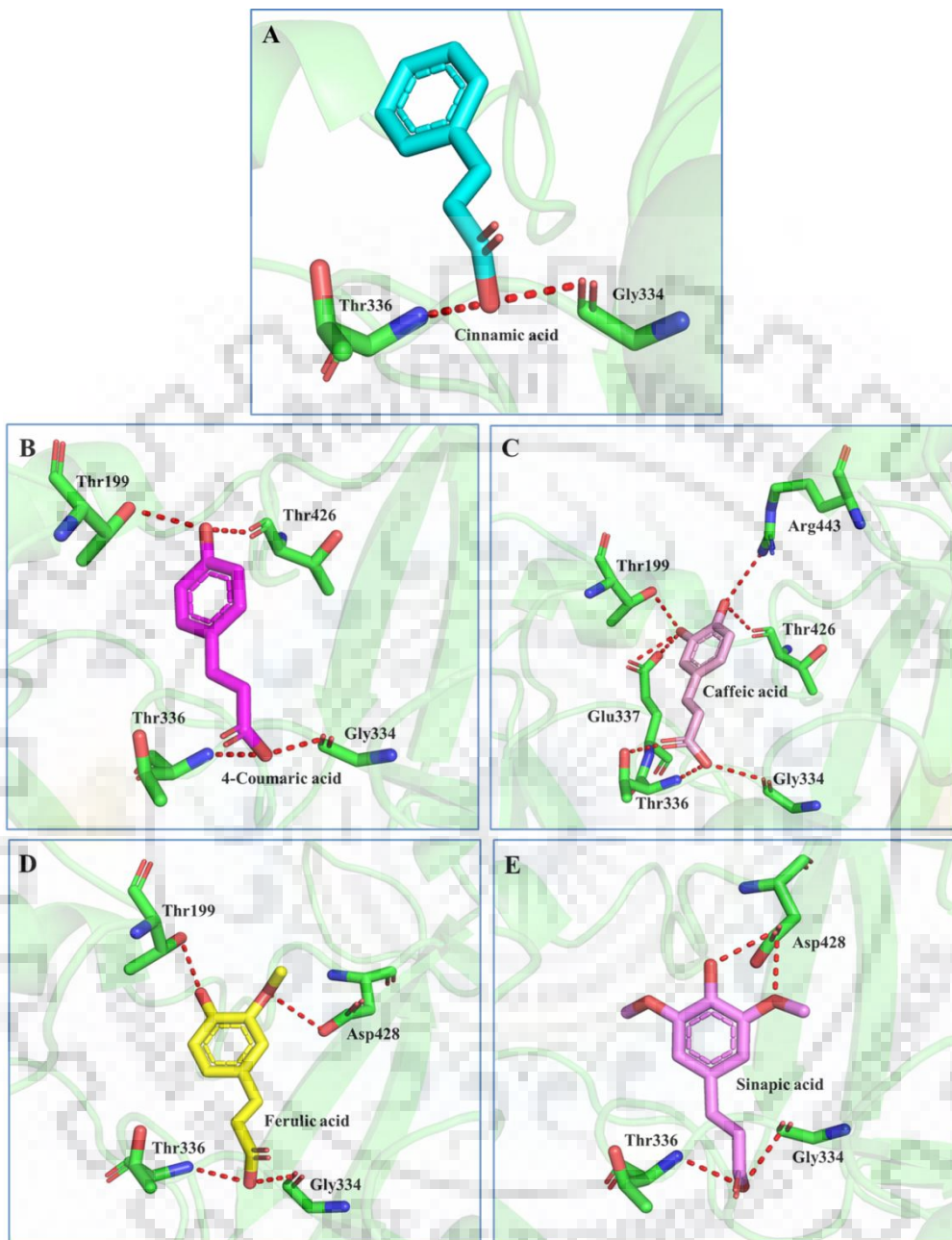


Figure 3.33: The cartoon representation of *MdcCNL* from showing binding with: (A) cinnamic acid (cyan color); (B) 4-coumaric acid (magenta color); (C) caffeic acid (pink color); (D) ferulic acid (yellow color) and E) sinapic acid (violet color). Interacting residues of *MdcCNL* are shown in stick format while red dotted lines show the intermolecular hydrogen bond interactions.

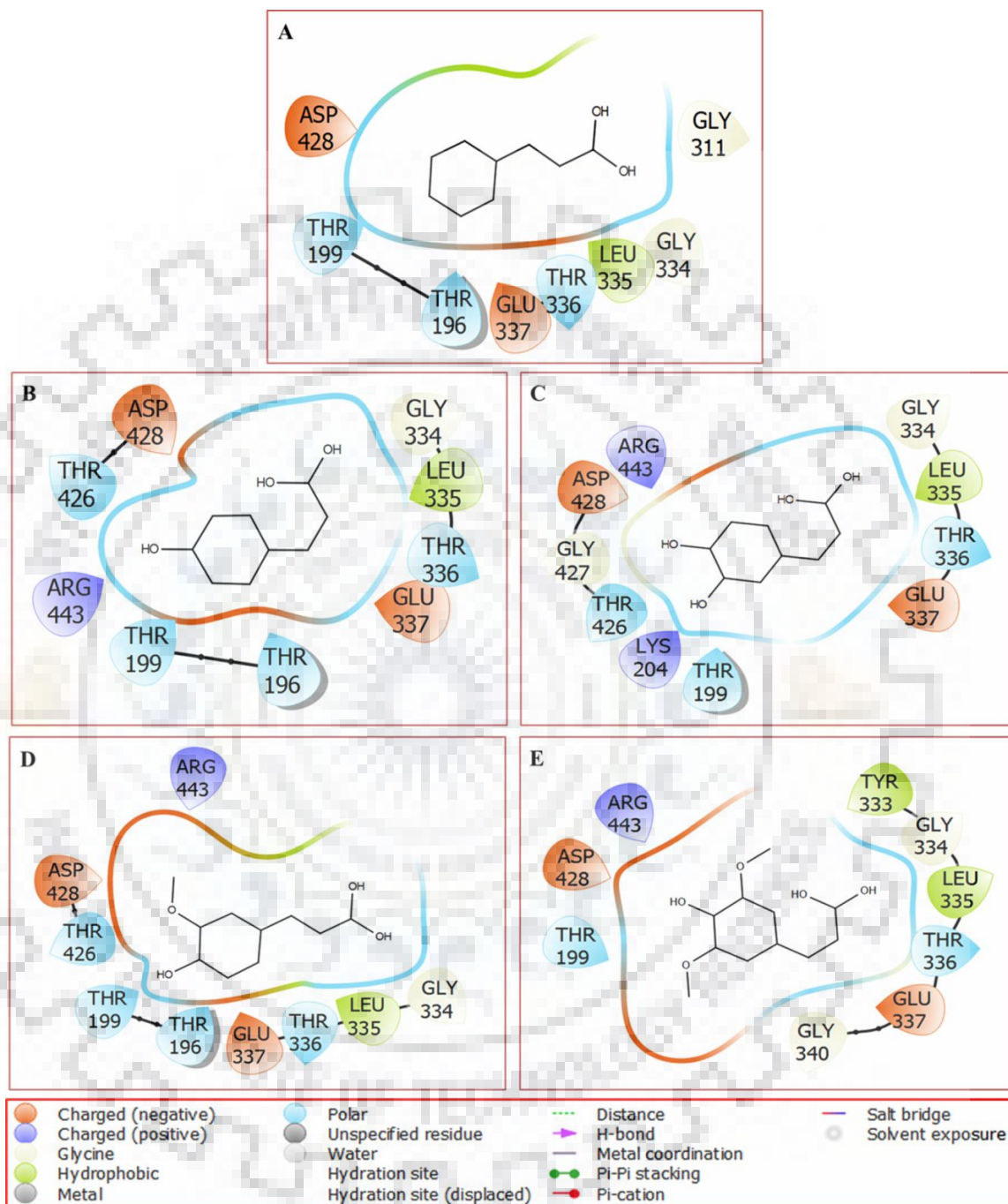


Figure 3.34: Pictographic representation of hydrophobic interaction involved in *MdcCNL* with: (A) cinnamic acid, (B) 4-coumaric acid, (C) caffeic acid, (D) ferulic acid and (E) sinapic acid.

Table 3.7: Docking results of *MdCNL* with cinnamic acid (CID444539), 4-coumaric (CID637542), caffeic (CID689043), ferulic (CID445858) and sinapic acids (CID637775) along with their binding energy and interacting residues.

S.No.	Name	PubChem	Binding affinity (K cal/mol)	Interacting residues	
				Hydrogen bonding	Hydrophobic
1	Cinnamic acid	CID444539	-5.0	Gly334, Thr336	Thr196, Thr198, Gly311, Leu335, Glu337, Asp428
2	4-Coumaric acid	CID637542	-4.55	T199, T426, Gly334, Thr336	Thr196, Leu335, Glu337, Asp428, Arg443
3	Caffeic acid	CID689043	-4.35	Gly334, Thr336, Glu337, Thr426, Asp428	Lys204, Leu335, Thr426, Gly427, Asp428
4	Ferulic acid	CID445858	-4.3	Thr199, Gly334, Thr336, Asp428	Thr196, Leu335, Glu337, Thr426, Arg443
5	Sinapic acid	CID637775	-4.2	Gly334, Thr336, Asp428	Thr199, Tyr333, Leu335, Glu337, Gly340, Arg443

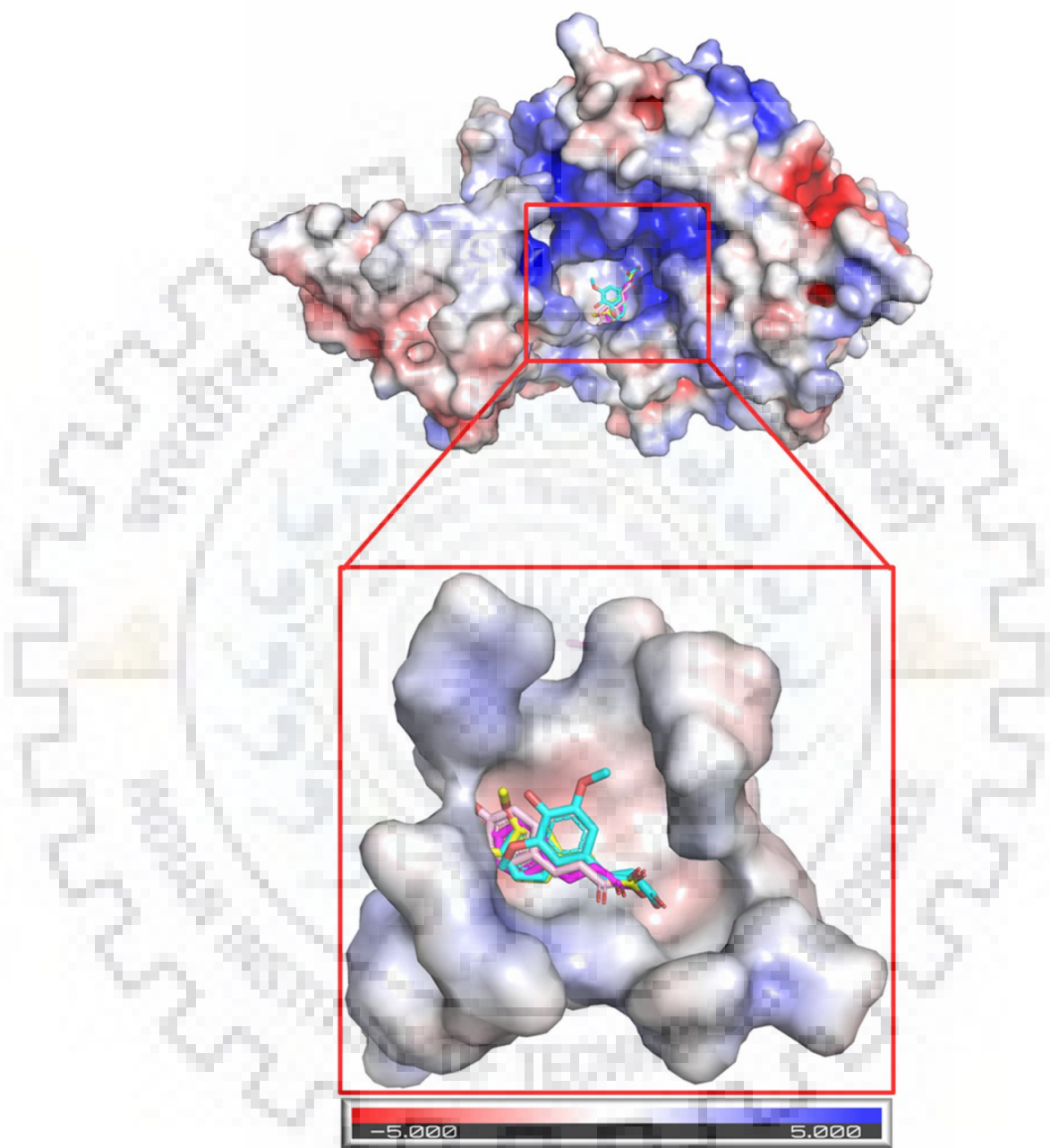


Figure 3.35: Electrostatic potential surface view of *MdCNL*. Zoom window shows the binding pocket with cinnamic acid (cyan color), 4-coumaric acid (magenta color), caffeic acid (pink color), ferulic acid (yellow color) and sinapic acid (violet color).

Chapter 4

Discussion

4.1. General Discussion:

Apple (*Malus domestica*) is an important fruit crop grown in India and other parts of the world. In orchards, apple trees are mostly propagated by clonal propagation of single tree, thereby bringing genetic uniformity within the population, which adversely affect plant's pathogen resistance potential (Gessler and Patocchi, 2007). The scab disease caused by the fungus *Venturia inaequalis* is disastrous for apple cultivation. Apple plants infected by scab fungus produces infected low quality fruits with massively reduced commercial value. Except for multiple fungicides spraying, there is no efficient technique to control this disease, and the underlying metabolic response of apple plants to *Venturia inaequalis* infection remains largely unknown. Considering the economic importance of apple, breeding of new scab-resistant apple cultivar is urgently needed to manage the scab disease and its adverse impacts. The resistance provided by scab resistant genes (*Rvi1-Rvi17*) in existing scab-resistant apple cultivars are either already broken by emerging races of *V. inaequalis* or will be broken soon in near future. In the view of the above, search for new scab-resistance gene in apple with durable resistance is required. Interestingly, a number of scab-resistant wild apple cultivars have evolved diverse endogenous mechanisms to combat with the scab infections, such as production of specialized class of defense metabolites, the biphenyl and the dibenzofurans (Kokubun and Harborne, 1994) and several other anti-fungal phenolics (Veberic et al., 2008; Mikulic-Petkovsek et al., 2009). However, systematic understanding the disease resistance mechanism in apples and underlying biochemical and molecular details is largely elusive. In this thesis work, the responses of an economically important apple cultivar, Golden Delicious, which is moderately scab-susceptible, was investigated using metabolomics, biochemical and molecular biological methods. A number of scab-induced defense metabolites were identified through GC-MS-based metabolomics analysis. The expression levels *PAL*, *F3H*, *AOX* and *BIS3* genes involved in the formation of some crucial defense-associated metabolites were studied through quantitative real-time PCR. In addition, a novel gene cinnamate-CoA-ligase (*MdCNL*), involved in the biosynthesis of benzoyl-CoA and subsequent biphenyl phytoalexin have

been cloned and functionally characterized from *Venturia inaequalis* elicitor-treated cell culture of Golden Delicious. Expression pattern of *MdCNL* upon scab-fungus infection to green house grown apple plants of scab resistant cultivar “Shireen” and moderately scab susceptible cultivar Golden Delicious were compared. Overall this thesis work increases our understanding of the complex interaction response apple-Venturia pathosystem. Based on the objectives and results, discussion section is sub-divided into following four sections.

4.1.1. Development of cell suspension culture of apple cv. Golden Delicious:

Considering the economic importance of apple cultivar cv. Golden Delicious and availability of published genome sequence (www.rosaceae.org) this cultivar has been selected for the initiation of the cell suspension culture. Plant cell suspension cultures offer excellent system to study plant metabolism under various change environments (Bhatia and Bera, 2015). Moreover, plant cell culture could potentially provide information on what metabolites are produced upon elicitor treatment, for those metabolites which play key role in plant defense (Pérez-Clemente et al., 2013). This approach provides several advantages such as little or no seasonal variation, easy extraction of metabolites, less presence of interfering substances (lignin and chlorophylls) and less production time. In this study, growth of cell suspension culture in liquid LS-medium showed best result with 2 µM 2,4-D and 1 µM NAA. Addition of kinetin in cell suspension culture showed cell clumping, thereby kinetin was removed. Although there are a few studies on callus induction in apple (Hrazdina et al., 1997; Kumar et al., 2016), no previous report on detailed characterization of callus induction in terms of frequency and biomass are available. It was earlier reported that callus induction in McIntosh and Liberty cultivar requires 2, 4-D, indole-3-butyric acid and kinetin in MS medium (Hrazdina et al., 1997). The differential response of different cultivars of the same species towards callus induction is possibly due to their unique physiological and biochemical response potential towards growth regulators. Factors such as plant genotype, nature of explant, in vitro growth conditions and optimal concentration of growth regulators often influence the callus induction properties (Delporte et al., 2014).

4.1.2. Development of a validated HPLC method for the simultaneous detection of biphenyl and dibenzofuran phytoalexins:

Upon pathogen attack, the Malinae sub-tribe of Rosaceae family forms two specialized class of phytoalexins, biphenyls and dibenzofurans (Chizzali and Beerhues, 2012). The ability to produce these two classes of inducible defence compounds is confined to the members of Malinae only (Saini et al., 2017). These phytoalexins from Malinae have gained immense attention due to their antibacterial and antifungal properties and their presence has been shown to be closely related to scab-disease tolerance of apple. These antimicrobial phytoalexins inhibit the growth of pathogens during plant-pathogen interactions. In the Malinae, the most abundant biphenyl phytoalexins are aucuparin and noraucuparin, whereas eriobofuran represent most important dibenzofuran phytoalexin (Chizzali and Beerhues, 2012). The content of these inducible phytoalexins varied widely in different apple cultivars depending on factors such as genotype, climate and pathogen infection. Presence of these phytoalexin in apple and pear serves as marker compound for scab and fire-blight tolerance. In order to obtain scab or fire-blightresistant apple and pear for commercial plantation, it is essential to rapidly determine the level of these phytoalexins in different cultivars of apple and pear. Till date, analysis and characterization of biphenyl and dibenzofuran phytoalexins from Malinae has relied mainly on gas chromatography (GC) based method (Huttner et al., 2010). However, the use of GC presents a number of difficulties including the instability of the derivatized phytoalexin and the self-destructive analytical process, hence not being suitable for preparative work. In this study a rapid HPLC-based method coupled with diode array detection (DAD) and mass-spectrometry was developed for the simultaneous detection and identification of biphenyl and dibenzofuran phytoalexins. Identification of each phytoalexin was accomplished by comparison of retention time (RT) and UV-spectral properties with known standards. Chemical identity of aucuparin, noraucuparin and eriobofuran was further confirmed by ESI-MS/MS analyses. The method can easily be extended to the routine analysis of apple phytoalexins to determine their scab-tolerance. The main advantage of this method is the rapid separation and quantification of noraucuparin, aucuparin and eriobofuran which are among the most important phytoalexins of Malinae. Furthermore, the monitoring of the level of these phytoalexin is essential for the assessment of pathogen defense potential of Malinae plants, such as apples and pear. HPLC analyses coupled with PDA detector and mass-spectrometry proved to be an efficient method for the simultaneous detection and quantification of biphenyl and dibenzofuran

phytoalexins from rosaceous plants. The evaluated validation characteristics showed that the technique is very simple, sensitive, reproducible and accurate. The detection limits for the measured compounds are excellent. Sample extraction and preparation process prior to analysis is very simple and fast, which could be applied to nearly any type of plant material containing biphenyl and dibenzofuran phytoalexins. Furthermore, the separation was performed using isocratic condition, thereby no re-equilibration is required in between two successive HPLC runs.

4.1.3. GC-MS based metabolomics analyses of *Venturia inaequalis* elicitor (VIE)-treated cell culture of apple cv. Golden Delicious:

The Golden Delicious cell cultures were treated with *Venturia inaequalis* elicitor to identify the scab-induced differentially accumulating metabolites. These differentially accumulating metabolites could be a very good target for developing metabolite marker for scab resistance. In this study, GC-MS based non-targeted metabolomics coupled with multivariate data analysis such as principal component analyses (PCA) were performed to delineate the scab-induced metabolites. Furthermore, the metabolomics data were integrated with the gene expression data of selected crucial secondary metabolite biosynthetic genes, to obtain a generalized view of the molecular and biochemical basis of scab-tolerance. As elicitors can mimic the pathogenesis related symptoms by triggering similar biochemical reactions as induced by original pathogen infection. Elicitor-treated plant cell suspension culture provides an easy system to study plant-pathogen interaction at biochemical and molecular levels ([Bektas and Eulgem, 2014](#)).

Metabolomics data showed changes in both primary and secondary metabolites. A speedy hydrolyses of sucrose was observed in the VIE-treated cell culture. This indicates that sucrose catabolism was higher in VIE-treated cell culture. Likewise, high glucose and fructose levels were probably due to rapid break-down of sucrose upon elicitation or higher rate of synthesis of glucose. Although photosynthetic rate of glucose formation have not been estimated in this study. Upon elicitation, conversion of fructose to mannose was up-regulated, resulting into higher mannose accumulation. A number of organic acid accumulations were enhanced after VIE-treatment, which was possibly due to increase turnover number of glycolysis and TCA cycle. High organic acid concentration facilitates better ion absorption/mobilization and thereby known to be associated with higher disease tolerance ([Hudina and Štampar, 2000](#)). Ascorbic acid level found to be up-

regulated after VIE-treatment, no significant change in vitamin E content was observed. Ascorbic acid is known to be associated with the enhanced defense responses in many plant species (Pastori et al., 2003). In contrast, Pavet et al., (2005) have shown that ascorbic acid deficiency activates higher disease resistance in *Arabidopsis*. So, whether high ascorbic acid content really helps in elevating resistance towards scab disease, needs to be investigated in detail. VIE-treatment leads to the massive up-regulation of a number of phenolics. The content of these phenolics were first up-regulated after VIE-treatment and thereafter declined to the basal level. Similar array of polyphenol compositions were previously detected in the leaves of Golden Delicious apple (Picinelli et al., 1995). However, in contrast to previous report, quercetin and avicularin has not been detected from VIE-treated Florina cell cultures. The phenolic acids and their derivatives are known to oxidize proteins, thereby inhibiting important enzyme functions of pathogen and restricting the disease progression. Phenolics also deposited along the cell wall and provide first line of defense against infection (Mikulic Petkovsek et al., 2008; Underwood, 2012).

In earlier studies, it has been demonstrated that differential accumulation of flavonols (catechins and proanthocyanidins) was key factors in providing scab resistance in apple cultivars (Treutter and Feucht, 1990; Mayr et al. 1997) have shown a positive association between proanthocyanidin content and scab resistance in apple. In contrast, Sierotzki and Gessler (1993) have shown that there was no positive correlation between scab-resistance and basal level of flavonols in terms of scab susceptibility of apples. In this study, high basal level of catechin, epicatechin and rutin content were also observed in the Golden Delicious cell culture. Upon elicitor-treatment, a significant up-regulation of all the three detected flavonoids (catechin, epicatechin and rutin) was observed. High basal catechin and epicatechin level is known to be associated with higher resistance against fungal infection (Amil-Ruiz et al., 2011). Earlier it has been shown that strawberry plant bearing high catechin content exhibit powerful resistance against *Botrytis cinerea* and *Alternaria alternata* (Hébert et al., 2002). It was also reported that scab-resistant apple cultivars are particularly rich in the content of caffeic, chlorogenic, and ferulic acid and their concentration rapidly increases after scab-infection as compared to susceptible cultivars (Mikulic Petkovšek et al., 2003). High phenolic content of scab-resistant apple is known to be associated with higher nutritional quality and antioxidant properties (Liaudanskas et al., 2014). In this study a rapid enhancement of benzoic acid was observed after elicitor-treatment. It was known that benzoic acid serves as the precursor for biphenyl and dibenzofuran class of phytoalexins of apple and other

members of Malinae (Hrazdina et al., 1997; Chizzali et al., 2012, 2016; Saini et al., 2017). Upon scab-infection, benzoic acid forms benzoyl-CoA, which combines with malonyl-CoA to produce 3,5-dihydroxybiphenyl, the precursor for all other biphenyl and dibenzofurans. Enhanced biosynthesis of benzoic acid in elicitor-treated cells might attribute its higher resistance against scab fungus *V. inaequalis* (Chizzali et al., 2012) by facilitating rapid formation of biphenyl phytoalexins upon pathogen attack. Equally, high content of chlorogenic, caffeic and protocatechuic acids are also known to be associated with enhanced resistance towards fungal infection (Mikulic Petkovsek et al., 2008; Mandal, 2010). In our study, enhanced accumulation of trans-cinnamic, chlorogenic, caffeic, p-coumaric, ferulic and protocatechuic acids in apple cell cultures were observed, which probably attribute resistance against scab infection in apple cultivar cv. Golden Delicious. *Trans*-cinnamic acid serves as the precursor of many defense metabolites, such as phenylpropanoids, benzoic acid, lignans and flavonoids (Gaid et al., 2012). High level of *p*-coumaric acid is linked with synthesis of flavonoids. Accordingly, the peak of *p*-coumaric acid precedes the peak of catechin, epicatechin and rutin formation in elicitor-treated cell cultures. Furthermore, a considerable up-regulation of salicylic acid biosynthesis was observed after elicitor treatment. Salicylic acid can induce local resistance in form of hypersensitive reaction or long distance systemic acquired resistance by triggering the production of pathogenesis-related proteins (PR proteins) (Vasyukova and Ozeretskovskaya, 2007). Both these defense reactions are linked with the biosynthesis of salicylic acid at the infection site or in the systemic parts of the plant. The crucial role of salicylic acid as signaling molecule in plant defense response is well established (Vlot et al., 2009). Nevertheless, in addition to elicitor-induced salicylic acid accumulation, a little amount of constitutive salicylic acid level was also detected. Under stress conditions, apple plants are known to produce enhanced levels of salicylic acid (Wang et al., 2016). Perhaps up-regulation of salicylic acid provides scab-tolerance in apple. However, whether, scab infection to green house grown plants actually synthesize salicylic acid or not need to be investigated in future to get a clear picture of salicylic acid-mediated scab tolerance.

Elicitor-treatment to apple cell culture led to production of aucuparin and noraucuparin, the marker phytoalexins of Malinae (Saini et al., 2017). Earlier studies have shown that the aucuparin and noraucuparin phytoalexins are derived from benzoic acid, which in turns originate from the cinnamic acid through intermediate formation of benzaldehyde (Sircar and Mitra, 2008; Sarkate et al., 2018). Up-regulation of *trans*-cinnamic acid level in apple cell cultures thereby explains the reason

underlying enhanced benzoic acid accumulation. It was worth speculating that after scab-infection, benzoic acid is further converted into biphenyl –dibenzofuran phytoalexins, which confers next level of resistance against scab-infection. Notably, peak of cinnamic acid accumulation precedes the peak of biphenyl and dibenzofuran phytoalexin accumulation in apple cell culture, suggesting a biogenic relationship. The biphenyl phytoalexin have shown efficacy towards inhibiting the growth of *Venturiainaequalis* (Chizzali et al., 2012). Interestingly, in this study, biphenyl phytoalexins were absent from the un-treated control cells and only detected after elicitor application. Notably, the dibenzofuran eriobofuran and malusfuran (2,4-methoxy- 3-hydroxy-9-*O*-*b*-D-glucosyloxydibenzofuran), detected earlier from the elicited cell culture of *Sorbus aucuparia* and apple cv. Liberty, respectively, has not been detected from Golden Delicious cell cultures. A similar situation was observed with *Pyruspyrifolia* cell cultures, where dibenzofurans were not detected after elicitor-treatment (Saini et al., 2017). Furthermore, the hierarchical clustering offered excellent separation of the metabolite trend between the non-elicited (0h) and elicitor-treated (6-48h). Elicitor-treated cells were the major source of variance in the result, which indicated that change in metabolite concentration by elicitor-treatment. When metabolic pathway network was considered, the significant different components in elicitor-treated cells were, histidine, isoleucine, glycine, aspartic acid, glucose, sucrose, fructose, TCA cycle intermediates, aucuparin, noraucuparin, benzoic acid, chlorogenic acid, protocatechuic acid, caffeic acid, *p*-coumaric acid, *trans*-cinnamic acid, catechin, epicatechin, rutin and ascorbic acid.

After elicitor treatment, expression level of all the four studied genes (*PAL*, *F3H*, *AOX* and *BIS3*) were up-regulated suggesting that phenolics and biphenyl biosynthesis was triggered by the elicitor-treatment. These gene expression data were well correlated with the enhanced accumulation of phenylpropanoids such as cinnamic acid, flavonoids and biphenyls in the elicited cell cultures of apple. Enhanced expression of *PAL* gene is known to be associated with increase in the phenylpropanoid and flavonoid biosynthesis (Gaid et al., 2012; Mukherjee et al., 2016). Likewise, high *F3H* expression is associated with higher accumulation of catechin. High *AOX* expression level in the VIE-treated cells is probably associated with the enhanced biosynthesis of phenylpropanoids (Arnholdt-Schmitt et al., 2006). Similar to *PAL*, a rapid up-regulation of *BIS3* expression was observed. The expression of *PAL* and *BIS3* preceded the accumulation of noraucuparin and aucuparin, suggesting involvement of these genes in biphenyl phytoalexin biosynthesis in apple. *BIS3* gene is known to contribute pathogen induced biphenyl biosynthesis

(Chizzali et al., 2012). Taken together, this study illustrates that elicitor (VIE)-treatment to Golden Delicious cell culture leads to the induction of metabolites that can have contrasting effects on scab resistance.

4.1.4. Molecular cloning and functional analyses of cinnamate-CoA-ligase (MdCNL) from VIE-treated cell culture of cv. Golden Delicious:

Few wild apple cultivars and several members of sub-tribe Malinae synthesize two special classes of phytoalexins, the biphenyl and the dibenzofurans, upon pathogen infection. In plants, benzoic acid and its derivatives serve as a biosynthetic building block for the synthesis of an array of metabolites that have established roles in plant-pathogen interactions. One of the most important examples of benzoate-derived plant secondary products is biphenyl-phytoalexins of *Malus*, which are the inducible defense compound of Malinae. Biosynthesis of benzoic acid is not completely understood in Malinae. PAL is the first enzyme in the benzoic acid biosynthetic pathway, which channels metabolic carbon flux from primary to secondary metabolism by synthesizing first stable phenylpropanoid, the cinnamic acid. Cinnamic acid is the first branch point of phenylpropanoid pathway, which diverts carbon flux in various sub-pathways. In most of the plant species, cinnamic acid is first converted into 4-coumaric acid, in a reaction catalyzed by cinnamate-4-hydroxylase (Yang et al., 2005). 4-Coumaric acid is then thioesterified by 4CL to form 4-coumaroyl-CoA, which serve as precursors for an array of plant natural products, such as lignin, flavonoids, anthocyanins and cell wall-bound phenolics (Li et al., 2015). In many plants, in addition to 4CL route, cinnamic acid is thioesterified with CoA by CNL to form cinnamoyl-CoA, which then directs carbon flow from the general phenylpropanoid pathway into benzenoid metabolism and subsequently to biphenyl phytoalexin backbone (Figure 4.1 A and B). *MdCNL* catalyzes thioesterification of cinnamic acid to form cinnamoyl-CoA. *MdCNL* contains a conserved AMP-binding domain, which is characteristic feature of the members of the adenylate-forming enzymes, such as 4CLs, luciferases and fatty acid CoA ligases (Fulda et al., 1994). The AMP-binding domain (box I) present in *MdCNL* is also a characteristic feature in CNL from *H. calycinum* (*HcCNL*), *P. hybrid* (*PhCNL*), *A. thaliana* (*AtCNL/ AtBZO*) and OSBZL sequence from *M. truncatula*. Furthermore, a second conserved domain (box II) is also present in all these proteins.

Earlier, cDNA cloning and functional expression of CNL from *H. calycinum* cell cultures (Gaid et al., 2012) and *P. hybrida* petals (Klempien et al., 2012) has been reported. The affinity of *MdCNL*

for cinnamic acid (K_m 19.6 μM) is markedly higher than the affinity of *PhCNL* for cinnamic acid ($K_m = 285.7 \mu\text{M}$), but slightly lower than the *HcCNL* affinity for cinnamic acid ($K_m = 11.14 \mu\text{M}$). Similarly, turn over number of *MdCNL* ($k_{\text{cat}} = 0.88 \text{ s}^{-1}$) is lower than the turn over number of *HcCNL* ($k_{\text{cat}} = 1.73 \text{ s}^{-1}$) but higher than the previously reported turn over number of *PhCNL* ($k_{\text{cat}} = 0.472 \text{ s}^{-1}$). For all the three studied CNLs, 4-coumaric acid was the second best substrate and, notably, benzoic acid was not accepted as substrate. The affinity of *MdCNL* for CoA ($K_m = 108.6 \mu\text{M}$) was slightly lower than that of *HcCNL* ($K_m = 95.6 \mu\text{M}$), but markedly higher than that of *PhCNL* ($K_m = 775.2 \mu\text{M}$). However, the *MdCNL* affinity towards ATP ($K_m = 102.4 \mu\text{M}$) was slightly higher than that of *HcCNL* ($K_m = 104.7 \mu\text{M}$). The K_m value of *PhCNL* for ATP was not reported. Notably, the activities of *MdCNL*, *HcCNL* and *PhCNL* were strictly dependent on the presence of cations, the combination of Mg^{2+} and K^+ provided the best result. A similar affinity of carboxylic acid:CoA ligases from cattle liver mitochondria towards cations were previously observed and reported (Vessey and Kelley, 1998). These carboxylic acid:CoA ligases had an absolute requirement for both monovalent and divalent cations for accepting benzoic acid as substrate. Since the use of divalent cation is associated to form complex with ATP, its optimum concentration was found to be directly related ATP concentration in the assay. The requirement of the bovine liver enzymes for monovalent cation was satisfied by 50 mM potassium ion (Vessey et al., 2000). Highest *MdCNL* activity was observed with 100 mM potassium ion. Previously reported *HcCNL*, also showed highest activity at 100 mM potassium concentration. However, in case of *PhCNL*, 10.5 mM potassium was reported to show half of the maximum activity in the presence of 2.5 mM divalent magnesium ion (Klempien et al., 2012).

The preferred substrate for *MdCNL*, *HcCNL* and *PhCNL* were cinnamic acid. However, 4CLs showed very little or no activity with cinnamic acid, rather it prefers 4-coumaric acid as substrate (Lindermayr et al., 2003; Schneider et al., 2003). In addition, the *Ri4CL2* isoform isolated from *Rubus idaeus* (Kumar and Ellis, 2003) showed cinnamic acid (153%) as preferred substrate over 4-coumaric acid (100%). It was reported that the twelve amino acids surrounding the substrate-binding pocket of 4CL actually function as a signature motif for 4CL substrate specificity (Stuible and Kombrink, 2001; Schneider et al., 2003) reported a 4CL triple mutant from *Arabidopsis* (*At4CL2*), which showed around 30-fold higher affinity towards cinnamic acid as substrate. The triple mutation N256A/M293P/K320L was known to enhance the hydrophobicity of the substrate-binding pocket. It was presumed that CNL enzymes may particularly carry a hydrophobic residue

at the corresponding position to Asn-256 in *At4CL2* (Figure 4; Schneider et al., 2003). Indeed, *MdCNL*, *HcCNL*, *PhCNL* and *AtCNL*, have hydrophobic glycine residues at the corresponding positions. In contrast, the cinnamate-preferring 4CL2 isoenzyme from *R. idaeus* bears an asparagine residue at the comparable position (Kumar and Ellis, 2003). The other two positions that were altered in the *At4CL* triple mutant are occupied by hydrophilic histidine and threonine residues in all functionally characterized CNLs.

Phylogenetic analyses showed that the benzenoid-related CoA ligases and 4CLs form two evolutionarily separate clusters, indicating their origin from a common ancestral gene. Since the 4CL clade included amino acid sequences from angiosperms, gymnosperms, pteridophytes and bryophytes, the 4CLs and benzenoid-related CoA ligases clusters appear to have separated prior to the divergence of the higher plant lineages.

In cell cultures of *M. domestica*, C₂-side-chain shortening of cinnamic acid appeared to proceed via a CoA-dependent and non β -oxidative route, yielding free benzoic acid (Gaid et al., 2009). It is likely that CNL-catalyzed cinnamoyl-CoA is first converted into benzaldehyde and then benzaldehyde is converted into benzoic acid by a dehydrogenase activity. A *Chyl* gene encoding 3-hydroxyisobutyryl-CoA hydrolase, which converts cinnamoyl-CoA into benzaldehyde, was reported in *A. thaliana* (Ibdah and Pichersky, 2009). Very recently a salicylaldehyde synthase activity was detected in apple (cv. 'Florina') cell suspension cultures. A 1.8 fold-increase in salicylic acid content after treatment with *Venturia* suggesting a role of salicylaldehyde in plant defense (Sarkate et al., 2017). Benzaldehyde dehydrogenase (BD) activity has been detected from the cell culture of two other members of Malinae, *Sorbus aucuparia* (Gaid et al., 2009) and *Pyrus pyrifolia* (Saini et al., 2017). The benzoic acid thus formed appears to be converted into benzoyl-CoA in a reaction catalyzed by benzoate CoA-ligase (BZL). Benzoyl-CoA then enters into biphenyl phytoalexin biosynthetic pathway by combining with three molecules of malonyl-CoA, in a reaction catalyzed by biphenyl synthase (Chizzali et al., 2012). BZL activity has been reported from *Clarkia breweri* (Beuerle and Pichersky, 2002b), cell cultures of *Hypericum androsaemum* (Abd El-Mawla and Beerhues, 2002) and *P. pyrifolia* (unpublished data). Thus, in *M. domestica* cv. Golden Delicious cell culture, biphenyl biosynthetic pathway appears to involve CNL, BD and BZL activities. Increase in the transcript level of both *PAL* and *CNL* preceded the VIE-induced accumulation of biphenyl phytoalexins (aucuparin and noraucuparin) which functions as a phytoalexin in a Malinae (Chizzali and Beerhues, 2012). While *CNL* transcripts were not

detectable before elicitation, a basal level of *PAL* mRNA was present because this enzyme also supplies precursors for other secondary metabolic pathways, such as lignin and flavonoids biosynthesis. The changes in the *PAL* and *CNL* transcript levels provide evidence for the involvement of these enzymes in formation of biphenyl phytoalexin through intermediate formation of benzoic acid and its derivatives. Three plant CoA-ligases exhibiting affinity towards benzoic acids were previously reported, BZL from *Clarkia breweri* (Beuerle and Pichersky, 2002b), BZL from cell culture of *P. pyrifolia* (unpublished data), 3-hydroxybenzoate:CoA ligase from *C. erythraea* (Barillas and Beerhues, 2000) and OSBZL from *Galium mollugo* (Sieweke and Leistner, 1992). BZL and 3-hydroxybenzoate:CoA were AMP-forming enzymes and lacked any activity with (hydroxy-) cinnamic acids, whereas OSBZL was an ADP-forming enzyme which showed activity with 4-coumaric acid. Earlier, a putative BZL gene (*BZO1*, At1g65880) associated with benzoyloxyglucosinolate biosynthesis has been detected in *A. thaliana* (Kliebenstein et al., 2007), which was later found to be a functional *CNL* (Lee et al., 2012).

Similar to *HcCNL*, *MdCNL* was also localized into peroxisomes, which are the site of β -oxidation in plants. Masking of SRL tri-peptide in the C-terminus of *MdCNL* resulted into cytoplasmic localization. A similar observation was made before with *HcCNL* (Gaid et al., 2012) and *PhCNL* (Klempien et al., 2012). *HcCNL* carried a C-terminal SRL tripeptide while *PhCNL* carried C-terminal ARL tri-peptide as peroxisomal localization signal. *CNL* proteins from *A. thaliana* (Lee et al., 2012) and BZL from *C. breweri* also contain a PTS1 (SRL) signal at the C-terminal end. A PTS1 signal is also present in the predicted OSBZL sequences from *M. truncatula* (Young et al., 2011). Interestingly, the enzyme 3-ketoacyl thiolase (*PhKAT*) converting 3-oxo-3-phenylpropionyl-CoA to benzoyl-CoA in the β -oxidative pathway is also localized inside peroxisomes (Van Moerkercke et al., 2009). *PhKAT* utilizes 3-oxo-3-phenylpropionyl-CoA as substrate, which is derived from cinnamoyl-CoA in a reaction catalyzed by cinnamic acid-CoA hydratase / dehydrogenase (*PhCHD*; Qualley et al., 2012; Bussell et al., 2014). Furthermore, Chy1 from *A. thaliana* is a peroxisomal protein (Ibdah and Pichersky, 2009). In contrary to this, BD from *Antirrhinum majus*, involved in the non- β -oxidative biosynthesis of benzoic acid, was localized in mitochondria (Long et al., 2009). However, BD activity from *S. aucuparia* and *P. pyrifolia* was found to be present in cell-free extract (Gaid et al., 2009; Saini et al., 2017). However, after forming *CNL*-catalyzed cinnamoyl-CoA, whether it further follows non- β -

oxidative or β -oxidative pathway to produce benzoyl-CoA is an open question and needs future investigation.

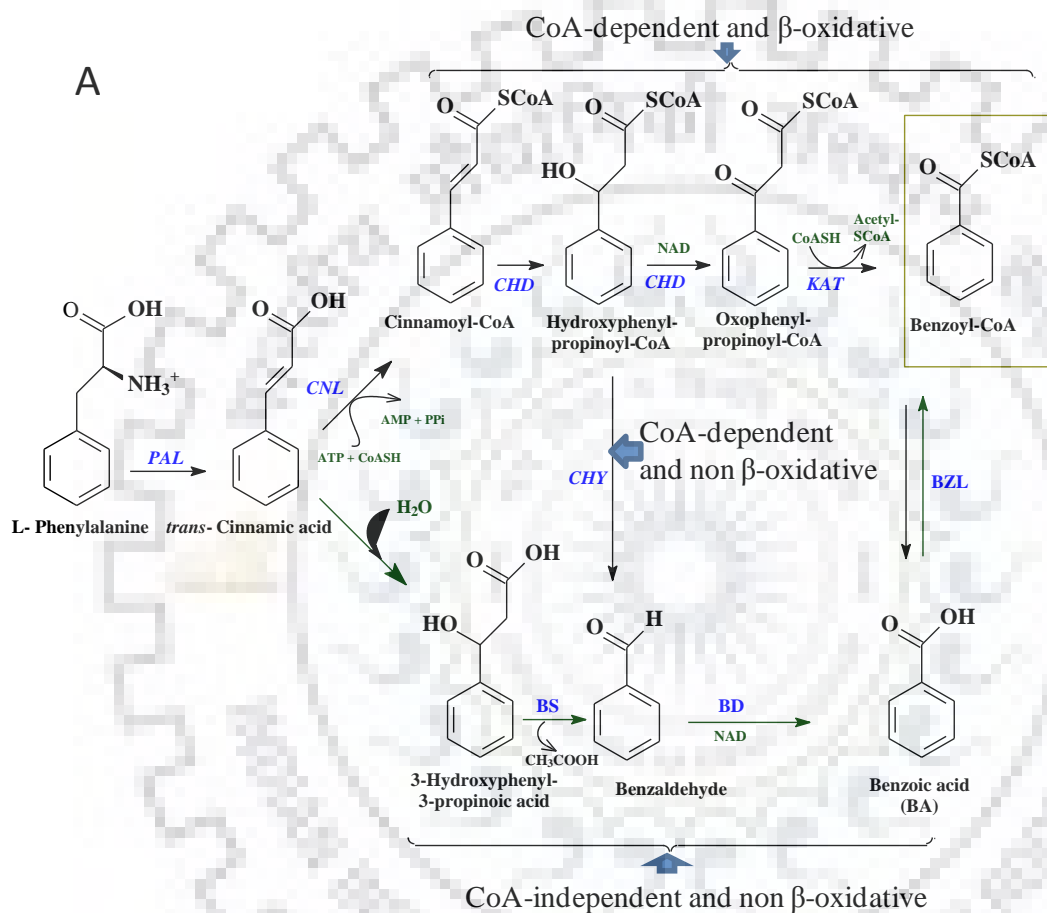


Figure 4.1. Proposed role of cinnamate-CoA ligase (CNL) in benzoyl-CoA biosynthesis.

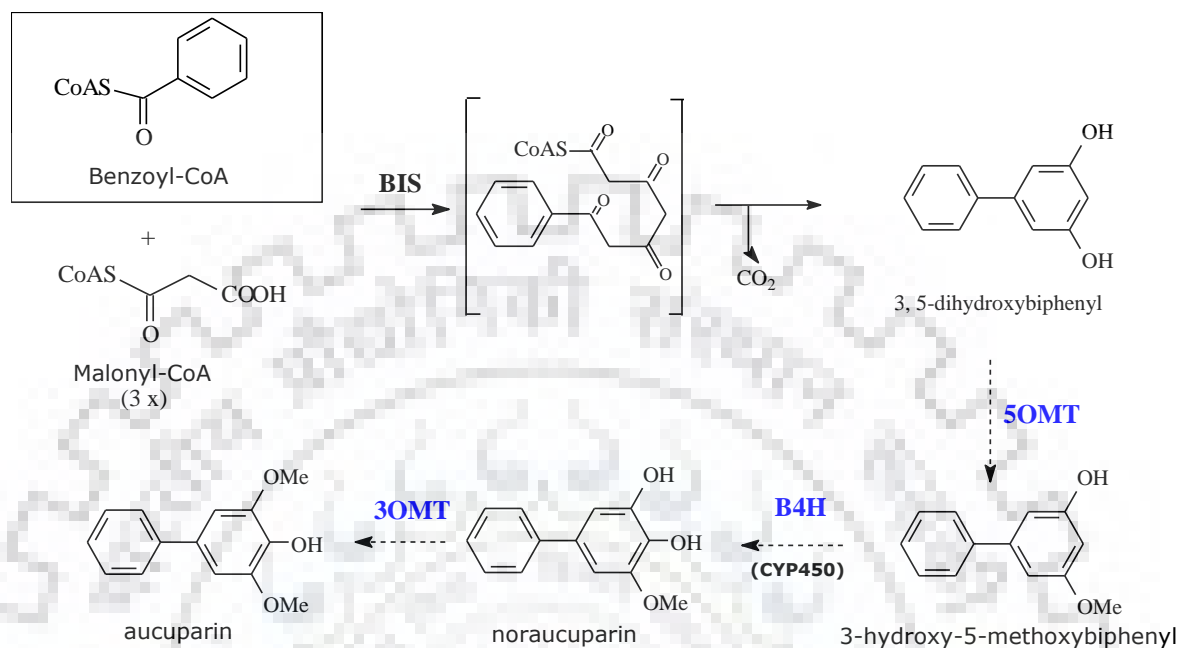
B

Figure 4.2. Figure showing incorporation of benzoyl-CoA into biphenyl phytoalexin backbone. PAL, phenylalanine ammonia lyase; CHD, cinnamoyl-CoA hydratase dehydrogenase; KAT, ketoacylthiolase; *CHY*, 3-hydroxyisobutyryl-CoA hydrolase; BZL, benzoate-CoA ligase; BS, benzaldehyde synthase; BD, benzaldehyde dehydrogenase; BIS, biphenyl synthase; OMT, o-methyl transferase; B4H, biphenyl-4-hydroxylase.

Chapter 5

Summary, Conclusion and Future scopes

5.1. Summary:

5.1.1: Development of cell suspension culture of apple cv. Golden Delicious:

- Apple cell suspension culture (cv. Golden Delicious) was developed which showed excellent growth in LS-medium supplemented with μM 2,4-D and 1 μM NAA. Better growth was observed in dark.

5.1.2: Development of a validated HPLC method for the simultaneous detection of biphenyl and dibenzofuran phytoalexins:

- A validated HPLC method was developed for the simultaneous detection of aucuparin, noraucuparin and eriobofuran, three most abundant phytoalexins from sub-tribe Malinae.
- Chromatographic separation was achieved on Luna C₁₈ reversed-phase column 250 x 4.6 mm, 5 μm particle size (Phenomenex, Torrance, California, USA) coupled with a Phenomenex Security Guard™ C18 guard column 4 x 3 mm (Torrance, California, USA). The mobile phase was degassed as well as vacuum filtered through 0.45 μm nylon membranes. The mobile phase consisted of an isocratic solvent mixture comprising 1mM TFA in water: methanol [40:60; (v/v)] with a flow rate of 0.5 mL min⁻¹. Detection wavelength was set at 254 nm. Peaks were identified by comparing their retention time and UV-spectra with those of authentic standards.
- Chemical identity of aucuparin, noraucuparin and eriobofuran was further confirmed by ESI-MS/MS analyses. The method can easily be extended to the routine analysis of apple phytoalexins to determine their scab-tolerance. The main advantage of this method is the rapid separation and quantification of noraucuparin, aucuparin and eriobofuran which are among the most important phytoalexins of Malinae. The evaluated validation characteristics showed that the technique is very simple, sensitive, reproducible and accurate.

- The limit of detection was found to be 0.76 $\mu\text{g mL}^{-1}$ for noraucuparin, 0.40 $\mu\text{g mL}^{-1}$ for aucuparin and 3.77 $\mu\text{g mL}^{-1}$ for eriobofuran. Corresponding limits of quantification were found to be 2.5, 1.3 and 12.6 $\mu\text{g mL}^{-1}$ respectively.
- Furthermore, the separation was performed using isocratic condition, thereby, no re-equilibration is required in between two successive HPLC runs.

5.1.3. GC-MS based metabolomics analyses of *Venturia inaequalis* elicitor (VIE)-treated cell culture of apple cv. Golden Delicious:

- In this study, the metabolomics analysis of moderately scab resistant apple cv. Golden Delicious cell cultures treated with elicitor preparation from *Venturia inaequalis* has been performed using gas chromatography-mass spectrometry (GC-MS). A total 43 differentially accumulating metabolites has been identified in the elicitor-treated cells. The score plots of principal component analysis (PCA) exhibited clear discrimination between untreated and elicitor-treated samples. The metabolomic analyses indicated elicitor-treatment could cause significant alternation in the metabolite levels, mainly on sugars, amino acids and phenolic metabolites. Furthermore, two new metabolites, aucuparin and noraucuparin were detected only in elicitor-treated cells.
- Kyoto Encyclopedia of Genes and Genomes (KEGG) pathway analysis of integration data demonstrated the possible biosynthetic relationship between carbohydrates, amino acids, organic acids and secondary metabolites biosynthesis. Taken together, these results suggest that Golden Delicious exhibited a metabolic re-programming by synthesizing an array of differentially accumulating metabolites, especially phenolics and biphenyl-phytoalexins phytoalexins after onset of elicitor-treatment.
- Alteration in the metabolite level were correlated with the up-regulation in the transcript level of *phenylalanine ammonia-lyase (PAL)*, *flavones-3-hydroxylase (F3H)*, *alternate oxidase (AOX)* and *biphenyl synthase isoform 3 (BIS3)* gene.

5.1.4. Molecular cloning and functional analyses of cinnamate-CoA-ligase (*MdCNL*) from VIE-treated cell culture of cv. Golden Delicious:

- Apples and other genera belonging to the sub-tribe Malinae of Rosaceae family produce benzoic acid-derived unique phytoalexins, the biphenyls and the dibenzofurans. Although biphenyl biosynthesis is well-studied in apple and many other members of Malinae, biosynthesis of its structurally simple precursor, benzoic acid, is poorly understood.
- *Malus domestica* cv. Golden Delicious cell cultures accumulate a benzoic acid-derived biphenyl phytoalexin, aucuparin and noraucuparin, in response to *Venturia inaequalis* elicitor (VIE)-treatment. Using a genome database of Rosaceae and sequence information from plant secondary metabolism- specific CoA ligase, a cDNA encoding cinnamate:CoA ligase (CNL) was cloned and functionally characterized from the VIE-treated cell cultures of cv. Golden Delicious.
- This enzyme channels carbon flux from the phenylpropanoid pathway towards benzenoid-metabolism and finally towards biphenyl phytoalexin biosynthesis. *MdCNL* preferred cinnamic acid as a substrate but failed to accept benzoic acid. *MdCNL* activity was found to be strictly dependent on the presence of K^+ and Mg^{2+} ions in the assay buffer at optimum concentrations of 100 and 2.5 mM, respectively. Coordinated increase in the *phenylalanine ammonia-lyase* (*PAL*) and *MdCNL* transcript levels preceded accumulation of biphenyl phytoalexin noraucuparin and aucuparin in VIE-treated cell cultures of apple cv.
- When greenhouse-grown apple plants of cv. Shireen (scab-resistant cultivar) and cv. Golden Delicious (moderately scab-susceptible cultivar) were infected with the scab fungus *V. inaequalis*, up-regulation of *MdCNL* transcript levels was observed in the internodal region with accumulation of aucuparin and noraucuparin phytoalexins. Both phytoalexin levels and *MdCNL* transcript levels were significantly higher in the cultivar Shireen than that of Golden Delicious. No phytoalexins were detected in the leaves.
- *MdCNL* contained a C-terminal type 1 peroxisomal targeting signal consisting of SRL tri-peptide, which directed an N-terminal reporter fusion (YFP-CNL) to the peroxisomes. Phylogenetic analyses showed two evolutionarily distinct clusters, one cluster consisting of CoA ligases associated with the benzoic acid metabolism and the other cluster comprised of 4-coumarate:CoA ligases from plants. Together, the data suggest that *MdCNL* catalyzed cinnamoyl-CoA formation is required for biphenyl phytoalexin biosynthesis in apple.

5.2. Conclusions:

- In conclusion, the cell suspension culture of apple cv. Golden Delicious provides excellent system to study apple-*Venturia* interaction at cellular level and to understand the early biosynthetic pathway of biphenyl biosynthesis.
- A validated HPLC method was developed to rapidly detect and quantify aucuparin, noraucuparin and eriobofuran.
- Application of GC-MS based metabolomics in combination with PCA on the cell suspension culture undoubtedly revealed an altered metabolite profiles of VIE-treated cells as compared to the untreated control cells during a time course of 0–48 h. A rapid up-regulation of a number of phenolics occurred after VIE-treatment with biosynthesis of two new phytoalexins, the aucuparin and the noraucuparin. Overall the metabolic response probably exhibited an immediate biochemical response of VIE-treatment which mimics scab fungus infection.
- *MdCNL* is a peroxisomally localized CoA-ligase was cloned and functionally characterized from the elicitor-treated cell culture of Golden Delicious. *MdCNL* is involved in the biosynthesis of cinnamoyl-CoA from cinnamic acid. Cinnamoyl-CoA later converted into benzoyl-CoA and contributes towards biphenyl biosynthesis. Upon scab infection in green house-grown apple plants, *MdCNL* expression was observed in the internodal stem region with subsequent accumulation of aucuparin and noraucuparin. Further, the genes and enzymes of benzoic acid biosynthesis in Malinae need to be studied at the molecular level to better understand spatial and temporal regulation of this important metabolite. The transport process of various benzoate-biosynthetic-intermediates between different compartments is also elusive. Apple is an economically important fruit crop where benzoic acid serves as the precursor for the biosynthesis of biphenyl and dibenzofuran phytoalexin. Since biphenyl and dibenzofuran phytoalexins play crucial role in combating disease resistance in apple and other members of Malinae, a better understanding of benzoic acid metabolism will help to fortify defense potential of apples through phytoalexin metabolic engineering using biotechnological means.

5.3. Future scopes:

- How scab elicitor infection triggers enhanced phenolic and phytoalexin biosynthesis need to be investigated in details. Differential accumulation of metabolites accumulated upon scab fungus infection to field grown cab resistant and scab-susceptible apple plants needs to be investigated in future.
- How scab-induced differentially accumulating metabolites inhibit / kill scab fungus growth and what is the underlying mechanism of actions, need to be investigated in future with isolated pure metabolites.
- The expression of level of *MdCNL* showed differences between the scab resistant cultivar Shireen and moderately scab-tolerant cultivar Golden Delicious. In future promoter region of *MdCNL* from both scab resistant and susceptible cultivars should be cloned and characterized.
- *MdCNL* should be cloned and characterized from one strongly scab resistant cultivar such as Florina or Shireen or Liberty to see if there is any functional difference exists in the sequence from the reported *MdCNL* from Golden Delicious.

References

1. Abd El-Mawla AMA, Beerhues L (2002). Benzoic acid biosynthesis in cell cultures of *Hypericum androsaemum*. *Planta*, 214: 727-733.
2. Abd El-Mawla AMA, Schmidt W, Beerhues L (2001). Cinnamic acid is a precursor of benzoic acids in cell cultures of *Hypericum androsaemum* L. but not in cell cultures of *Centaureum erythraea* RAFN. *Planta*, 212: 288-293.
3. Amil-Ruiz F, Blanco-Portales R, Muñoz-Blanco J, Caballero JL (2011). The strawberry plant defense mechanism: A molecular review. *Plant and Cell Physiology*, 52: 1873–1903.
4. Aprea E, Gika H, Carlin S, Theodoridis G, Vrhovsek U, Mattivi F (2011). Metabolite profiling on apple volatile content based on solid phase microextraction and gas-chromatography time of flight mass spectrometry. *J Chromatogr A*, 1218: 4517–4524.
5. Arnholdt-Schmitt B, Costa JH, de Melo DF (2006). AOX-a functional marker for efficient cell reprogramming under stress? *Trends in Plant Science*, 11: 281–287.
6. Babst B, Harding S, Tsai C (2010). Biosynthesis of phenolic glycosides from phenylpropanoid and benzenoid precursors in *Populus*. *J Chem Ecol*, 36: 286-297.
7. Baldwin IT, Halitschke R, Paschold A, von Dahl CC, Preston CA (2006). Volatile signaling in plant-plant interactions: “talking trees” in the genomics era. *Science*, 311: 812-815.
8. Bao K, Fan A, Dai Y, Zhang L, Zhang W, Cheng M, Yao X (2009). Selective demethylation and debenzoylation of aryl ethers by magnesium iodide under solvent-free conditions and its application to the total synthesis of natural products. *Org Biomol Chem*, 7: 5084.
9. Barillas W, Beerhues L (1997). 3-Hydroxybenzoate:coenzyme A ligase and 4-coumarate:coenzyme A ligase from cultured cells of *Centaureum erythraea*. *Planta*, 202: 112-116.
10. Barillas W, Beerhues L (2000). 3-Hydroxybenzoate:coenzyme A ligase from cell cultures of *Centaureum erythraea*: isolation and characterization. *Biol Chem*, 381: 155–160.
11. Bartsch M, Bednarek P, Vivancos PD, Schneider B, von Roepenack-Lahaye E, Foyer CH, Kombrink E, Scheel D, Parker JE (2010). Accumulation of isochorismate-derived

- 2,3-dihydroxybenzoic 3-O- β -D-xyloside in *Arabidopsis* resistance to pathogens and ageing of leaves. *J Biol Chem*, 285: 25654-25665.
12. Bektas Y, Eulgem T (2014). Synthetic plant defense elicitors. *Front Plant Sci*, 5: 804.
 13. Belete T, Boyraz N (2017). Critical review on apple scab (*Venturia inaequalis*) biology, epidemiology, economic importance, management and defense mechanisms to the causal agent. *J Plant Physiol Pathol*, 5: 2.
 14. Belfanti E, Barbieri M, Tartarini S, Vinatzer B, Gennari F, Paris R, et al., (2004a). Gala apple transformed with the putative scab resistance gene HcrVf2. *Acta Hort*, 663: 453-456.
 15. Benaouf G, Parisi L (2000). Genetics of host-pathogen relationships between *Venturia inaequalis* races 6 and 7 and *Malus* species. *Phytopathology*, 90: 236-242.
 16. Bennett BC (2010). Economic botany- twenty five economically important plant families. *Encyclopedia of life support systems*, Oxford, UK: UNESCO-EOLSS Publishers.
 17. Bera P, Mukherjee C, Mitra A (2017). Enzymatic production and emission of floral scent volatiles in *Jasminum sambac*. *Plant Science: An International Journal of Experimental Plant Biology*, 256: 25-38.
 18. Beuerle T, Pichersky E (2002a). Enzymatic synthesis and purification of aromatic coenzyme A esters. *Anal Biochem*, 302: 305-312.
 19. Beuerle T, Pichersky E (2002b). Purification and characterization of benzoate:coenzyme A ligase from *Clarkia breweri*. *Arch Biochem Biophys*, 400: 258-264.
 20. Bhatia S, Bera T (2015). Chapter 7 – Classical and nonclassical techniques for secondary metabolite production in plant cell culture. *Modern applications of plant biotechnology in pharmaceutical sciences*. Pages 231-291.
 21. Bisht S, Kant R, Kumar V (2013). α -D-Glucosidase inhibitory activity of polysaccharide isolated from *Acacia tortilis* gum exudate. *International Journal of Biological Macromolecules*, 59: 214-220.
 22. Block A, Widhalm JR, Fatih A, Cahoon RE, Wamboldt Y, Elowsky C, Mackenzie SA, Cahoon EB, Chapple C, Dudareva N, Basset GJ (2014). The origin and biosynthesis of the benzenoid moiety of ubiquinone (coenzyme Q) in *Arabidopsis*. *Plant Cell*, 26: 1938-1948.

23. Boatright J, Negre F, Chen X, Kish CM, Wood B, Peel G, Orlova I, Gang D, Rhodes D, Dudareva N (2004). Understanding in vivo benzenoid metabolism in petunia petal tissue. *Plant Physiol*, 135: 1993-2011.
24. Bolar JP, Norelli JL, Wong KW, Hayes CK, Harman GE and Aldwinckle HS (2000) Expression of endochitinase from *Trichoderma harzianum* transgenic apple increases resistance to apple scab and reduces vigor. *Phytopathology*, 90: 72-77.
25. Bolar JP, Norelli JL, Wong KW, Hayes CK, Harman GE, Brown SK, Aldwinckle HS (2001). Synergistic activity of endochitinase and exochitinase from *Trichoderma atroviride* (*T. harzianum*) against the pathogenic fungus (*Venturia inaequalis*) in transgenic apple plants. *Transgenic Res*, 10: 533-543.
26. Bowen JK, Mesarich CH, Bus VGM, Beresford RM, Plummer KM, Templeton MD. (2011). *Venturia inaequalis*: the causal agent of apple scab. *Mol Plant Pathol*, 12: 105–22.
27. Borejsza-Wysocki W, Lester C, Attygalle A, Hrazdina G (1999). Elicited cell suspension cultures of apple (*Malus × domestica*) cv. Liberty produce biphenyl phytoalexins. *Phytochemistry*, 50: 231–235.
28. Boyer J, Liu RH (2004). Apple phytochemicals and their health benefits. *Nutrition Journal*, 3: 5-12.
29. Bradford MM (1976). A rapid and sensitive method for the quantitation of microgram quantities of protein utilizing the principle of protein-dye binding. *Anal Biochem*, 72: 248–254.
30. Bussell JD, Reichelt M, Wiszniewski AAG, Gershenzon J, Smith SM (2014). Peroxisomal ATP-binding cassette transporter COMATOSE and the multifunctional protein abnormal inflorescence meristem are required for the production of benzoylated metabolites in *Arabidopsis* seeds. *Plant Physiol*, 164: 48–54.
31. Bus VGM, Laurens FND, van de Weg WE, et al., (2005). “The Vh8 locus of a new gene-for-gene interaction between *Venturia inaequalis* and the wild apple *Malus sieversii* is closely linked to the Vh2 locus in *Malus pumila* R12740-7A. *New Phytologist*, 166: 1035–1049.
32. Bus VGM, Rikkerink EHA, Caffier V, Durel CE, Plummer KM (2011). Revision of the nomenclature of the differential host-pathogen interactions of *Venturia inaequalis* and *Malus*. *Annu Rev Phytopathol*, 49: 391–413.

33. Campos MD, Campos C, Cardoso HG, Simon PW, Oliveira M, Nogales A, Arnholdt-Schmitt B (2016a). Isolation and characterization of plastid terminal oxidase gene from carrot and its relation to carotenoid accumulation. *Plant Gene*, 5: 13–21.
34. Campos MD, Nogales A, Cardoso HG, Kumar SR, Nobre T, Sathishkumar R, Arnholdt-Schmitt B (2016b). Stress-induced accumulation of DCAOX1 and DCAOX 2a transcripts coincides with critical time point for structural biomass prediction in carrot primary cultures (*Daucus carota* L.). *Frontiers in Genetics*, 7: 1.
35. Carisse O, Bernier J (2002). Effect of environmental factors on growth, pycnidial production and spore germination of *Microspphaeropsis* isolates with biocontrol potential against apple scab. *Mycol Res*, 106: 1455–1462.
36. Catinot J, Buchala A, Abou-Mansour E, Mettraux JP (2008). Salicylic acid production in response to biotic and abiotic stress depends on isochorismate in *Nicotiana benthamiana*. *FEBS Lett*, 582: 473-478.
37. Chizzali C, Beerhues L (2012). Phytoalexins of the Pyrinae: biphenyls and dibenzofurans. *Beilstein Journal of Organic Chemistry*, 8: 613-620.
38. Chizzali C, Khalil MNA, Beuerle T, Schuehly W, Richter K, Flachowsky H, Peil A, Hanke MV, Liu B, Beerhues L (2012). Formation of biphenyl and dibenzofuran phytoalexins in the transition zones of fire blight-infected stems of *Malus domestica* cv. ‘Holsteiner Cox’ and *Pyrus communis* cv. ‘Conference’. *Phytochemistry*, 77: 179–185.
39. Chizzali C, Swiddan AK, Abdelaziz S, Gaid M, Richter K, Fischer TC, Beerhues L (2016). Expression of biphenyl synthase genes and formation of phytoalexin compounds in three fire blight-infected *Pyrus communis* cultivars. *PLoS ONE*, 11: e0158713.
40. Christenhusz MJM and JW Byng (2016). The number of known plants species in the world and its annual increase. *Phytotaxa*, 261: 201–217.
41. Colquhoun TA, Marciniak DM, Wedde AE, Kim JY, Schwieterman ML, Levin LA, Van Moerkercke A, Schuurink RC, Clark DG (2012). A peroxisomally localized acyl-activating enzyme is required for volatile benzenoid formation in a *Petunia*×*hybrida* cv. “Mitchell Diploid” flower. *J Exp Bot*, 63: 4821–4833.
42. Cornille A, Gladieux P, Smulders MJM, Roldán-Ruiz I, Laurens F, Le Cam B, Nersesyan A, Clavel J, Olonova M, Feugey L, Gabrielyan I, Zhang XG, Tenaillon MI, Giraud T (2012). New insight into the history of domesticated apple: Secondary contribution of the European wild apple to the genome of cultivated varieties. *PLoS Genet*, 8: e1002703.

43. Costa JH, Cardoso HG, Campos MD, Zavattieri A, Frederico AM, Fernandes de Melo D, Arnholdt-Schmitt B (2009). *Daucus carota* L.- an old model for cell reprogramming gains new importance through a novel expansion pattern of alternative oxidase (AOX) genes. *Plant Physiology and Biochemistry*, 47: 753–759.
44. Costa JH, Santos CP, de Sousa E Lima B, Netto ANM, Saraiva KD, Arnholdt-Schmitt B (2017). In silico identification of alternative oxidase 2 (AOX2) in monocots: A new evolutionary scenario. *Journal of Plant Physiology*, 210: 58–63.
45. Cuthbertson D, Andrews PK, Reganold JP, Davies NM, Lange BM (2012). Utility of metabolomics toward assessing the metabolic basis of quality traits in apple fruit with an emphasis on antioxidants. *J Agric Food Chem*, 60: 8552–8560.
46. Delgado-Pelayo R, Gallardo-Guerrero L, Hornero-Méndez D (2014). Chlorophyll and carotenoid pigments in the peel and flesh of commercial apple fruit varieties. *Food Research International*, 65: 272-281.
47. Delporte F, Pretova A, du Jardin P, Watillon B (2014). Morpho-histology and genotype dependence of in vitro morphogenesis in mature embryo cultures of wheat. *Protoplasma*, 251: 1455-1470.
48. Dewick PM (2009). *Medicinal natural products. A biosynthetic approach* (Ed 3). Wiley, Chichester, UK.
49. Dianne AH (2011). A Comprehensive reviews of apples and apple components and their relationship to human health. *Advances in Nutrition*, 2: 408-420.
50. Dudareva N, Klempien A, Muhlemann JK, Kaplan I (2013). Biosynthesis, function and metabolic engineering of plant volatile organic compounds. *New Phytol*, 198: 16-32.
51. Dudareva N, Pichersky E (2008). Metabolic engineering of plant volatiles. *Curr Opin Biotech*, 19: 181-189.
52. Dzhangaliev AD (2003). *The wild apple tree of Kazakhstan*. Horticulture Rev John Wiley & Sons, Inc; pp. 63–303.
53. Eberhardt M, Lee C, Liu RH (2000). Antioxidant activity of fresh apples. *Nature*, 405: 903-904.
54. Eisenmann P, Ehlers M, Weinert CH, Tzvetkova P, Silber M, Rist MJ, Luy B, Muhle-Goll C (2016). Untargeted nmr spectroscopic analysis of the metabolic variety of new apple cultivars. *Metabolites*, 6: 29.

55. Evans RC, Alice LA, Campbell CS, Kellogg EA, Dickinson TA (2000). The granule-bound starch synthase (GBSSI) gene in the Rosaceae: multiple loci and phylogenetic utility. *Mol Phylogen Evol*, 17: 388–400.
56. Evans RC, Campbell CS (2002). The origin of the apple subfamily (Rosaceae: Maloideae) is clarified by DNA sequence data from duplicated GBSSI genes. *Am J Bot*, 89: 1478–1484.
57. Faize M, Sourice S, Dupuis F, Parisi L, Gautier MF and Chevreau E (2004). Expression of wheat puroindoline-b reduces scab susceptibility in transgenic apple (*Malus x domestica* Borkh.). *Plant Sci*, 167: 347-354.
58. Fiser A, Sali A (2003). ModLoop: automated modeling of loops in protein structures. *Bioinformatics*, 19: 2500-2501.
59. Flor HH (1971). Current status of the gene-for-gene concept. *Ann Rev Phytopathol*, 9: 275–96.
60. Francini A, Sebastiani L (2013). Phenolic compounds in Apple (*Malus x domestica* Borkh.): Compounds characterization and stability during postharvest and after processing. 2: 181-193.
61. French CJ, Vance CP, Neil Towers GH (1976). Conversion of p-coumaric acid to p-hydroxybenzoic acid by cell free extracts of potato tubers and *Polyporus hispidus*. *Phytochemistry*, 15: 564-566.
62. Fulda M, Heinz E, Wolter FP (1994). The fadD gene of *Escherichia coli* K12 is located close to rnd at 39.6 min of the chromosomal map and is a new member of the AMP-binding protein family. *Mol Gen Genet*, 242: 241-9.
63. Gaid MM, Scharnhop H, Ramadan H, Beuerle T, Beerhues L (2011). 4-Coumarate:CoA ligase family members from elicitor-treated *Sorbus aucuparia* cell cultures. *Journal of Plant Physiology*, 168: 944-951.
64. Gaid MM, Sircar D, Beuerle T, Mitra A, Beerhues L (2009). Benzaldehyde dehydrogenase from chitosan-treated *Sorbus aucuparia* cell cultures. *J Plant Physiol*, 166: 1343-1349.
65. Gaid MM, Sircar D, Müller A, Beuerle T, Liu B, Ernst L, Hänsch R, Beerhues L (2012). Cinnamate:CoA ligase initiates the biosynthesis of a benzoate-derived xanthone phytoalexin in *Hypericum calycinum* cell cultures. *Plant Physiol*, 160: 1267-80.

66. Gallage NJ, Hansen EH, Kannangara R, Olsen CE, Motawia MS, Jørgensen K, Holme I, Hebelstrup K, Grisoni M, Møller BL (2014). Vanillin formation from ferulic acid in *Vanilla planifolia* is catalysed by a single enzyme. *Nat Commun*, 5: 4037.
67. Garcia A, Cuadros L, Ales F, Roman M, Sierra JL (1997). ALAMIN: a chemometric program to check analytical method performance and to assess the trueness by standard addition methodology. *Trends Anal Chem*, 16: 381-385.
68. Gerhauser C (2008). Cancer chemo preventive potential of apples, apple juice and apple components. *Planta Medica*, 74: 1608-1624.
69. Gessler C, Patocchi A (2007). Recombinant DNA technology in apple. *Adv Biochem Eng Biotechnol*, 107: 113–32.
70. Gessler C, Pertot I (2011). Vf scab resistance of *Malus*. *Trees*, 26: 95–108.
71. Gross GG, Zenk MH (1966). Darstellung und Eigenschaften von Coenzym A-Thioestern substituierter Zimtsäuren. *Z Naturforsch*, 21b: 683-690.
72. Gross J, Cho WK, Lezhneva L, Falk J, Krupinska K, Shinozaki K, Seki M, Herrmann RG, Meurer J (2006). A plant locus essential for phyloquinone (vitamin K1) biosynthesis originated from a fusion of four eubacterial genes. *J Biol Chem*, 281: 17189-17196.
73. Guex N, Peitsch MC (1997). SWISS- MODEL and the Swiss- Pdb Viewer: an environment for comparative protein modeling. *Electrophoresis*, 18: 2714-2723.
74. Hammerschmidt R (1999). Phytoalexins: What have we learned after 60 years? *Annual review of Phytopathol.* 37: 285-306.
75. Hanson AD, Gregory JF (2011). Folate biosynthesis, turnover, and transport in plants. *Annu Rev Plant Biol*, 62: 105-125.
76. Harish MC, Dachinamoorthy P, Balamurugan S, BalaMurugan S, Sathishkumar R (2013). Enhancement of α -tocopherol content through transgenic and cell suspension culture systems in tobacco. *Acta Physiologiae Plantarum*, 35: 1121–1130.
77. Harris SA, Robinson JP, Juniper BE (2002). Genetic clues to the origin of the apple. *Trends Genet*, 18: 416–430.
78. Hébert C, Charles MT, Gauthier L, Willemot C, Khanizadeh S, Cousineau J (2002). Strawberry proanthocyanidins: biochemical markers for *Botrytis cinerea* resistance and shelf-life predictability. *Acta Hort*, 567: 659-661.

79. He X, Liu RH (2007). Triterpenoids isolated from apple peels have potent anti proliferative activity and may be partially responsible for apple's anticancer activity. *Journal of Agricultural and Food Chemistry*, 55: 4366-4370.
80. Hisanaga Y, Ago H, Nakagawa N, Hamada K, Ida K, Yamamoto M, Hori T, Arii Y, Sugahara M, Kuramitsu S (2004). Structural basis of the substrate-specific two-step catalysis of long chain fatty acyl-CoA synthetase dimer. *Journal of Biological Chemistry*, 279: 31717-31726.
81. Holzapfel C, Meisel B, Thummler F, Leser C, Treutter D (2012). Differential gene expression in leaves of a scab susceptible and a resistant apple cultivar upon *Venturia inaequalis* inoculation. *Trees*, 26: 121-129.
82. Hrazdina G, Borejsza-Wysocki W, Lester C (1997). Phytoalexin production in an apple cultivar resistant to *Venturia inaequalis*. *Phytopathology*, 87: 868-876.
83. Hrazdina G (2003). Response of scab-susceptible (McIntosh) and scab-resistant (Liberty) apple tissues to treatment with yeast extract and *Venturia inaequalis*. *Phytochemistry*, 64: 485-492.
84. Hudina M, Stampar F (2000). Sugars and organic acids contents of European (*Pyrus communis* L.) and Asian (*Pyrus serotina* Rehd.) pear cultivars. *Acta alimentaria*, 29: 217-230.
85. Hüttner C, Beuerle T, Liu B, Beerhues L, Richter K, Flachowsky H, Peil A, Hanke MV (2011). Biphenyl and dibenzofuran formation in fire blight-infected *Malus domestica* cultivars. *Acta Hort*, 896: 547-553.
86. Hüttner C, Beuerle T, Scharnhop H, Ernst L, Beerhues L (2010). Differential effect of elicitors on biphenyl and dibenzofuran formation in *Sorbus aucuparia* cell cultures. *J Agric Food Chem*, 58: 11977-11984.
87. Ibdah M, Chen YT, Wilkerson CG, Pichersky E (2009). An aldehyde oxidase in developing seeds of *Arabidopsis* converts benzaldehyde to benzoic acid. *Plant Physiol*, 150: 416-423.
88. Ibdah M, Pichersky E (2009). *Arabidopsis Chyl* null mutants are deficient in benzoic acid-containing glucosinolates in the seeds. *Plant Biol*, 11: 574-581.
89. ICH Topic Q2 B (1996). Validation of analytical procedures: Methodology, the European agency for the evaluation of medicinal products, Geneva.

90. Ishii H, Udagawa H, Nishimoto S, Tsuda T and Nakashima H (1992). Scab resistance in pear species and cultivars. *Acta Phytopathol Entomol Hung*, 27: 293-298.
91. Ishikura N, Hayashida S, Tazaki K (1984). Biosynthesis of gallic and ellagic acids with ¹⁴C-labeled compounds in *Acer* and *Rhus* leaves. *Bot Mag Tokyo*, 97: 355-367.
92. Janick J (2005). The origin of fruits, fruit frowning and fruit breeding. *Plant Breed Rev*, 25: 255–320.
93. Jarvis AP, Schaaf O, Oldham NJ (2000). 3-Hydroxy-3-phenylpropanoic acid is an intermediate in the biosynthesis of benzoic acid and salicylic acid but benzaldehyde is not. *Planta*, 212: 119–126.
94. Jha G, Thakur K, Thakur P (2009). The *Venturia* apple pathosystem: pathogenicity mechanisms and plant defense responses. *J Biomed Biotechnol*, 2009: 680160, 10 pages.
95. Jones JDG, Dangl JF (2006). The plant immune system. *Nature*, 444: 323–29.
96. Kanwal Q, Hussain I, Latif Siddiqui H, Javaid A (2010). Antifungal activity of flavonoids isolated from mango (*Mangifera indica* L.) leaves. *Nat Prod Res*, 24: 1907–14.
97. Kaufholdt D, Baillie CK, Bikker R, Burkart V, Dudek CA, Von Pein L, Hänsch R (2016). The molybdenum cofactor biosynthesis complex interacts with actin filaments via molybdenum insertase Cnx1 as anchor protein in *Arabidopsis thaliana*. *Plant Science*, 244: 8–18.
98. Kaufholdt D, Baillie CK, Wille T, Lang C, Hallier S, Herschbach C, Hänsch R (2015). Chapter 18: Prospective post-translational regulation of plant sulfite oxidase. In, *Molecular physiology and ecophysiology of sulfur*. Cham: Springer International Publishing, pp. 179–187.
99. Kelley LA, Mezulis S, Yates CM, Wass MN, Sternberg MJ (2015). The Phyre2 web portal for protein modeling, prediction and analysis. *Nature protocols*, 10: 845.
100. Khalil MNA, Beuerle T, Muller A, Ernst L, Bhavanam VBR, Liu B, Beerhues L (2013). Biosynthesis of the biphenyl phytoalexin aucuparin in *Sorbus aucuparia* cell cultures treated with *Venturia inaequalis*. *Phytochem*, 96: 101-109.
101. Khalil MNA, Brandt W, Beuerle T, Reckwell D, Groeneveld J, Hänsch R, Gaid MM, Liu B, Beerhues L (2015). O-Methyltransferases involved in biphenyl and dibenzofuran biosynthesis. *Plant J*, 83: 263–76.

102. Kim JK, Choi SR, Lee J, Park SY, Song SY, Na J, Kim SW, Kim SJ, Nou IS, Lee YH, Park SU, Kim H (2013). Metabolic differentiation of diamondback moth (*Plutella xylostella* (L.)) resistance in cabbage (*Brassica oleracea* L. ssp. capitata). *J Agric Food Chem*, 61: 11222–11230.
103. Klempien A, Kaminaga Y, Qualley A, Nagegowda DA, Widhalm JR, Orlova I, Shasany AK, Taguchi G, Kish CM, Cooper BR, D’Auria JC, Rhodes D, Pichersky E, Dudareva N (2012). Contribution of CoA ligases to benzenoid biosynthesis in *Petunia* flowers. *Plant Cell*, 24: 2015–2030.
104. Kliebenstein DJ, D’Auria JC, Behere AS, Kim JH, Gunderson KL, Breen JN, Lee G, Gershenzon J, Last RL, Jander G (2007). Characterization of seed-specific benzoyloxyglucosinolate mutations in *Arabidopsis thaliana*. *Plant J*, 51: 1062–1076.
105. Kokubun T, Harborne JB (1994). A survey of phytoalexin induction in leaves of the Rosaceae by copper ions. *J Biosci*, 49: 628–634.
106. Kokubun T, Harborne JB (1995). Phytoalexin induction in the sapwood of plants of the Maloideae (Rosaceae): biphenyls or dibenzofurans. *Phytochemistry*, 40: 1649-1654.
107. Kokubun T, Harborne JB, Eagles J, Waterman PG (1995b). Dibenzofuran phytoalexins from the sapwood tissue of *Photinia*, *Pyracantha* and *Crataegus* species. *Phytochemistry*, 39:1033-1037.
108. Köllner TG, Lenk C, Zhao N, Seidl-Adams I, Gershenzon J, Chen F, Degenhardt J (2010). Herbivore-induced SABATH methyltransferases of maize that methylate anthranilic acid using S-adenosyl-L-methionine. *Plant Physiol*, 153: 1795-1807.
109. Kumar A, Ellis BE (2003). 4-coumarate: CoA ligase gene family in *Rubus idaeus*: cDNA structures, evolution, and expression. *Plant Mol Biol*, 31: 327-340.
110. Kumar RS, Joshi C, Nailwal TP (2016). Callus induction and plant regeneration from leaf explants of apple (*Pyrus malus* L.) cv. Golden Delicious. *Int J Curr Microbiol App Sci*, 5: 502-510.
111. Kumar V, Nagar S (2014). Studies on *Tinospora cordifolia* monosugars and correlation analysis of uronic acids by spectrophotometric methods and GLC. *Carbohydrate Polymers*, 99: 291–296.
112. Kumar SR, Kiruba R, Balamurugan S, Cardoso HG, Arnholdt-Schmitt B, Zakwan A, Sathishkumar R (2014). Carrot antifreeze protein enhances chilling tolerance in transgenic tomato. *Acta Physiologiae Plantarum*, 36: 21–27.

113. Lakhera AK, Kumar V (2017). Monosaccharide composition of acidic gum exudates from Indian *Acacia tortilis* ssp. *raddiana* (Savi) Brenan. *International Journal of Biological Macromolecules*, 94: 45–50.
114. Laskowski RA (2001). PDBsum: summaries and analyses of PDB structures. *Nucleic acids research*, 29: 221-222.
115. Laskowski RA, Rullmann JAC, MacArthur MW, Kaptein R, Thornton JM (1996). AQUA and PROCHECK-NMR: programs for checking the quality of protein structures solved by NMR. *Journal of biomolecular NMR*, 8: 477-486.
116. Lattanzio V, Di Venere D, Linsalata V, Bertolini P, Ippolito A, Salerno M (2001). Low-temperature metabolism of apple phenolics and quiescence of *Phlyctaena vagabunda*. *J Agr Food Chem*, 49: 5817-5821.
117. Lattanzio V, Lattanzio VM, Cardinali A (2006). Role of phenolics in the resistance mechanisms of plants against fungal pathogens and insects. *Phytochemistry: Advances in research*, 661: 23–67.
118. Lee CY, Mattick LR (1989). Composition and nutritive value of apple products, In: D. Downing. (ed.). *Processed Apple Products*. Van Nostrand Reinhold, New York. pp. 303-322.
119. Le Cam B, Parisi L, Arene L. (2002). Evidence of two formae speciales in *Venturia inaequalis*, responsible for apple and pyracantha scab. *Phytopathology*, 92:314–20.
120. Lee K, Kim Y, Kim D, Lee H, Lee C (2003). Major phenolics in apple and their contribution to the total antioxidant capacity. *Journal of Agricultural and Food Chemistry*, 51: 6516-6520.
121. Lee S, Kaminaga Y, Cooper B, Pichersky E, Dudareva N, Chapple C (2012). Benzoylation and sinapoylation of glucosinolate R-groups in *Arabidopsis*. *Plant J*, 72: 411-422.
122. Leontowicz H, Gorinstein S, Lojek A, Leontowicz M, Ciz M, Soliva-Fortuny R, Park Y, Jung S, Trakhtenberg S, Martin-Belloso O (2002). Comparative content of some bioactive compounds in apples, peaches and pears and their influence on lipids and antioxidant capacity in rats. *Journal of Nutritional Biochemistry*, 13: 603-610.

123. Liaudanskas M, Viskelis P, Raodonis R, Kviklys D, Uselis N, Janulis V (2014). Phenolic composition and antioxidant activity of *Malus domestica* leaves. *Scientific World Journal*, 2014: 1-10.
124. Lindermayr C, Fliegmann J, Ebel J (2003). Deletion of a single amino acid residue from different 4-coumarate: CoA ligases from soybean results in the generation of new substrate specificities. *The Journal of Biological Chemistry*, 278: 2781-2786.
125. Linsmaier EM, Skoog F (1965). Organic growth factor requirements of tobacco tissue cultures. *Physiol Plant*, 18: 100-127.
126. Lisec J, Schauer N, Kopka J, Willmitzer L, Fernie AR (2006). Gas chromatography mass spectrometry-based metabolite profiling in plants. *Nature Protocols*, 1: 387–96.
127. Liu B, Beuerle T, Klundt T, Beerhues L (2004). Biphenyl synthase from yeast-extract-treated cell cultures of *Sorbus aucuparia*. *Planta*, 218: 492-496.
128. Liu B, Raeth T, Beuerle T, Beerhues L (2007). Biphenyl synthase, a novel type III polyketide synthase. *Planta*, 225: 1495–1503.
129. Li Y, Jeong I K, Len P, Clint C (2015). Four isoforms of *Arabidopsis* 4-coumarate: CoA ligase have overlapping yet distinct roles in phenylpropanoid metabolism. *Plant Physiol*, 169: 2409–2421.
130. Li Z, Nair SK (2015). Crystal structure of 4-coumarate:CoA ligase delta-V341 mutant complexed with feruloyl adenylate. *Structure*, 23: 2032-2042.
131. Long MC, Nagegowda DA, Kaminaga Y, Ho KK, Kish CM, Schnepf J, Sherman D, Weiner H, Rhodes D, Dudareva N (2009). Involvement of snapdragon benzaldehyde dehydrogenase in benzoic acid biosynthesis. *Plant J*, 59: 256–65.
132. Luby J, Forsline P, Aldwinckle H, Bus V, Geibel M (2001). Silk road apples: collection, evaluation and utilization of *Malus sieversii* from Central Asia. *Hort. Science*, 36: 225–31.
133. MacHardy WE (1996). *Apple scab: biology, epidemiology and management*. St. Paul, MN: APS Press, USA. 545 pp.
134. Malinowski J, Krzymowska M, Godo K, Hennig J, Podstolski A (2007). A new catalytic activity from tobacco converting 2-coumaric acid to salicylic aldehyde. *Physiol Plant*, 129: 461-471.
135. Malnoy M, Xu M, Borejsza-Wysocka E, Korban SS, Aldwinckle HS (2008). Two receptor-like genes, Vf1 and Vf2, confer resistance to the fungal pathogen *Venturia inaequalis* inciting apple scab disease. *Mol Plant Microbe Interact*, 21: 448-458.

136. Mandal S (2010). Induction of phenolics, lignin and key defense enzymes in eggplant (*Solanum melongena* L.) roots in response to elicitors. African Journal of Biotechnology, 9: 8038–8047.
137. Mandal S, Das RK, Mishra S (2011). Differential occurrence of oxidative burst and antioxidative mechanism in compatible and incompatible interactions of *Solanum lycopersicum* and *Ralstonia solanacearum*. Plant Physiology and Biochemistry, 49: 117–123.
138. Masakapalli SK, Kruger NJ, Ratcliffe RG (2013). The metabolic flux phenotype of heterotrophic *Arabidopsis* cells reveals a complex response to changes in nitrogen supply. The Plant Journal, 74: 569–582.
139. Masakapalli SK, Ratcliffe RG, Anneli R, Kirsi-Marja O, Sweetlove LJ (2014). Metabolic flux phenotype of tobacco hairy roots engineered for increased geraniol production. Phytochemistry, 99: 73-85.
140. Matsumoto S (2014). Apple pollination biology for stable and novel fruit production: Search system for apple cultivar combination showing incompatibility, semicompatibility and full-compatibility based on the S-RNase allele database,” International Journal of Agronomy 1-9. Article ID 138271, 2014.
141. Mayr U, Michalek S, Treutter D, Feucht W (1997). Phenolic compounds of apple and their relationship to scab resistance. J Phytopathol, 145: 69-75.
142. Mikulic Petkovšek M, Usenik V, Stampar F (2003). The role of chlorogenic acid in the resistance of apples to apple scab (*Venturia inaequalis* (Cooke) G. Wind. Aderh.). Research Reports Biotechnical Faculty University of Ljubljana, 81: 233-242.
143. Mikulic Petkovsek M, Stampar F, Veberic R (2008). Increased phenolic content in apple leaves infected with the apple scab pathogen. Journal of Plant Pathology, 90: 49-55.
144. Mikulic-Petkovsek M, Stampar F, Veberic R (2009). Accumulation of phenolic compounds in apple in response to infection by the scab pathogen, *Venturia inaequalis*. Physiological and Molecular Plant Pathology, 74: 60-67.
145. Mikulic Petkovsek M, Slatnar A, Stampar F, et al. (2011). Phenolic compounds in apple leaves after infection with apple scab. Biol Plant, 55: 725.
146. Mir JI, Ahmed N, Singh DB, Rashid R, Shafi W, Zaffer S, Rather I (2013). Fast and efficient in-vitro multiplication of apple clonal root stock MM-106. Vegetos, 26: 198–202.

147. Mir JI, Ahmed N, Wani SH, Rashid R, Mir H, Sheikh MA (2010). In vitro development of microcorms and stigma like structures in saffron (*Crocus sativus* L.). *Physiology and Molecular Biology of Plants*, 16: 369–373.
148. Mitra A, Mayer MJ, Mellon FA, Michael AJ, Narbad A, Parr AJ, Waldron KW, Walton NJ (2002). 4-Hydroxycinnamoyl-CoA hydratase/lyase, an enzyme of phenylpropanoid cleavage from *Pseudomonas*, causes formation of C6-C1 acid and alcohol glucose conjugates when expressed in hairy roots of *Datura stramonium* L. *Planta*, 215: 79–89.
149. Moreno PRH, van der Heijden R, Verpoorte R (1994). Elicitor-mediated induction of isochorismate synthase and accumulation of 2,3-dihydroxybenzoic acid in *Catharanthus roseus* cell suspension and shoot cultures. *Plant Cell Rep*, 14: 188-191.
150. Morris GM, Huey R, Lindstrom W, Sanner MF, Belew RK, Goodsell DS, Olson AJ (2009). AutoDock4 and AutoDockTools4: Automated docking with selective receptor flexibility. *Journal of computational chemistry*, 30: 2785-2791.
151. Mukherjee C, Samanta T, Mitra A (2016). Redirection of metabolite biosynthesis from hydroxybenzoates to volatile terpenoids in green hairy roots of *Daucus carota*. *Planta*, 243: 305–20.
152. Mustafa NR, Kim HK, Choi YH, Erkelens C, Lefeber AWM, Spijksma G, van der Heijden R, Verpoorte R (2009). Biosynthesis of salicylic acid in fungus elicited *Catharanthus roseus* cells. *Phytochemistry*, 70: 532-539.
153. Mutui TM, Mibus H, Serek M (2012). Effect of meta-topolin on leaf senescence and rooting in *Pelargonium x hortorum* cuttings. *Postharvest Biol Technol*, 63: 107-110.
154. Nieuwenhuizen NJ, Green SA, Chen X, Bailleul EJD, Matich AJ, Wang MY, Atkinson RG (2013). Functional genomics reveals that a compact terpene synthase gene family can account for terpene volatile production in apple. *Plant Physiol*, 161: 787–804.
155. Nowak K, Luniak N, Meyer S, Schulze J, Mendel RR, Hänsch R (2004). Fluorescent proteins in Poplar: a useful tool to study promoter function and protein localization. *Plant Biol*, 6: 1-9.
156. O'Boyle NM, Banck M, James CA, Morley C, Vandermeersch T, Hutchison GR (2011). Open Babel: An open chemical toolbox. *Journal of cheminformatics*, 3: 33.
157. Parisi L, Lespinasse Y, Guillaumes J, et al. (1993). A new race of *Venturia inaequalis* virulent to apples with resistance due to the Vf gene. *Phytopathology*, 83: 533–537.

158. Park YJ, Thwe AA, Li X, Kim YJ, Kim JK, Arasu MV, et al. (2015). Triterpene and flavonoid biosynthesis and metabolic profiling of hairy roots, adventitious roots and seedling roots of *Astragalus membranaceus*. *J Agric Food Chem*, 63: 8862–9.
159. Pastori GM, Kiddle G, Antoniw J, Bernard S, Veljovic-Jovanovic S, Verrier PJ, Noctor G, Foyer CH (2003). Leaf vitamin C contents modulate plant defense transcripts and regulate genes that control development through hormone signaling. *Plant Cell*, 15: 939–51.
160. Pavet V, Olmos E, Kiddle G, et al. (2005). Ascorbic acid deficiency activates cell death and disease resistance responses in *Arabidopsis*. *Plant Physiology*, 139: 1291-1303.
161. Pérez-Clemente RM, Vives V, Zandalinas SI, López-Climent MF, Muñoz V, Gómez-Cadenas A (2013). Biotechnological approaches to study plant responses to stress. *BioMed Research International*. 2013: 654120.
162. Pereira-Lorenzo S, Ramos-Cabrer AM, DÍaz-Hernández MB (2007). Evaluation of genetic identity and variation of local apple cultivars (*Malus x domestica*) from Spain using microsatellite markers. *Genet Resour Crop Ev*, 54: 405-420.
163. Pfaffl MW (2001). A new mathematical model for relative quantification in real-time RT-PCR. *Nucleic Acids Res*, 29: e45.
164. Phipps JB (2014). *Flora of North America North of Mexico, Vol. 9, Magnoliophyta: Picramniaceae to Rosaceae*. New York and Oxford: Oxford University Press.
165. Picinelli A, Dapena E, Mangas JJ (1995). Polyphenolic pattern in apple tree leaves in relation to scab resistance. A preliminary study. *J Agr Food Chem*, 43: 2273-2278.
166. Podstolski A, Havkin-Frenkel D, Malinowski J, Blounta JW, Kourteva G, Dixon RA (2002). Unusual 4-hydroxybenzaldehyde synthase activity from tissue cultures of the vanilla orchid *Vanilla planifolia*. *Phytochemistry*, 61: 611–620.
167. Potter D, Eriksson T, Evans RC, Oh S, et al (2007). Phylogeny and classification of Rosaceae. *Plant Systematics and Evolution*, 266: 5–43.
168. Qualley AV, Widhalm JR, Adebessin F, Kish CM, Dudareva N (2012). Completion of the core -oxidative pathway of benzoic acid biosynthesis in plants. *Proc Natl Acad Sci*, 109: 16383–16388.
169. Rana,S, Bhushan S (2016). Apple phenolics as nutraceuticals: assessment, analysis and application. *Journal of Food Science and Technology* 53: 1727-1738.
170. Ribnicky DM, Shulaev V, Raskin I (1998). Intermediates of salicylic acid biosynthesis in *Tobacco*. *Plant Physiol*, 118: 565–572.

171. Rottensteiner H, Kramer A, Lorenzen S, Stein K, Landgraf C, Volkmer-Engert R, Erdmann R (2004). Peroxisomal membrane proteins contain common Pex19p-binding sites that are an integral part of their targeting signals. *Mol Biol Cell*, 15: 3406–3417.
172. Rowan DD, Hunt MB, Alspach PA, Whitworth CJ, Oraguzie NC (2009). Heritability and genetic and phenotypic correlations of apple (*Malus × domestica*) fruit volatiles in a genetically diverse breeding population. *J Agric Food Chem*, 57: 7944–7952.
173. Rupasinghe HPV, Paliyath G, Murr DP (1998). Biosynthesis of α -farnesene and its relation to superficial scald development in ‘Delicious’ apples. *J Am Soc Hortic Sci*, 123: 882–886.
174. Saha AK, Brewer CF (1994). Determination of the concentrations of oligosaccharides, complex type carbohydrates, and glycoproteins using the phenol-sulfuric acid method. *Carbohydrate Research*, 254: 157-167.
175. Saini SS, Teotia D, Gaid M, Thakur A, Beerhues L, Sircar D (2017). Benzaldehyde dehydrogenase-driven phytoalexin biosynthesis in elicitor-treated *Pyrus pyrifolia* cell cultures. *Journal of Plant Physiology*, 215: 154–162.
176. Sarkate A, Banerjee S, Mir JI, Roy P, Sircar D (2017). Antioxidant and cytotoxic activity of bioactive phenolic metabolites isolated from the yeast-extract treated cell culture of apple. *Plant Cell Tiss Organ Cult*, 130: 641-649.
177. Sarkate A, Saini SS, Kumar P, Sharma AK, Sircar D (2018). Salicylaldehyde synthase activity from *Venturia inaequalis* elicitor-treated cell culture of apple. *J Plant Physiol*, 221: 66-73.
178. Schauer N, Fernie AR (2006). Plant metabolomics: towards biological function and mechanism. *Trends Plant Sci*, 11: 508–516.
179. Schmarr HG, Bernhardt J (2010). Profiling analysis of volatile compounds from fruits using comprehensive two-dimensional gas chromatography and image processing techniques. *J Chromatogr A*, 1217: 565–574.
180. Schneider K, Hovel K, Witzel K, Hamberger B, Schomburg D, Kombrink E, Stuible HP (2003). The substrate specificity-determining amino acid code of 4-coumarate:CoA ligase. *Proc Natl Acad Sci*, 100: 8601–8606.
181. Schneider K, Kienow L, Schmelzer E, Colby T, Bartsch M, Miersch O, Wasternack C, Kombrink E, Stuible HP (2005). A new type of peroxisomal acyl-coenzyme A synthetase

- from *Arabidopsis thaliana* has the catalytic capacity to activate biosynthetic precursors of jasmonic acid. *J Biol Chem*, 280: 13962–1397.
182. Schnitzler JP, Madlung J, Rose A, Ulrich Seitz H (1992). Biosynthesis of p-hydroxybenzoic acid in elicitor-treated carrot cell cultures. *Planta*, 188: 594-600.
 183. Schouten HJ, Brinkhuis J, van der Burgh A, Schaart JG, Groenwold R, Broggin GAL, Gessler C (2014). Cloning and functional characterization of the *Rvi15 (Vr2)* gene for apple scab resistance. *Tree Genetics & Genomes*, 10: 251–260.
 184. Schouten HJ, Soriano JM, Joshi SG, Kortstee AJ, Krens FA, Schaart JG, van der Linden K, Allan AC, Hellens RP, Espley RV, Jacobsen E (2009). Cisgenesis is a promising approach for fast, acceptable and safe breeding of pip fruit. *Acta Hort. (ISHS)*, 814: 199-204.
 185. Schwalb P, Feucht W (1999). Changes in the concentration of phenolic substances in the bark during the annual development of the cherry tree (*Prunus avium L.*). *Advances in Horticultural Science*, 13: 71-75.
 186. Sciubba F, di Cocco ME, Gianferri R, Capuani G, de Salvador FR, Fontanari M, Goriotti D, Delfini M (2015). Nuclear Magnetic Resonance-based metabolic comparative analysis of two apple varieties with different resistances to apple scab attacks. *J Agric Food Chem*, 63: 8339–8347.
 187. Shay JR, Hough LF (1952). Evaluation of apple scab resistance in selections of *Malus*. *Am J Bot*, 39: 288– 97.
 188. Shen J, Wang Y, Chen C, Ding Z, Hu J, Zheng C, et al. (2015). Metabolite profiling of tea (*Camellia sinensis L.*) leaves in winter. *Sci Hortic (Amsterdam)*, 192: 1–9.
 189. Shulaev V, Sargent DJ, Crowhurst RN, Mockler TC, Folkerts O, Delcher AL, Jaiswal P, Mockaitis K, Liston A, Mane SP, et al. (2011). The genome of woodland strawberry (*Fragaria vesca*). *Nat Genet*, 43: 109–116.
 190. Shuman JL, Cortes DF, Armenta JM, Pokrzywa RM, Mendes P, Shulaev V (2011). Plant metabolomics by GC–MS and differential analysis. In *Plant Reverse Genetics: Methods and Protocols*; Pereira, A., Ed.; Humana Press: Totowa, NJ, 229–246.
 191. Sierotzki H, Gessler C (1993). Flavan-3-ols content and the resistance of *Malus x domestica* to *Venturia inaequalis* (Cooke.) Wind. *Physiological and Molecular Plant Pathology*, 42: 291-297.

192. Sieweke HJ, Leistner E (1992). o-Succinylbenzoate:coenzyme A ligase from anthraquinone producing cell suspension cultures of *Galium mollugo*. *Phytochemistry*, 31: 2329–2335.
193. Sircar D, Gaid M, Chizzali C, Reckwell D, Kaufholdt D, Beuerle T, Broggin GA, Flachowsky H, Liu B, Haensch R, Beerhues L (2015). Biphenyl 4-Hydroxylases involved in aucuparin biosynthesis in rowan and apple are CYP736A proteins. *Plant Physiol*, 168: 428-442.
194. Sircar D, Mitra A (2008). Evidence for p-hydroxybenzoate formation involving enzymatic phenylpropanoid side-chain cleavage in hairy roots of *Daucus carota*. *J Plant Physiol*, 165: 407–414.
195. Stewart C, Woods K, Macias G, Allan AC, Hellens RP, Noel JP (2017). Molecular architectures of benzoic acid-specific type III polyketide synthases. *Acta Cryst*, D73: 1007-1019.
196. Stöckigt J, Zenk MH (1975). Chemical syntheses and properties of hydroxycinnamoyl-coenzyme A derivatives. *Z Naturforsch*, C30: 352–358.
197. Stuible HP, Kombrink E (2001). Identification of the substrate specificity-conferring amino acid residues of 4-coumarate:coenzyme A ligase allows the rational design of mutant enzymes with new catalytic properties. *J Biol Chem*, 276: 26893-7.
198. Szankowski I, Waidmann S, Degenhardt J, Patocchi A (2008). Functional characterization of the native promoter of the apple scab resistance gene HcrVf2. In *Biotech fruit ISHS First International Symposium on Biotechnology of Fruit Species*. September 1-5. Julius-Kühn Institut, Bundesanstalt für Kulturpflanzen (JKI), Dresden, Germany.
199. Tamura K, Peterson D, Peterson N, Stecher G, Nei M, Kumar S (2011). MEGA5: molecular evolutionary genetics analysis using maximum likelihood, evolutionary distance and maximum parsimony methods. *Mol Biol Evol*, 28: 2731–2739.
200. Teotia D, Saini SS, Gaid M, Beuerle T, Beerhues L, Sircar D (2016). Development and validation of a new HPLC method for the determination of biphenyl and dibenzofuran phytoalexins in Rosaceae. *J Chromatogr Sci*, 54: 918–922.
201. Thakur K, Chawla V, Bhatti S, Swarnkar MK, Kaur J, et al. (2013). *De Novo* transcriptome sequencing and analysis for *Venturia inaequalis*, the devastating apple scab pathogen. *PLOS ONE*, 8: e53937.
202. Thomson S (2000). Epidemiology of fire blight. In JL Vanneste, eds, *Fire blight: the*

- disease and its causative agent, *Erwinia amylovora*. Wallingford: CAB International, pp 9–36.
203. Trapman M (2006). Resistance management in Vf resistant organic apple orchards. *Bull OILB/SROP*, 29: 253–257.
 204. Treutter D, Feucht W (1990). The pattern of flavan-3-ols in relation to scab resistance of apple cultivars. *Journal of Horticultural Science*, 65: 511-517.
 205. Trott O, Olson AJ (2010). AutoDock Vina: improving the speed and accuracy of docking with a new scoring function, efficient optimization, and multithreading. *Journal of computational chemistry*, 31: 455-461.
 206. Tsao R, Yang R, Young JC, Zhu H (2003). Polyphenolic profiles in eight apple cultivars using high-performance liquid chromatography (HPLC). *J Agric Food Chem*, 51: 6347–6353.
 207. Underwood W (2012). The Plant Cell Wall: A dynamic barrier against pathogen invasion. *Frontiers in plant science*, 3: 85.
 208. Vaclavic L, Schreiber A, Lacina O, Cajka T, Hajslova J (2012). Liquid chromatography-mass spectrometry-based metabolomics for authenticity assessment of fruit juices. *Metabolomics*, 8: 1-11.
 209. Vaillancourt LJ, Hartman JR (2000). Apple scab. *The Plant Health Instructor*. DOI: 10.1094/PHI-I-2000-1005-01 Updated 2005.
 210. Valadon LRG, Rosemary SM (1967). Carotenoids of certain compositae flowers. *Phytochemistry*, 6: 983-988.
 211. Vanblaere T, Szankowski I, Schaart J, Schouten H, Flachowsky H, Brogini GA, et al., (2011). The development of a cisgenic apple plant. *Journal of biotechnology*, 154: 304–11.
 212. Vanblaere T, Flachowsky H, Gessler C, Brogini GAL (2014). Molecular characterization of cisgenic lines of apple ‘Gala’ carrying the Rvi6 scab resistance gene. *Plant Biotechnology Journal*, 12: 2–9.
 213. Van Moerkercke A, Schauvinhold I, Pichersky E, Haring MA, Schuurink RC (2009). A plant thiolase involved in benzoic acid biosynthesis and volatile benzenoid production. *Plant J*, 60: 292-302.

214. Vanzo A, Jenko M, Vrhovsek U, Stopar M (2013). Metabolomic profiling and sensorial quality of 'Golden Delicious', 'Liberty', 'Santana', and 'Topaz' apples grown using organic and integrated production systems. *J Agric Food Chem*, 61: 6580–6587.
215. Vasco C, Riihinen K, Ruales J, Kamal-Eldin A (2009). Phenolic compounds in Rosaceae fruits from Ecuador. *Journal of Agricultural and Food Chemistry*, 57: 1204-1212.
216. Vasyukova NI, Ozeretskovskaya OL (2007). Induced plant resistance and salicylic acid: A review. *Appl Biochem Microbiol*, 43: 367-373.
217. Veberic R, Mikulic-Petkovsek M, Stampar F (2008). Increased phenolic content in apple leaves infected with the apple scab pathogen. *Journal of Plant Pathology*, 90: 49-55.
218. Velasco R et al., (2010). The genome of the domesticated apple (*Malus × domestica* Borkh.). *Nature Genetics*, 42: 833-839.
219. Verde I, Abbott AG, Scalabrin S, Jung S, Shu S, Marroni F, Zhebentyayeva T, Dettori MT, Grimwood J, Cattonaro F, et al., (2013). The high-quality draft genome of peach (*Prunus persica*) identifies unique patterns of genetic diversity, domestication and genome evolution. *Nat Genet*, 45: 487–494.
220. Vessey DA, Kelley M (1998). Characterization of the monovalent and divalent cation requirements for the xenobiotic carboxylic acid: CoA ligases of bovine liver mitochondria. *Biochim Biophys Acta*, 1382: 243-248.
221. Vessey DA, Kelley M, Lau E, Zhang SZ (2000). Monovalent cation effects on the activity of the xenobiotic/medium-chain fatty acid:CoA ligases are substrate specific. *J Biochem Mol Toxicol*, 14: 162-168.
222. Villarino M, Sandín-España P, Melgarejo P, De Cal A (2011). High chlorogenic and neochlorogenic acid levels in immature peaches reduce *Monilinia laxa* infection by interfering with fungal melanin biosynthesis. *J Agric Food Chem*, 59: 3205–3213.
223. Vinson J, Su X, Zubik L, Bose P (2001). Phenol antioxidant quantity and quality in foods: fruits. *Journal of Agricultural and Food Chemistry*, 49: 5315-5321.
224. Vlot AC, Dempsey DA, Klessig DF (2009). Salicylic acid, a multifaceted hormone to combat disease. *Annu Rev Phytopathol*, 47: 177-206.
225. Wang CZ, Maier UH, Eisenreich W, Adam P, Obersteiner I, Keil M, Bacher A, Zenk MH (2001). Unexpected biosynthetic precursors of amarogentin - a retrobiosynthetic ¹³C NMR study. *Eur J Org Chem*, 8: 1459-1465.

226. Wang QJ, Sun H, Dong QL, Sun TY, Jin ZX, Hao YJ, Yao YX (2016). The enhancement of tolerance to salt and cold stresses by modifying the redox state and salicylic acid content via the cytosolic malate dehydrogenase gene in transgenic apple plants. *Plant Biotechnol J*, 14: 1986–1997.
227. Werbrouck SPO, Strnad M, Van Onckelen HA, Debergh PC (1996). *Meta*-topolin, an alternative to benzyladenine in tissue culture? *Physiol Plant*, 98: 291-297.
228. Werner I, Bacher A, Eisenreich W (1997). Retrobiosynthetic NMR studies with ¹³C-labeled glucose. Formation of gallic acid in plants and fungi. *J Biol Chem*, 272: 25474-25482.
229. Widhalm JR, Dudareva N (2015). A familiar ring to it: Biosynthesis of plant benzoic acids. *Mol Plant*, 8: 83–97.
230. Wildermuth MC (2006). Variations on a theme: synthesis and modification of plant benzoic acids. *Curr Opin Plant Biol*, 9: 288-296.
231. Wolfe K, Wu X, Liu RH (2003). Antioxidant activity of apple peels. *Journal of Agricultural and Food Chemistry*, 51: 609-614.
232. Wong KW, Harman GE, Norelli JL, Gustafson HL, Aldwinckle HS (1999). Chitinase-transgenic lines of ‘Royal Gala’ apple showing enhanced resistance to apple scab. *Acta Hort*, 484: 595-599.
233. Wu J, Wang Z, Shi Z, Zhang S, Ming R, Zhu S, Khan MA, Tao S, Korban SS, Wang H, et al., (2013). The genome of the pear (*Pyrus bretschneideri* Rehd.). *Genome Res*, 23: 396–408.
234. Wurdig J, Flachowsky H, Andrea Saß, Peil A, Magda-Viola Hanke (2015). Improving resistance of different apple cultivars using the Rvi6scab resistance gene in a cisgenic approach based on the Flp/FRT recombinase system. *Mol Breeding*, 35: 95.
235. Xiang Y, Huang CH, Hu Y, Wen J, Li S, Yi T, Chen H, Xiang J, Ma H (2017). Evolution of Rosaceae Fruit Types Based on Nuclear Phylogeny in the Context of Geological Times and Genome Duplication. *Mol Biol Evol*, 34: 262-281.
236. Yang DH, Chung BY, Kim JS, et al., (2005). cDNA cloning and sequence analysis of the rice Cinnamate-4-hydroxylase gene, a cytochrome P450-dependent monooxygenase involved in the general phenylpropanoid pathway. *J Plant Biol*, 48: 311.

237. Yazaki K, Heide L, Tabata M (1991). Formation of p-hydroxybenzoic acid from p-coumaric acid by cell free extract of *Lithospermum erythrorhizon* cell cultures. *Phytochemistry*, 30: 2233–2236.
238. Young ND, Debellé F, Oldroyd GED, Geurts R, Cannon SB, Udvardi MK, Benedito VA, Mayer KF, Gouzy J, Schoof H, et al., (2011). The *Medicago* genome provides insight into the evolution of rhizobial symbioses. *Nature*, 480: 520–524.
239. Zhang CH, Mei XG, Liu L, Yu LJ (2000). Enhanced paclitaxel production induced by the combination of elicitors in cell suspension cultures of *Taxus chinensis*. *Biotechnology Letters*, 22: 1561-1564.
240. Zhang Q, Chen W, Sun L, Zhao F, Huang B, Yang W, Tao Y, Wang J, Yuan Z, Fan G, et al., (2012b). The genome of *Prunus mume*. *Nat Commun*, 3: 1318.
241. Zhang H, Cha S, Yeung ES (2007). Colloidal graphite-assisted laser desorption/ionization MS and MSn of small molecules. 2. Direct profiling and MS imaging of small metabolites from fruits. *Anal Chem*, 79: 6575–6584.
242. Zuckerkandl E, Pauling L (1965). Molecules as documents of evolutionary history. *Journal of Theoretical Biology*, 8: 357-366.

Publications

A. Research papers

1. **Teotia D**, Saini SS, Gaid M, Beuerle T, Beerhues L, **Sircar D** (2016). Development and validation of a new HPLC method for the determination of biphenyl and dibenzofuran phytoalexins in Rosaceae. **Journal of Chromatographic Science**, 54: 918–922.
2. Saini SS, **Teotia D**, Gaid M, Thakur A, Beerhues L, **Sircar D** (2017). Benzaldehyde dehydrogenase-driven phytoalexin biosynthesis in elicitor treated *Pyrus pyrifolia* cell cultures. **Journal of Plant Physiology**, 215: 154–162.

B. Conference paper/poster

1. **Teotia D**, Sircar D (2014): Contribution of cytochrome P450 hydroxylase to noraucuparin biosynthesis in apple. **International Conference on Molecular Signaling: Recent Trends in Biomedical and Translational Research**, Department of Biotechnology, IIT Roorkee, Roorkee (India), December 2014, PP- 35. [Poster Presentation]
2. **Teotia D**, Sircar D (2015): Contribution of cinnamate: CoA ligase to benzoyl-CoA biosynthesis in apple. **International conference on Molecular Signaling: Recent Trends in Biosciences**, Department of Zoology, NEHU, Shilong, Guwahati (India). November 2015, PP-25. [Poster Presentation].

C. Manuscript Under Review

1. **Teotia D**, Gaid M, Saini SS, Dalal V, Verma A, Ambatipudi K, Kumar P, Beuerle T, Hänsch R, Roy P, Agrawal PK, Beerhues L, **Sircar D** (2018). A peroxisomally localized cinnamate:CoA-ligase is involved in benzoate-derived biphenyl phytoalexin biosynthesis in *Malus × domestica* cv. ‘Golden Delicious’ cell cultures. Manuscript submitted to **Plant Physiology** (Under Review).